UNIVERSIDADE FEDERAL DE PERNAMBUCO
CENTRO DE BIOCIÊNCIAS
DEPARTAMENTO DE ZOOLOGIA
PROGRAMA DE PÓS-GRADUAÇÃO EM BIOLOGIA ANIMAL – PPGBA

DENISE FABIANA DE MORAES COSTA SCHWAMBORN

ESPECTROS DE TAMANHOS E BIOMASSA DO ZOOPLÂNCTON, COM ÊNFASE EM DECÁPODES, EM AMBIENTES COSTEIROS DO NORDESTE DO BRASIL

RECIFE

2024

DENISE FABIANA DE MORAES COSTA SCHWAMBORN

ESPECTROS DE TAMANHOS E BIOMASSA DO ZOOPLÂNCTON, COM ÊNFASE EM DECÁPODES, EM AMBIENTES COSTEIROS DO NORDESTE DO BRASIL

Tese apresentada ao Programa de Pós-graduação em Biologia Animal da Universidade Federal de Pernambuco, como requisito parcial para obtenção do título de Doutora em Biologia Animal. Área de concentração: Biologia Animal

Orientador: Prof. Dr. Alexandre Oliveira de Almeida.

Coorientadora: Profa. Dra. Catarina da Rocha Marcolin.

Recife

2024

Catalogação na Fonte
Bibliotecário: Marcos Antonio Soares da Silva
CRB4/1381

Schwamborn, Denise Fabiana de Moraes Costa
Espectros de tamanhos e biomassa do zooplâncton, com ênfase em decápodes, em ambientes costeiros do Nordeste do Brasil. / Denise Fabiana de Moraes Costa Schwamborn. – 2024.

213 f. : il., fig.; tab.

Orientador: Alexandre Oliveira de Almeida.
Coorientadora: Catarina da Rocha Marcolin.

Tese (doutorado) – Programa de Pós-Graduação em Biologia Animal da Universidade Federal de Pernambuco, 2024.

Inclui referências e apêndices.

1. Decapoda. 2. Zooplâncton. 3. Espectros de tamanhos. 4. Série temporal. 5. Índices climáticos I. Almeida, Alexandre Oliveira de (Orient.). II. Marcolin, Catarina da Rocha (Coorient.). III. Título.

590 CDD (22.ed.) UFPE/CB – 2024-102

DENISE FABIANA DE MORAES COSTA SCHWAMBORN

ESPECTROS DE TAMANHOS E BIOMASSA DO ZOOPLÂNCTON, COM ÊNFASE EM DECÁPODES, EM AMBIENTES COSTEIROS DO NORDESTE DO BRASIL

Tese apresentada ao Programa de Pós-Graduação em Biologia Animal da Universidade Federal de Pernambuco, como requisito parcial para a obtenção do título de Doutor em Biologia Animal. Área de concentração: Biologia Animal

Aprovada em: 30 / 01 / 2024

COMISSÃO EXAMINADORA:

Prof. Dr. Alexandre Oliveira de Almeida (Orientador) – Presidente
Universidade Federal de Pernambuco – UFPE

Profa. Dra. Catarina da Rocha Marcolin (Coorientadora)
Universidade Federal do Sul da Bahia – UFSB

Profa. Dra. Rosangela Paula Teixeira Lessa – Titular Interno
Universidade Federal Rural de Pernambuco – UFRPE

Prof. Dr. André Morgado Esteves – Titular Interno
Universidade Federal de Pernambuco – UFPE

Profa. Dra. Sigrid Neumann Leitão – Titular Externo
Universidade Federal de Pernambuco – UFPE

Profa. Dra. Xiomara Franchesca García Díaz – Titular Externo
Universidade Federal Rural da Amazônia – UFRA

Prof. Dr. Ralf Tarciso Silva Cordeiro – Suplente Interno
Universidade Federal Rural de Pernambuco – UFPE

Profa. Dra. Jussara Moretto Martinelli-Lemos – Suplente Externo
Universidade Federal do Pará – UFPA

AGRADECIMENTOS

Agradeço ao meu bom Deus por ser a fonte de minha força e conforto nos dias difíceis.

Agradeço a minha mãe Mirian, meu exemplo de vida, por toda dedicação, amor incondicional, conselhos. Sempre vou ser a sua Fabí. Sigamos fortes, enfrentando os desafios que a vida nos traz.

Ao meu irmão Pedro, por suas risadas e espírito leve. Obrigada por ter me dado meu sobrinho Calebe, que tantas alegrias traz para nossa família. Te amo, Calebinho!

Ao meu amor Ralf, meu companheiro de todas as estradas, sejam boas ou ruins. Você é meu presente de Deus. Obrigada por seu senso de humor, conseguindo tirar risadas minhas em tempos difíceis. Obrigada por sua proteção e amor. E muito obrigada por toda sua ajuda nesta caminhada do doutorado, não conseguiria sem você.

À Coordenação de Aperfeiçoamento de Pessoal de Nível Superior (CAPES), pela concessão da minha bolsa de doutorado.

Ao Programa de Pós-graduação em Biologia Animal da UFPE, por ter me proporcionado esta oportunidade.

Aos Projetos ST-Esplan-Tropic (processo CNPq nº 471038/2012-1) e INCT AmbTropic (CNPq/CAPES/FAPESB) que possibilitaram as coletas que fazem parte da minha tese.

Ao centro de pesquisa CEPENE/ICMBio em Tamandaré pelo apoio laboratorial e logístico. Ao Ministério do Meio Ambiente (MMA) pela licença do SISBIO nº. 38428-4 e 34067. Ao Instituto Recifes Costeiros (IRCOS, apoiado pelas Fundações ICMBio, SOS Mata Atlântica e Toyota do Brasil), pelo apoio logístico com amostragem.

Ao projeto TRIATLAS, que recebeu financiamento do programa Horizon 2020 da União Europeia do acordo de subvenção nº. 817578.

Ao meu orientador, professor Alexandre Almeida, por ter aceitado me orientar, pelos ensinamentos que me ajudaram a construir a minha tese. Obrigada pela confiança.

À minha coorientadora, professora Catarina Marcolin, por ter aceitado me coorientar e que não mediu esforços para me ajudar sempre. Obrigada por tentar me deixar calma e me fazer acreditar na frase “Vai dar tudo certo, viu.” Obrigada Catarina!

À professora Rosangela Lessa que me acompanha desde o Mestrado. Obrigada por suas palavras sempre amáveis.

À professora Xiomara F. G. Díaz por tantos ensinamentos e momentos especiais compartilhados no laboratório de zooplâncton. Sentimos sua falta por aqui.

Aos meus professores do Centro de Biociência (Programa de Pós-graduação em Biologia Animal) da Universidade Federal de Pernambuco, principalmente a Professora

Luciana, Professor Simão, Professor André que me acompanham da graduação até agora. E em especial para a Professora Bruna e o professor Ulisses que sempre tiraram dúvidas e me ajudaram nesta caminhada do doutorado.

Ao secretário da Pós-graduação em Biologia Animal, Manoel Guimarães, por toda dedicação e atenção dispensadas para resolver qualquer solicitação, muitas vezes, escutando nossos problemas e angústias do dia a dia. Muito obrigada Manoel.

A Bruna Teixeira, representante dos alunos de doutorado, que sempre esteve disposta a tirar dúvidas e ajudar no que for preciso.

Agradeço aos professores e técnicos responsáveis pelo Laboratório de Zooplâncton, Museu de Oceanografia e Departamento de Oceanografia por permitir que eu desenvolvesse todo o meu trabalho.

À professora do Departamento de Oceanografia da Universidade Federal de Pernambuco, Sigrid Neumann Leitão, por todo carinho e cuidado. Suas palavras serviram de alento em muitos momentos dessa caminhada! Que Deus ilumine seu caminho sempre!

Aos professores do Departamento de Oceanografia da Universidade Federal de Pernambuco, Pedro Melo, Fernando Feitosa e Manuel Flores, que sempre foram amistosos ao me encontrarem em qualquer tempo.

A secretária do Departamento de Oceanografia da Universidade Federal de Pernambuco, Marília, por ajudar sempre no que fosse preciso.

Obrigada Sylvain Févre (Hydroptic - França), por toda dedicação e ajuda com o *ZooScan*. Obrigada a Marc Picheral (Laboratoire d' Oceanographie de *Villefranche* - França), pelo apoio com o aparelho *ZooScan* e o software *Zooprocess*. Obrigada a Rainer Kiko (GEOMAR - Kiel - Alemanha) pelo auxílio com o ECOTAXA (Software de banco de dados).

Agradeço a todas as pessoas envolvidas no trabalho de campo desses projetos INCT AmbTropic e ESPLAN: Aislan, Ralf, Igor, Alejandro, Simone, Gleice, Richard, Mikaelle, Morgana, Lucas, Nize, Renata, Glenda, Romero, Gabi, Cynthia, Alexandre, Everton, Gabriel, Leonardo, Pedro Melo, Isaac e a todos os barqueiros que possibilitaram nossa ida a campo. Todos nós fomos importantes na concretização desses projetos!

Meu agradecimento especial a Nathália Lins Silva nas coletas do INCT AmbTropic e ESPLAN, que não mediu esforços na ajuda com o *ZooScan* e tantas outras dúvidas que apareceram ao longo desta tese. Muito obrigada Nathália.

Agradeço também a Simone M. A. Lira por sua ajuda nos meus primeiros passos com o *Zooscan* e depois com o Ecotaxa. Obrigada por sempre estar disposta a ajudar, por seus abraços e por suas risadas.

Obrigada a Claudeilton S. Santana (”Claus”) por me ajudar na identificação dos Decapoda e na ajuda com Ecotaxa, em qualquer lugar do globo e a qualquer hora. Nunca vou esquecer.

Obrigada a Gabriela G.A.A. Figueiredo por me ajudar com o Ecotaxa, por seu otimismo e palavras de compreensão. Sempre preciso de seus abraços!

Obrigada Gleice por sua prestativa ajuda com alguns problemas do Ecotaxa.

Agradeço aos colegas do Laboratório de Zooplâncton - Labzoo (Cynthia, Gabriel, Mikaelle, Richard, Anne, Glenda, Kaio, Renata, Ályssa, Éverton, Ìtala, Fillipe) que estiveram comigo nesta jornada, compartilhando aprendizagens, experiências e boas risadas. Vocês são importantes para mim.

Agradeço a minha amiga Morgana Brito Lolaia a quem eu chamo carinhosamente de "pequena". Foram tantos momentos compartilhados, tantas experiências trocadas, tantos pedidos de oração, tantos abraços, tantos desabafos. Te amo pequena. Obrigada por sempre me motivar a ser melhor. Que bom que estamos juntas desde a graduação!

A Aurinete e Fabíola que sempre me receberam com abraços apertados no museu de Oceanografia da UFPE.

Aos meus amigos da graduação, Marcela e Fábio, que são irmãos que a vida me deu. Sempre são os primeiros a saber qualquer novidade minha. Gosto de estar perto de vocês, dar risadas e poder compartilhar minha vida. Vocês estão no meu coração sempre!

Aos meus amigos desde a graduação na UFPE, Fábio Correia (Fabinho), Gilberto (Gil), Helcy e Rama. Que venham mais encontros!

Um agradecimento especial a Ralf, Morgana, Simone e Nathália que nas últimas semanas para a conclusão da minha tese, no momento mais difícil, não largaram minhas mãos! Foram minha força e refúgio. Muito obrigada de coração!

Aos membros da banca por aceitarem o convite e poderem participar de mais essa etapa da minha vida.

A todos aqueles que de alguma forma fizeram parte dessa minha jornada nestes últimos quatro anos.

RESUMO

As contribuições dos decápodes planctônicos tropicais para a comunidade zooplanctônica foram avaliadas através de análises da estrutura de comunidades, séries temporais, e espectros de tamanho e biomassa. Também foram investigadas as variações interanuais de decápodes planctônicos e outros organismos do macrozooplâncton e relacionadas com índices climáticos, como o TSA ("Tropical South Atlantic index"). Testou-se a hipótese central de que as larvas de decápodes são importantes componentes do plâncton costeiro tropical, que respondem de forma significativa às variações climáticas. Amostras de zooplâncton foram coletadas bimestralmente no Estuário do Rio Formoso (2013 a 2015), na Baía de Tamandaré (2013 a 2019) e na Plataforma Continental ao largo de Tamandaré (2013 a 2015), Pernambuco, (Brasil), com uma rede de malha de 300 micrômetros, e analisadas utilizando um equipamento ZooScan. As imagens (vinhetas) foram depositadas no banco de dados ECOTAXA. Os decápodes foram o segundo grupo de organismos mais importante (após os copépodes), em abundância e biovolume. O total de decápodes contribuiu em média com 33,6%, 4,4% e 7,1% de abundância relativa e 30,9%, 30,9% e 15,2% de biovolume relativo no estuário, baía e plataforma, respectivamente. Os táxons e estágios de decápodes mais relevantes nas três áreas de amostragem foram zoeas e megalopas de caranguejos (Brachyura), pós-larvas de camarões peneídeos (principalmente Penaeus spp.), luciferídeos holoplanctônicos (adultos, protozoeas e mísis), zoeas de Anomura, zoeas de camarões-estalo (Alpheidae) e zoeas de Porcellanidae. Zoeas de Brachyura contribuíram com até 81,3% de abundância e até 69% de biovolume, no estuário. As pós-larvas de camarões peneídeos representaram até 28,1% do total de abundância e até 94,7% do biovolume total, na plataforma. Espectros de tamanho de biomassa normalizado (NBSS) foram construídos para o zooplâncton total, larvas de decápodes e outros organismos do mero- e ictioplâncton. Os declives do NBSS foram mais íngremes do que o esperado (estuário: inclinação = -2,45 +- 0,16, baía: inclinação = -1,81 +- 0,10, plataforma: inclinação =

-1,80 +- 0,09), o que foi claramente devido à alta abundância de copépodes calanóides, especialmente no estuário. Nossos resultados mostram que os espectros de tamanho, são moldados por interações estruturadas por tamanho, estratégias de nicho de tamanho específico dos táxons e processos de regulação “top-down” da cadeia alimentar. Essa regulação depende da densidade dos predadores (zoeas de Brachyura). Na série temporal de 2013 a 2019, um ponto de inflexão (“tipping point”) significativo (ponto de mudança, p <0,001), com um aumento abrupto na temperatura, foi detectado no índice TSA. Pós-larvas de camarões peneídeos (Penaeus spp.), copépodes, apendiculárias e quetognatos, apresentaram abundâncias significativamente mais baixas no período após o evento EN. Medusas de cnidários e ovos de teleósteos foram destacados entre os poucos “vencedores” desta série temporal. O forte evento EN (o “El Niño Godzilla”) de 2015-2016, em conjunto com o aquecimento antropogênico global, atuou como um gatilho (“trigger”), desencadeando uma mudança de regime de temperaturas na região da TSA, que afetou diretamente os ecossistemas costeiros estudados.

Palavras-chave: Decapoda; zooplâncton; espectros de tamanhos; série temporal; índices climáticos.

ABSTRACT

The contributions of tropical planktonic decapods to the zooplankton community were assessed through analyzes of community structure, time series, and size and biomass spectra. Interannual variations of planktonic decapods and other macrozooplankton organisms were also investigated and related to climate indices, such as the TSA (Tropical South Atlantic) index. The central hypothesis tested was that decapod larvae are important components of tropical coastal plankton, which respond significantly to climate variations. Zooplankton samples were collected bimonthly in the Rio Formoso Estuary (2013 to 2015), in Tamandaré Bay (2013 to 2019) and on the Continental Shelf off Tamandaré (2013 to 2015), Pernambuco, (Brazil), with a plankton net of 300 micrometer mesh, and analyzed using a ZooScan equipment, with images deposited in the ECOTAXA database. Decapods were the second most important group of organisms (after copepods), in abundance and biovolume. The total number of decapods contributed on average 33.6%, 4.4% and 7.1% relative abundance and 30.9%, 30.9% and 15.2% relative biovolume in the estuary, bay and shelf, respectively. The most relevant taxa and stages of decapods in the three sampling areas were zoeae and megalopae of brachyuran crabs, post-larvae of penaeid shrimps (mainly *Penaeus* spp.), holoplanktonic luciferid shrimps (adults, protozoeae, and mysis), anomuran zoeae, zoeae of pistol shrimps (Alpheidae), and porcellanid zoeae. Brachyuran zoeae contributed up to 81.3% in abundance and up to 69% in biovolume in the estuary. Post-larvae of penaeid shrimp represented up to 28.1% of the total abundance and up to 94.7% of the total biovolume on the shelf. Normalized biomass size spectra (NBSS) were constructed for total zooplankton, decapod larvae, and other mero- and ichthyoplankton. NBSS slopes were steeper than expected (estuary: slope = -2.45 +- 0.16, bay: slope = -1.81 +- 0.10, shelf: slope = -1.80 +- 0.09), which was clearly due to the high abundance of calanoid copepods, especially in the estuary. Our results show that size spectra are shaped by size-structured

interactions, taxon-specific size niche strategies, and top-down food-web regulation processes. This regulation depends on the density of predators (brachyuran zoea). In the time series from 2013 to 2019, a significant tipping point ($p < 0.001$), with an abrupt increase in temperature, was detected in the TSA index. Post-larvae of penaeid shrimp (*Penaeus* spp.), copepods, appendicularians and chaetognaths showed significantly lower abundances in the period after the EN event. Cnidarian jellyfish and teleost eggs were highlighted among the few "winners" of this time series. The strong EN event (the "Godzilla El Niño") of 2015-2016, together with anthropogenic global warming, acted as a trigger, triggering a change in the temperature regime in the TSA region, which directly affected the coastal ecosystems studied.

Key words: Decapoda; zooplankton; size spectra; time series; climate indices.

LISTA DE ILUSTRAÇÕES

ARTIGO 1 – SYNCHRONOUS CONTRIBUTIONS OF DECAPOD LIFE HISTORY STAGES TO THE ZOOPLANKTON OF TROPICAL ESTUARINE, COASTAL AND SHELF ECOSYSTEMS – NEW INSIGHTS FROM SEMI-AUTOMATIC IMAGE ANALYSIS

ARTIGO 3 – DECLINES IN COASTAL MACROZOOPLANKTON COMMUNITIES WITHIN A RECENT CLIMATE AND OCEAN TIPPING POINT IN THE TROPICAL SOUTH ATLANTIC

SUMÁRIO

1 INTRODUÇÃO

Os decápodos são um grupo de crustáceos majoritariamente bentônicos, com vários representantes amplamente conhecidos e de importância socioeconômica, como os camarões, as lagostas e os caranguejos. Ao longo de seu desenvolvimento larval, a maioria dos decápodes sofrem metamorfoses na morfologia, tamanho corporal, anatomia, comportamento, ecologia, nutrição, fisiologia e composição bioquímica (ANGER, 2001). Com mais de 15000 espécies e cerca de 175 famílias, estão entre os táxons mais representativos do zooplâncton, com as suas formas larvais planctônicas e espécies holoplanctônicas (BRACKEN *et al*., 2009). Quase 90% das espécies de decápodes vivem nos oceanos ou em áreas próximas como a costa e em ambientes com complexa hidrodinâmica e alta flutuação na temperatura e salinidade como os estuários (ANGER, 2001; NG; GUINOT; DAVIE, 2008), além de serem encontrados em profundidades de até 6000 m nos oceanos (NG; GUINOT; DAVIE, 2008). Geralmente, larvas de decápodes contribuem de 1 a 10% da biomassa do mesozooplâncton (LINDLEY; WILLIAMS; CONWAY, 1994) e se destacam na ecologia marinha e biologia pesqueira. Sua importância comercial, disponibilidade e diversidade morfológica dão arcabouço para modelos da estrutura trófica que integram muitos gradientes ambientais (NG; GUINOT; DAVIE, 2008; BRACKEN *et al.*, 2009; STENECK *et al.*, 2011; TOON *et al.*, 2016). Atuam nos ambientes bentônicos como herbívoros, comensais, ou predadores vorazes (BOUDREAU; WORM, 2012). São responsáveis por regular processos biogeoquímicos e ecossistêmicos através da laceração da matéria orgânica facilitando a decomposição por outros organismos (FRECKMAN *et al.*, 1997). As larvas de crustáceos sofrem predação de um grande número de invertebrados e vertebrados, em sua defesa, as larvas utilizam artifícios como espinhos, pequenos disparos para escapar dos predadores e migrações verticais e horizontais (BASHEVKIN; MORGAN, 2020). Como estratégia de evitar a predação, algumas espécies de decápodes lançam suas larvas para serem exportadas fora dos ecossistemas estuarinos, que são ambientes de alta densidade de predadores planctófagos (HOVEL; MORGAN, 1997).

A maioria dos estudos sobre decápodes planctônicos tropicais foi realizada em estuários (por exemplo, SCHWAMBORN; BONECKER, 1996; SCHWAMBORN *et al.*, 2001; SCHWAMBORN *et al*., 2002; ALMEIDA *et al.*, 2006; MELO JÚNIOR *et al*., 2007; MELO JÚNIOR *et al.*, 2016), em áreas recifais (por exemplo, SEKIGUCHI, 1983; ALMEIDA *et al*., 2010; ALMEIDA *et al.*, 2012; SANTOS; SOLEDADE; ALMEIDA, 2012; SANTOS *et al*,

2019) e águas oceânics (por exemplo, VALENTIN; MONTEIRO-RIBAS, 1993; SCHWAMBORN *et al.*, 1999; EPIFANIO; GARVINE, 2001; ROCHA *et al.*, 2003; LOPES *et al.*, 2006; BRANDÃO; GARCIA; FREIRE, 2015; LIMA *et al.*, 2021; RODRIGUES-INOUE; DOS SANTOS; MARTINELLI-LEMOS, 2021), muitas vezes em estudos baseados em um único cruzeiro oceanográfico (por exemplo, SANTANA *et al.*, 2018). Dentre os decápodos planctônicos, destacam-se os pequenos camarões holoplanctônicos da família Luciferidae, apresentando 7 espécies, com apenas duas espécies ocorrendo na costa brasileira: *Belzebub faxoni* (Borradaile, 1915) e *Lucifer typus* (Milne Edwards, 1837). Essas espécies possuem uma distribuição geográfica ampla e características morfológicas marcantes, como a parte anterior da carapaça alongada (D'INCAO, 1997). Indivíduos de *Lucifer typus* (Milne Edwards, 1837) são frequentemente encontrados na região oceânica, enquanto *Belzebub faxoni* (Borradaile, 1915) em áreas próximas da costa e nas desembocaduras dos estuários (HANSEN, 1922). Recentemente, um novo gênero de Luciferidae, *Sume marcosi* n. gen. n. sp., foi descoberto na Bacia do Araripe, nordeste do Brasil. O material estava bem preservado em xisto calcário da Formação Romualdo do final do Cretáceo Inferior (SARAIVA; PINHEIRO; SANTANA, 2018). Outros decápodes planctônicos muito comuns em àreas costeiras são as larvas meroplanctônicas, como por exemplo, as zoeas de Brachyura (caranguejos e siris), Penaeidae (camarões marinhos), Alpheidae (camarões-estalo), e Porcellanidae (caranguejos-porcelana, SCHWAMBORN *et al.*, 2001).

Os decápodes planctônicos tornaram-se se organismos extremamente exitosos e abundantes, nas suas formas larvais e como adultos, devido grande parte, às suas diferentes adaptações morfológicas, crescimento rápido e ecologia, sendo importantes nas cadeias alimentares como fonte de alimentos de outros invertebrados, larvas de peixes e peixes planctófagos. São importantes componentes do zooplâncton estuarino e marinho. O zooplâncton é um conjunto de animais, majoritariamente microscópicos, que pairam nas águas sem conseguir vencer as correntes. O zooplâncton é classificado como holoplanctônico, quando seus indivíduos passam todo o seu ciclo de vida no plâncton (como os copépodes calanóides e camarões luciferídeos) ou como meroplanctônico, cujos indivíduos permanecem no plâncton apenas durante uma fase de suas vidas (como as larvas de crustáceos decápodos e de outros invertebrados). Além de serem extremamente abundantes, o zooplâncton marinho possui grande diversidade de formas corporais, tamanhos e tipos de reprodução e abrangem diferentes níveis tróficos em teias alimentares pelágicas (STEINBERG; LANDRY, 2017; MCENNULTY

et al., 2020). O sucesso da transferência de energia das teias alimentares está intrinsecamente ligado ao tamanho do corpo da presa e do predador.

As populações de zooplâncton enfrentam inúmeras variações sazonais de temperatura ao longo de sua existência. Normalmente, as variações de temperatura e sazonalidade são diárias e repetitivas, o que as torna esperadas. Usando estratégias fisiológicas, comportamentais e de distribuição, o zooplâncton consegue reduzir os danos, que são desfavoráveis a seu crescimento e sobrevivência (MACKAS *et al.*, 2012). Quando analisamos dados de uma série temporal, procuramos identificar mudanças nos ciclos sazonais e do zooplâncton, ano após ano. Estudos de longo prazo são uma combinação de partes de tendência, sazonais e irregulares (HARVEY; SHEPHARD, 1993) que fornecem informações importantes sobre as oscilações da comunidade e das espécies e o que causa essas oscilações (CLARK; FRID; BATTEN, 2001). A temperatura, disponibilidade de nutrientes, produtividade primária, concentração de clorofila estão entre as principais variáveis ambientais que participam da variância total de tempo (MACKAS *et al.*, 2012). Como o zooplâncton reage às alterações de longo prazo, pode ser averiguado em mudanças na variabilidade da biomassa (Valdés *et al.*, 2007), composição de espécies (Mackas *et al.*, 2012), abundância (VALDÉS *et al.*, 2007; MAZZOCCHI *et al.*, 2011), alterações de tamanho (AYÓN *et al.*, 2011) e flutuações do zooplâncton (BERLINE *et al.*, 2012).

As distribuições de tamanho, biovolume e biomassa contêm informações importantes sobre o funcionamento das comunidades planctônicas (HOBBIE *et al.*, 1972; PLATT, 1985; MORIARTY *et al*, 2013). A análise dos espectros de tamanho fornece parâmetros da dinâmica populacional do zooplâncton e da produtiviade do ecossistema (SPRULES; MUNAWAR, 1986; ZHOU; HUNTLEY, 1997; SPRULES; BARTH, 2016). Com base em observações de que a biomassa em ambientes aquáticos é relativamente constante ao longo de uma distribuição de lei de potência (distribuição Pareto), numerosos conceitos teóricos e modelos de espectro de tamanho foram desenvolvidos (por exemplo, SHELDON; PRAKASH; SUTCLIFFE, 1972; SHELDON; SUTCLIFFE; PARANJAPE, 1977; KERR, 1974; PLATT; DENMAN, 1978; RAY *et al.*, 2001; BLANCHARD *et al.*, 2017). O espectro de tamanho de biomassa (ou biovolume) normalizado (NBSS, PLATT; DENMAN, 1977) usa uma transformação simples, onde o valor Y (abundância, biovolume ou biomassa) para cada tamanho de compartimento é dividido pela largura correspondente do compartimento (PLATT; DENMAN, 1977; DICKIE; KERR; BOUDREAU, 1987; RODRÍGUEZ, 1994; GAEDKE; STRAILE, 1998). Muitos estudos recentes sobre zooplâncton usaram a abordagem NBSS para analisar a variabilidade

sazonal, interanual ou espacial (por exemplo, SAN MARTIN; HARRIS; IRIGOIEN, 2006; VANDROMME *et al.*, 2014; MARCOLIN; GAETA; LOPES, 2015; KE *et al.*, 2018, SOUZA *et al.*, 2020; ATKINSON *et al.*, 2021; COURET *et al.*, 2023). Diversos descritores de espectro de tamanho (inclinação, intercepto, elevação média, linearidade, dispersão média, homocedasticidade da dispersão, formato do contorno, altura e distribuição de picos e cúpulas, diversidade de tamanhos, etc.) podem fornecer subsídios para a compreensão, previsão e gerenciamento dos ecossistemas. Entre estes descritores, o declive do NBSS é de longe o mais intensamente estudado e mais frequentemente investigado, uma vez que pode ser utilizado para avaliar a eficiência trófica (TE) de cadeias alimentares (FIGUEIREDO *et al.*, 2020).

As observações de longo prazo (séries temporais) nos permitem documentar o funcionamento de um sistema e suas variações. Através das séries temporais, é possível desenvolver modelos e testar hipóteses da dinâmica do sistema (GREVE *et al.*, 2004; WELLS *et al.*, 2022). Um conjunto substancial de evidências sobre a mudanças de regime do ecossistema marinho foram relatados com base em séries temporais de zooplâncton altamente informativas e sensíveis (ARONÉS *et al.*, 2009; AYÓN *et al.*, 2008; JIAO, 2009; MACKAS; BEAUGRAND, 2010; WELLS *et al.*, 2022). As comunidades zooplanctônicas são sistemas extremamente sensíveis e responsivos, respondendo de forma dinâmica e rápida até mesmo as alterações mais sutis, sendo assim potentes amplificadores de sinal para estágios iniciais de alterações climáticas e oceânicas deletérias (RICHARDSON, 2008). Extremos climáticos cada vez mais frequentes, como eventos de chuva extrema (“enxurradas”) foram relatados recentemente em diversas partes do mundo, incluindo o Nordeste do Brasil (MARENGO *et al.*, 2023). Porém, ainda não foram descritas as consequências destes eventos extremos, assim como do recente evento El Niño 2015/16, excepcionalmente forte (o El Niño “Godzilla”), para os ecossistemas pelágicos costeiros do Nordeste do Brasil.

1.1 OBJETIVOS

1.1.1 Objetivo geral

Determinar a composição taxonômica e biomassa dos decápodes planctônicos em ambientes estuarinos e marinhos no Nordeste do Brasil e sua contribuição para os espectros de tamanhos, biovolume e biomassa do mesozooplâncton (>300 micrômetros), assim como a sua variação temporal e espacial.

1.1.2 Objetivos específicos

- Caracterizar e comparar as larvas de decápodes e demais zooplâncton nos ambientes estuarino, costeiro e de plataforma continental de Tamandaré (PE - Brasil).

- Analisar a distribuição espacial da abundância e do biovolume das larvas de decápodes e comparar com os demais organismos (zooplâncton total) dos ambientes estuarino, costeiro e nerítico de Tamandaré (PE - Brasil).

- Avaliar a contribuição relativa (%) das larvas de decápodes, em abundância e biovolume, para o zooplâncton total nos ambientes estuarino, costeiro e nerítico de Tamandaré (PE - Brasil).

- Analisar as distribuições de tamanhos e espectros de biomassa (ou biovolume) normalizados (NBSS, normalized biomass size spectra) do zooplâncton nos ambientes estuarino, costeiro e nerítico e a contribuição das larvas de decápodes para esses espectros, nestes ambientes.

- Detectar possíveis efeitos do forte evento El Niño de 2015/16 sobre as larvas de decápodes e demais comunidades zooplanctônicas costeiras de Tamandaré, ao longo de uma série temporal de 2013 a 2019 (6 anos).

- Organizar um banco de dados (EcoTaxa) com as imagens (vinhetas) de zooplâncton marinho e dados descritivos das imagens.

2 ESTRUTURA DA TESE

Esta tese baseia-se em três capítulos com resultados inéditos. O primeiro capítulo foi publicado recentemente no periódico científico *Journal of Marine Systems.* Os demais dois capítulos estão preparados em formato de manuscrito para serem submetidos a periódicos científicos. No início da tese abrimos com uma introdução geral, na qual abordamos diversos aspectos do zooplâncton marinho e estuarino, espectros de tamanho e biomassa, e a ecologia de decápodos planctônicos. Finalizamos a tese com um capítulo sobre conclusões gerais, no qual abordamos os principais avanços obtidos ao longo destes anos.

Artigo 1 - Asynchronous contributions of decapod life history stages to the zooplankton of tropical estuarine, coastal and shelf ecosystems – new insights from semi-automatic image analysis.

Estado: publicado - *Journal of Marine Systems*

DOI: https://doi.org/10.1016/j.jmarsys.2023.103943

Hipótese:

Os diversos estágios da história de vida dos decápodes exibem padrões de recrutamento e dispersão bem definidos em áreas estuarinas, costeiras e de plataforma continental adjacentes, constituindo contribuições relevantes para o zooplâncton nessas áreas.

Objetivo geral:

Estudar decápodes planctônicos em três ambientes estuarinos e marinhos tropicais, usando dados obtidos por meio de um método padronizado, quantitativo e semiautomático de análise de imagem. O foco principal foi comparar áreas de estudo e estações e as diversas contribuições dos decápodes para o abundância, biomassa e biovolume de zooplâncton, como resultado da sincronicidade dos processos de reprodução, dispersão e recrutamento. Além disso, investigamos as possíveis inter-relações entre diferentes estágios da história de vida dos decápodes e de outros organismos do zooplâncton (copépodos, larvas e ovos de peixes, etc.) nesses ecossistemas pelágicos costeiros tropicais.

Artigo 2 - Size niche interactions between mero- and holoplankton shape the size spectrum of tropical estuarine and marine ecosystems.

Estado: a ser submetido

Hipótese:

Pretendemos testar a hipótese geral de que a liberação massiva de larvas meroplanctônicas na coluna de água afeta significativamente a forma dos espectros de tamanho do zooplâncton em ambientes estuarinos e costeiros tropicais.

Mais especificamente, testamos as cinco hipóteses de trabalho de que 1.) os picos no espectro de tamanho do zooplâncton podem estar relacionados a grupos taxonômicos específicos do meroplâncton, 2.) existem interações de nicho de tamanho significativas entre o mero- e o holoplâncton (ou seja, existem correlações significativas entre picos e os vales em suas distribuições de tamanho), 3.) tais interações de nicho de tamanho são dependentes da densidade, 4.) aportes de organismos não-holoplanctônicos na coluna de água podem alterar a inclinação do espectro de tamanho e o seu intercepto, 5.) e que o meroplâncton preenche lacunas graves (“classes vazias”) no espectro de tamanho do zooplâncton.

Objetivo geral:

Elaborar espectros de tamanho de biovolume normalizado (NBSS) como forma sintética de descrever o zooplâncton total, larvas de decápodes e outros organismos do mero- e ictioplâncton em três áreas de Tamandaré, Brasil.

Artigo 3 - Declines in coastal macrozooplankton communities within a recent climate and ocean tipping point in the Tropical South Atlantic

Estado: a ser submetido

Hipótese:

As variações interanuais das comunidades de decápodos planctônicos tropicais (incluindo espécies de relevância socioeconómica) e de outros organismos do macrozooplâncton, em um série temporal de 6 anos (2013-2019), em uma área marinha protegida costeira do Nordeste brasileiro, podem ser explicadas por variações climáticas em escala global, sintetizadas em índices climáticos comuns (por exemplo, ONI e TSA).

Objetivo geral:

Examinar os efeitos potenciais de alterações climáticas específicas e fenômenos climáticos bem definidos, como o forte EN 2015/16 e eventos de chuvas extremas, sobre as comunidades pelágicas de substancial relevância ecológica e socioeconômica.

3 ARTIGO 1 – ASYNCHRONOUS CONTRIBUTIONS OF DECAPOD LIFE HISTORY STAGES TO THE ZOOPLANKTON OF TROPICAL ESTUARINE, COASTAL AND SHELF ECOSYSTEMS - NEW INSIGHTS FROM SEMI-AUTOMATIC IMAGE ANALYSIS

Observação: Este artigo foi publicado on-line no **Journal of Marine Systems**. https://doi.org/10.1016/j.jmarsys.2023.103943. Para seguir o padrão da tese, o abstract, acknowledgements, fundings foram extraídos deste artigo.

1 INTRODUCTION

Decapod crustaceans include many species of interest to fisheries and aquaculture (e.g., shrimps, crabs and lobsters). They are key components of estuarine and marine zooplankton communities, as holoplanktonic adults and as meroplanktonic larvae (Schwamborn *et al.*, 2001). Many studies on planktonic decapods have been based on visual counting (i.e., abundance), and the abundance composition of planktonic decapod assemblages has thus been intensively studied in numerous tropical areas (Schwamborn *et al.*, 2001; Melo Júnior *et al.*, 2016; Costa and Schwamborn 2016; Santana *et al.*, 2018; Santos *et al.*, 2019). Yet, there are considerable knowledge gaps regarding the biomass and biovolume composition of tropical estuarine and coastal zooplankton, especially regarding the contributions of meroplankton, such as decapod larvae.

Most studies on tropical planktonic decapods have been conducted in estuaries (e.g., Schwamborn *et al.*, 1996; Schwamborn *et al.*, 2001; Schwamborn *et al.*, 2002; Almeida *et al.*, 2006; Melo Júnior *et al.*, 2007; Schwamborn *et al.*, 2008; Melo Júnior *et al.*, 2016), in reef areas (e.g.,Sekiguchi, 1983; Almeida *et al.*, 2010; Almeida *et al.*, 2012; Santos *et al.*, 2012; Santos *et al.*, 2019) and offshore waters (e.g., Valentin and Monteiro-Ribas, 1993; Schwamborn *et al.*, 1999; Epifanio and Garvine *et al.*, 2001; Rocha *et al.*, 2003; Lopes *et al.*, 2006; Brandão *et al.*, 2015; Lima *et al.*, 2021; Rodrigues-Inoue *et al.*, 2021), often based on one single oceanographic cruise (e.g., Santana *et al.*, 2018).

One of the most common ways to estimate the space occupied by an individual of a certain species in an ecosystem is through the calculation of its biovolume (Binggeli *et al.*, 2011). Previously, it was very common to determine biovolume through simple geometric shapes (Hillebrand *et al.*, 1999; Mustard and Anderson 2005), linear measurements (Alcaraz *et al.*, 2003), or total biovolume by displacement in glass cylinders (Kramer *et al.*, 1972, Turner,

1982). Few studies conducted the measurement of individual biovolume before the arrival of automated systems, such as the ZooScan (Remsen *et al.*, 2004; Gorsky *et al.*, 2010; Dai *et al.*, 2016 and 2017; Colas *et al.*, 2018; Ibarbalz *et al.*, 2019).

The ZooScan (Gorsky *et al.*, 2010) is a fast and non-destructive method that provides a large amount of information and data about body shape, size, and area, allowing us to estimate the sizes, abundance, biovolume and biomass, and securing the image archives for future comparisons and validations. However, there is little or incipient information on the biomass and biovolume of decapods from ZooScan-based zooplankton studies (García-Comas *et al.*, 2011; Vandromme *et al.*, 2012; Santos *et al.*, 2019). No specific study has been conducted until now to investigate a planktonic decapod community in detail using the ZooScan.

Peaks in zooplankton biomass have been observed in association with the synchronized release of larvae (meroplankton) by benthic invertebrates (e.g., for cirripedian larvae, Barnes, 1957; Crisp, 1962; Lang and Ackenhusen, 1981). Seasonal reproductive peaks are well documented in temperate decapod larval communities, usually coinciding with peak summer temperatures or food availability in spring blooms (González-Gordillo and Rodríguez, 2003; Pan *et al.*, 2011; Vieira and Calazans, 2015). Only few studies assessed the effect of larval inputs on the zooplankton. Highfield *et al.* (2010) quantified this contribution to the zooplankton collected with a 200 micron mesh net off the coast of Plymouth, UK, in terms of maximum relative abundance (numbers), and stated that "meroplankton (predominantly Cirripedia) can account for up to 42.5% of the total zooplankton community following spawning events linked to phytoplankton blooms".

For a long time, a continuous reproduction has been generally assumed for tropical and subtropical marine invertebrates (Hernáez *et al.*, 2012), due to favorable temperatures and phytoplankton biomass throughout the year. Indeed, studies in subtropical offshore zooplankton revealed a very weak seasonality, for highly diverse decapod larval assemblages (Reyns and Sponaugle 1999; Landeira and Lozano-Soldevilla, 2018).

The few studies that have quantified the larval phenology of decapods in tropical waters focused only on estuaries (Schwamborn and Bonecker, 1996), or on one species only (Hernáez *et al.*, 2012), little being known about the triggers that shape the timing of larval and postlarval peaks. Hernáez *et al.* (2012) related the peak in reproduction of ghost shrimp Lepidophthalmus

bocourti (Milne-Edwards, 1870) to the decrease in salinity at the onset of the rainy season in Costa Rican mangroves.

So far, no attempts have been made to compare the seasonal and spatial synchronicity of planktonic decapods in tropical estuarine and coastal zooplankton, and to quantify the impact of such larval inputs (in terms of abundance, biovolume, and biomass) on the zooplankton communities in these ecosystems.

Here, we test the hypothesis that decapod taxa and life history stages exhibit well defined recruitment and dispersal patterns in adjacent estuarine, coastal and shelf areas, that are relevant contributions to the zooplankton in these areas. The objective of this study was to investigate planktonic decapods in three tropical estuarine and marine environments, using data obtained through a standardized, quantitative, semi-automatic image analysis approach.
The main focus was to compare study areas and seasons and the varying contributions of decapods to the zooplankton abundance, biomass and biovolume, as a result of the synchronicity of reproduction, dispersal and recruitment processes. Also, we investigated the potential interrelationships between distinct life history stages of decapods, and other plankton, in these tropical coastal pelagic ecosystems.

2 MATERIALS AND METHODS

2.1 Study Area

Sampling was conducted in the Rio Formoso estuary, in Tamandaré bay, and along a transect on the continental shelf off Tamandaré, Pernambuco State, northeastern Brazil (Fig. 1). This study is the result of 37 bimonthly sampling campaigns conducted in the context of two projects: St-ESPLAN-Tropic (estuary and bay stations) and INCT AmbTropic (shelf stations). The three areas surveyed are included in the Costa dos Corais Environmental Protection Area, which extends over 120 km of the coast, including extensive estuarine mangroves, coral reefs and sandy beaches, and has its limit in the continental shelf break (ICMBio - MMA).

Figure 1. Map of the study area and sampling stations in the Rio Formoso estuary (EST1 to EST3, in red), in Tamandaré bay (BA1 to BA3, in orange), and on the adjacent continental shelf (PE1 to P6, in blue), Pernambuco, Brazil.

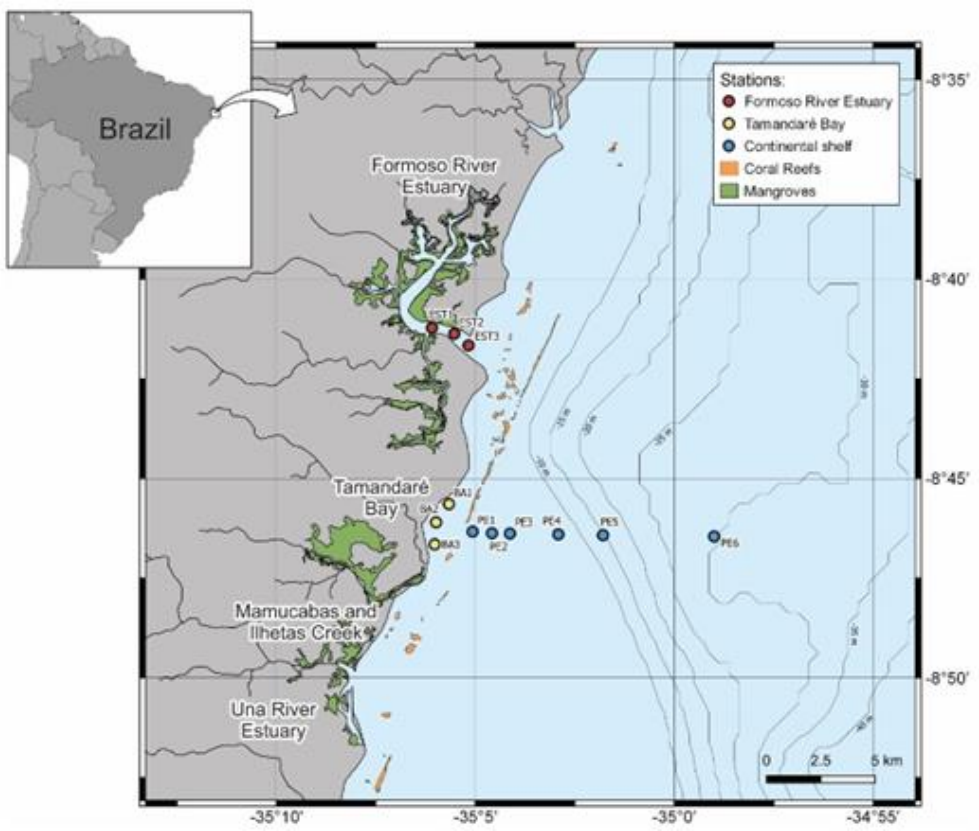

Fonte: A autora (2023).

The Rio Formoso estuary is located in the Environmental Protection Area "APA do Rio Formoso", an extensive riverine mangrove with 204.31 ha (CONDEPE/FIDEM) and a "restinga" ecosystem (i.e., a sandy coastal plain with characteristic herbaceous plants and shrubs), that extends for about 3 km (Duarte, 1993). Tamandaré bay extends over approximately 3 km². It is a semi-open bay, protected by lines of sandstone and coral reefs, and receives water from a lagoon-like shallow reef labyrinth at the north and from several mangrove estuaries at the south (Duarte, 1993; Maida and Ferreira, 1997). It receives water indirectly from the nearby large-scale Una River, which is the main watershed in the region with an extension of 290 km, and directly from the Mamucabas and Ilhetas creeks, which are surrounded by mangroves and drain into the bay. The adjacent continental shelf off Tamandaré has a series of sandstone and coral reefs lines that run parallel to the coast and are an effective protection against wave energy, and calcareous silt flats and rhodolith beds (Manso *et al.*, 2003; Camargo *et al.*, 2007).

The average annual rainfall (mean from 1990 to 2020) in this area is 1,631 mm (Silva *et al.*, 2022), with strong variations between dry (September to February, 367 mm, 22,5% of the total rainfall) and rainy seasons (March to August, 1.264 mm, 77.5% of the accumulated rainfall, Silva *et al.*, 2022).

At the Pernambuco continental shelf and coastal areas, the high-pressure system of the South Atlantic controls the trade wind regime (Domingues *et al.*, 2017). The wind regime has a considerable seasonality (Rollnic and Medeiros, 2006), with strong southeasterly trades in the second semester. Low wind speeds occur in the first semester, with minimum wind speeds in March, April and May (early rainy season), and weaker winds from E-NE especially in December and January, coinciding with the peak dry season. The peak windy season, with strong shoreward winds from E-SE, lasts from June to October, extending from the peak of the rainy season to the early dry season.

2.2 Zooplankton sampling

Sampling was always conducted during the day, at new moon spring tides, at 12 fixed stations (Fig. 1) totaling 121 samples. The sampling strategy in the estuary had the objective to capture larvae that were recently released and exported from tropical mangroves, and was designed accordingly to obtain estuarine zooplankton, with a minimum marine influence (sampling during the transition from late ebb tide to early low tide, between approx. 09:00 to

11:00 am). Conversely, sampling in Tamandaré bay was designed to minimize the influence of estuarine plumes, and to sample coastal marine zooplankton, with maximum influence of the adjacent shelf and coral reef ecosystems (sampling during the transition from late flood tide to early high tide, between approx. 1:00 to 3:00 pm). Along the transect on the shelf, the sampling schedule was designed to obtain organisms transported shoreward at the surface, by common shoreward trade winds and flood tides (from approx. 10:00 am to 2:00 pm, during flood tide). Since the sampling tides were always during the new moon, daytime hours and tidal situations (i.e., low, flood, high, and ebb tides) were well standardized throughout the time series.

During each field campaign, diurnal subsurface (0 to 60 cm depth stratum) horizontal tows were conducted with a conical plankton net (mesh size: 300 μm, diameter: 60 cm, length: 2.5 m), equipped with a calibrated flowmeter (Hydro-Bios, Kiel) to estimate the filtered volume. Tows had a duration of 5 minutes at a speed of 2 to 3 knots. Abiotic data (temperature, salinity and Secchi depth) were measured at each station using a CTD probe (YSI/SonTek CastAway) and a Secchi disk. All zooplankton samples were immediately placed in flasks with seawater and preserved with 4% formaldehyde (buffered with 0.5 g / L sodium tetraborate).

2.3 ZooScan analyses

In the laboratory, samples were divided into two size fractions by sieving with a 1000 μm mesh. This separation was important to avoid underestimating large organisms and particles, considering that large objects are less abundant (Gorsky *et al.*, 2010). Each size fraction was split with a Motoda splitter (Omori and Ikeda, 1984) to achieve quantitative aliquots (subsamples) of approx. 1,000 to 2,000 objects per subsample. The ZooScan device (Hydroptic model ZSCAN03), a modified scanner (resolution: 2400 dpi), was used to digitize the wet zooplankton samples. The software ZooProcess (http://www.obs-vlfr.fr/LOV/ZooPart/ZooScan) and Plankton Identifier (PkID) were used to semi-automatically analyze and classify each subsample, thus generating digital images (i.e., “vignettes”) of all organisms and particles. For each vignette, a vector of descriptive parameters was calculated (e.g., size, area, ellipsoid axes, gray level, feret diameter, etc.).

These parameters were used for the semi-automatic identification that was conducted with the Plankton Identifier software, applying the Random Forest algorithm (Breiman, 2001) to classify all vignettes, which were later visually verified (validated) by a specialist and

separated by categories, thus manually correcting any classification errors. This procedure allowed the identification of organisms at the level of taxonomic groups and life history stages (zoeae, megalopae, postlarvae, protozoeae, mysis, and adults).

From the size and area data, and the axes lengths of the equivalent ellipse, we calculated the individual biovolume (in mm^3 per ind.) and the individual biomass (in carbon units) of each organism.

The ellipsoid biovolume was calculated from the axes of the equivalent ellipse (that is, the ellipse that best fits the object) using the following equation: $*pi*a^2*b$, where a = minor axis and b = major axis (Stemmann and Boss, 2012; Vandromme *et al.*, 2012).

The individual biomass of organisms (in carbon units) was calculated from specific equations obtained by Marcolin (2013). Individual biovolume (mm^3 per ind.), individual biomass, filtered volume (m^{-3}) and subsampling factors (for each size fraction), were then used to calculate total biovolume (mm^3 m^{-3}) and total carbon biomass (micrograms C m^{-3}) for each size fraction, before pooling the two size fractions in each sample. Biovolume was preferred over biomass as the main unit in this study, since 1) biovolume is the most common unit in ZooScan-based studies, thus allowing comparisons with other publications, and 2) biovolume obtained from high-resolution ZooScan vignettes is a more direct, precise, accurate, reliable and robust information, than carbon biomass calculated using a list of equations obtained from several literature sources. However, biovolume and biomass were highly correlated within a perfectly linear relationship (for total zooplankton and for total decapods). Only biovolume is presented in analyses and graphs, to avoid collinearity and repetition of results. All data are available in units of frequency of occurrence, abundance, carbon biomass and biovolume.

2.4 Statistical analyses

To test for significant temporal (sampling months, “rainy *vs* dry”, “windy *vs* calm”, and “four seasonal trimesters”) and spatial (sampling areas) variations of the main univariate parameters of the zooplankton and decapod community (total zooplankton abundance, decapod abundance, decapod biovolume, decapod carbon biomass, abundance and biovolume of key decapod taxa), we used a univariate Kruskal-Wallis ANOVA (Kruskal and Wallis, 1952)

When significant effects of a spatial or temporal factor were detected, we conducted a non-parametric *post-hoc* Kruskal-Nemenyi test (Nemenyi, 1963), for pairwise comparisons among the three areas, in relation to total zooplankton abundance, biovolume, carbon biomass, and decapod carbon biomass in absolute and relative units (%, referring to the total zooplankton). The *post-hoc* Kruskal-Nemenyi test was conducted using the "kwAllPairsNemenyiTest" function from the "PMCMRplus" package (Pohlert, 2022).

Correlations between abiotic parameters (surface salinity, surface water temperature, Secchi depth), biotic parameters (total zooplankton, copepods, fish larvae, fish eggs, etc.), and abundance and biovolume of each decapod taxon were tested with non-parametric Spearman rank correlation tests. Also, pairwise tests with Spearman correlations between all decapod taxa and stages were conducted, for abundance and biovolume. These tests were conducted semi-automatically within a Spearman correlation plot matrix ("corrplot"), at alpha = 0.05. Correlation plot matrices were built with all samples, and for each sampling area ("estuary", "bay", and "shelf") separately.

Multiple mixed linear (GLM) and non-linear (GAM) models were built using abiotic variables (surface salinity, surface water temperature and Secchi depth), seasonality vectors ("dry *vs* rainy", "windy *vs* calm", "four seasons") and spatial factors ("sampling area", "distance from the coast", "local depth") as initial explanatory variables, to investigate variables or combinations of variables that can potentially explain the variability of the main univariate parameters of the zooplankton and decapod communities (log(x+1) transformed total zooplankton abundance, decapod abundance, decapod biovolume, decapod carbon biomass, abundance and biovolume of key decapod taxa. For all linear models, stepwise backward regression was used to select the significant variables using the function "stepAIC" in the R Package "MASS" (Venables and Ripley, 2002). The contribution of each explanatory variable or factor to the overall variability explained by linear models was assessed with the "Relative importance" approach, by calculating the "lmg" index (R^2 partitioned by averaging over orders, Lindeman *et al.*, 1980), within the R package "relaimpo" (Grömping, 2007). Univariate, multivariate and mixed GAM models were built using the R package "gam" (Hastie and Tibshirani, 1990). The statistical significance of linear and non-linear models (either univariate or multivariate) was checked with non-parametric permutation tests (function "avperm") within the R package "permuco" (Frossard and Renaud, 2021).

Multivariate analyses (RDA and PERMANOVA) were used to investigate variables or combination of variables that can potentially explain the variability in biovolume and abundance matrices of decapods (Rao 1964; Legendre *et al.*, 2011; Anderson, 2017), using the "vegan" R package (Oksanen *et al.*, 2022), by applying the functions "rda", "ordistep", and "adonis2". Prior to these multivariate analyses, all biological matrices were Hellinger-transformed (i.e., the square root of the relative abundance or relative biovolume within a sample was calculated). Abiotic variables (surface salinity, surface water temperature and Secchi depth), seasonality vectors ("dry vs rainy", "windy vs calm seasons", "four seasons") and spatial factors ("sampling area", "distance from the coast", "local depth") were used together, as initial explanatory matrices. From these, significant variables were selected using the "ordistep" function. Finally, significant variables were tested using PERMANOVA (function "adonis2"), based on Bray-Curtis similarities. These multivariate analyses were conducted for all data and for each sampling area separately.

All statistical analyses were performed at alpha = 0.05, using the "R" programming environment, software and language (version 4.0.2, R Core Team, 2022) through the "RStudio" interface (version 1.1.463, RStudio Team, 2022).

3 RESULTS

3.1 Abiotic conditions

Abiotic conditions displayed evident spatial and seasonal patterns (Fig. 2). In the three sampling areas, surface water temperature ranged from 26.38°C to 30.54°C. Surface salinity ranged from 27.03 in the estuary to 37.44 on the shelf. Water transparency (Secchi depth) ranged from less than 1 m in the estuary to more than 19 m on the shelf. Spatial gradients were very strong and conspicuous for Secchi depth and salinity. When comparing abiotic parameters between rainy *vs* dry seasons, only differences in Secchi depth in the bay were significant ($p < 0.05$, Mann-Whitney U tests), with more transparent waters in the dry season.

3.2 Zooplankton composition

In the present study, 182,281 digital images were semi-automatically pre-classified, measured regarding their biovolume and biomass, and validated manually regarding their taxonomic classification and larval stage. Zooplankton was classified into 31 taxonomic groups.

Zooplankton was dominated by copepods, in units of abundance and biovolume, followed by decapods. Average abundance of copepods was 2,448.2 ind. m^{-3} (std. dev.: 8,129.4 ind. m^{-3}) in the estuary, 149.4 ± 354.2 ind. m^{-3} in the bay, and 133.4 ± 267.3 ind. m^{-3} on the shelf, followed by Decapoda (650.52 ± 1202.93 in the estuary, 2.79 ± 3.39 ind. m^{-3} in the bay, and 3.31 ± 6.18 on the shelf, Fig. 3). On average, copepods showed 56.7%, 77.7%, and 70.4% relative abundance and 60.1%, 50.4% and 53.9% relative biovolume in estuary, bay and shelf areas, respectively.

Total decapods showed very relevant contributions (> 30%) in units of relative abundance in the estuary. In terms of relative biovolume, total decapods were very important in the estuary and in the bay. Decapods contributed on average with 33.6%, 4.4% and 7.1% relative abundance and 30.9%, 30.9%, and 15.2% relative biovolume in the estuary, in the bay, and on the shelf, respectively.

Figure 2. Abiotic conditions: salinity (top), temperature (center) and Secchi depth (bottom) in the three study areas (Rio Formoso estuary, Tamandaré bay, and on the adjacent continental shelf, Pernambuco, Brazil), from June 2013 to May 2015. Blue line: loess smooth, obtained by local polynomial regression fitting (span: 0.75). Gray area: standard error envelope. Asterisk: significant difference between rainy and dry season ($p < 0.05$, M-W test). Dashed lines in lower graph: offshore waters with Secchi depths > 18 m, except for one measurement with Secchi depth = 12 m. Center panel: no significant differences were found between areas. Letters in violplots ("a", "b") indicate similar data sets that did not show significant differences ($p > 0.05$, K-N post-hoc test).

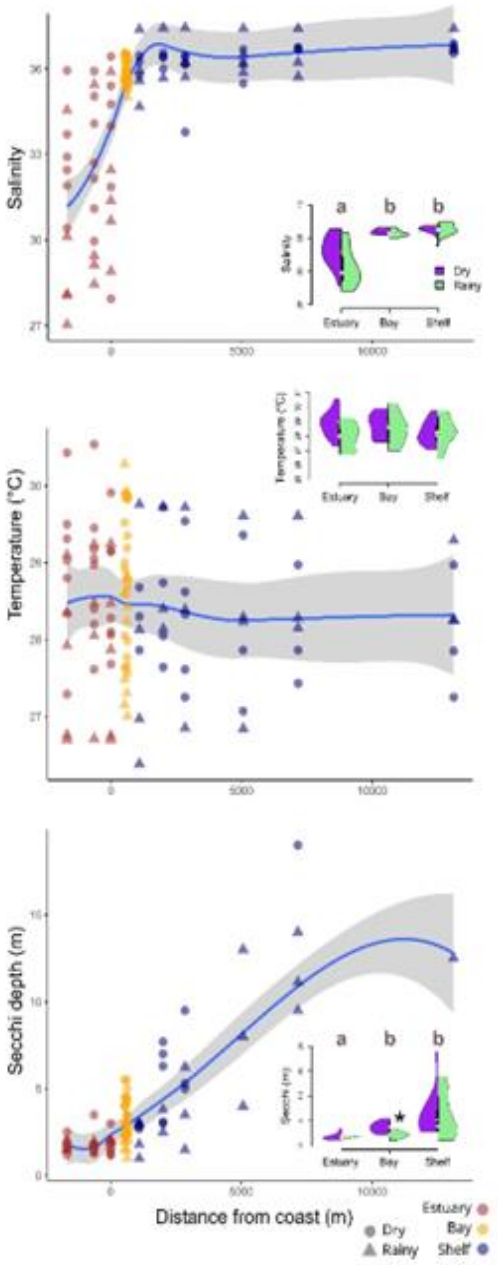

Fonte: A autora (2023)

Twenty decapod crustacean taxonomic categories (taxonomic groups and larval stages) were classified using digital images. Several decapod groups showed considerable contributions in terms of relative abundance and biovolume. Brachyuran zoeae contributed with up to 81.3% abundance (mean: 29.7%) and up to 69% biovolume (mean: 22.7%), in the estuary. Penaeid postlarvae contributed with up to 28.1% of the abundance (mean: 1%) and up to 94.7% of the zooplankton biovolume (mean: 5.9%), on the shelf. Important non-decapod larval groups were fish eggs (up to 41,6% biomass, on the shelf, mean: 5.5%), fish larvae (up to 20,2% biomass, on the shelf, mean: 1%), and cirripedian nauplii. Although cirripedian nauplii were infrequent (and thus were not suitable for subsequent statistical analyses), they did occur in considerable patches and contributed to peaks in meroplankton (up to 40.5% abundance, in the estuary, mean: 2.7%).

For total decapods, there were clear and highly significant differences between the three sampling areas ($p < 0.001$, univariate PERMANOVA, Figs. 3, 4 and 5). Decapod abundance was significantly higher in the estuary ($p < 0.001$, K-N post-hoc test) than in the other two areas (Figs. 2 and 3). Mean decapod abundance in the estuary (656.8 ind. m^{-3}) was higher than that observed in the bay and shelf areas by two orders of magnitude (bay mean: 2.86 ind. m^{-3}; shelf mean: 6.62 ind. m^{-3}).

Total decapod abundance was similar between bay and shelf areas ($p > 0.05$, K-N post-hoc test). No significant differences were detected between seasons, for total decapod abundance, when considering all areas together (e.g., “rainy *vs* dry”, “windy *vs* calm”, “four seasons”, $p > 0.05$, univariate PERMANOVA).

The composition of the planktonic decapod community was highly variable between samples, areas, and months (Fig. 6). The most relevant decapod crustacean taxa and stages (in terms of frequency, abundance and biovolume) found in the three sampling areas, were brachyuran crab zoeae and brachyuran crab megalopae, penaeid shrimp postlarvae (mostly *Penaeus* spp.), holoplanktonic luciferid adults, protozoeae and mysis, anomuran (mostly Paguridae and Diogenidae hermit crabs) zoeae, pistol shrimp (Alpheidae) zoeae, and porcelain crab (Porcellanidae) zoeae (Fig. 6).

Figure 3. Stacked barplots of mean abundance (top) and mean biovolume (bottom) of total zooplankton groups (right) and decapod life history stages (left). Samples were taken bimonthly in the Rio Formoso estuary, in Tamandaré bay, and on the adjacent continental shelf (Pernambuco, Brazil), from June 2013 to May 2015. N: 121 samples. Cop: copepods, Dec: decapods; Fish_L: fish larvae; Fish_E: fish eggs; OTHzoo: other zooplankton; BraZ: brachyuran zoeae; BraM: brachyuran megalopae; PenPL: Penaeidae, postlarvae; AlphZ: Alpheidae, zoeae; PorcZ: Porcellanidae, zoeae; LuciAd: Luciferidae, adult; LuciPZ: Luciferidae, protozoeae; LuciMy: Luciferidae, mysis; AnomZ: Anomura, zoeae; OTHDec: other decapods.

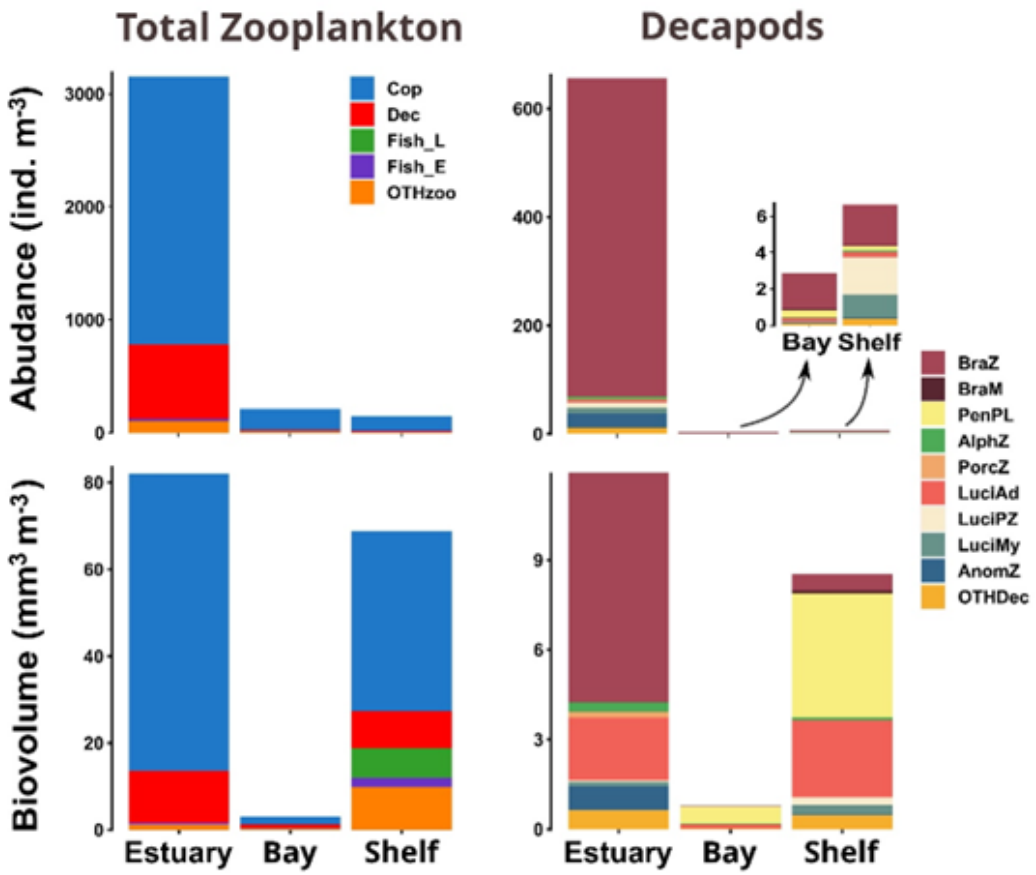

Fonte: A autora (2023)

Figure 4. Spatial patterns of abundance (ind. m^{-3}) and biovolume (mm^3 m^{-3}) of total zooplankton (right) and planktonic decapods (left). Samples were taken bimonthly in the Rio Formoso estuary, in Tamandaré bay, and on the adjacent continental shelf (Pernambuco, Brazil), from June 2013 to May 2015. N: 121 samples. Blue line: loess smooth, obtained by local polynomial regression fitting (span: 0.75). Gray area: standard error envelope. Violin plots ("vioplots") show kernel density distributions with inserted boxplots. White points: medians. Letters in vioplots ("a", "b") indicate similar data sets, without significant differences ($p > 0.05$, K-N post-hoc test). Note the logarithmic scale.

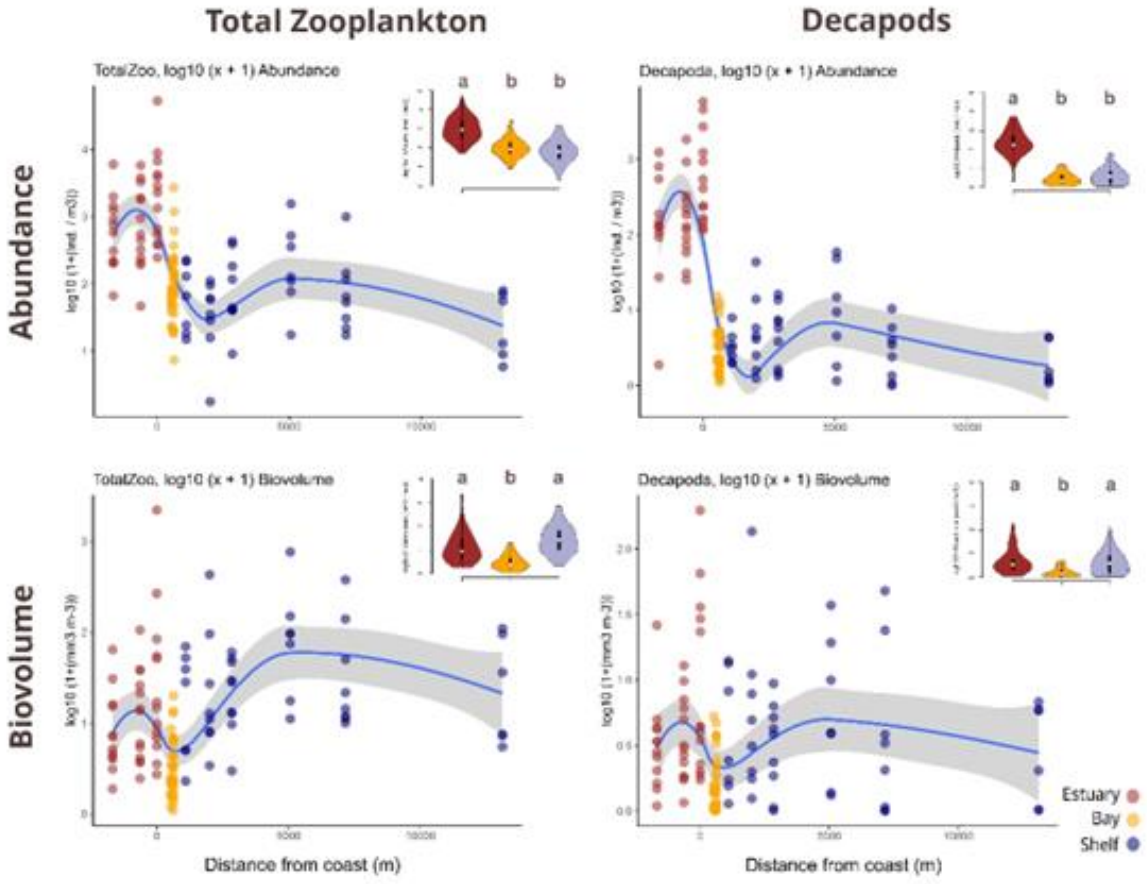

Fonte: A autora (2023).

Figure 5. Spatial patterns of relative abundance (%) and relative biovolume (%) of planktonic decapods, in relation to the total zooplankton. Samples were taken bimonthly in the Rio Formoso estuary, in Tamandaré bay, and on the adjacent continental shelf (Pernambuco, Brazil), from June 2013 to May 2015. N: 121 samples. Blue line: loess smooth, obtained by local polynomial regression fitting (span: 0.75). Gray area: standard error envelope. Violin plots ("vioplots") show kernel density distributions with and inserted boxplots. White points: medians. Letters in vioplots ("a", "b") indicate similar data sets that did not show significant differences ($p > 0.05$, K-N post-hoc test).

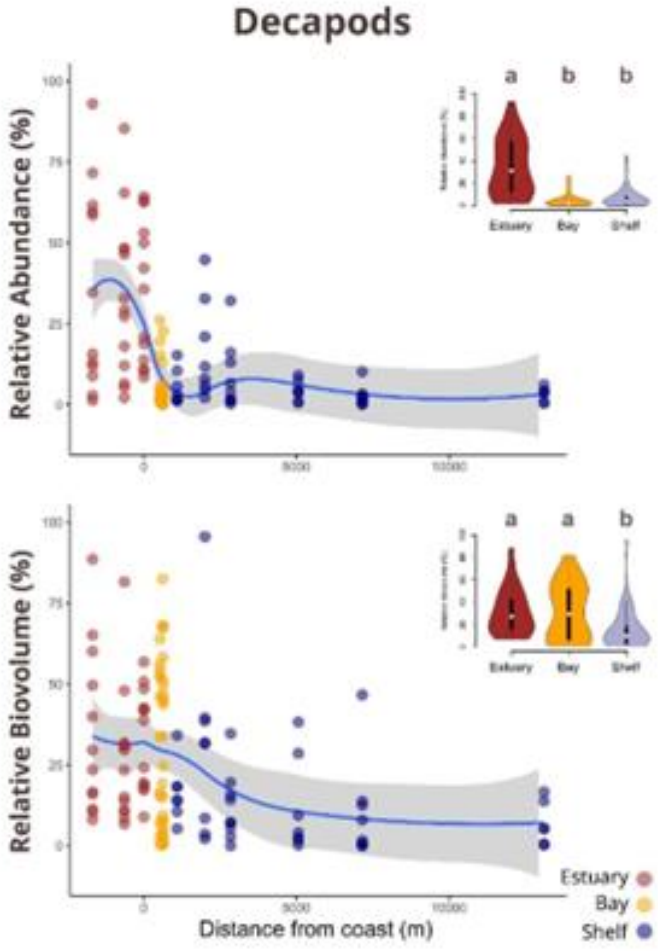

Fonte: A autora (2023).

Figure 6. Variability in relative abundance composition of decapods. Samples were taken bimonthly in the Rio Formoso estuary, in Tamandaré bay, and on the adjacent continental shelf (Pernambuco, Brazil), from June 2013 to May 2015. N: 121 samples. BraZ: brachyuran zoeae; BraM: brachyuran megalopae; PenPL: penaeid shrimp postlarvae; AlphZ: pistol shrimp (Alpheidae) zoeae; PorcZ: porcelain crab (Porcellanidae) zoeae; LuciAd: Luciferidae adults; LuciPZ: Luciferidae, protozoeae; LuciMy: Luciferidae, mysis; AnomZ: Anomura, zoeae; OthDec; other decapods.

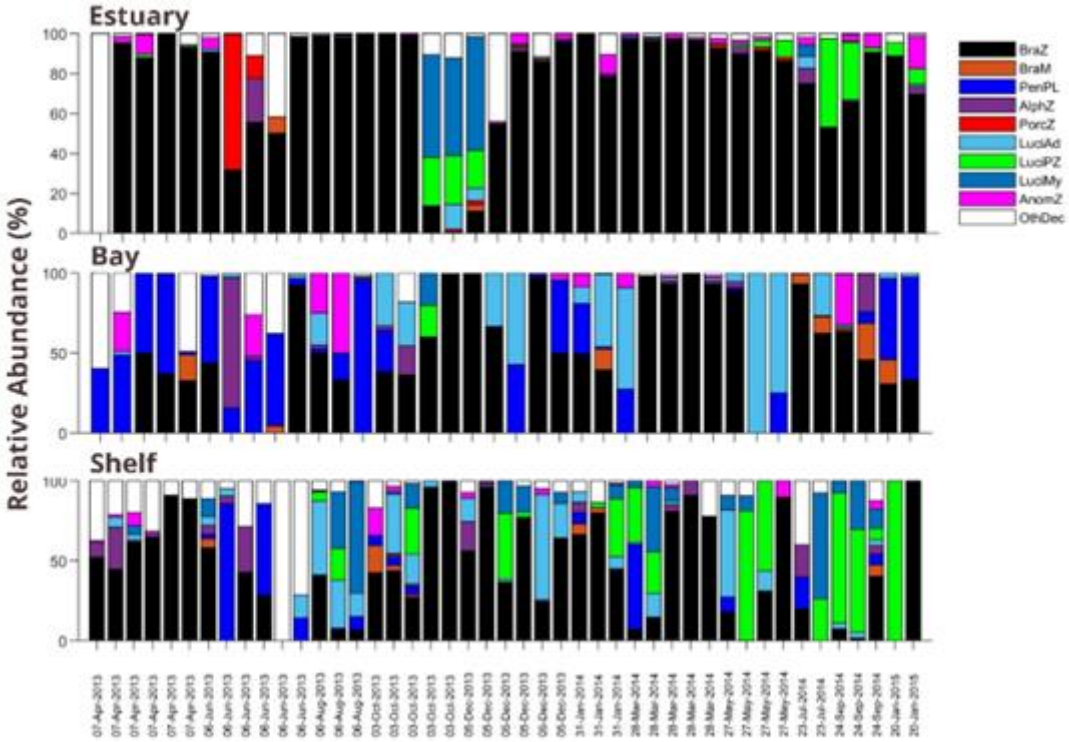

Fonte: A autora (2023)

Figure 7. Vioplots of abundance and biovolume for key planktonic decapods (Brachyuran zoeae and penaeid postlarvae, by area. Letters in vioplots (“a”, “b”, “c”) indicate similar data sets that did not show significant differences ($p > 0.05$, K-N post-hoc test). Samples were taken bimonthly in the Rio Formoso estuary, in Tamandaré bay, and on the adjacent continental shelf (Pernambuco, Brazil), from June 2013 to May 2015. N: 121 samples. Violin plots (“vioplots”) show kernel density distributions with inserted boxplots. White points: medians. Note the logarithmic scale. Brachy. Z.: brachyuran zoeae; Penaeid P.-L.: penaeid postlarvae.

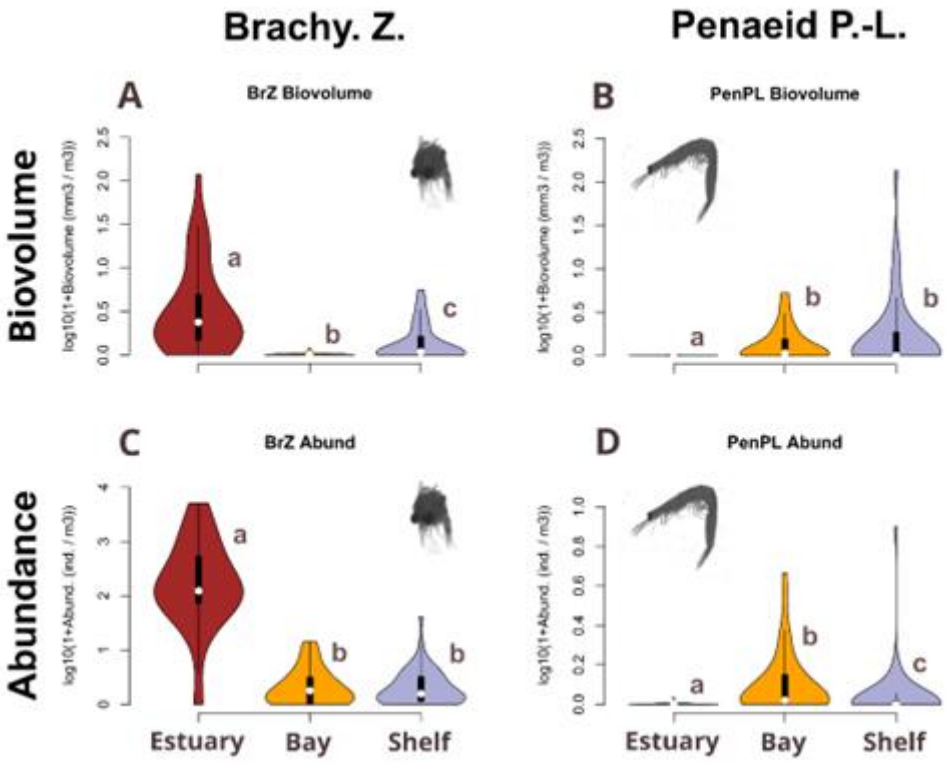

Fonte: A autora (2023).

3.3 Asynchronous seasonal cycles, dispersal and recruitment events of key decapod taxa

Brachyuran crab zoeae were the most important decapods in this study, in terms of frequency of occurrence, abundance, carbon biomass and biovolume, in all three sampling areas. They occurred in all sampling areas throughout the year, with a strong inshore-offshore gradient. Brachyuran zoeal abundance, carbon biomass and biovolume in the estuary were two orders of magnitude higher than in the other two areas (Fig. 7A).

Figure 8. Seasonal patterns of abundance, biovolume, and relative biovolume (%) of total decapods, and total zooplankton biovolume, by sampling month. Samples were taken bimonthly in the Rio Formoso estuary, in Tamandaré bay, and on the adjacent continental shelf (Pernambuco, Brazil), from June 2013 to May 2015. N: 121 samples. Violin plots ("vioplots") show kernel density distributions with inserted boxplots. White points: medians. Note the logarithmic scale in plots A-I. Images not to scale.

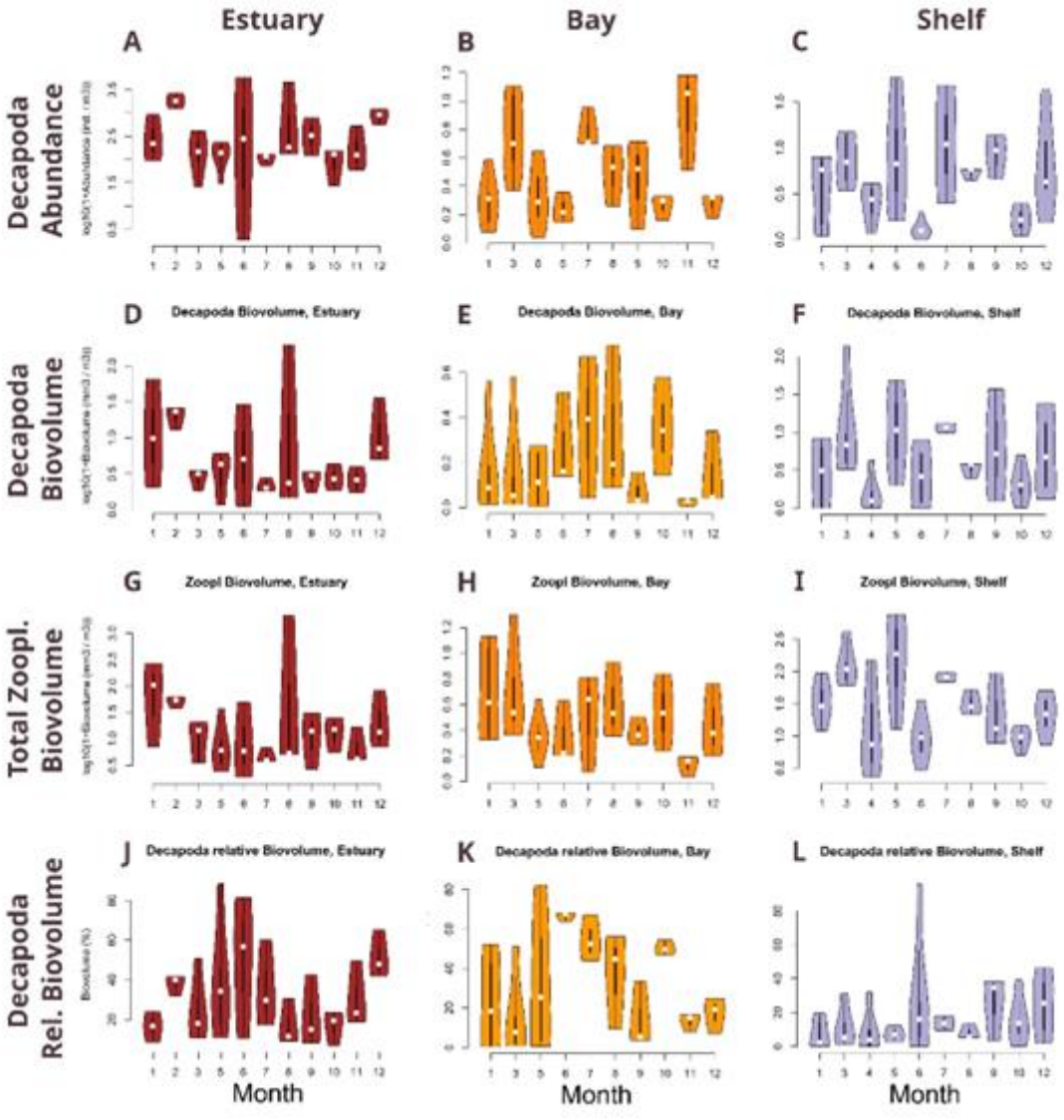

Fonte: A autora (2023).

Figure 9. Seasonal patterns in biovolume (mm³ m^{-3}) of selected taxa. BrZ: Brachyura, zoeae; PorcZ: Porcellanidae, zoeae; PenPL: Penaeidae, postlarvae; LuciAd: Luciferidae, adults; LuciMy: mysis; LuciPZ: protozoeae. Samples were taken bimonthly in the Rio Formoso estuary, in Tamandaré bay, and on the adjacent continental shelf (Pernambuco, Brazil), from June 2013 to May 2015. N: 121 samples. Images ("vignettes") are not to scale. Violin plots ("vioplots") show kernel density distributions with and inserted boxplots. White points: medians. Note the logarithmic scale.

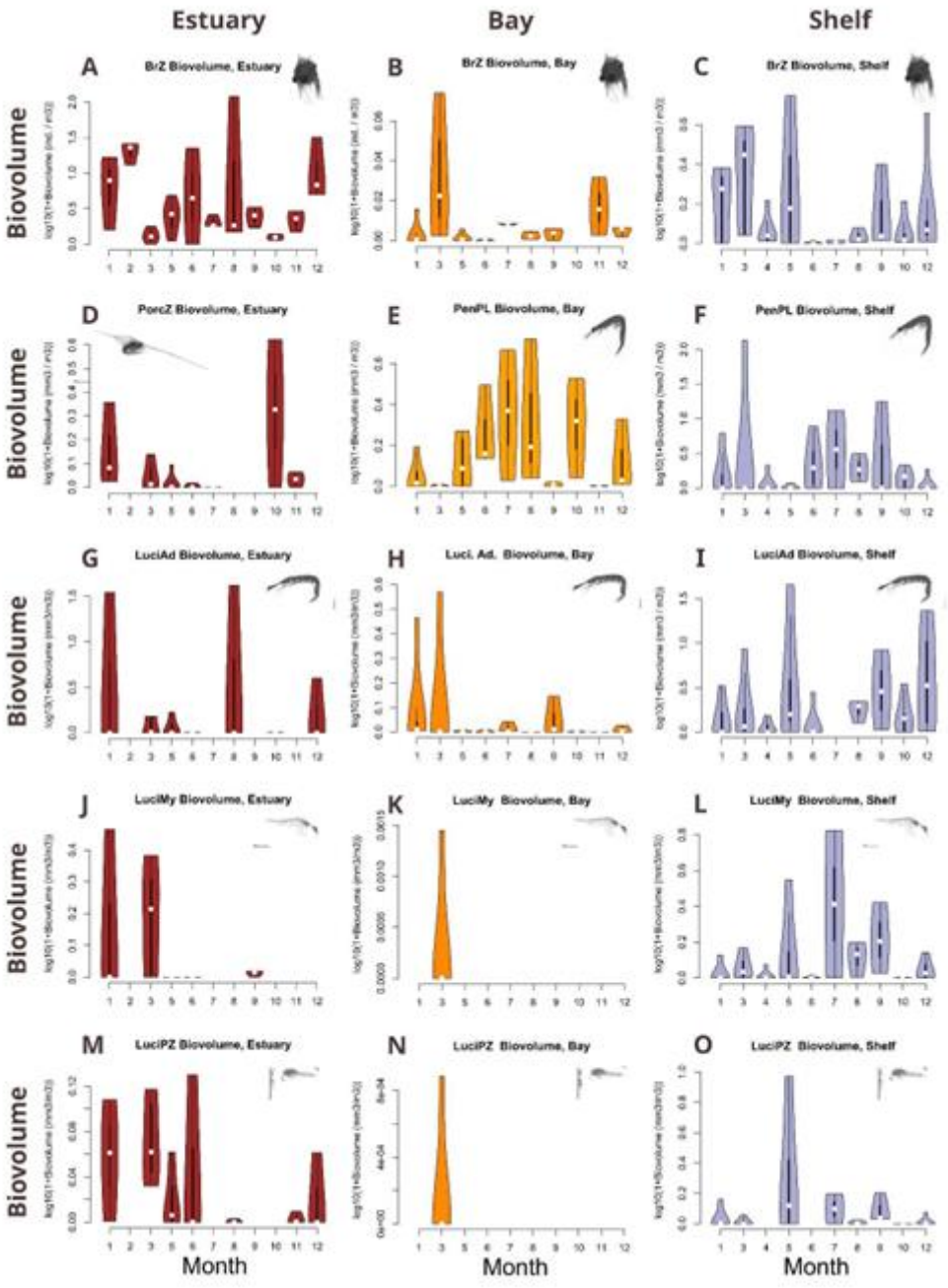

Fonte: A autora (2023).

In the estuary, clear seasonal peaks in abundance and carbon biomass of total decapods (dominated by brachyuran zoeae) were observed in December and in February (late dry season, or peak austral summer, Fig. 8). Brachyuran zoeae occurred in the estuary throughout the year in considerable numbers. However, there were clear, significant peaks in brachyuran crab zoeae in December, January and February (Fig. 9). These peaks coincided with the late dry season, peak austral summer, and less windy months. In the bay and on the shelf, crab zoeae also showed a clear seasonality, since they were observed in very low numbers from June to October (windy season, from peak austral winter to early spring), and showed peaks mainly in the dry season and early rainy season, with a clear maximum in March (onset of the rainy season), in the bay and on the shelf (Fig. 9). Differences in brachyuran zoea biovolume were significant between areas (Fig. 7A) and months (K-W-ANOVA, $p < 0.0001$ and $p = 0.04$, for areas and months, respectively). For each sampling area, differences between months were also significant (K-W-ANOVA, $p = 0.0271$, $p = 0.0053$, $p = 0.0487$ for estuary, bay and shelf, respectively), indicating a relevant seasonality in all sampling areas (Fig. 9).

The seasonal peak in brachyuran zoeae was synchronous with the peak in estuarine copepod biovolume and thus, in total zooplankton biovolume (Fig. 8G). Thus, the relative biovolume contribution (in %) of brachyuran zoeae was less relevant in December, January and February (peak zoeal abundance), increasing on occasions when total zooplankton biovolume in the estuary was lower than average. Brachyuran megalopae (pre-settlement stages) occurred sporadically in all three sampling areas throughout the year, in very low numbers.

Penaeid shrimp postlarvae (pre-settlement stages, mostly *Penaeus* spp.) were the second most important decapod group in this study, in terms of biovolume and biomass, especially on the shelf and in the bay. They were virtually absent in the estuary, except for a few individuals caught in May and September. In contrast to brachyuran zoeae, they occurred in higher numbers and biovolumes in the windy months of the second semester. Peak abundance, carbon biomass and biovolume were found from June to October (Figs. 9E,F). This coincides with the windy season months, from peak rainy season to early dry season, from peak austral winter to early spring, and was asynchronous to the seasonal pattern observed in brachyuran zoeae. In these windy months, penaeid postlarvae contributed considerably to the zooplankton biomass in the oligotrophic bay and shelf ecosystems.

Differences between areas were highly significant ($p < 0.0001$, K-W-ANOVA), except for the pairwise post-hoc comparison between bay and shelf, which did not differ regarding penaeid postlarval biovolume (Fig. 7B). When pooling all areas, seasonal variations were not significant, when using the factors “month” or “dry vs rainy”, but were highly significant ($p =$

0.005, K-W test) for the factor “windy vs calm”, indicating a strong effect of the wind regime in this group, with much higher abundance and biovolume of penaeid postlarvae in the windy season (June to October).

Adults of luciferid holoplanktonic shrimps, (comprising only two species: *Belzebub faxoni* (Borradaile, 1915) and *Lucifer typus* Milne Edwards, 1837), were also very relevant in units of biovolume. These adults occurred in all sampling areas in considerable numbers, with more than tenfold higher average abundance in the estuary (mean, estuary: 4.25 ind m^{-3}; mean, bay: 0.19 ind m^{-3}; mean, shelf: 0.28 ind m^{-3}). In contrast to penaeid postlarvae and brachyuran zoeae, adult luciferids did not present a consistent seasonality in the three sampling areas. However, luciferid larvae showed complex seasonal patterns with conspicuous peaks, with higher numbers in the windy months (June-October) on the shelf, and an asynchronous, inverted pattern (peaks of luciferid larvae in January and March), in the estuary. One unexpected, striking result, was the virtual absence of luciferid larvae (mysis and protozoeae) in the bay, except for one sample in March, with very low numbers (Fig. 9K,N).

Porcellanid zoeae (mostly the estuarine porcelain crab *Petrolisthes armatus* (Gibbes, 1850) occurred almost exclusively in the estuary. They were virtually absent in the bay and at the shelf. In the estuary, they occurred throughout the year, with peaks in January and in October, which are dry season months (Fig. 9D). They were virtually absent from March to September (rainy season and austral winter). Anomuran zoeae (mostly hermit crabs of the families Paguridae and Diogenidae) occurred in all areas throughout the year in considerable numbers, without a conspicuous seasonality. Alpheid pistol shrimp zoeae (Caridea: Alpheidae) also occurred over the whole year in all study areas, with no clear seasonality (Fig. 6). They were considerably more abundant in the estuary than in the other two areas (mean, estuary: 4.63 ind. m^{-3}; mean, bay: 0.06 ind. m^{-3}; mean, shelf: 0.1 ind. m^{-3}).

3.4 Correlation matrices

Correlation matrices revealed numerous significant ($p < 0.05$) Spearman rank correlations (positive and negative) between abiotic and biological variables, and between the total biovolumes (mm^3 m^{-3}) of key zooplankton, ichthyoplankton and decapod taxa.

Correlations between biological variables, salinity and Secchi depths were well within the results expected from the spatial gradients (e.g., brachyuran crab zoeae and porcelain crab zoeae showed negative correlations with salinity and Secchi depths, since both occur predominantly in the estuary). Porcellanid zoeae showed a positive correlation with water

temperature, which can be well explained by their virtual absence, in the estuary, during the colder months (July to September).

Several significant positive correlations were found between biological variables, such as between copepod biovolume and total zooplankton biovolume, for all areas and for each area separately, due to the overall dominance of these holoplanktonic organisms in the zooplankton, in all areas. Also, there were positive correlations between fish eggs and fish larvae, due to synchronous spawning and recruitment seasons in the dry season, in the bay and on the shelf.

Copepod biovolume was positively correlated with brachyuran crab zoeae biovolume, for the whole dataset, with a very high degree of significance ($p < 0.000001$, Spearman rank test, $n = 121$ samples), which was clearly due to the spatially congruent distribution of these two abundant and frequent taxa, that both occur in much higher numbers in the estuary. Similarly, this was also observed on the shelf ($p = 0.0043$, Spearman rank test, $n = 45$ samples from the shelf). When using data from the estuary only, this correlation was also highly significant ($p = 0.0089$, Spearman rank test, $n = 39$ samples from the estuary), with no obvious explanation, except for a functional interrelationship. Thus, the potential relationship between copepods and crab zoeae was further investigated by linear and nonlinear models.

Several decapod taxa had pairwise positive relationships, such as between brachyuran zoeae and porcellanid zoeae, when using data from all areas (since both zoeae occur predominantly in the estuary).

Penaeid postlarvae and crab megalopae showed significant positive correlations, for all data, for the estuary only, and for the continental shelf only, showing a very strong and consistent co-occurrence of these two pre-settlement organisms.

Conversely, penaeid postlarvae (pre-settlement stages) and brachyuran crab zoeae (early life history stages) showed consistently negative correlations, for the whole data set, with crab zoeae being much more abundant in the estuary, and shrimp postlarvae being virtually absent there. This negative correlation was also observed when looking at data in the bay only, which was clearly due to seasonally asynchronous peaks of crab zoeae (peaks in March and November, transition periods), and penaeids (peaks in the windy season).

3.5 Linear models - brachyuran zoeae

For brachyuran zoeae, the most important factor when considering all variables and factors, for a complete data set with all sampling areas, was the spatial factor “Area”, showing the marked differences between areas, specifically, the much higher numbers of crab larvae in the estuary than in the other two areas. The effect of seasonal factors, for crab zoeae, was not significant, when using “months”, “rainy vs dry”, “windy vs calm”. The seasonal factor was significant only when testing seasons using a vector of four seasonal trimesters. This indicates the importance of discrete seasonal peaks in brachyuran zoeae, especially in summer (estuary), spring (bay) and autumn (bay). The best spatio-temporal two-way-ANOVA-like model was obtained with the three factors “Area”, “four seasons”, and the interaction term “Area x four seasons”, all of which were significant ($p < 0.0001$, with ANOVA, $p < 0.05$ with PERMANOVA). Including other variables (e.g. abiotic parameters) into such spatio-temporal ANOVA models hardly brought any improvements.

When looking at correlations only, Spearman Rank correlation tests showed a significant effect of Secchi depth (and salinity) on Brachyuran crab zoeae, for all regions, obviously due to the consistently lower Secchi depth (and lower salinities) in the estuary, and huge abundances and biovolumes of Brachyuran zoeae in the estuary. A very similar spatial covariance was observed for the relationship between crab zoeae, Secchi depth and salinity. When analyzing the three areas separately, there were no relevant relationships between crab zoeae and any abiotic parameters.

3.6 Linear models - penaeid postlarvae

Penaeid shrimp postlarvae were virtually absent in the estuary, but occurred in high biovolumes, over the whole year, in the bay and on the shelf. When considering all areas together, Penaeid shrimp postlarvae were not correlated to any parameters, except for salinity ($p = 0.005$ for biovolume vs salinity, $p = 0.01$ for abundance vs salinity, Spearman rank correlation). This was clearly due to the virtual absence of these organisms in low-salinity estuarine waters.

When analyzing data from the bay only (Fig. 10A), abundance and biovolume of penaeid postlarvae was highly correlated with Secchi depth ($p < 0.00001$ for abundance vs Secchi depth, $p = 0.002$ for biovolume vs Secchi depth, Spearman rank correlation, $n = 21$ samples with Secchi depths). The log-linear model for penaeid PL biovolume *vs* Secchi depth

in the bay (Fig. 10A) was significant (parametric $p = 0.017$, permutation $p = 0.027$, $R^2 = 0.21$, $n = 21$).

This means that they were occurring in higher biovolumes in relatively turbid "green" waters in the bay, during the rainy and windy periods, and in lower biovolumes during the peak dry and calm seasons, when there were extremely transparent "blue" waters (Secchi depth > 4 m) in the bay (Fig. 10A). The remaining taxa investigated did not show any significant correlations with abiotic parameters.

3.7 Linear models - copepods and brachyuran zoeae

Similarly to Spearman rank correlations, linear models were also highly significant for the relationship "copepods *vs* brachyuran crab zoeae", when analyzing all data, for "shelf only" and for "estuary only". In the bay, there was no significant relationship between these two abundant taxa. Models with all data were improved by adding spatial factors and were clearly dominated by spatial covariance (i.e., by the factor "Area"). In a mixed linear model with all samples (n = 121), the factor "Area" explained 12.0 % of the variability, and log (1+x) transformed biovolumes of brachyuran crab zoeae explained 9.5 % of the total variability in log (1+x) transformed copepod biovolumes ("lmg" index, totaling 21.5 % of the variability explained by the model).

The underlying structure of the copepods vs crab zoeae - relationship in the estuary, and on the shelf was not obvious and required a detailed investigation. The basic linear model for $\log_{10}(x+1)$ transformed copepod biovolumes and $\log_{10}(x+1)$ transformed crab zoeae biovolumes from the estuary (Fig. 10C) was highly significant (parametric $p = 0.0058$, permutation $p = 0.0042$ with "aovperm", $R^2 = 0.19$, $n = 38$ samples from the estuary). In contrast to the "All data" and the "shelf only" models, the linear model for "estuary only" was not improved (AIC, BIC, adjusted R^2, and significance of added variables) by adding spatial ("Station") or temporal (months, seasons, etc.) factors or any abiotic variables, or combinations. Instead, adding such factors and variables did only lead to non-significant linear (or non-linear) models. It is actually unsurprising that abiotic variables did not contribute to these models, since the variability in copepod biovolume could not be explained by any abiotic variables in the estuary. When building nonlinear models (GAM), non-parametric effects were not significant ($p > 0.05$), showing that the linear models are better suited than the more complex GAM, to explain this interrelationship. In summary, there was a highly significant positive relationship between copepods and brachyuran zoeae that cannot be explained by spatio-temporal effects or

abiotic variables, and has no other explanation than a functional relationship between these two ecosystem components in the estuary.

A similar result was also found on the shelf, where the linear model for $\log_{10}(x+1)$ transformed copepod biovolumes and $\log_{10}(x+1)$ transformed crab zoeae biovolumes (Fig. 10C) was also significant (parametric $p = 0.01$, permutation $p = 0.01$ with "aovperm", $R^2 = 0.14$, $n = 45$ samples from the shelf). Similarly to the situation found in the estuary, this simple linear model for shelf samples could also not be improved by adding factors and variables or by using a nonlinear (GAM) model.

Figure 10. Log-linear relationships between planktonic decapod (penaeid shrimp postlarvae and brachyuran crab zoeae) biovolumes ($mm^3\ m^{-3}$), total biovolume of copepods, and Secchi depth (m). Only significant linear models ($p < 0.05$) are shown. Samples were taken bimonthly in the Rio Formoso estuary, in Tamandaré bay, and on the adjacent continental shelf (Pernambuco, Brazil), from June 2013 to May 2015. N: 121 samples. Log-linear relationships between total biovolumes of penaeid postlarvae and Secchi depth in the bay (A); total biovolumes of brachyuran zoeae and copepods in the estuary (B); total biovolumes of brachyuran zoeae and copepods on the shelf (C).

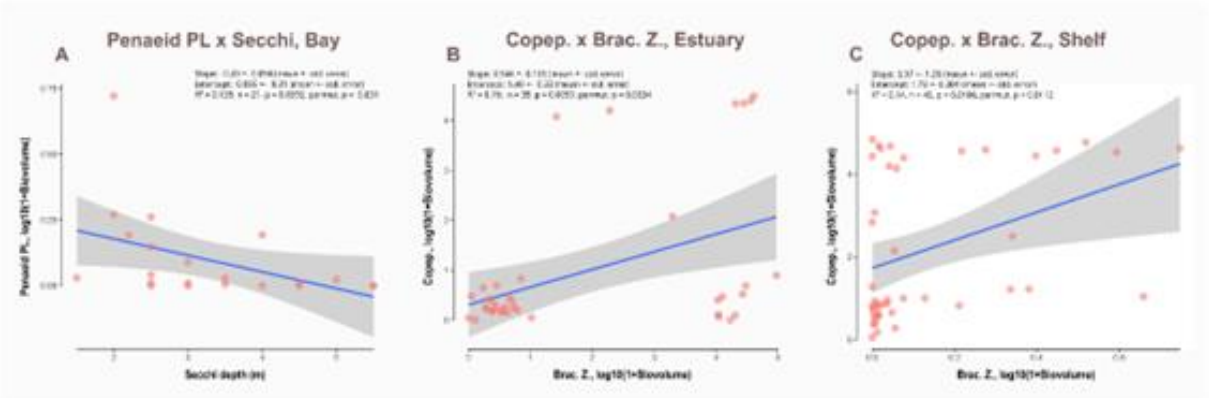

Fonte: A autora (2023).

Figure 11. Redundancy analysis (RDA) plots based on Hellinger-transformed biovolume matrices ($mm^3\ m^{-3}$) of ten planktonic decapod taxa and stages. Only significant ($p < 0.05$) vectors were used in the analyses and plots. Samples were taken bimonthly in the Rio Formoso estuary, in Tamandaré bay, and on the adjacent continental shelf (Pernambuco, Brazil), from June 2013 to May 2015. A: All samples (N: 121 samples), B: Rio Formoso estuary only (N: 38 samples), C: Tamandaré bay only (N: 38 samples).

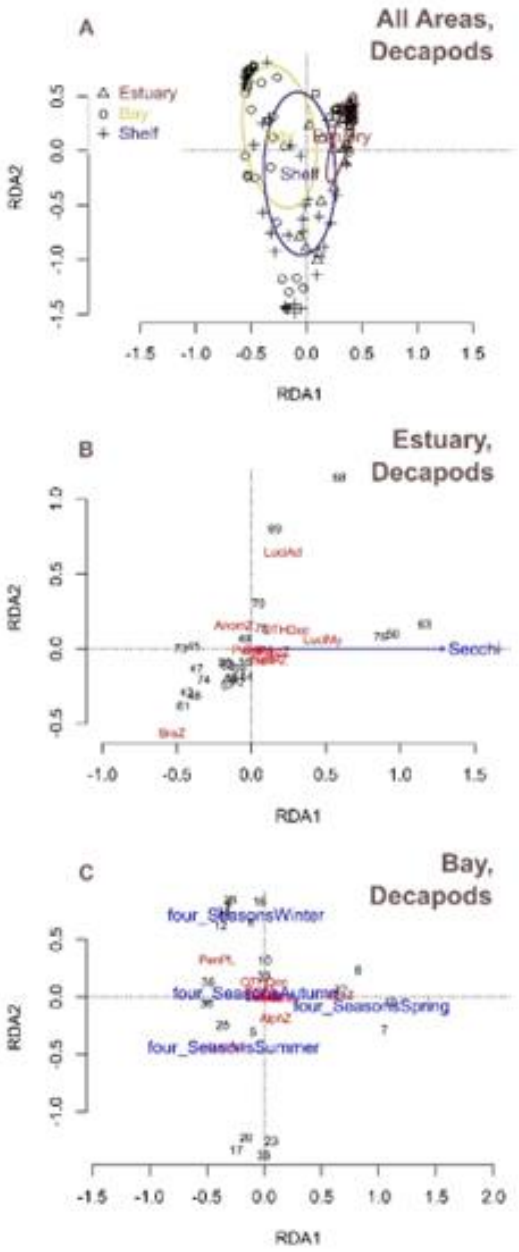

Fonte: A autora (2023)

3.8 Multivariate analyses (RDA, dbRDA and PERMANOVA) - Abiotic variables and space-time factors

The RDA models for all sampling areas (N = 69 samples with complete abiotic factors) were dominated by the factor "Area". This full RDA (Fig 11A) explained 13.4 % of the variability in decapod composition in the first RDA axis (only 2 % were explained by the second RDA axis).

When analyzing the decapod relative biovolume composition in the estuary (N = 24 samples with compete abiotic factors), no significant seasonality was detected, for any temporal factors used (probably because the time series is dominated by only one brachyuran zoeae peak in February). However, there was a significant effect of the factor Secchi depth on the relative biovolume composition of the planktonic decapod community (Fig 11B). Brachyuran zoeae associated to more turbid waters and luciferids (adults and mysis-stage larvae) associated with more transparent waters, in the estuary (Fig 11B).

In the bay (N = 21 samples with complete abiotic factors), seasonality was the key factor in explaining the variability in decapod relative abundance and relative biovolume composition, more specifically, the vector with four discrete seasonal trimesters. For the relative biovolume matrix from the bay, "four seasons" ($p < 0.01$) was the only significant vector. For the relative abundance matrix from the bay, models for "four seasons" only ($p < 0.01$) and salinity only ($p = 0.04$) were significant. The dominance of the vector "four seasons" in explaining decapod variability in the bay (Fig. 11C) can be explained by the conspicuous abundance peaks of penaeids in winter, of luciferid adults in summer, and brachyuran zoeae in autumn and spring (Fig. 10, Fig. 11C). For the shelf (N = 24 samples with complete abiotic factors), the multivariate models were inconclusive for biovolume (no signif. effects). For the decapod relative abundance matrix from the shelf, "Local depth" ($p = 0.025$, multivariate PERMANOVA) was the only significant variable.

3.9 Multivariate analyses (RDA, dbRDA and PERMANOVA) - key space-time factors only

RDA was also conducted using a matrix without abiotic data (121 samples), using only descriptors of space (sampling area, local depth and distance from coast) and time (seasonality vectors: “dry vs rainy”, “windy vs calm”, “four seasons”).

Biovolume

Seasonality vectors “windy vs calm seasons”, “four seasons” and the spatial factors “Area” and “distance from the coast” were useful to explain the variability in decapod biovolume. Complex models with “windy vs calm seasons” ($p = 0.001$), “four seasons” ($p = 0.003$), “Area” ($p = 0.001$) and “distance from the coast” ($p = 0.013$), and the interaction term “four seasons x Area” ($p = 0.010$), were highly significant (multivariate PERMANOVA). Numerous multivariate RDA and dbRDA models with the above-mentioned variables could be built that were highly significant. Surprisingly, the seasonal factor “dry vs rainy” was not significantly related to the variability of the decapod biovolume matrix.

Abundance

Seasonality vectors “windy vs calm seasons”, “four seasons” and the spatial factor “Area” were useful to explain the variability in numbers (decapod abundance). Complex models with “windy vs calm seasons” and “Area”, or “four seasons” and “Area” were highly significant ($p = 0.001$, PERMANOVA). The factors “dry vs rainy” and “distance from the coast” were not significantly related to the variability of the decapod abundance matrix.

4 DISCUSSION

The present study revealed and quantified, for the first time, the ecosystem-shaping impacts of decapods during their seasonal peaks in abundance and biovolume, on estuarine and marine zooplankton. The seasonal peaks (i.e., biomass input events) were clearly asynchronous between taxa and areas (e.g., in January-March for brachyuran crab zoeae and in June-October for penaeid postlarvae). Thus, these massive events (e.g., release of early-stage brachyuran crab larvae in the mangroves and shoreward migration of pre-settlement penaeid shrimp on the shelf) are asynchronous and spatially segregated, having huge impacts on coastal pelagic ecosystems.

4.1 Synchronous reproduction of mangrove crabs - effects on pelagic food webs

Our study revealed a strong variability in decapod larvae, with extremely relevant peaks, especially for brachyuran crab zoeae, which were present in all months, in all sampling areas, thus confirming the "constant reproduction" hypothesis (Hernáez *et al.*, 2012). These crab zoeae are constantly being washed from the estuarine mangrove forests, every month. However, these early-stage larvae occurred in much higher numbers and biomass (characterizing a "massive biomass input event"), when large-sized semi-terrestrial mangrove crabs (*Ucides cordatus* and *Cardisoma guanhumi*) have their unique synchronous reproduction events ("andada"), in austral summer (Botelho *et al.* 2001; Schmidt *et al.*, 2012; Costa and Schwamborn, 2016; Schwamborn and Schwamborn, 2021). This suggests a very strong seasonality in estuarine zooplankton biomass, forced not by abiotic factors, but rather by the precise timing of mangrove crab larval release events. In contrast, studies in subtropical offshore zooplankton revealed a very weak seasonality for highly diverse decapod larval assemblages (Reyns and Sponaugle, 1999; Landeira and Lozano-Soldevilla, 2018).

Hernáez *et al.* (2012) related the peak in reproduction of the ghost shrimp Lepidophthalmus bocourti to the decrease in salinity at the onset of the rainy season in Costa Rican mangroves. Conversely, our study did not relate the brachyuran larval peaks (or any other larval peaks) to any abiotic parameters, probably due to a rigorously and precisely predetermined reproduction calendar, that is manifested in adult crab populations during simultaneous molting and massive migration and mating events, in a series of events that starts several months before the zoeae hatch (Schmidt *et al.*, 2012). Thus, there is no way that the abiotic conditions at the time of hatching can influence this precise larval timing, in a highly dynamic and variable estuarine environment.

Yet, our multivariate analyses (RDA and PERMANOVA) revealed important structuring factors and the importance of four discrete seasonal situations in shaping decapod communities. In the estuary, there was a multivariate structuring gradient related to Secchi depth, from turbid waters that were recently washed from the mangroves, rich in early-stage larvae of mangrove crabs, particles, and mangrove sediments, towards more transparent waters, that were rich in coastal luciferids (adults and mysis-stage larvae). This may seem contradictory, at first sight, to the idea that abiotic conditions are not determining the timing of larval release. However, the observation that samples with less mangrove crab zoeae and more luciferids came from more transparent waters can be well accommodated with the hypothesis of precise larval timing, if one embraces a conceptual mixing model with two endmembers (Brito-Lolaia *et al.*, 2022), where some samples are more "mangrove-related" (more turbid and with more zoeae) and others are more "coastal-related" (less turbid and with more luciferids), within a complex tidally-driven mixture at the estuarine inlet.

A precise lunar and spatial synchrony in the reproduction of the mangrove crab *Ucides cordatus* was reported by Schmidt *et al.* (2012). This large-sized, abundant semi-terrestrial crab spawns in Brazilian mangroves only from January to March, and usually dominates the decapod larval assemblages in these months, in estuarine plumes, together with zoeae-stage larvae of Uca spp. (Schwamborn *et al.*, 2001).

These crabs mate in December to February, at precisely synchronized new moon or full moon nights, depending on which is going to be the maximum tidal amplitude lunar phase in the subsequent month, which is an unprecedentedly precise lunar synchronicity (Schmidt *et al.*, 2012).

Brazilian mangroves harbor a huge biomass of parental crab populations composed of numerous brachyuran species (Coelho *et al.*, 2008), most of which do not have any published information regarding their phenology. A recent study by Lima *et al.* (2021) found that all larval stages (all zoea stages and the megalopa) of the common mangrove crab *Panopeus lacustris* were found throughout the year off northern Brazil, confirming the "continuous reproduction" hypothesis, for this species. The existence of crab species with constant reproduction in the mangroves is also confirmed by our observations. We found a near-constant background of high crab zoeal biomass, and a few massive biomass peaks, that coincide with the hatching period of the large-sized mangrove crab *U. cordatus* that is of great socio-economic relevance for artisanal fisheries. Although the present study did not distinguish brachyuran larvae at species level (this would require the dissection of larval mouthparts), it seems likely that large-

sized, conspicuous mangrove crabs, such as *U. cordatus*, were important in the Rio Formoso estuary, as found in previous studies in this region (Diele, 2000; Schwamborn *et al.*, 2001).

4.2 Shoreward migration of decapod pre-settlement stages - community-shaping events in tropical coastal and shelf ecosystems

Penaeid shrimp postlarvae were the dominant decapods on the shelf, in biomass and biovolume. These zooplanktivorous predators are well known to migrate from the offshore spawning grounds towards coastal and estuarine nurseries, growing and becoming increasingly benthos-associated on the way, with strong vertical migrations (Schwamborn and Criales 2000; Zetina-Rejón *et al.*, 2004). In our study, we showed that these pre-settlement stages enter Tamandaré bay, an oligotrophic reef-lined environment, poor in zooplankton, where they dominate decapod biomass and biovolume. It seems likely that the postlarval peaks found in the windy months, when strong shoreward trade winds usually predominate, are related to an optimized shoreward migration strategy from the offshore shelf towards the coast. Further studies are necessary to investigate the variability in wind and rainfall patterns in the context of ongoing climate change, and how these processes affect the recruitment and dispersal of decapods and other organisms in tropical pelagic ecosystems.

The generally neglected high relative biomass of these voracious zooplanktivores has obvious implications for pelagic food webs, as predators and as an important food source for upper trophic levels. In spite of the very high relative biomass revealed here, and their importance for fisheries, postlarval shrimps have been generally ignored in food web models, with few exceptions (e.g., Zetina-Rejón *et al.*, 2004).

Many studies have investigated penaeid postlarval abundance in situ and documented their wind-driven dispersal patterns in shelf and offshore waters off South Florida, U.S.A. (Criales *et al.*, 2000; 2005; 2011; 2015; Browder *et al.*, 2002; Ogburn *et al.* 2013).

Several studies showed that the two most common penaeid shrimp species at the temperate southern Brazilian coast (*Penaeus brasiliensis* and *P. paulensis*) have asynchronous reproduction cycles. *P. paulensis* is usually highly abundant in summer, and *P. brasiliensis* in autumn (Brisson, 1977; D'Incao, 1991; Albertoni *et al.*, 1999; Lüchmann *et al.*, 2008). For Calazans (1978), and D'Incao (1978, 1983, 1984), winds and rainfall were responsible for the higher densities of penaeid postlarvae at different times in the large-scale Lagoa dos Patos estuary (South Brazil).

Yet, all these investigations of these pre-settlement shrimps were focused on their transport and quantified abundance only, not biomass. The detailed investigations of dispersal patterns of penaeid postlarvae in previous studies had been generally justified by their socio-economic importance, being a key part of the life cycle of important shrimp fisheries stocks. However, the importance as key components of food webs (i.e., their contribution to pelagic ecosystem biomass) had not yet been highlighted in previous studies. This is the first systematic quantification of biomass and relative biomass of penaeid postlarvae and other decapods in estuarine and coastal marine ecosystems.

Very few studies have been dedicated to the study of brachyuran crab megalopae sampled *in situ*. Similarly to our results, considerable patches of high abundance ("blooms") of megalopae of the mangrove crab *Panopeus lacustri*s were detected by de Lima *et al.* (2021) at the offshore shelf off Northern Brazil. In our study, penaeid postlarvae and crab megalopae showed significant positive correlations, for all data, for data for the estuary only, and for the shelf data only. Thus, our unprecedented comparison revealed very strong and consistent patterns of co-occurrence of these two pre-settlement organisms. This indicates congruent optimized shoreward transport, and similar settlement and recruitment strategies for both taxa.

4.3 Life-history dynamics of holoplanktonic decapods

One of the main characteristics of the Luciferidae is their holoplanktonic life history. They are found along the entire Brazilian coast and many other tropical and subtropical regions. There are seven recognized species in this family (Vereshchaka *et al.*, 2016), of which only two occur in the study area: *Lucifer typus* Milne-Edwards, 1837 and *Belzebub faxoni* (Borradaile, 1915). Similarly to our results, many studies have shown very high numbers of larvae and adults of these holoplanktonic decapods in estuarine coastal, shelf and offshore waters, highlighting their huge importance for tropical pelagic food webs (Longhurst and Pauly, 1987; D´Incao, 1997; Schwamborn *et al.*,1999; Melo *et al.*, 2014; Santana *et al.*, 2020). In these previous studies, *Lucifer typus* Milne-Edwards, 1837, was generally found in more offshore oceanic waters, with very high and constant salinity. Conversely, *Belzebub faxoni* (Borradaile, 1915) has a more nearshore distribution in estuarine, coastal and shelf waters. At the mouth of the Amazon River, on the North Brazilian shelf and adjacent large-scale oceanic plume retroflection, *Belzebub faxoni* is exported far offshore and plays an essential role in tropical neritic and oceanic zooplankton (Melo *et al.*, 2014; Neumann-Leitão *et al.*, 2018; Santana *et*

al., 2020. In the Amazon plume region off northern Brazil, both *B. faxoni* and *L. typus* were abundant in most neritic samples, even very far offshore (Melo *et al.*, 2014).

A “constant oceanic ecosystem” pattern was observed by Landeira and Soldevilla (2018) in the subtropical waters off Gran Canaria, where *Lucifer typus* Milne-Edwards, 1837 was present throughout the year. In our study, the presence of adult individuals of Luciferidae in all areas showed the contribution of significant numbers of these holopelagic decapods in all months, and all areas, with very important contributions in abundance and especially in biomass. Yet, our data indicate that luciferid larvae exhibit complex spatio-temporal patterns, with asynchronous peaks on the shelf and in the estuary, possibly due to different dispersal and retention strategies in these areas, or due to the existence of two species with different spatial and temporal distribution patterns. However, both species are morphologically indistinguishable in their early larval forms, even for a taxonomist dissecting them under the microscope.

4.4 Asynchronous biomass inputs from decapod life history cycles - retention and dispersal strategies and their effects on pelagic food webs

Our study revealed seasonal peaks (i.e., biomass input events), which were clearly asynchronous between taxa and areas (e.g., in January-March for brachyuran crab zoeae in the estuary and in June-October for penaeid postlarvae in the bay and on the shelf). Both are probably related to optimized retention, dispersal and transport strategies, which differ between life history stages, taxonomic groups, and geographic areas. We documented the larvae that were exported from the hyper-eutrophic estuary, and the shoreward migrating pre-settlement stages on the oligotrophic continental shelf. These were two very different situations in the life histories of these organisms, within two distinct ecosystems.

Larval export from estuaries to adjacent marine areas seems to be an effective solution for gene dispersal, to avoid competition for space, osmoregulation stress (in view of the low salinity of estuaries) and to flee the extremely high predation pressure that may occur, especially on young, small larvae (Morgan, 1989). Coping with predation is a key factor for these small organisms, in oligotrophic, nutrient-rich mangrove estuaries that are rich in phytoplankton and other food particles (Silva *et al.*, 2019), but also rich in pelagic predators, such as sardines and anchovies (Ooi and Chong 2011; Castellanos-Galindo *et al.*, 2013; Amin *et al.*, 2019), and

young stages of numerous fish species (Sheridan and Hays, 2003; Blaber, 2007; Whitfield, 2017).

The extremely high predation pressure on zooplankters in estuarine environments may also have another unexpected consequence, regarding the distribution of copepods and brachyuran zoeae, or more specifically, regarding the impacts of crab larval release events on copepods. Adding decapods to the water column dramatically increased the total zooplankton abundance, biomass and biovolume. This additive effect was especially strong and significant during synchronous massive larval release events of zoea-stage crab larvae in February-March, in the estuary, but also on the shelf. Surprisingly, there was not only an additive effect of crab zoeae to the total zooplankton biomass, but we also detected a functional relationship between small-sized larvae (zoeae) and holoplankton (copepods), that is mediated through key physical and trophic processes, such as patchiness and trophic cascades. These highly significant positive correlations between crab zoeae and copepods in the estuary and on the shelf may be the result of small-scale patchiness effects (accumulation of surface-dwelling organisms at small-scale aggregations, especially at convergence zones and fronts). However, such an aggregation would have led to positive correlations with many other surface-dwelling organisms. Thus, the observed strong and significant correlations are most likely also mediated through trophic cascades. One likely explanation for this phenomenon is an increase in prey availability for zooplanktivores and subsequently reduced predation mortality for copepods in the estuary during peak brachyuran zoea larval release events in the mangroves, which could be advantageous for both taxa. Actually, both explanations (patchiness or reduced predation) are not contradictory at all, but rather complementary, since accumulation in patches that are rich in brachyuran zoea may be advantageous for copepods (in comparison with patches without brachyuran zoeae), with regard to predation avoidance (Johnson and Shanks 2003). Conversely, the results obtained by the experiments of Schwamborn *et al.* (2006) indicate that crab zoeae may feed effectively on several types of organisms and particles, including adult copepods, which would suggest a negative (prey-predator) relationship between these two taxonomic groups.

Our study quantified the contribution of mangrove ecosystems to the zooplankton, in terms of decapod larval biomass (especially brachyuran zoeae), that fuel the seasonal dynamics of pelagic food webs, thus contributing to our knowledge on tropical estuarine and marine ecosystems.

4.5 Advantages and limitations of the ZooScan for the study of decapods

In this study, semi-automated analyses based on digital images proved to be useful to investigate planktonic decapods. Relative biovolume or biomass composition is a key descriptor of the importance of a species or species group within the food web. It describes the composition of the food available to pelagic predators and filter feeders within the energy and matter flows in the ecosystem. These are key input data for any quantitative trophic model, urgently needed for reliable ecosystem predictions (Pauly *et al.*, 2000). Also, the biovolume or biomass relative composition can be used to predict the trophic level of an ecosystem (Brito-Lolaia *et al.*, 2022).

However, images were generally only informative enough to identify decapods to infraorder or family level, since an identification to species and exact larval stage (e.g, zoea I, II, II, …) would require the time-consuming and complex dissection of setae on mouthparts of all organisms under a microscope. These are extremely delicate and time-consuming procedures that can only be performed by experienced taxonomists, and will provide abundance data only. This has been the standard approach for the study of planktonic decapods up to now (Schwamborn, 1999; Santana *et al.*, 2018; Da Silva *et al.*, 2021). It is important to note, however, that even for experienced taxonomists who specialized on these larval organisms, identification to species level is absolutely not possible for many of the larval decapods sampled here, since larval descriptions and identification keys for decapod larvae are available for only few among the thousands of extant species (Anger, 2001; Schwamborn, 2001, 2002).

Another important issue of taxonomic identification under the microscope is that within a time series, the subjective and arbitrary identification of larvae by many different laboratory technicians and students with varying levels of skill and willingness to dedicate time and effort to dissect and describe mouthparts and other larval structures, will inevitably lead to serious artifacts in the data matrices (Highfield *et al.*, 2010). Even when all samples are analyzed and identified by one taxonomist only, the increasing identification skill during the analysis of a time series will obviously also lead to artifacts. Most seriously, these identifications cannot be verified and cross-checked afterwards, since many organisms are completely destroyed during dissection. Thus, one important advantage of the non-destructive ZooScan approach is that it permits the preservation of all complete zooplankton samples in formalin, without destroying, removing, or any other modifications of these extremely valuable archival treasures. Most importantly, scanning these samples with a ZooScan generates databases and digital archives

of images (vignettes) that can be readily accessed, cross-checked and validated as often as necessary, by many different specialists. Thus, the ZooScan approach considerably improves the issues related to subjectivity and lack of consistency in identification, especially when combining specialist knowledge with classification algorithms, as in the present study.

Another alternative for taxonomic identification is the use of molecular techniques, such as DNA barcoding, but up to now, no published study has been able to demonstrate this efficiently for the whole decapod community yet. This technique was recently used for the study of brachyuran crab larvae (Brandão *et al.*, 2016), and to study the larvae of a single shrimp species (Landeira *et al.*, 2019). As a drawback, most DNA barcoding techniques do not provide information on life history stage (e.g., zoea I, II, III, …, megalopa, postlarvae, juveniles, adults) nor any quantitative estimates of abundance, biomass or biovolume.

Image processing systems such as ZooScan also have a number of intrinsic limitations, such as their relatively low taxonomic refinement and accuracy, and the impossibility to dissect mouthparts and appendages. In the step of sampling and sample processing, one serious drawback of this approach is the loss of fragile structures, and the destruction of aggregates and delicate organisms, such as gelatinous taxa (e.g., ctenophores). *In situ* imaging systems (such as the VPR, LOKI, and UVP, Lombard *et al.*, 2019) do not destroy particles and organisms, but their image quality is much lower than in laboratory bench systems, such as the ZooScan, often impeding any useful identification. An in-depth comparison of available imaging systems, their advantages and limitations, was recently provided by Lombard *et al.* (2019).

Our study revealed and quantified new, unexpected phenomena in tropical coastal ecosystems, such as the relevant inputs of brachyuran zoeae and penaeid shrimp postlarvae in terms of biomass and biovolume. The practical and simple approach presented here paves the path towards standardized quantitative analysis of decapod larval contributions to the zooplankton biomass. In the future, a combination of microscopy, DNA barcoding, and ZooScan analysis may become standard for a complete evaluation of the zooplankton.

REFERENCES

Albertoni, E.F., Palma-Silva, C., Esteves, F.D.A., 1999. Larvae and postlarvae of Penaeidae and Palaemonidae in coastal lagoons of the north of Rio de Janeiro (Macaé, RJ). Rev. Bras. Biol. 59, 109-117. https://doi.org/10.1590/S0034-71081999000100014.

Alcaraz, M., Saiz, E., Calbet, A., Trepat, I., Broglio, E., 2003. Estimating zooplankton biomass through image analysis. Mar. Biol. 143, 307-315. https://doi.org/10.1007/s00227-003-1094-8

Almeida, A.O.D., Bohs, G., Silva, C.D.L. A., Bezerra, L.E.A., 2012. Shallow-water caridean shrimps from southern Bahia, Brazil, including the first record of *Sinalpheus ul* (Rios and Duffy, 2007) in the southwestern Atlantic Ocean. Zootaxa 3347, 1–35.

Almeida, A.O.D., Coelho, P.A., Santos, J.T.A.D., Ferraz, N.R, 2006. Crustáceos decápodos estuarinos de Ilhéus, Bahia, Brasil. Biota Neotrop. 6(2). https://doi.org/10.1590/S1676-06032006000200024

Almeida, A.O., Souza, G.B., Boehs, G., Bezerra, L.E.A. (2010). Shallow-water anomuran and brachyuran crabs (Crustacea: Decapoda) from southern Bahia, Brazil. Lat. Am. J. Aquat. Res. 38, 329–376. https://doi.org/10.3856/vol38-issue3-fulltext-2.

Amin, S., Azmir, I.A., Esa, Y., Yasin, I.S.M., Ara, R., 2019. A snapshot study on larval fish diversity in selected mangrove areas of Peninsular Malaysia, Malaysia. Journal of Academia, 7(2), 112-123. https://doi.org/10.13057/biodiv/d220250.

Anderson, M.J., 2017. Permutational Multivariate Analysis of Variance (PERMANOVA). In Wiley StatsRef: Statistics Reference Online (eds N. Balakrishnan, T. Colton, B. Everitt, W. Piegorsch, F. Ruggeri and J.L. Teugels). https://doi.org/10.1002/9781118445112.stat07841.

Anger, K., 2001. The biology of decapod crustacean larvae. Crustacean Issues 14, 1-420. Lisse, A. A. Balkema Publishers.

Barnes, H., 1957. Processes of restoration and synchronization in marine ecology. The spring diatom increase and the spawning of the common barnacle *Balanus balanoides* (L.). Année biol. 33, 67-85.

Binggeli, C., Waring, A., Mihuc, T., 2011. Methods for Determining New Biovolumes for Copepods and Cladocerans. Plattsburgh State University of New York.http://hdl.handle.net/1951/70021.

Blaber, S.J., 2007. Mangroves and fishes: issues of diversity, dependence, and dogma. Bull. Mar. Sci. 80, 457-472.

Botelho, E.R.O., Santos, M.C.F., Souza, J.R.B., 2001. Aspectos populacionais do guaiamum, Cardisoma guanhumi Latreille, 1825, do estuário do rio Una (Pernambuco – Brasil). Boletim Técnico Científico do CEPENE 9, 123-46.

Brandão, M.C., Garcia, C.A.E., Freire, A.S., 2015. Large-scale spatial variability of decapod and stomatopod larvae along the South Brazil shelf. Cont. Shelf Res. 107, 11-23. https://doi.org/10.1016/j.csr.2015.07.012.

Brandão, M.C., Freire, A.S., Burton, R.S., 2016. Estimating diversity of crabs (Decapoda: Brachyura) in a no-take marine protected area of the SW Atlantic coast through DNA barcoding of larvae. Systematics and Biodiversity 14, 288-302. https://doi.org/10.1080/14772000.2016.1140245.

Breiman, L., 2001. Random forests. Machine Learning, 45, 5–32. doi: 10.1023/A:1010933404324

Brisson, S., 1977. Estudo da população de peneídeos na área de Cabo Frio. 11. Distribuição sazonal de pós-larvas de camarão-rosa (*P. brasiliensis* e *P. paulensis*) na entrada de canal da laguna de Araruama-Cabo Frio-RJ-BR. Publ. lnst. Pesp. Marinha. 101, 1-20.

Brito-Lolaia, M., Figueiredo, G.G.A.A., Neumann-Leitão, S., Yogui, G.T., Schwamborn, R., 2022. Can the stable isotope variability in a zooplankton time series be explained by its key species? Mar. Environ. Res. 181, 105737. https://doi.org/10.1016/j.marenvres.2022.105737.

Browder, J.A., Zein-Eldin, Z., Criales, M.M., Robblee, M.B., Wong, S., Jackson, T.L., Johnson, D., 2002. Dynamics of pink shrimp *(Farfantepenaeus duorarum*) recruitment potential in relation to salinity and temperature in Florida bay. Estuaries 25, 1355-1371.

Calazans, D.K., 1978. Penetração das post-larvas do "camarão-rosa" (*Penaeus paulensis*) no estuário da Lagoa dos Patos, RS, Brasil. V Simpósio Latinoamericano sobre Oceanografia Biológica. São Paulo, 125-126 (Resumos).

Camargo, J.M.R., Araújo, T.C.M., Maida, M., Ushizima,T.M., 2007. Morfologia da plataforma continental interna adjacente ao município de Tamandaré, sul de Pernambuco – Brasil. Rev. Bras. Geof. 25(1) São Paulo. https://doi.org/10.1590/S0102-261X2007000500008.

Castellanos-Galindo, G.A., Krumme, U., Rubio, E.A., Saint-Paul, U., 2013. Spatial variability of mangrove fish assemblage composition in the tropical eastern Pacific Ocean. Rev. Fish. Biol. Fisher. 23, 69-86. https://doi.org/10.1007/s11160-012-9276-4.

Coelho, P.A., Alemida, A.O., Bezerra, L. E. A., 2008. Checklist of the marine and estuarine Brachyura (Crustacea: Decapoda) of northern and northeastern Brazil. Zootaxa 1956, 1-58.

Colas, F., Tardivel, M., Perchoc, J., Lunven, M., Forest, B., Guyader, G., Danielou, M.M., Le Mestre, S., Bourriau, P., Antajan, E.,Sourisseau M., Huret, M., Petitgas, P., M., Romagnan, J.

B., 2018. The zoocam, a new in-flow imaging system for fast onboard counting, sizing and classification of fish eggs and metazooplankton. Prog. Oceanogr. 166, 54-65. https://doi.org/10.1016/j.pocean.2017.10.014.

Costa, D.F.M., Schwamborn, R., 2016. Biologia populacional e ecologia trófica de *Cardisoma guanhumi* Latreille, 1825 em um manguezal de acesso restrito em Itamaracá, Pernambuco, Brasil. Tropical Oceanography (Online) 44, 89-105.

Criales, M.M., Cherubin, L.M., Browder, J.A., 2015. Modeling larval transport and settlement of pink shrimp in South Florida: dynamics of behavior and tides. Mar. Coast. Fish. 7(1), 148-176. https://doi.org/10.1080/19425120.2014.1001541.

Criales, M. M., Bello, M.J., Yeung, C., 2000. Diversity and recruitment of penaeoid shrimps (Crustacea: decapoda) at Bear Cut, Biscayne bay, Florida, USA. Bull. Mar. Sci. 67(2), 773-788.

Criales, M.M., Wang, J., Browder, J.A., Robblee, M.B., 2005. Tidal and seasonal effects on transport of pink shrimp postlarvae. Mar. Ecol. Prog. Ser. 286, 231-238. https://doi.org/doi:10.3354/meps286231.

Criales, M.M., Zink, I.C., Browder, J.A., Jackson, T.L., 2011. The effect of acclimation salinity and age on the salinity tolerance of pink shrimp postlarvae. J. Exp. Mar. Biol. Ecol. 409, 283-289. https://doi.org/10.1016/j.jembe.2011.09.007.

Crisp, D.J., 1962. Release of larvae by barnacles in response to the available food supply. Anim. Behav. 10, 382-383.

Dai, L., Li, C., Yang G., Sun, X., 2016. Zooplankton abundance, biovolume and size spectra at western boundary currents in the subtropical North Pacific during winter 2012. J. Mar. Syst. 155, 73-83, ISSN 0924-7963. https://doi.org/10.1016/j.jmarsys.2015.11.004.

Dai, L., Tao, Z.,Yang, G.,Wang, X., Zhu, M., 2017. Zooplankton abundance, bio-volume and size spectra down to 3000m depth in the western tropical North Pacific during autumn 2014. Deep Sea Res. Part I Oceanogr. Res. Pap. 121,1– 13. http://dx.doi.org/10.1016/j.dsr.2016.12.015.

Da Silva, L.S., Cavalcante-Braga, D. V., Lourenço, C.B., Schwamborn, R., Martinelli-Lemos, J.M., 2021. Factors affecting the seasonal variability of planktonic shrimps (Dendrobranchiata) along an estuary–ocean gradient on the Amazon continental shelf. J. Mar. Biol. Assoc. U.K. 101(2), 331-342. https://doi.org/10.1017/S0025315421000308.

Diele, K., 2000. Life history and population structure of the exploited mangrove crab Ucides cordatus cordatus (Decapoda: Brachyura) in the Caete Estuary, North Brazil. (PhD thesis). Universität Bremen, Bremen, Germany. http://researchrepository.napier.ac.uk/id/eprint/6575

D'Incao, F., 1978. Curva de crescimento do “camarão-rosa” (*Penaeus paulensis* Pérez Farfante, 1967) na lagoa dos Patos,RS, Brasil. Atlântica 3, 75-78.

D'Incao, F., 1983. Estudo do crescimento e da mortalidade de *Penaeus (Farfantepenaeus) paulensis* Pérez Farfante,1967, na Lagoa dos Patos, RS, Brasil. Porto Alegre, Univ. Fed. do Rio Grande do Sul, 122p. (Dissertação de Mestrado).

D'Incao, F., 1984. Estudo sobre o crescimento de *Penaeus (Farfantepenaeus) paulensis* Pérez Farfante, 1967 da Lagoa dos Patos, RS, Brasil. (Decapoda, Penaeidae). Atlântica 7, 73-84.

D'Incao, F., 1991. Pesca e biologia de *Penaeus paulensis* na Lagoa dos Patos, RS. Atlântica 13(1), 159-169.

D'incao, F., 1997. Espécies do gênero *Lucifer* Thompson, 1829 no litoral brasileiro (Decapoda: Luciferidae). Nauplius 5(2),139-145.

Domingues, E.D.C., Schettini, C.A.F., Truccolo, E.C., Oliveira, J.C.D., 2017. Hydrography and currents on the Pernambuco Continental shelf. Rbrh, 22. https://doi.org/10.1590/2318-0331.0217170027.

Duarte, R.X., 1993. Mapeamento do quaternário costeiro do extremo sul de Pernambuco: Área 05 – Tamandaré. Relatório apresentado à graduação do curso de Geologia da Universidade Federal de Pernambuco. Recife, 86p.

Epifanio, C.E., Garvine, R.W., 2001. Larval transport on the Atlantic continental shelf of North America: a review. Estuar. Coast. Shelf S. 52(1), 51-77. https://doi.org/10.1006/ecss.2000.0727.

Frossard, J., Renaud, O., 2021. Permutation tests for regression, ANOVA, and comparison of signals: the permuco package. Journal of Statistical Software, 99, 1-32. https://doi: 10.18637/jss.v099.i15.

García-Comas, C., Stemmann, L., Ibanez, F., Berline, L., Mazzocchi, M.G., Gasparini, S., Picheral M., Gorsky, G., 2011. Zooplankton long-term changes in the NW Mediterranean Sea: Decadal periodicity forced by winter hydrographic conditions related to large-scale atmospheric changes? J. Mar. Syst. 8, 216–226. https://doi.org/10.1016/j.jmarsys.2011.04.003.

González-Gordillo, J.I., Rodríguez, A., 2003. Comparative seasonal and spatial distribution of decapod larvae assemblages in three coastal zones off the south-western Iberian Peninsula. Acta Oecologica, 24, S219-S233.https://doi.org/10.1016/S1146-609X(03)00032-8.

Gorsky, G., Ohman, M.D., Picheral, M., Gasparini, S., Stemmann, L., Romagnan, J.B., Cawood, A., Prejger, F., 2010. Digital zooplankton image analysis using the ZooScan integrated system. Journal of plankton research, 32(3), 285-303. https://doi.org/10.1093/plankt/fbp124.

Grömping, U., 2007. Relative importance for linear regression in R: the package relaimpo. Journal of statistical software 17, 1-27. https://doi.org/10.18637/jss.v017.i01.

Hastie, T. J.,Tibshirani, R. J., 1990. Generalized Additive Models, New York: Chapman and Hall.

Hernáez, P., Villegas-Jiménez, E., Villalobos-Rojas, F., Wehrtmann, I.S., 2012. Reproductive biology of the ghost shrimp *Lepidophthalmus bocourti* (A. Milne-Edwards, 1870) (Decapoda: Axiidea: Callianassidae): a tropical species with a seasonal reproduction. Marine Biology Research *8*(7), 635-643. https://doi.org/10.1080/17451000.2011.653369.

Highfield, J.M., Eloire, D., Conway, D.V., Lindeque, P.K., Attrill, M.J., Somerfield, P.J., 2010. Seasonal dynamics of meroplankton assemblages at station L4. Journal of plankton research *32*(5), 681-691. https://doi.org/10.1093/plankt/fbp139.

Hillebrand, H., Dürselen, C.D., Kirschtel, D., Pollingher, U., Zohary, T., 1999. Biovolume calculation for pelagic and benthic microalgae. J. Phycol. 35, 403-424. https://doi.org/10.1046/j.1529-8817.1999.3520403.x.

Ibarbalz, F.M., Henry, N., Brandão, M.C., Martini, S., Busseni, G., Byrne, H., Coelho, L.P., Endo, H., Gasol, J.M., …; Zinger, L., 2019. Global trends in marine plankton diversity across kingdoms of life. Cell *179*(5), 1084-1097. https://doi.org/10.1016/j.cell.2019.10.008.

ICMBIO : https://www.icmbio.gov.br/apacostadoscorais/ Accessed in 29/10/2010.

Johnson, K. B., Shanks, A. L., 2003. Low rates of predation on planktonic marine invertebrate larvae. Mar. Ecol. Prog. Ser. 248, 125-139.

Kramer, D., Kalin, M.J., Stevens, E.G., Thrailkill, J.R., Zweifel J.R.l., 1972. Collectingand processingdata on fish e m and larvae in the California Current region. NOAA Tech. Rep. NMFS CIRC- 370, l-38.

Kruskal, W.H., Wallis, W.A., 1952. Use of Ranks in One-Criterion Variance Analysis. J. Am. Stat. Assoc. 47, 583–621

Landeira, J.M., Lozano-Soldevilla, F., 2018. Seasonality of planktonic crustacean decapod larvae in the subtropical waters of Gran Canaria Island, NE Atlantic. Sci. Mar. 82(2), 119-134. https://doi.org/10.3989/scimar.04683.08A.

Landeira, J., Yang, C., Komai, T., Chan, T., Wakabayashi, K., 2019. Molecular confirmation and description of the larval morphology of *Thalassocaris lucida* (Dana, 1852) (Decapoda, Caridea, Pandaloidea). J. Mar. Biol. Assoc. U.K. 99(8), 1797-1805. doi:10.1017/S0025315419000791.

Lang, W.H., Ackenhusen-Johns, A., 1981. Seasonal species composition of barnacle larvae (Cirripedia: Thoracica) in Rhode Island waters, 1977–1978. J. Plankton Res. 3(4), 567-575. https://doi.org/10.1093/plankt/3.4.567.

Legendre, P., Oksanen, J., ter Braak, C.J.F., 2011. Testing the significance of canonical axes in redundancy analysis. Methods Ecol. Evol. 2, 269-277. https://doi.org/10.1111/j.2041-210X.2010.00078.x.

Lima, F.A., Butturi-Gomes, D., Martinelli-Lemos, J.M., 2021. Megalopa bloom of *Panopeus lacustris* (Decapoda: Panopeidae) on the Amazon Continental shelf. Reg. Stud. Mar. Sci. 47, 101960. doi: 10.1016/j.rsma.2021.101960.

Lindeman, R.H., 1980. Introduction to Bivariate and Multivariate Analysis. Glenview IL: Scott, Foresman. (No. 04; QA278, L553.).

Lombard, F., Boss, E., Waite, A.M., Vogt, M., Uitz, J., Stemmann, L., Sosik H.M., Schulz J., Romagnan, J.B., Picheral, M., Pearlman, J., Ohman, M.D., Niehoff, B., Möller, K.O., Miloslavich, P., Lara-Lpez, A., Kudela, R., Lopes, R.M., Kiko, R., Karp-Boss, L., Jaffe, J.S. Iversen, M.H., Irisson, J.O., Fennel, K., Hauss, H., Guidi, L., Gorsky, G., Giering, S.L.C., Gaube, P., Gallager, S., Dubelaar, G., Cowen, R. K. Carlotti, F., Briseño-Avena, C., Berline, L., Benoit-Bird, K., Bax, N., Batten, S., Ayata, S.D., Artigas, L.F., Appeltans, W., 2019. Globally consistent quantitative observations of planktonic ecosystems. Front. Mar. Sci. 6, 196. https://doi.org/10.3389/fmars.2019.00196.

Lira, S. M., Schwamborn, R., de Melo Júnior, M., Varona, H. L., Queiroz, S., Veleda, D., ... & Marcolin, C. R. 2024. Multiple island effects shape oceanographic processes and zooplankton size spectra off an oceanic archipelago in the Tropical Atlantic. J. Mar. Sys., 242, 103942.

Longhurst, A,R., Pauly, D., 1987. (Eds.). Ecology of tropical oceans. San Diego: Academic Press. 407 p.

Lopes, R.M., Katsuragawa, M., Dias, J.F., Montú, M.A., Muelbert, J.H., Gorri, C., Brandini, F.P. 2006. Zooplankton and ichthyoplankton distribution on the southern Brazilian shelf: an overview. Sci. Mar. 70(2), 189-202. https://doi.org/10.3989/scimar.2006.70n2189.

Lüchmann, K.H., Freire, A.S., Ferreira, N.C., Daura-Jorge, F.G., Marques, M.R.F., 2008. Spatial and temporal variations in abundance and biomass of penaeid shrimps in the subtropical Conceição Lagoon, southern Brazil. J. Mar. Biol. Assoc. U.K. 88(2), 293-299. https://doi.org/10.1017/S0025315408000556.

Maida, M., Ferreira, B. P., 1997. Coral reefs of Brazil: an overview. Proc. 8th International. Coral Reef Sym, v.1, 263-274.

Manso, V.D.A.V., Correa, I.C. S., Guerra, N., 2003. Morfologia e sedimentologia da plataforma continental interna entre as Praias Porto de Galinhas e Campos-Litoral Sul de Pernambuco, Brasil. Pesquisas em geociências 30(2), 17-25. https://doi.org/10.22456/1807-9806.19587.

Marcolin, C.D.R., 2013. Plankton and particle biomass size spectra on the Southwest Atlantic: Case studies in tropical and subtropical areas (Doctoral dissertation, Universidade de São Paulo). doi:10.11606/T.21.2013.tde-12052014-173357. Available in: 2020-10-30.

Marcolin, C.D.R.,C., Schultes, S., Jackson, G.A., Lopes, R.M., 2013. Plankton and seston size spectra estimated by the LOPC and ZooScan in the Abrolhos Bank ecosystem (SE Atlantic). Cont. Shelf Res. 70, 74-87. https://doi.org/10.1016/j.csr.2013.09.022.

Melo Júnior, M., Paranaguá, M.N., Schwamborn, R., Neumann-Leitão, S., Ekau, W. (2007). Fluxes of zooplankton biomass between a tidal estuary and the sea in northeastern Brazil. Braz. J. Oceanogr. 55(4): 239-249.

Melo, N.F.A.C., Neumann-Leitão, S., Gusmão, L.M.O., Martins Neto, F.E., Palheta, G.D.A., 2014. Distribution of the planktonic shrimp Lucifer (Thompson, 1829)(Decapoda,

Sergestoidea) off the Amazon. Brazilian Journal of Biology *74*, S045-S051.https://doi.org/10.1590/1519-6984.20612.

Melo Júnior, M., Melo, M.P., Paranagua, M.N., Neumann-Leitão, S., Schwamborn, R. (2016). Composition of decapod larvae in a northeastern Brazilian estuarine inlet over a full tidal cycle. Latin American Journal of Aquatic Research 44, 401–410. https://doi:10.3856/vol44-issue2-fulltext-21.

Morgan, S.G., 1989. Adaptive significance of spination in estuarine crab zoeae. Ecology 70(2), 464-482. https://doi.org/10.2307/1937551.

Mustard, A.T., Anderson, T.R., 2005. Use of spherical and spheroidal models to calculate zooplankton biovolume from particle equivalent spherical diameter as measured by an optical plankton counter. Limnol. Oceanogr. Methods 3(3), 183-189. https://doi.org/10.4319/lom.2005.3.183.

Nemenyi, P. 1963. Distribution-free Multiple Comparisons. Ph.D. thesis, Princeton University.

Neumann-Leitão, S., Melo, P.A.M. C., Schwamborn, R., Diaz, X.F.G., Figueiredo, L.G.P.,Silva, A.P., Campelo, R.P.S., Melo Júnior, M. de, Melo, N.F.A.C., Costa, A.E.S.F., 2018. Zooplankton from a reef system under the influence of the Amazon River Plume. Front. Microbiol. 9, 355. https://doi.org/10.3389/fmicb.2018.00355.

Ogburn, M.B., Criales, M.M., Thompson, R.T., Browder, J.A., 2013. Endogenous swimming activity rhythms of postlarvae and juveniles of the penaeid shrimp *Farfantepenaeus aztecus, Farfantepenaeus duorarum,* and *Litopenaeus setiferu*s. J. Exp. Mar. Biol. Ecol., 440, 149-155. https://doi.org/10.1016/j.jembe.2012.12.007.

Oksanen, J., Simpson, G.L., Blanchet, F.G., Kindt, R., Legendre, P., Minchin, P. R., O'Hara, R.B., Solymos, P., Stevens, M. H. H.…., 2022. vegan: Community Ecology Package. R package version 2.6-2 https://CRAN.R-project.org/package=vegan

Omori, M., Ikeda, T., 1984. Methods in marine zooplankton ecology. Wiley, New York

Ooi, A.L., Chong, V.C., 2011. Larval fish assemblages in a tropical mangrove estuary and adjacent coastal waters: Offshore–inshore flux of marine and estuarine species. Cont. Shelf Res. 31, 1599-1610. https://doi.org/10.1016/j.csr.2011.06.016.

Pan, M., Pierce, G.J., Cunningham, C.O., Hay, S.J., 2011. Seasonal and interannual variation of decapod larval abundance from two coastal locations in Scotland, UK. J. Mar. Biol. Assoc. U.K. 91, 1443-1451. https://doi.org/10.1017/S0025315411000191.

Pauly, D., Christensen, V., Walters, C., 2000. Ecopath, Ecosim, and Ecospace as tools for evaluating ecosystem impact of fisheries. – ICES J. Mar. Sci. 57, 697–706. https://doi.org/10.1006/jmsc.2000.0726.

Pohlert, T., 2022. PMCMRplus: Calculate Pairwise Multiple Comparisons of Mean Rank Sums Extended. R package version 1.9.4. https://cran.r-project.org/web/packages/PMCMRplus/index.html

R Core Team, 2022. R: A Language and Environment for Statistical Computing. R Foundation for Statistical Computing, Vienna, Austria, 2022, Version 4.1.3

RStudio Team, 2022. RStudio: Integrated Development for R, Version 2022.02.0. https://www.rstudio.com.

Rao, C.R., 1964. The use and interpretation of principal component analysis in applied research. Sankhyā: The Indian Journal of Statistics. Series A 26, 329– 358.

Remsen, A., Hopkins, T.L., Samson, Scott., 2004. What you see is not what you catch: a comparison of concurrently collected net, Optical Plankton Counter, and Shadowed Image Particle Profiling Evaluation Recorder data from the northeast Gulf of Mexico, Deep Sea Research Part I: Oceanographic Research Papers 51(1), 129-151. ISSN 0967-0637. https://doi.org/10.1016/j.dsr.2003.09.008.

Reyns, N., Sponaugle, S., 1999. Patterns and processes of brachyuran crab settlement to Caribbean coral reefs. Mar. Ecol. Prog. Ser., 185, 155-170.

Rocha, G.R., Rossi-Wongtschowski, C.L., Pires-Vanin, A.M., Jarre-Teichmann, A., 2003. Seasonal budgets of organic matter in the Ubatuba shelf system, SE Brazil. I. Planktonic and benthic components. Oceanologica Acta 26(5-6), 487-495. https://doi.org/10.1016/S0399-1784(03)00043-4.

Rodrigues-Inoue, A.C.M., Dos Santos, A., Martinelli-Lemos, J.M., 2021. Distribution patterns of Anomura, Axiidea and Gebiidea (Crustacea, Decapoda) larvae at the Amazon shelf. Reg. Stud. Mar. Sci. 47, 101946. https://doi.org/10.1016/j.rsma.2021.101946.

Rollnic, M., Medeiros, C., 2006. Circulation of the coastal waters off Boa Viagem, Piedade and Candeias beaches Pernambuco, Brazil. Journal of Coastal Research 648-650. https://www.jstor.org/stable/25741656

Santana, C.S., de Albuquerque Lira, S.M., Varona, H. L., Neumann-Leitão, S., Araujo, M., Schwamborn, R., 2020. Amazon river plume influence on planktonic decapods in the tropical Atlantic. J. Mar. Syst. 212, 103428. https://doi.org/10.1016/j.jmarsys.2020.103428.

Santana, C.S., Schwamborn, R., Neumann-Leitão, S., Montes, M.J.F., Lira, S.M.A., 2018. Spatio-temporal variation of planktonic decapods along the leeward coast of the fernando de noronha archipelago. Brazil. Braz. J. Oceanogr. 66, 1–14. https://doi: 10.1590/s1679-87592018147206601.

Santos, G.S., Stemmann, L., Lombard, F., Schwamborn, R. 2019. Are tropical coastal reefs sinks or sources of mesozooplankton? A case study in a Brazilian marine protected area. Coral Reefs. 38:1107–1120. https://doi.org/10.1007/s00338-019-01860-2.

Santos, P. S., Soledade, G.O., Almeida, A.O., 2012. Decapod crustaceans on dead coral from reef areas on the coast of Bahia, Brazil. Nauplius 20, 145-169.

Schmidt, A.J., Bemvenuti, C.E., Diele, K., 2012. Effects of geophysical cycles on the rhythm of mass mate searching of a harvested mangrove crab. Anim. Behav. 84(2), 333-340. ISSN 0003-3472, https://doi.org/10.1016/j.anbehav.2012.04.023.

Schwamborn, R. A.C.T. Bonecker., 1996. Seasonal changes in the transport and distribution of meroplankton into a Brazilian estuary with emphasis on the importance of floating mangrove leaves. Braz. Arch. Biol. Technol. 39(2): 451-462.

Schwamborn, R., Ekau, W., Silva, A.P., Silva, T.A., Saint-Paul, U., 1999. The contribution of estuarine decapod larvae to marine zooplankton communities in North-East Brazil. Arch. Fish. Mar. Res. 47, 167-182.

Schwamborn, R., Voss, M., Ekau, W., Saint-Paul, U., 1999. Stable isotope composition of particulate organic matter and zooplankton in North-East Brazilian shelf waters. Arch. Fish. Mar. Res. 47, 201-210.

Schwamborn, R., Criales, M.M., 2000. Feeding strategy and daily ration of juvenile pink shrimp (*Farfantepenaeus duorarum*) in a South Florida seagrass bed. Mar. Biol. 137, 139-147. https://doi.org/10.1007/s002270000317.

Schwamborn, R., Silva, T.A., Silva, Andréa P., Ekau, Werner, Saint-Paul, Ulrich., 2001. Distribution and dispersal of decapod crustacean larvae and other zooplankton in the Itamaracá estuarine system, Brazil. Tropical Oceanography, Recife, Brasil. 29(1), 1-13.

Schwamborn, R., Ekau, W., Voss, M., Saint-Paul, U., 2002. How important are mangroves as a carbon source for decapod crustacean larvae in a tropical estuary? Mar. Ecol. Prog. Ser. 229, 195-205. https://doi:10.3354/meps229195.

Schwamborn, R., Ekau, W., Silva, A.P., Schwamborn, S.H.L., Silva, T.A., Neumann-Leitão, S., Saint-Paul, U., 2006. Ingestion of large centric diatoms, mangrove detritus, and zooplankton by zoeae of *Aratus pisonii* (Crustacea: Brachyura: Grapsidae). Hydrobiologia 560(1), 1-13.

Schwamborn, R., Júnior, M.D.M., Leitão, S.N., Ekau, W., Paranaguá, M.N., 2008. Dynamic patterns of zooplankton transport and migration in Catuama Inlet (Pernambuco, Brazil), with emphasis on the decapod crustacean larvae. Lat. Am. J. Aquat. Res. 36, 109-113. https://doi: 10.3856/vol36-issue1-fulltext-10.

Schwamborn, R., Schwamborn, D. F. M. C. Growth and mortality of the endangered land crab *Cardisoma guanhumi* assessed through tagging with PITs and novel bootstrapped methods. 2021. Pan-Am. J. Aquat. Sci., 16(1): 57-78.

Sekiguchi H. (1983). Distribution of larvae of P*innixa rathbuni* Sakai (Decapoda: Pinnotheridae) in Ise bay and its neighboring coastal waters, central Japan. 3. Aggregation of the benthic adult population with reference to the spatial distribution of the planktonic larvae. J. Oceanogr. Soc. Japan. 39, 119-128.

Sheridan P, Hays C., 2003. Are mangroves nursery habitat for transient fishes and decapods? Wetlands, 23, 449–458

Silva, N.L., Marcolin, C.R., Schwamborn, R., 2019. Using image analysis to assess the contributions of plankton and particles to tropical coastal ecosystems. Estuar. Coast. Shelf S. 219, 252-261. https://doi.org/10.1016/j.ecss.2019.02.010.

Silva, T.R.B.F.; Santos, C.A.C.d.; Silva, D.J.F.; Santos, C.A.G.; da Silva, R.M.; de Brito, J.I.B. Climate Indices-Based Analysis of Rainfall Spatiotemporal Variability in Pernambuco State, Brazil. Water 2022, 14, 2190. https://doi.org/10.3390/w14142190

Stemmann, L., Boss, E., 2012. Plankton and Particle Size and Packaging: From determining Optical Properties to Driving the Biological Pump. Ann. Rev. Mar. Sci. 4, 263–290.

Turner, J.T., 1982. The annual cycle of zooplankton in a Long Island estuary. Estuaries 5, 261–274. https://doi.org/10.2307/1351749.

Valentin, J.L., Monteiro-Ribas, W.M., 1993. Zooplankton community structure on the east-southeast Brazilian continental shelf (18–23 S latitude). Cont. Shelf Res. 13(4), 407-424. https://doi.org/10.1016/0278-4343(93)90058-6.

Vandromme, P., Stemmann, L., Garcìa-Comas, C., Berline, L., Sun, X., Gorsky, G., 2012. Assessing biases in computing size spectra of automatically classified zooplankton from imaging systems: a case study with the ZooScan integrated system. Methods in Oceanography 1–2, 3–21. https://doi.org/10.1016/j.mio.2012.06.001.

Venables, W.N., Ripley, B.D., 2002. Modern applied statistics with S, 4th edn Springer. *New York*.

Vereshchaka A.L., Olesen J., Lunina A.A. 2016. A phylogeny-based revision of the family Luciferidae (Crustacea: Decapoda). Zool. J. Linn. Soc., 178: 15– 32. doi: 10.1111/zoj.12398

Vieira, R.R.R., Calazans, D.K.D., 2015. Abundance and distribution of Portunidae larval phases (Crustacea: Brachyura) in the estuarine and coastal region of the Patos Lagoon, southern Brazil. Nauplius *23*(2), 132-145. https://doi.org/10.1590/S0104-64972015002303.

Whitfield, A.K., 2017. The role of seagrass meadows, mangrove forests, salt marshes and reed beds as nursery areas and food sources for fishes in estuaries. Rev. Fish Biol. Fisher. 27(1), 75-110. https://doi.org/10.1007/s11160-016-9454-x.

Zetina-Rejón, M.J., Arreguín-Sánchez, F., Chávez, E. A., 2004. Exploration of harvesting strategies for the management of a Mexican coastal lagoon fishery. Ecol. Model. 172(2–4), 361-372. https://doi.org/10.1016/j.ecolmodel.2003.09.017.

4 ARTIGO 2 - SIZE NICHE INTERACTIONS BETWEEN MERO- AND HOLOPLANKTON SHAPE THE SIZE SPECTRUM OF TROPICAL ESTUARINE AND MARINE ECOSYSTEMS

1 INTRODUCTION

Body size is considered to be a “master trait” within functional analyses of natural ecosystems (Ray *et al.*, 2001; Brown *et al.*, 2004; Blanchard *et al.*, 2017; Wang *et al.*, 2022). All physiological, behavioral, and food web-related processes are intrinsically dependent on an organism's body size (Sheldon *et al.*, 1977; Gaedke, 1993; Zhang *et al.*, 2023). Size distributions of organisms can be easily quantified and used as powerful and simple descriptors (Woodward *et al.*, 2005; Krupica *et al.*, 2012).

Many theoretical frameworks and practical methods have been developed to study the distribution of body size in natural ecosystems (Sprules and Munawar, 1986; Zhou and Huntley, 1997; Zhou, 2006; Sprules and Barth, 2016). The relationship between size and abundance (size spectra analysis, SSA) is particularly useful for the study of zooplankton communities. Since the development of automated methods that allow obtaining large numbers of size measurements, such as the ZooScan (Gorsky *et al.*, 2010), increasing numbers of articles on marine zooplankton size spectra have been published, mostly from temperate and polar seas (Lombard *et al.*, 2019). Conversely, little has been done to study the size spectra of tropical estuarine zooplankton and to compare them to adjacent coastal and shelf ecosystems (Ke *et al.*, 2018). Generally, the size spectrum of marine zooplankton is considered to be stable at around -1, with notable exceptions (San Martin *et al.*, 2006; Marcolin *et al.*, 2015). Based on a meta-analysis of recent publications and their own extensive data obtained at a fixed station in temperate marine waters off Plymouth (UK), Atkinson *et al.* (2021) obtained a median plankton size spectrum slope close to the theoretical optimum (median slope: −1.11), but varying seasonally. They propose a dome-shaped relationship between size spectra slopes and plankton biomass, with steeper slopes towards far hypereutrophic and oligotrophic systems and the flattest (“optimum”) slope in mesotrophic, productive, temperate systems.

Size, biovolume, and biomass distributions contain key information on the functioning of planktonic communities (Hobbie, 1972; Platt, 1985; Moriarty, 2013). Size spectrum analysis provides parameters of zooplankton population dynamics and ecosystem production (Sprules and Munawar, 1986; Zhou and Huntley, 1997; Sprules and Barth, 2016). Based on observations that the biomass in aquatic environments is relatively constant along a power-law (Pareto) distribution, numerous theoretical concepts and size spectrum models have been developed (e.g., Sheldon *et al.*, 1972,1977; Kerr, 1974; Platt and Denman, 1978; Ray *et al.*, 2001; Blanchard *et al.*, 2017). The normalized biomass size spectrum (NBSS, Platt and Denman, 1977) uses a simple transformation, where the Y value (abundance, biovolume, or biomass) for each size bin is divided by the corresponding bin width (Platt and Denman, 1977; Dickie and Boudreau, 1987; Rodríguez, 1994; Gaedke and Straile, 1998). Many recent zooplankton studies have used the NBSS approach to address seasonal, interannual, or spatial variability (e.g., San Martin *et al.*, 2006; Vandromme *et al.*, 2014; Marcolin *et al.*, 2015; Ke *et al.*, 2018, Souza *et al.*, 2020; Atkinson *et al.*, 2021; Couret *et al.*, 2023).

Several size spectrum descriptors (slope, intercept, mean elevation, linearity, mean dispersion, homoscedasticity of the dispersion, outline shape, height and distribution of peaks and domes, size diversity, etc.) may provide subsidies for the understanding, prediction, and management of ecosystems. Among these descriptors, the NBSS slope is by far the most intensively studied and most commonly investigated, since it can be used to assess the trophic efficiency (TE) of aquatic food webs (Figueiredo *et al.*, 2020). Conversely, the number of empty bins within a given size spectrum has been generally ignored as a source of information.

A possible effect of meroplankton inputs on the zooplankton size spectrum has not yet been investigated. Here, we intend to test the general hypothesis that the massive release of meroplanktonic larvae into the water column significantly affects the shape of zooplankton size spectra in tropical estuarine and coastal environments. More specifically, we tested the five working hypotheses that 1.) peaks in the zooplankton size spectrum can be related to specific meroplankton taxonomic groups, 2.) there are significant size niche interactions between mero- and holoplankton (i.e., there are significant correlations between peaks and throughs in their size distributions), 3.) such size niche interactions are density-dependent, 4.) inputs of non-holoplanktonic organisms into the water column may change the size spectrum slope and intercept, 5.) and that meroplankton fills severe gaps (“empty bins”) in the zooplankton size spectrum.

2 MATERIALS AND METHODS

2.1 Field sampling

The study areas (Fig. 1) are located in the coastal zone of Pernambuco State (northeastern Brazil) and are part of the "*Costa dos Corais"* Environmental Protection Area. Surveys were carried out in a hypereutrophic mangrove-lined estuary (Rio Formoso Estuary), in a reef-lined semi-enclosed oligotrophic coastal ecosystem (Tamandaré Bay), and at the adjacent oligotrophic continental shelf, with rhodolith beds, silt flats and deep reefs (Tamandaré Shelf). Surface water temperature in the study area ranges from 26.4 °C to 30.5°C, surface salinity ranges from 27.03 in the estuary to 37.44 on the shelf, and water transparency (Secchi depth) ranges from less than 1 m in the estuary to more than 19 m on the shelf (Schwamborn *et al.*, 2024). Thirty-seven cruises were carried out in these areas between 2013 and 2015 through two projects: 1.) St-ESPLAN-Tropic (CNPq) and 2.) INCT AmbTropic (CNPq/CAPES/FAPESB).

Figure 1. Map of the study area showing the sampling stations in the coastal region of Tamandaré, Pernambuco State, Brazil. Formoso River Estuary (red), Tamandaré Bay (yellow), Continental Shelf (blue).

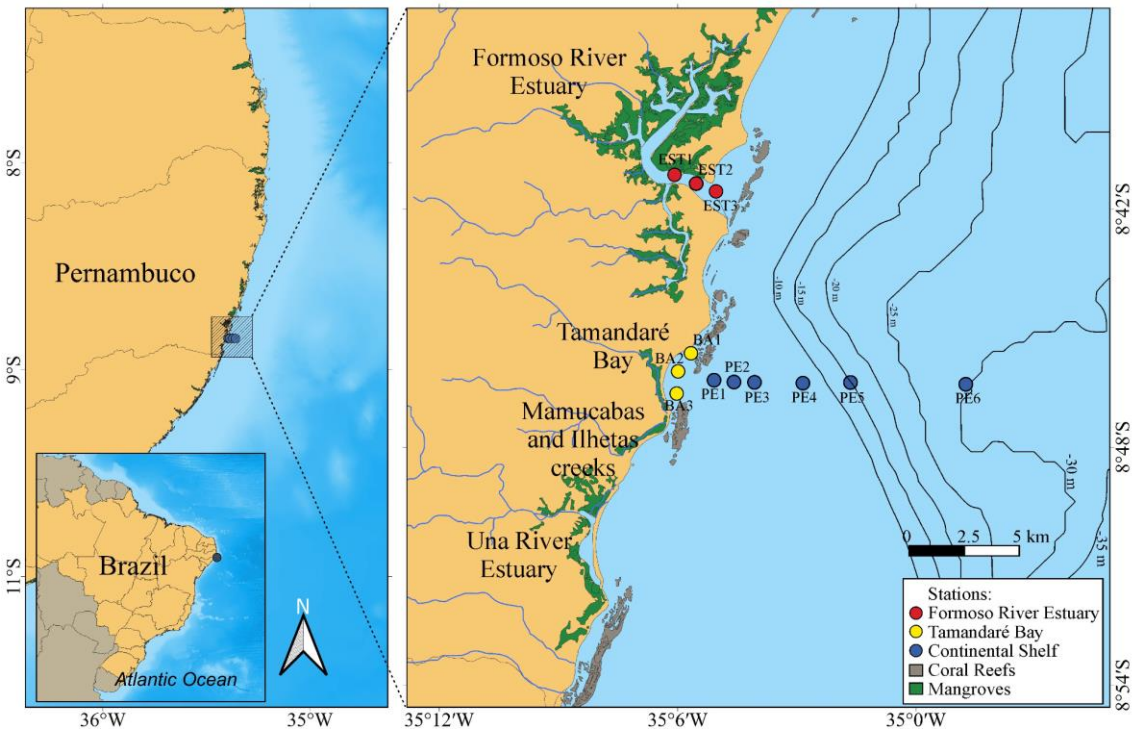

Fonte: A autora (2024).

A 300 μm mesh plankton net (net diameter: 60 cm) equipped with a Hydro-Bios (Kiel, Germany) flow meter was towed at subsurface (5 minutes duration, speed: 2 to 3 knots) to collect zooplankton samples that were preserved with a sodium-tetraborate-buffered formaldehyde solution (4%) in seawater. At each station, salinity, temperature, and depth were measured using a CTD probe (YSI/SonTek CastAway) and a Secchi disk. Campaigns were conducted in bimonthly intervals, during daytime. A total of 121 zooplankton samples were obtained successfully and analyzed in this study.

2.2 ZooScan analysis

In the laboratory, zooplankton samples were scanned using a ZooScan, a semi-automatic scanner (resolution: 2400 dpi) (Hydroptic model ZSCAN03, Gorsky *et al.*, 2010). To optimize the extraction of vignettes, samples were divided into two fractions, using a 1000 μm mesh. Aliquots were taken from these two fractions with a Motoda-type subsampler (Omori and Ikeda, 1984), determining an amount between approx. 1000 and 2000 objects (incl. particles and organisms) for each fraction to be digitized. Scans were processed using the ZooProcess software (http://www.obs-vlfr.fr/LOV/ZooPart/ZooScan) and Plankton Identifier (Gorsky *et al.*, 2010) generating digital images (vignettes) of each organism and particle. Descriptive parameters such as area, feret diameter, fractal dimension of the object's boundary, equivalent ellipse axes, descriptors of gray levels, etc. were calculated for each vignette, for subsequent semi-automatic classification.

2.3 Classification of vignettes

A total of 182,281 digital images (vignettes) were obtained and analyzed in this study. Images were initially checked for artifacts (e.g., bubbles) where necessary and semi-automatically classified into taxonomic categories. The numerical descriptors of each vignette were used for semi-automatic pre-classification through a Random Forest algorithm (Breiman, 2001). After pre-classification, all vignettes were visually classified and validated by an experienced plankton taxonomist. The ellipsoid biovolume (mm^3) was calculated for each vignette based on the minor and major axes of the equivalent ellipse (http://www.obs-vlfr.fr/LOV/ZooPart/ZooScan).

2.4 Data analysis

2.4.1 Taxon-specific size spectra

Taxon-specific size spectra (in units of abundance and of biovolume) were built to analyze the effects of different taxonomic groups on the shape of the overall zooplankton size spectrum. For each taxonomic group, abundance (ind. m^3) and biovolume (mm^3 m^{-3}) matrices were compiled by study area (Estuary, Bay, and Shelf), and size class.

Meroplankton (especially decapod larvae), copepods, and other holoplankton were identified in detail, for all samples, by an experienced taxonomist, to the best level possible based on the visual examination of thousands of ZooScan vignettes (Schwamborn *et al.*, 2024). Considering the well-known dominance of copepods in estuarine and marine zooplankton, and the need to analyze specific appendages and body parts for their accurate identification, an additional effort was made towards a detailed identification of copepods under a stereomicroscope by an experienced taxonomist. For this detailed identification of copepods, 27 samples were randomly selected (9 samples from each area, Estuary, Bay and Shelf). Subsamples (the same aliquots as for the Zooscan analysis) were poured into a Bogorov chamber, and all copepods (total: 7,035 individuals) were identified, usually at genus level (Boltovskoy, 1999).

Based on the ZooScan results, taxon-specific abundance-size and biovolume-size spectra were built to evaluate the contributions of the main taxonomic groups to the abundance and biovolume of each size class and the shapes of these size spectra (range, slope, occurrence and position of peaks and throughs, relative contribution (%) to the total zooplankton within each size range) were analyzed for each taxon. These contributions and size spectra shapes (location of peaks and troughs of the taxon-specific size spectrum, for the most abundant taxa) were evaluated for each sample separately (sample-by-sample analysis) and for the overall mean size spectrum, for each sampling area (Estuary, Bay and Shelf).

2.4.2 Size niche interactions between holo- and meroplankton

To verify the existence of statistically significant size niche interactions between taxonomic groups, pairwise Spearman rank correlation analysis was used to test for significant ($p < 0.05$) correlation between size distributions (peaks and throughs in the size spectrum) for pairs of key taxa (most abundant and frequent), such as copepods (holoplankton) and brachyuran zoeae (meroplankton). This pairwise correlation analysis was done within the size range that corresponds to the peak zooplankton size spectrum (from 0.5 to 2.2 mm Feret length), to avoid the effects of dominant zeros at the tails of the spectrum. Prior to correlation analysis, the two original spectra (normalized abundance or biomass in each size bin) of both taxa to be correlated were log10(x+1)-transformed and standardized (i.e., transformed into their relative contributions (%) to the total zooplankton normalized abundance or biomass of in each size bin).

2.4.3 Density-dependence of size niche interactions

To test whether the interaction between copepods (holoplankton) and brachyuran zoeae (meroplankton) is density-dependent, permutational linear regression analysis (function "lmp" within the R package "lmPerm", Wheeler and Torchiano, 2016) was conducted between the total density of copepods (ind. m^3, Fig. 8) and the Spearman rank correlation coefficient ("rho") of the rank correlation analysis described above (correlations between size distributions of copepods and brachyuran zoeae). The same linear regression analysis for density-dependence was also conducted between the Spearman rank correlation coefficient ("rho") and the total density of brachyuran crab zoeae (ind. m^3, Fig. 8).

2.4.4 Comparison of NBSS slopes with and without meroplankton

Normalized biovolume size spectra (NBSS) analysis was conducted to compare size spectra slopes and intercepts between study areas (Estuary, Bay, Shelf). Also, we used the NBSS to verify the potential effects of non-holoplanktonic organisms (e.g., decapod larvae and other meroplankton) on the total zooplankton community size spectrum shape. Thus, we calculated and compared the slopes and intercepts of linear NBSS models between three

datasets: 1.) for the total zooplankton, 2.) without meroplanktonic decapod larvae, 3.) for holoplankton only (i.e., without ichthyoplankton, meroplankton, or any other non-holoplanktonic organisms).

NBSSz: Total **zooplankton** (including holo- and meroplankton). These data include all multicellular heterotrophic organisms found in the plankton samples but exclude micro- and macroalgae and non-organismic particles, such as aggregates, biogenic detritus, and microplastics.

NBSSnmd (no meroplankton decapods). As above, but without meroplanktonic decapod larvae (i.e., without brachyuran zoeae, without penaeid post-larvae, without caridean and anomuran zoeae, etc., but with holoplanktonic luciferids and sergestids).

NBSSho (**holoplankton** only). As above, but without meroplankton and without ichthyoplankton or any other non-holoplanktonic organisms. These datasets are without any larvae (except for larvae of holoplanktonic luciferids and sergestids, which were included here) without parasites, without benthopelagic organisms (e.g., without polychaete and mollusk larvae, without cirripedian nauplii, without parasitic copepods, without cumaceans, isopods and amphipods, without any meroplanktonic decapod larvae, but with holoplanktonic luciferid and sergestid adults and larvae).

These three types of NBSS were built for the three sampling areas (Estuary, Bay, Shelf), totaling 3 x 3 = 9 NBSS models built in this study. The main objective was to compare slopes and intercepts of NBSSz vs NBSSho and NBSSz vs NBSSnmd, as to test for potential effects of non-holoplankton and of meroplanktonic decapods, on the total zooplankton community size spectrum shape.

Size spectra were normalized as described by Vandromme *et al.*, (2014), based on biovolume data. As the size class width varies according to the size, the normalization divides the biovolume (V), by the width of the size class (Δs), where NBSS(s) = V(s) / Δs.

Slope and intercept were calculated for each NBSS by using ordinary least squares regression (OLSR) and robust regression (Hampel *et al.*, 1986). The latter method is robust to outlier effects and to deviations from the prerequisites of common OLSR. To avoid mesh

selection and gear avoidance effects, we excluded the extremely small and extremely large size groups. The effective size range used for regression was from -1.5 log10 mm3 to 0.1 log10 mm3 biovolume (i.e., from 0.39 mm esd to 1.34 mm esd size), encompassing nine size classes. Robust linear regression and robust ANCOVA (robust statistical testing for differences in slopes and intercepts, Hampel *et al.*, 1986) were conducted using the "robust" package in R (Wang *et al.*, 2019).

2.4.5 Finding and filling the gaps: analysis of empty bins within the NBSS

To test the hypothesis that the input of non-holoplanktonic organisms into the water column fills significant gaps ("empty bins") that would otherwise exist in the zooplankton size spectrum, we investigated the effect of total non-holoplanktonic organisms and of meroplanktonic decapods, on the number of empty bins (blue arrows in Fig. 2). This was done by comparing the datasets with and without meroplankton or any other non-holoplanktonic organisms regarding their relative numbers of empty bins ("0") and bins with data ("1"), by applying a permutation test ("emptiness test") to these presence-absence data. Differences between NBSSz and NBSSho regarding the number of empty bins were tested using a non-parametric permutation test (function independence_test in the R package coin, Hothorn *et al.*, 2006). This permutation test was applied for the size range from -1.5 log10 mm3 to 0.1 log10 mm3 biovolume (i.e, from 0.39 mm esd to 1.34 mm esd size), encompassing nine size classes ("small"-sized organisms) and for a "large" size group, that encompasses nine NBSS size classes from 0.1 log10 mm3 to 1.7 log10 mm3 biovolume (i.e, from 1.34 mm esd to 4.47 mm esd size). All analyses were conducted at alpha = 0.05, using the R programming environment, software, and language (version 4.0.2, R Core Team, 2022) with the RStudio interface (version 1.1.463, RStudio Team, 2022).

3 RESULTS

3.1 Taxon-specific contributions to the size spectrum

Detailed analyses of the contributions of key taxa to the overall community size spectra using different units and transformations showed that the biovolume-biovolume (NBSS, Fig. 2), abundance-size (Figs. 3 and 4) and biovolume-size spectra (Fig. 5) displayed considerably different shapes, for both total zooplankton and for the main taxonomic groups. Yet, regardless of units and transformations, calanoid copepods were the overall dominating taxon in all three areas, in units of abundance and biovolume (Figs. 2 to 5). These small-sized holoplankters were dominating in the indiv. biovolume range < -0.8 log10 mm3 (Fig. 2) and in the body size range < 3 mm Feret length (Fig. 5). The calanoid *Acartia* sp. was the most abundant taxon in all areas, being especially dominant in the Estuary. In the Bay and Shelf area, large-sized copepods, such as *Labidocera* spp., were also relevant.

In the Estuary, brachyuran zoeae, anomuran zoeae, alpheid zoeae, other caridean shrimp zoeae and holoplanktonic luciferid shrimps (adults and larvae) were important groups in the size classes larger than -0.8 log10 mm3 (i.e., larger than 3 mm Feret length, Fig. 2, Fig. 5). In Bay and Shelf areas, chaetognaths, luciferid shrimp, fish larvae and *Penaeus* post-larvae were dominant in the size range > 3mm Feret length (Fig. 5).

Figure 2. Mean *Normalized Biovolume Size Spectra* (NBSS) for the total zooplankton and for key taxonomic groups in the three study areas. Dominant taxa (in units of biovolume) for each size range, are highlighted above each spectrum. Zooplankton was sampled bimonthly in the Rio Formoso Estuary, in Tamandaré Bay, and on the adjacent continental shelf (Pernambuco, Brazil), from June 2013 to May 2015. n: 121 samples.

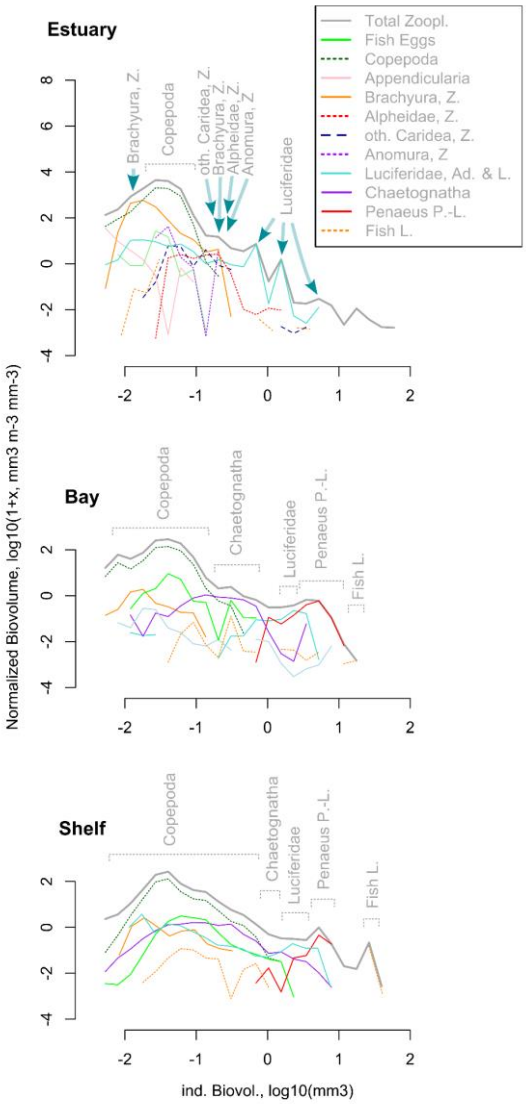

Fonte: A autora (2024).

Figure 3. Example ("sample no. 73", taken in the Rio Formoso Estuary) of a taxon-specific abundance-size spectrum showing the occurrence of two empty bins (at 0.75 mm and 0.85 mm Feret length) in the holoplankton (copepod) distribution, that are both filled by meroplankton (brachyuran zoea larvae). Note that between 0.75 and 0.85 mm Feret length, there is a "gap" (empty bins) in the size spectrum of copepods. Spearman Rank correlation analysis of the contributions of copepods and brachyuran zoeae to the total zooplankton abundance detected a significantly negative correlation (p = 0.007, rho = -0.7), for this sample.

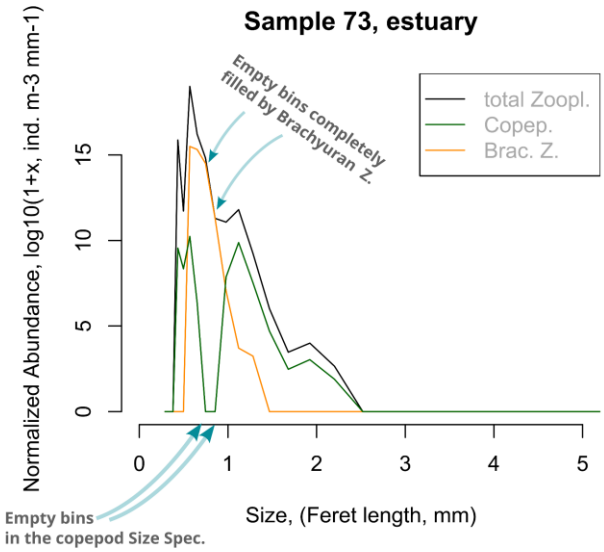

Fonte: A autora (2024).

In all three sampling areas, harpacticoid and cyclopoid copepods were negligible in units of biovolume, as well as parasitic copepods and benthic migrants (Cumacea, Isopoda, Amphipoda). The most striking difference between the three study areas was that calanoid copepods (< 1 mm Feret length) were more abundant in the Estuary than in the other two study areas, by more than six orders of magnitude (Fig. 4), and by more than five orders of magnitude, in units of biovolume (Fig. 5). A secondary peak for large calanoids, at approx. 1 to 2 mm Feret length, frequently appeared in the copepod abundance-size spectrum (Figs. 3 and 4). Within the mean biovolume-size spectrum in Bay and Shelf areas, this strong secondary peak, made of large calanoids (Feret length = 1.7 mm), was most clearly visible (Fig. 5).

Figure 4. Mean abundance-size spectra (Feret size vs log10 Abundance) of total zooplankton, copepods, and brachyuran zoeae, for the three study areas. Mean abundances for each size bin were calculated considering empty bins (zeros). Zooplankton was sampled bimonthly in the Rio Formoso estuary, in Tamandaré bay, and on the adjacent continental shelf (Pernambuco, Brazil), from June 2013 to May 2015. n: 121 samples.

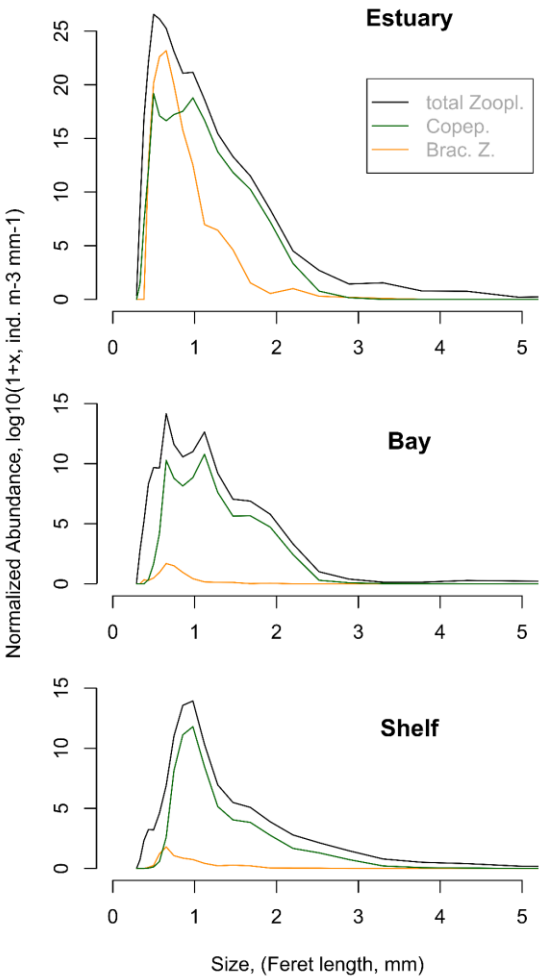

Fonte: A autora (2024).

Figure 5. Mean biovolume-size spectra (Feret size *vs* log10 Biovolume) of total zooplankton and main holo-, mero- and ichthyoplankton taxa, for the three study areas. Mean biovolumes for each size bin were calculated considering empty bins (zeros). Zooplankton was sampled bimonthly in the Rio Formoso estuary, in Tamandaré bay, and on the adjacent continental shelf (Pernambuco, Brazil), from June 2013 to May 2015. n: 121 samples.

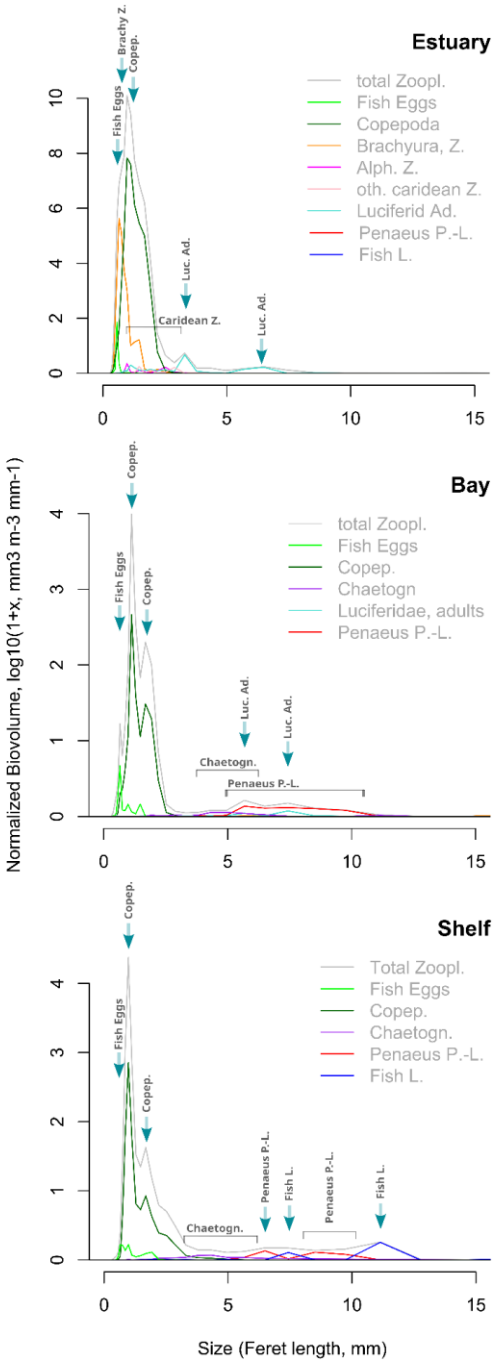

Fonte: A autora (2024).

Brachyuran crab zoeae were the most abundant meroplankton taxon in all three areas. Overall, these crab larvae were the second most relevant taxon in our dataset, in abundance and biovolume, after calanoid copepods. Crab zoeae were particularly abundant and relevant in the Estuary (Figs. 3 and 4). In the Estuary, brachyuran zoeae clearly dominated, in abundance and biovolume, within the size range from 0.5 mm to 1 mm Feret length (Figs 3 to 5). This size range corresponds to a "gap" within the copepod abundance size spectrum of several samples (e.g., Fig. 3), generating the empty bins shown in Fig. 8. Also, this size range (0.5 mm to 1mm Feret length) corresponds to a "through" within two peaks (0.5 and 1.1 mm Feret length) in the mean copepod size spectrum in the Estuary and in the Bay (Fig. 4).

Additionally to brachyuran crab zoeae, other decapod larvae, such as caridean shrimp zoeae (e.g. Palaemonidae, Hippolytidae, Alpheidae, and "other" caridean zoeae), were also relevant, in units of abundance and biovolume, as "gap fillers" and especially as contributors to the larger size classes (> 1.1 mm Feret length), in the Estuary, together with many other meroplankton groups.

In the Bay and Shelf areas, penaeid post-larvae were extremely relevant as "gap fillers" and contributors to the larger size classes (> 3 mm Feret length), in units of abundance and biovolume (Fig. 5), together with caridean shrimp zoeae and fish larvae.

Fish larvae and Fish eggs were also extremely relevant, especially at the Shelf. Fish eggs occurred in all areas in high numbers, and were dominant among the smallest organisms in this study (approx 0.4 to 0.7 mm Feret length), with peaks usually at the lower fringe of the copepod size distribution (Fig 5). Conversely, fish larvae (mostly late pre-settlement stages) were most important in the largest size classes, larger than 7 mm Feret length, at the Shelf (Fig. 5).

Considering the location of the peaks within the size spectrum, we observed that on the shelf, fish larvae and *Penaeus* spp. post-larvae had four intermittent successive peaks (two peaks for each group) with no overlap, indicating a possible size niche utilization strategy or overlap avoidance (Fig. 5). This phenomenon was observed regardless of the units of the size spectrum (i.e., regardless of whether in units of abundance-size, biovolume-size or biovolume-biovolume).

3.2 Correlations between taxon-specific size spectra

A detailed sample-by-sample (Fig. 3) analysis of peaks and throughs, for each taxon, revealed features and interactions between taxa that were not visible in the mean spectrum. Sample-by-sample analysis (Fig. 3) revealed evident inverse peak *vs* through features of throughs in copepod size spectrum that coincided with peaks in brachyuran zoeae size spectra in 95 % (36 out of 38 samples) of the analyzed samples in the Estuary, where brachyuran crab zoeae often exhibited a maximum that coincided with a minimum in the copepod size spectrum, a phenomenon that would not be visible when looking only at the overall mean spectrum. The consistently negative effect of crab zoeae on copepods occurred regardless of the mean size of the brachyuran zoeae (e.g., regardless of the position, where the peak in crab zoeae abundance was located within the size spectrum), within the varying shapes, locations and numbers of peaks in crab zoea size spectra observed along the seasonal cycle, which depend on the crab species and zoeal stages (zoea I, II, III, IV, etc.) that occurred in the plankton samples.

Non-parametric Spearman rank correlation analysis confirmed this negative interaction, by detecting highly significantly negative correlations between copepods and brachyuran crab zoeae, the two most abundant taxa. For the whole data set (n = 121 samples), rank correlation between copepods and brachyuran zoeae was negative and highly significant ($p < 10^{-5}$, n = 121). When testing correlations for each sampling area (Estuary, Bay, Shelf), highly significant negative correlations between copepods and crab zoeae were found in all areas (Estuary: p-value $< 10^{-15}$, n = 38 ; Bay: p-value = 0.0028, n = 38 ; Shelf: $p < 10^{-08}$, n = 45).

Detailed sample-by-sample Spearman rank correlation analysis revealed that in the whole dataset (121 samples) only one (1/121, less than 1%) significantly positive rank correlation result occurred (“sample 2”, collected in the Bay). In contrast, we found 34 significant negative rank correlations, distributed within all three sampling areas. This analysis revealed a common and strong negative interaction between copepods and crab zoeae (i.e., peaks in zoeae contributions consistently and significantly coincided with throughs in copepod contributions within 34 size spectra).

3.3 Density-dependence of size-niche interactions

In the Estuary, for most samples (55%, 21 out of 38 samples) there was a significantly negative correlation between contributions of brachyuran zoeae and copepods to the total zooplankton. In Bay and Shelf areas, such gap-filling interactions between copepods and these larvae were much less frequent (Bay: 4 out of 38 samples with negative significant results, Shelf: 9 out of 45 samples with negative significant results), which may be due to overall lower abundances in oligotrophic marine areas than in the hypereutrophic mangrove Estuary. Accordingly, significant negative correlation was only found for samples above a minimum threshold of at least 0.3 brachyuran zoeae m^{-3}, indicating a density-dependent negative interaction between these two taxa. Furthermore, the value of Spearman's Rho (i.e, the “Rho” value of the Spearman rank correlation tests described above, between size spectra contributions of copepods and crab zoeae) was significantly related to the log-transformed total abundance of crab zoeae ($p < 10\text{-}16$, permutational linear regression, Fig. 6).

This proves that there is a density-dependent relationship between crab zoea abundance and their effect on copepods. Conversely, Spearman's Rho was not significantly related to copepod abundance. These results confirm the existence of a density-dependent negative interaction and that brachyuran crabs are negatively affecting same-sized copepods. This size-niche interaction analysis evidenced that increasing numbers of crab zoeae (e.g., during massive hatching events) produce a (probably predation-mediated) negative effect on the abundance of same-size copepods.

Figure 6. Linear and log-linear relationships between the values of Spearman's "Rho" and total abundances (ind. m^{-3}) of copepods and brachyuran crab zoeae. The "Rho" value is the Spearman rank correlation coefficient for the rank correlation between size spectra contributions of copepods and brachyuran crab zoeae. Negative "Rho" values indicate that peaks in crab zoeae coincide with throughs in copepod size spectra (i.e., depletion of copepods by same-sized crab zoeae). Linear models were fitted and tested with permutation tests ($R^2 = 0.25$, $p < e\text{-}16$, for the linear model of "Rho" vs log(1+total abundance of crab zoeae)). Zooplankton was sampled bimonthly in the Rio Formoso estuary, in Tamandaré bay, and on the adjacent continental shelf (Pernambuco, Brazil), from June 2013 to May 2015. n: 121 samples.

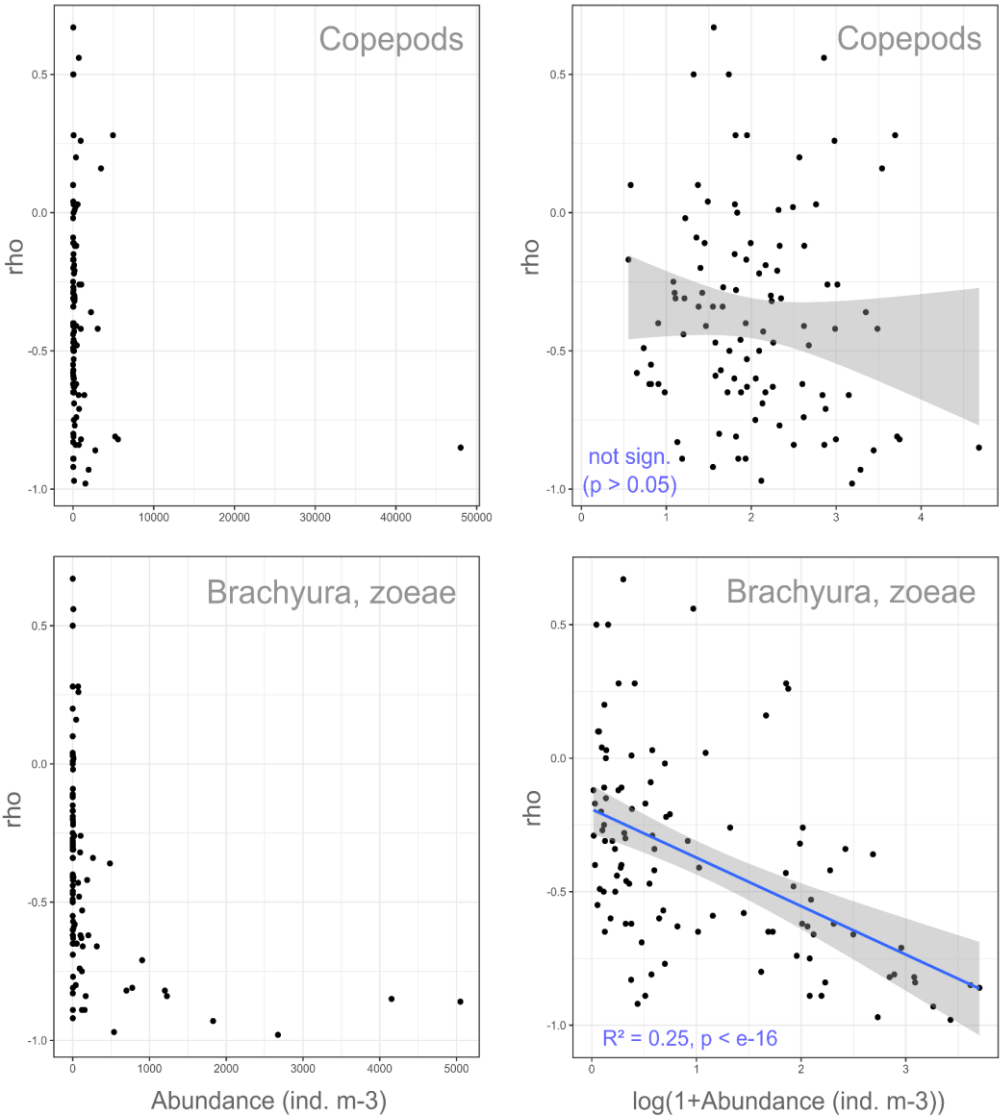

Fonte: A autora (2024).

3.4 NBSS slopes and intercepts

Normalized Biovolume Size Spectra (NBSS) for the total zooplankton showed a log-linear declining shape within the size range used for linear models, from -1.5 log_{10} mm^3 to 0.1 log_{10} mm^3 (Figs. 7 and 8).

Comparisons of NBSS slopes between Estuary, Bay, and Shelf ecosystems revealed several significant differences, with the Estuary showing significantly steeper slopes (Figs. 7 and 8). These slopes were always significantly steeper for estuarine zooplankton than for the other two areas, whether analyzing NBSSz, NBSSho, or NBSSnmd. By contrast, there were no significant differences in slopes between models from Bay and Shelf areas.

For NBSSz, the robust linear model slope in the Estuary (Estuary, NBSSz, slope = -2.455 +- 0.165 std. error, intercept = -1.050 +- 0.158 std. error, R2: 0.51, $p < 0.0001$, robust regression) was significantly steeper ($p = 0.0012$, permutation ANCOVA with lmperm) than in the Bay (Bay, NBSSz, slope = -1.806 +- 0.098, intercept = -1.006 +- 0.087 std. error, R2: 0.50, $p < 0.0001$, robust regression). Also, the NBSSz slopes in the Estuary were significantly steeper ($p < 0.0001$, permutation ANCOVA with lmperm) than NBSSz regression slopes at the Shelf (Shelf, NBSSz, slope = -1.803 +- 0.089, intercept = -0.7689 +- 0.077 std. error, robust regression).

The steeper robust linear model slopes observed in the Estuary were mainly due to considerably higher numbers and biovolumes of small-sized organisms (mostly small-sized calanoid copepods < 1.5 mm Feret length) at the estuarine stations, than in both adjacent marine areas. In our analyses, the NBSS slope was clearly determined by the size structure of the calanoid copepod community (i.e., the relative stage and species composition within the Calanoida). Small-sized calanoid copepods were more abundant in the Estuary than in the other two areas, by several orders of magnitude (Figs. 2 to 5). Also, copepods in the Estuary did not display a secondary peak in their size spectrum, for large calanoid copepods (> 1.5 mm Feret length), that was characteristic for Bay and Shelf areas (Fig. 4). The far higher abundance and biovolume of small calanoids (mostly *Acartia* sp.) in the Estuary and a secondary peak of large calanoids (> 1.5 mm Feret length, mainly *Labidocera* sp.), in Bay and Shelf areas can well explain the observed differences in NBSSz slope between these areas.

Figure 7. Normalized biovolume size spectra (NBSS) for the three study areas (estuary, bay and shelf) and community types. (NBSSz): Total zooplankton (above), NBSSnmd: zooplankton with no meroplanktonic decapods (center), NBSSho: holoplankton only, e.g., zooplankton without mero- and ichthyoplankton (below). Blue arrows highlight conspicuous changes in the shape of the NBSS after mero- and ichthyoplankton (NBSSho) or meroplanktonic decapods (NBSSnmd) were removed from the total zooplankton (NBSSz). Areas where points "disappear" in the lower graphs indicate the occurrence of empty bins due the removal of mero- and ichthyoplankton from the data (i.e., possibly relevant contributions of mero- and ichthyoplankton to the zooplankton community). Zooplankton was sampled bimonthly in the Rio Formoso Estuary, in Tamandaré Bay, and on the adjacent continental shelf (Pernambuco, Brazil), from June 2013 to May 2015. n: 121 samples.

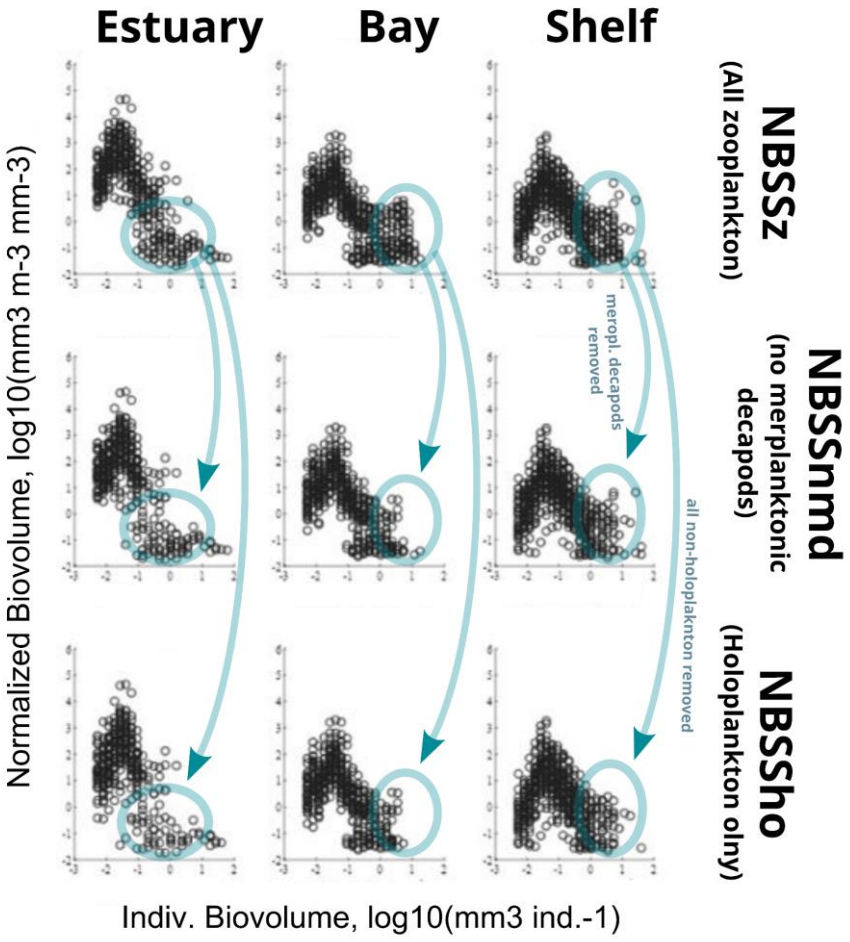

Fonte: A autora (2024).

Figure 8. NBSS for total zooplankton (NBSSz, above), for holoplankton only (NBSSho, holoplankton only, center), and NBSSz - NBSSho (bins which did not appear in NBSSho, below). In blue or green color: points within the size range used for linear models, from -1.5 log10 mm3 to 0.1 log10 mm3, encompassing nine size classes. Red line: Ordinary least squares linear regression. Green line: Robust linear regression. Blue horizontal bar: ”small-sized” fraction used, Orange horizontal bar: ”large-sized” fraction used for empty bin analysis. Regression slopes for NBSSz were not significantly different from NBSSho in any of the three regions. Asterisks: Size fractions with significant differences between numbers of empty bins (NBSSz vs NBSSho). Zooplankton was sampled bimonthly in the Rio Formoso Estuary, in Tamandaré Bay, and on the adjacent continental shelf (Pernambuco, Brazil), from June 2013 to May 2015. n: 121 samples.

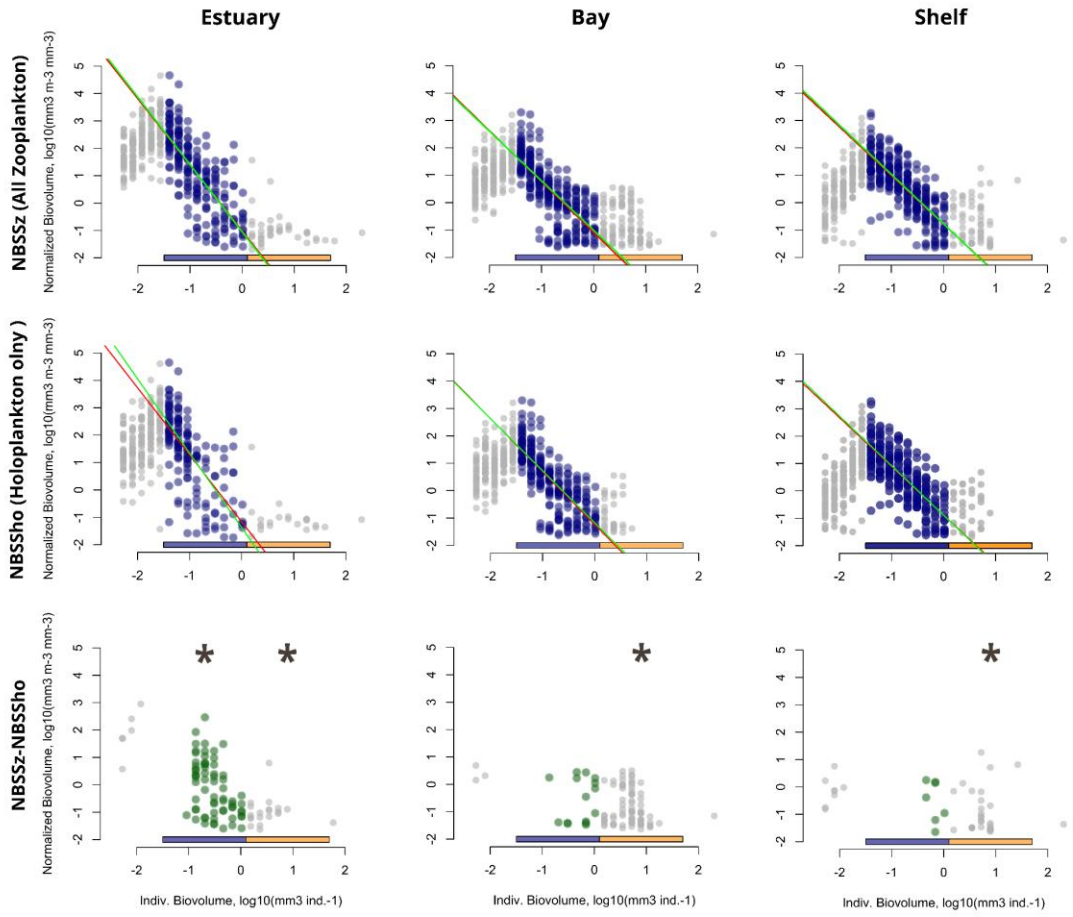

Fonte: A autora (2024).

Comparisons between communities with and without mero- and ichthyoplankton (NBSSz, NBSSho, NBBmd), and between fit methods (OLSR, robust regression) did not detect any significant differences in NBSS slope (permutation ANCOVA, $p > 0.05$). Also, our analyses did not detect any differences between regions, regarding NBSS intercepts (i.e., mean elevation at indiv. biovolume = 1 mm^3, log10 = 0, located at the large-sized limit of the useful linear size range).

3.5 Numbers of empty bins with and without meroplankton

In contrast to linear regression analysis, comparing the numbers of empty bins did actually detect conspicuous, relevant, and significant differences between communities (NBSSz, NBSSho, NBSSnmd), in all study areas (Figs. 7 and 8). There were conspicuous changes in "emptiness" of NBSS when non-holoplankton (NBSSho) or meroplanktonic decapods (NBSSnmd) were removed from the total zooplankton (NBSSz) data. Areas in the NBSS where points "disappear" in the lower graphs of Fig. 7 indicate an increase in empty bins due the removal of non-holoplankton from the data (i.e., conspicuously relevant contributions of mero- and ichthyoplankton to the zooplankton community).

The application of permutation tests detected significant differences in "emptiness" (i.e., the relative numbers of empty bins) between NBSSz and NBSSho, for several datasets (asterisks in Figure 8). In the Estuary, small-sized organisms (0.392 mm to 1.34 mm esd) had significantly ($p < 10\text{-}8$, permutation test) less empty bins in the NBSSz (all zooplankton), than in the NBSSho (without mero- and ichthyoplankton), indicating a significant effect of the input of small-sized meroplankton (e.g., brachyuran zoeae) on the NBSS, within this size fraction. Conversely, in the Bay and Shelf ecosystems, there was no significant difference between NBSSho and NBSSz within the small-sized fraction, indicating that small-sized meroplankton (e.g., brachyuran zoeae) is of lesser importance in these areas, as compared to the overall dominant holoplankton (mostly copepods) in the small-sized fractions of these areas.

A similar result was observed for the “large” size classes (1.34 mm to 4.57 mm esd, or from 0.1 log10 mm3 to 1.7 log10 mm3 biovolume). For large organisms in the Estuary, the difference in empty bins between NBSSz and NBSSho was also significant ($p = 0.01$, permutation test), indicating the existence of relevant contributions of small- (see above) and large-sized meroplankton (e.g., caridean shrimp zoeae) in the Estuary.

The “large-sized” meroplankton classes also displayed highly significant differences between NBSSz and NBSSho in the Bay ($p = 4.7 * 10\text{-}13$, permutation test) and on the Shelf ($p = 0.0025$, permutation test), indicating relevant contributions of large-sized mero- and ichthyoplankton (e.g., *Penaeus* spp. post-larvae and fish larvae) to the size spectrum in these two tropical marine sampling areas.

4 DISCUSSION

The present study analyzed the structure and functioning of tropical estuarine and coastal zooplankton communities through size spectra analysis (SSA), providing for the first time size spectra of decapods and other individual groups of tropical mero- and ichthyoplankton. Most importantly, we provide a theoretical framework and propose a simple, robust practical statistical test, based on the numbers of empty bins. This novel "emptiness test" allowed us to detect highly significant effects of meroplankton inputs on pelagic ecosystems.

Also, our sampling strategy allowed us to investigate the relationships between changes in zooplankton composition and slope and shape of size spectra in three study areas, showing that even the most radical change in meroplankton contributions (i.e., total removal of all non-holoplankton, including larvae of benthic invertebrates, fish eggs, and larvae, larvae of parasites and benthic migrants) did not affect the NBSS slope. This confirms the concept that the NBSS slope is a robust, conservative property of an ecosystem that is defined by food web (trophic transfer and its efficiency), population (e.g., mortality) and physiological (e.g., growth) processes that occur within the water column (Lira *et al.*, 2024). Also, the present study is the first to reveal the density-dependent predatory effect of brachyuran crab zoeae on same-sized copepods using a size-spectra approach.

Taxon-specific size spectra showed that brachyuran zoeae create and fill a gap within the copepod size spectrum, thus contributing to a continuous ("gap-free") total zooplankton spectrum (Figs. 3 and 4). In the estuary, brachyuran crab larvae were thus the single most important taxon to fill the "gaps" (empty bins) in the holoplankton and can thus be considered to be the main causative for the significant differences detected when comparing empty bins between NBSSz and NBSSho, for the "small" size fraction, in the estuary (green dots in Fig 8).

This study provided the first SSA for a tropical estuary. The NBSS slope of tropical estuarine zooplankton found in our study (slope = -2.45 +- 0.16) is the steepest median NBSS slope for any natural ecosystem reported so far. The NBSS slopes that we found in oligotrophic tropical marine systems, such as the reef-lined bay (slope = -1.81 +- 0.10) and shelf (slope = -1.80 +- 0.09) ecosystems, are also far steeper than most data found in the literature (e.g. San Martin *et al.*, 2006, Vandromme *et al.*, 2014, Marcolin *et al.*, 2015, Lira *et al.*, 2024), which is clearly due to the large abundance and "steep" (mostly small-sized) size structure of copepods, that overwhelmingly dominate the size range analyzed in our study.

Our detailed analyses proved that the observation of an unexpectedly steep slope is not due to meroplankton inputs (see test results above), nor due to contamination with detritus particles (removed from the data prior to analysis), but is rather an intrinsic property of the pelagic ecosystems studied herein, which has important consequences for the interpretation of size spectra.

4. 1 Empty bins - nuisance or valuable information?

Empty bins are a ubiquitous phenomenon in size spectra analyses, that are generally based on binning (i.e., grouping organisms into size classes). The existence of empty bins in NBSS, the need to use geometrically increasing bin widths, and subsequent normalization of the data, and the need to use log-log plots, are all due to the innate "heavy-tailed" characteristic of power-law (or Pareto) distributions, that generally become linear when log-log transformed (Vidondo *et al.*, 1997; Edwards *et al.*, 2020). In studies that dealt explicitly with empty bins in size spectra, they were regarded as a sign of serious flaw of the NBSS method, as an unsolved issue, or at best, as a nuisance to be avoided. Numerous analyses and approaches have been proposed to avoid or exclude empty bins in NBSS analysis (Yurista *et al.*, 2005; Edwards *et al.*, 2017; Edwards *et al.*, 2020). Furthermore, one of the main reasons for the development of non-binned alternative analysis approaches, such as maximum likelihood estimation of size spectra (Edwards *et al.*, 2017) has been the prerogative to avoid the deleterious effect of empty bins on spectra analyses, more specifically, the effect that these gaps have on the estimation of NBSS slopes.

This study proposes a new approach towards empty bins. Instead of simply avoiding and ignoring them, we consider the number of empty bins as a valuable source of information, and propose the analysis of empty bins as a tool for understanding the processes that shape size spectra in natural ecosystems. For instance, in our study, we successfully applied the analysis of empty bins to evaluate the changes in "emptiness" of the size spectrum that occur due to the input of specific taxonomic groups into the water column, such as the larvae of decapod crustaceans.

One apparent drawback of this approach is that the number of empty bins intrinsically depends on the chosen bin size. A choice of smaller bins will lead to overall more bins and also, relatively more empty bins. Obviously, the subjective choice of bin size and of the progressive exponent of the beginning vector will have an effect on the occurrence of empty bins. However, when different datasets are compared using the same bins sizes (as in our comparison of NBSSz, NBSSnmd, and NBSSho, all built with exactly the same binning vector), this effect can be ignored as a potential source of error within such comparisons. The comparison of the numbers of empty bins before and after removing specific groups, as applied here, can be a powerful tool to investigate the contributions of specific taxa or communities to the size spectrum.

4.2 NBSS slopes - conservative ecosystem descriptors

Our study confirms that the slope of the NBSS is a conservative parameter, characteristic of each ecosystem, that is not changed by the addition of meroplankton. Meroplankton is clearly not the cause for the extremely steep NBSS slope observed for estuarine zooplankton (slope = -2.45 +- 0.16). This slope value is considerably steeper than the often cited theoretical "constant" slope of -1 for zooplankton in the world's oceans (Zhou and Huntley, 1997).

Yet, it is still unclear which factors are responsible for the extremely steep size spectra slopes observed in this study, specifically in the estuary. Recent studies have attempted to explain variations in size spectra slopes through a trophic-metabolic approach (Figueiredo *et al.*, 2020), where the determinant factors were predator / prey size ratio (PPMR), trophic efficiency (TE), and metabolic scaling (MS). Both TE and MS may be influenced by ambient conditions, such as temperature, oxygen, and variations in salinity. Estuaries are extremely stressful, variable and turbulent environments. Physiological and physical stress may be one possible explanation for the observed steep NBSS slope. Under the assumption that the NBSS slope is a proxy for TE, our results could mean that tropical estuaries are extremely inefficient ecosystems, regarding the transfer of energy and matter from one trophic level to the next one. Also, the "apparent inefficiency" due to advective export (of holoplankton, but especially also of meroplanktonic larvae) from the estuary may contribute to the steep NBSS slopes. In this simple conceptual model of the tropical mangrove estuary, extremely high abundances of small-sized copepods are effectively preyed upon by decapod larvae (as proven by our analyses). According to the "apparent inefficiency" concept, these larvae are subsequently exported from

the estuary and complete their development in adjacent marine waters. Advective losses are usually not considered in the analysis and interpretation of NBSS slopes, but may be especially relevant in estuarine systems.

Our results confirm the idea that NBSS slopes are conservative characteristics of pelagic ecosystems. Although slopes steeper than - 1 have been observed in other tropical areas (e.g., Marcolin *et al.*, 2015), the slopes reported here are the steepest ever reported for natural zooplankton. This could be due to the fact that tropical estuarine zooplankton has not yet been intensively investigated regarding its NBSS slopes, as opposed to the vast literature on marine zooplankton from temperate and polar seas (e.g.,Vandromme *et al.*, 2014; Lombard *et al.*, 2019; Atkinson *et al.*, 2021). Ke *et al.* (2018) reported zooplankton size spectra slopes from −1.02 to zero in the subtropical Pearl River estuary (South China). The unusually flat NBSS slopes found in the Pearl River estuary were interpreted by the authors as being due to an unstable zooplankton community in the upper estuary (slope = zero) because of strong freshwater perturbations in the rainy season. However, the Pearl River estuary is one of the most polluted estuaries worldwide, and this effect may also have affected the zooplankton data. Our data are from the lower ranges of a well-preserved mangrove estuary, in a tropical marine protected area, with much higher temperature, constantly higher salinities and lower pollutant concentrations than the upper estuary regions of the Pearl River estuary.

A recent study based on Atlantic Meridional Transects across the Atlantic reported NBSS slopes from −0.93 to −1.46, with steeper slopes (steeper than -1) in the tropical oceanic stations (San Martin *et al.*, 2006). In a subtropical coastal upwelling ecosystem off São Paulo (southeastern Brazil) Marcolin *et al.* (2015) also found steep NBSS slopes, with values below -3 for several samples, but median with slopes of approximately -1.5 to -1, considerably less steep than in the present study.

In all three sampling areas, calanoid copepods (mostly *Acartia* spp.) were dominant and determinant for the slope of the NBSS. Cyclopoid and harpacticoid copepods were negligible in units of biovolume, in our study. The low abundance or absence of extremely small-sized cyclopoid copepods, such as the ubiquitous Oithonidae, is probably due to the relatively large mesh size used (300 micron) in our sampling program. Much smaller mesh sizes (e.g. 50, 64, or 100 micron meshes) were usually employed in studies that intend to quantify the copepod composition within the microzooplankton. Such studies with small mesh sizes, found

cyclopoid copepods of the family Oithonidae to be the key taxon (Yahia *et al.*, 2004; Dias and Bonecker, 2008; Bhattacharya et., 2015; Neumann Leitão *et al.*, 2019; Brito-Lolaia *et al.*, 2022). Yet, similarly to our study, in many studies that used larger mesh sizes (> 120 microns), copepods of the genus *Acartia* spp. were reported among the most important of the mesozooplankton in estuaries and coastal waters of the Southwest Atlantic (Silva *et al.*, 2003; Silva *et al.*, 2004; Sterza and Fernandes, 2006; Magalhães *et al.*, 2009; Escamilla *et al.*, 2011). *Acartia (odontacartia) lilljeborgii* is the most frequent *Acartia* species in Brazil. Similarly to our results, previous studies also showed that *A. lilljeborgii* is extremely abundant in estuaries, coastal waters and inner shelf areas, and disappears towards offshore areas under oligotrophic oceanic water influence (Lopes *et al.*, 2006; Sartori and Lopes, 2000).

The differences in slope (and hence, in relative biovolume of small sized calanoids) between areas can be possibly due to variations in species composition, but also due to variations in size structure within species. Intraspecific variations in size structure can be fully explained by a combination of higher productivity and higher mortality/growth ratios (Schwamborn, 2018). It is well known that productive ecosystems, such as estuaries, are “food heaven” and “predation hell” (Bakun, 2006). Whether this apparently high mortality in the Rio Formoso estuary is due to high predation (Schwamborn *et al.*, 2006) or non-predatory mortality (Silva *et al.*, 2020), apparent mortality due to advective export from the Estuary, or due to extreme physiological stress in such a highly variable and temporarily hypoxic environment (Schwamborn and Silva, 1996) are key questions that are still to be investigated by future studies.

4.4 Dynamic size-niche interactions between copepods and brachyuran zoeae

The present study revealed conspicuous and statistically significant size-niche interactions between holoplanktonic copepods (mostly the herbivorous *Acartia* spp.) and the dominant carnivorous meroplanktonic organisms (brachyuran zoeae). We found conspicuous peaks in brachyuran zoea size spectra that coincided with throughs and gaps in copepod size spectra. In the Estuary, such conspicuous negative interactions were observed for the vast majority of samples (32 out of 38 samples, 84 %). Also, for the whole estuarine data set, and in most estuarine samples, non-parametric Spearman rank correlation analysis detected

significantly negative correlation between these two taxa. Furthermore, no samples with positive correlations between these two taxa were found in any sample within our three study areas. A significant negative correlation was observed for most samples (21 out of 38 samples, 55%) in the Estuary, and for several samples in Bay and Shelf areas, where brachyuran zoeae were abundant. These results indicate a strong negative interaction between these two taxa.

Similarly, Schwamborn *et al.* (2024) also found strong and significant negative interactions between copepods and brachyuran zoeae when analyzing the correlation between their total abundances and total biomass in this study area, within a study on their spatiotemporal variability.

Conversely, positive correlations between any two given holoplankton taxa can be predicted by physical (accumulation of all organisms in discrete convergence zones, within patchy distributions) and biogeochemical models (variability in holoplankton abundance driven by biogeochemical drivers that affect nutrient flux, primary production and food availability). That is why positive correlations between many different taxa is an ubiquitous feature, found in most zooplankton surveys (Wiebe, 1970; Schwamborn *et al.*, 2001; Greer *et al.*, 2016).

This indicates that the unexpected negative correlations observed by Schwamborn *et al.* (2024) and in the present study are derived from hitherto ignored negative size-structured interactions between copepods and brachyuran zoeae. The size spectra analysis presented herein further confirms existence of a negative interaction between these two taxa within the estuarine zooplankton. Also, we proved that this interaction is density-dependent, being driven by brachyuran larval (predator) density only (Fig. 6), which indicates a relevant top-down regulation process.

Our size spectra analysis revealed new size-niche interaction phenomena that were hitherto ignored and opens up a new area of research within size-based community and food-web ecology. Interestingly, negative interaction was only observed when there were extremely high numbers of brachyuran zoeae added to the estuarine holoplankton, which already presented a record high abundance of copepods. This addition of brachyuran zoeae clearly and significantly removed significant and large numbers of copepods within the same size niche occupied by brachyuran zoeae. It is not completely impossible that estuarine copepods were avoiding the incoming patch of similarly sized-brachyuran zoeae (e.g., vertically, by diving into

deeper strata, or laterally, by leaping away from zoea-rich patches). Yet, the most obvious explanation for this phenomenon is that incoming patches of crab zoeae negatively affect similarly-sized copepods through active predation.

Such a predatory behavior of crab zoeae was already demonstrated by Schwamborn *et al.*, (2006), within controlled laboratory experiments. In their experiments, recently hatched zoea I larvae of the mangrove crab *Aratus pisonii,* a small-sized brachyuran zoea larva, preyed upon similar-sized copepods and significantly removed them from their experiments (Schwamborn *et al.,* 2006). Our study is the first to demonstrate this phenomenon in the field. Although there is vast evidence that such zoeae can feed upon smaller-sized particles, such as phytoplankton and protozoans (Factor and Dexter, 1993; Perez and Sulkin, 2005; Schwamborn *et al.*, 2006; Shaber and Sulkin, 2007), preying upon similarly-sized abundant copepods may be an additional, effective feeding strategy, especially when copepods are very abundant. However, it is not clear whether the zoeae feed upon living copepods or on carcasses of recently deceased adult copepods, which are highly abundant in the study area (Silva *et al.*, 2020). All planktonic copepod species ever investigated possess a range of highly effective predation advance strategies and behaviors, such as fast, directional, jumps (Kiørboe *et al.*, 1999; Ardeshiri *et al.*, 2017), although at least some species seem to exhibit fatigue after several successive escape jumps (van Duren and Videler, 2003). Given the ubiquitous nature of negative correlations between copepods and brachyuran zoeae in the mangrove estuary of our study area (it was observed in most estuarine samples, and in virtually all samples that contained large numbers of brachyuran zoeae), the large numbers of copepods removed, and the fact that for calanoid adult copepods, the numbers of carcasses are estimated at less than 10%, it is highly likely that brachyuran zoeae did effectively prey upon living calanoid copepods, under conditions of high abundance and intensive, frequent prey encounter, and high turbulence, in estuarine convergence zones. Predation upon carcasses and living prey does not exclude each other. Rather, utilizing both types of food (living or carcasses) is observed in most carnivores. The fact that decapod larvae are usually fed with living, large-sized *Artemia* nauplii in standard commercial larviculture and scientific experiments (e.g., Coelho-Filho *et al.*, 2018, Van Eyde *et al.*, 2019), is a further indication of the predatory capabilities of these meroplankters.

The densities of copepods and brachyuran zoeae in Northeast Brazilian estuaries are among the highest reported in the literature (Schwamborn *et al.*, 1999; Schwamborn *et al.*, 2001, Schwamborn *et al.*, 2024), probably due to the huge adult crab biomass and biodiversity

in these vast mangrove ecosystems. Furthermore, it is important to consider that abundance estimated from plankton tows represents an average across extremely patchy spatial distributions. Therefore, much higher *in situ* abundances likely occur, especially when considering accumulation within strong convergence zones that are very common in such estuaries (Schwamborn and Saint Paul, 1996; Schwamborn *et al.*, 2001; Melo *et al.*, 2007).

Instead of smooth additive effects, we found large numbers of discrete gaps that were revealed when removing these organisms within the meroplankton removal experiments (NBSSz vs NBSSholo). Most importantly, such interaction phenomena are not detectable when looking at the mean spectrum only (regardless of whether using mean NBSS or mean size-frequency distributions). Only when analyzing the spectrum station-by-station, such phenomena become evident.

The detailed sample-by-sample analysis (e.g., Figure 3) helps explain the gaps "filled" by meroplankton or rather, the gaps "carved" into the holoplankton size spectrum by these predatory larval organisms during pulses of larval release, wich are instantaneously filled by these added meroplankton. This key density-dependent negative interaction mechanism, that shapes the estuarine size spectrum, has not been considered in any previous studies, or in any theoretical work on size spectra theory.

4.4 Filling the gaps - taxon-specific size niche processes that lead to continuous size spectra

Few studies have analyzed the taxon-specific composition of marine zooplankton size spectra, and none have analyzed the contributions of meroplanktonic decapod larvae to estuarine size spectra. The vast majority of such studies concentrate on holoplankton groups such as copepods, appendicularian, chaetognaths, euphausiids, molluscs and thaliaceans.

Kwong *et al.* (2022) recorded the dominance of small copepods (*Acartia* spp., *Oithona* spp., *Pseudocalanus* spp.) throughout an entire time series, as large copepods were present in offshore regions in the NE Pacific. Mesozooplankton were well distributed among taxonomic groups. Crustaceans (copepods and malacostracans) and chaetognaths were the dominant groups. In the tropical Abrolhos shelf region (Brazil), chaetognaths and salps contributed most of all to the biomass due to their large size (Marcolin *et al.*, 2013), and additionally, the biomass

of decapods represented more than 5% of the total biomass of the mesozooplankton. Calanoids were more numerous in the shelf area, which agrees with what was described by Kwong *et al.* (2022). Quiroga *et al.* (2014) mentioned adult decapods in their evaluation of the macrobenthos size spectrum (Hippolytidae, Crangonidae), among other groups such as Cnidaraia, Mollusca, Bivalvia, and Gastropoda.

Several authors have used the specific contributions of multiple taxa to explain the log-linearity (i.e., power-law shape) and continuity of natural size spectra, with data obtained from natural ecosystems (Zhou and Huntley, 1997; Cavender-Bares *et al.*, 2001; Zhou, 2006), but without analyzing specific prey-predator interactions and evolutionary size niche processes. *A priori*, there is no obvious reason why a size spectrum should be continuous ("gap-free") and log-linear within a power-law distribution. Interestingly, continuous power-law distributions have been reported from numerous areas of science, including ecology, geography, astronomy, economy, semiotics, and sociology, for seston particles, and terrestrial invertebrate communities (Vidondo *et al.*, 1997). Continuous power-law distributions have been found for virtually all aquatic communities (pelagic and benthic, marine and freshwater) ever studied, including microbial communities (Cavender-Bares *et al.*, 2001).

For a community composed of numerous different species and life history stages, the question emerges what processes could force a given species to fill in a specific gap in the size spectrum, instead of superposing an existing peak in the spectrum (which would, in theory, lead to peak-shaped community spectra, instead of log-linear shapes). From an evolutionary perspective, the question is what selective advantage can be obtained by a species through filling a "gap" and fitting into a continuous power-law distribution, relative to other positions within the size spectrum. The most likely explanation is that evolutionary pressures lead species and life history stages to occupy and compete for vacant "size niches" in the size spectrum.

For example, *Penaeus* spp. post-larvae and pre-settlement stage fish larvae were found to be not displaying any superposition ever, of their size distributions in all mean spectra and in individual samples, indicating a competition avoidance strategy, from a "size-niche" perspective. However, the selective advantages of filling in gaps and avoiding size overlaps are not obvious. From a predation avoidance perspective, it may be advantageous not to stand out within the background size spectrum, as not to be the target of size-selective predators. Furthermore, from a feeding efficiency perspective, it may be advantageous to occupy available

prey size niches within the prey size spectrum. This will also lead to gap-filling within specific size niches, if predator size distributions are related to prey size and are directly related (see below). While the concept of "prey size niche" is well established within niche theory (Baker *et al.*, 2022), the concept of body size niche has not yet been analyzed in detail in the available literature.

All interpretations above are based on the assumption that there is a relationship between body size, prey size and trophic level (TL). The existence of a rigorously size-structured food web (where an organism's TL is defined primarily by body size) has been generally assumed in all theoretical approaches and size spectrum models (Zhou and Huntley, 1997; Zhou, 2006; Taniguchi *et al.*, 2014), but has rarely been tested in natural ecosystems. The existence of a significant size-TL relationship has recently been proven by using nitrogen stable isotope measurements of size-fractionated zooplankton samples (Figueiredo *et al.*, 2020). The ubiquitous observation that plankton size spectra are continuous and log-linear, with a constant slope across the communities (e.g., phyto- and zooplankton), supports the idea of trophic regulation between TLs (top-down and bottom-up), although multi-modal dome-shaped patterns may emerge under certain conditions, with trophic cascades (Rossberg *et al.*, 2019).

Top-down (predation avoidance) and bottom-up (feeding efficiency) processes also lead to size-selective pressures that drive a given species to find and fill gaps within the background size spectrum. In our study, density-dependency was only significant for predator (brachyuran zoeae) densities, indicating a relevant top-down regulation process in these ecosystems, with regular seasonal inputs of predatory carnivorous zoeae (Schwamborn *et al.*, 2024). Additionally to density-dependent negative (predation-mediated) interactions, such as observed for copepods and brachyuran zoeae, multiple food-web regulation processes may help explain the ubiquity of power law size spectra found in ecosystems with size-structured food webs.

REFERENCES

Ardeshiri, H., Schmitt, F. G., Souissi, S., Toschi, F., & Calzavarini, E. (2017). Copepods encounter rates from a model of escape jump behavior in turbulence. *Journal of Plankton Research*, *39*(6), 878-890.

Ara, K. (2001). Length-weight relationships and chemical content of the planktonic copepods in the Canan beta a Lagoon estuarine system, São Paulo, Brazil. *Plankton Biology and Ecology*, *48*(2), 121-127.

Atkinson, A., Lilley, M. K., Hirst, A. G., McEvoy, A. J., Tarran, G. A., Widdicombe, C., ... & Somerfield, P. J. (2021). Increasing nutrient stress reduces the efficiency of energy transfer through planktonic size spectra. *Limnology and Oceanography*, 66(2), 422-437. https://doi.org/10.1002/lno.11613

Bakun, A. (2006). Wasp-waist populations and marine ecosystem dynamics: navigating the "predator pit" topographies. *Progress in oceanography*, *68*(2-4), 271-288. https://doi.org/10.1016/j.pocean.2006.02.004

Baker, H. K., Bruggeman, C. E. F. & Shurin, J. B. (2022). Population niche width is driven by within-individual niche expansion and individual specialization in introduced brook trout in mountain lakes. *Oecologia*, 200, 1–10. https://doi.org/10.1007/s00442-022-05201-z

Bhattacharya, B. D., Hwang, J. S., Sarkar, S. K., Rakhsit, D., Murugan, K., & Tseng, L. C. (2015). Community structure of mesozooplankton in coastal waters of Sundarban mangrove wetland, India: a multivariate approach. *Journal of Marine Systems*, *141*, 112-121.

Blanchard, J. L., R. F. Heneghan, J. D. Everett, R. Trebilco, & A. J. Richardson. (2017). From bacteria to whales: Using functional size spectra to model marine ecosystems. *Trends in Ecology and Evolution*, 32, 174–186. https://doi.org/10. 1016/j.tree.2016.12.003

Breiman, L., (2001). Random forests. *Machine Learning*, 45, 5–32. https://doi: 10.1023/A:1010933404324

Boltovskoy, D. (1999). *South Atlantic Zooplankton*. Leiden, Backhuys Publishers. 1706p.

Brito-Lolaia, M., Figueiredo, G. G. A. A., Neumann, L., S., Yogui, G. T., & Schwamborn, R. (2022). Can the stable isotope variability in a zooplankton time series be explained by its key species? *Marine Environmental Research*, *181*, 105737. https://doi.org/10.1016/j.marenvres.2022.105737

Brown, J. H., Gillooly, J. F., Allen, A. P., Savage, V. M., & West, G. B. (2004). Toward a metabolic theory of ecology. *Ecology*, 85(7), 1771-1789.

Cavender-Bares, K. K., Rinaldo, A., & Chisholm, S. W. (2001). Microbial size spectra from natural and nutrient enriched ecosystems. *Limnology and Oceanography*, 46(4), 778-789. https://doi: 10.4319/lo.2001.46.4.0778

Chew, L. L., & Chong, V. C. (2011). Copepod community structure and abundance in a tropical mangrove estuary, with comparisons to coastal waters. *Hydrobiologia, 666*, 127-143.

Coelho-Filho, P. A., Gonçalvez, A. P., & Barros, H. P. (2018). Artemia nauplii intake by *Macrobrachium carcinus* at different larval stages in laboratory. Aquaculture, 484, 333-337.

Couret, M., Landeira, J. M., Tuset, V. M., Sarmiento-Lezcano, A. N., Vélez-Belchí, P., & Hernández-León, S. (2023). Mesozooplankton size structure in the Canary Current System. *Marine Environmental Research*, 188, 105976. https://doi.org/10.1016/j.marenvres.2023.105976

Dias, C. D. O., & Bonecker, S. L. C. (2008). Inter-annual variability of planktonic copepods in a tropical bay in southeastern Brazil. *Brazilian Archives of Biology and Technology*, 51(4),731–42.

Dickie, L. M., Kerr, S. R., & Boudreau, P. R. (1987). Size-dependent processes underlying regularities in ecosystem structure. *Ecological monographs*, 57(3), 233-250. https://doi.org/10.1111/gcb.12231

Edwards, A. M., Robinson, J. P. W., Plank, M. J., Baum, J. K., Blanchard, J. L., & Matthiopoulos, J. (2017). Testing and recommending methods for fitting size spectra to data. *Methods in Ecology and Evolution*, 8(1), 57–67. https://doi.org/10.1111/2041-210x.12641

Edwards, A. M., Robinson, J. P., Blanchard, J. L., Baum, J. K., & Plank, M. J. (2020). Accounting for the bin structure of data removes bias when fitting size spectra. *Marine Ecology Progress Series, 636*, 19-33.

Escamilla, B. J., Ordóñez-López, U., Suárez-Morales, E. (2011). Spatial and seasonal variability of Acartia (Copepoda) in a tropical coastal lagoon of the southern Gulf of Mexico. *Revista de Biología Marina y Oceanografía*, 46(3), 379:390.

Factor, J. R., & Dexter, B. L. (1993). Suspension feeding in larval crabs (Carcinus maenas). *Journal of the Marine Biological Association of the United Kingdom*, *73*(1), 207-211.

Figueiredo, G. G. A. A., Schwamborn, R., Bertrand, A., Munaron, J. M., Le Loc'h, F. (2020). Body size and stable isotope composition of zooplankton in the western tropical Atlantic. *Journal of Marine Systems*, 212, 103449. https://doi.org/10.1016/j.jmarsys.2020.103449

Gaedke, U. (1993). Ecosystem analysis based on biomass size distributions: a case study of a plankton community in a large lake. *Limnology and Oceanography*, 38(1), 112-127.

Gaedke, U., & Straile, D. (1998). Daphnids-Keystone species for the pelagic food web structure and energy flow: a body size-related analysis linking seasonal changes at the population and ecosystem levels. *Advances in Limnology*, 53, 587-610.

Gorsky, G., Ohman, M. D., Picheral, M., Gasparini, S., Stemmann, L., Romagnan, J. B., Cawood, A., Pesant, S., Garcia-Comas, C., Prejger, F. (2010). Digital zooplankton image analysis using the ZooScan integrated system. *Journal of Plankton Research*, 32, 285–303. https://doi.org/10.1093/plankt/fbp124

Greer, A. T., Woodson, C. B., Smith, C. E., Guigand, C. M., & Cowen, R. K. (2016). Examining mesozooplankton patch structure and its implications for trophic interactions in the northern Gulf of Mexico. *Journal of Plankton Research*, *38*(4), 1115-1134.

Hampel, F. R., Ronchetti, E. M., Rousseeuw, P. J., & Stahel, W. A. (1986). *Robust statistics*: *the approach based on influence functions*. John Wiley & Sons.

Hobbie, J. E., Holm-Hansen, O., Packard, T. T., Pomeroy, L. R., Sheldon, R. W., Thomas, J. P., & Wiebe, W. J. (1972). A study of the distribution and activity of microorganisms in ocean

water 1. *Limnology and oceanography*, 17(4), 544-555. https://doi.org/10.4319/lo.1972.17.4.0544

Hopcroft, R. R., & Roff, J. C. (1998). Zooplankton growth rates: the influence of female size and resources on egg production of tropical marine copepods. *Marine biology*, *132*, 79-86.

Hothorn, T., Hornik, K., Van de Wiel, M. & Zeileis, A. (2006). COIN: conditional inference procedures in a permutation test framework. World Wide Web electronic publication, accessible at https://cran.r-project.org/web/packages/coin/coin.pdf (Accessed 06/27/2020).

Ke, Z., Tan Y., Huang, L., Liu, J., Liu, H. (2018). Community structure and biovolume size spectra of mesozooplankton in the Pearl River estuary. *Aquatic Ecosystem Health & Management*, 21(1), 30–40. https://doi.org/10.1080/14634988.2018.1432948

Kerr, S. R. (1974). Theory of size distribution in ecological communities. *Journal of the Fisheries Board of Canada*, *31*(12), 1859-1862.

Kiørboe, T., Saiz, E., & Visser, A. (1999). Hydrodynamic signal perception in the copepod Acartia tonsa. *Marine Ecology Progress Series*, *179*, 97-111.

Krupica, K. L., Sprules, W. G., & Herman, A. W. (2012). The utility of body size indices derived from optical plankton counter data for the characterization of marine zooplankton assemblages. *Continental Shelf Research*, 36, 29-40.

Kwong, L. E., Ross, T., Lüskow, F., Florko, K. R., & Pakhomov, E. A. (2022). Spatial, seasonal, and climatic variability in mesozooplankton size spectra along a coastal-to-open ocean transect in the subarctic Northeast Pacific. *Progress in Oceanography*, 201, 102728. https://doi.org/10.1016/j.pocean.2021.102728

Lira, S. M., Schwamborn, R., de Melo Júnior, M., Varona, H. L., Queiroz, S., Veleda, D., Silva, A.J., Neumann-Leitão, S., Araujo, M. & Marcolin, C. R. 2024. Multiple island effects shape oceanographic processes and zooplankton size spectra off an oceanic archipelago in the Tropical Atlantic. J. Mar. Sys., 242, 103942.

Lombard F., Boss E., Waite A. M., Vogt M., Uitz J., Stemmann L., Sosik, H. M., … Appeltans, W. (2019). Globally consistent quantitative observations of planktonic ecosystems. *Frontiers in Marine Science*, 6, 196. https://doi.org/10.3389/fmars.2019.00196

Lopes, R. M., Katsuragawa, M., Dias, J. F., Montú, M. A., Muelbert, J. H., Gorri, C., & Brandini, F. P. (2006). Zooplankton and ichthyoplankton distribution on the southern Brazilian shelf: an overview. *Scientia Marina*, 70(2), 189-202.

Magalhães, A., Costa, R. D., Liang, T. H., Pereira, L. C. C., & Ribeiro, M. J. S. (2006). Spatial and temporal distribution in density and biomass of two Pseudodiaptomus species (Copepoda: Calanoida) in the Caeté river estuary (Amazon region-North of Brazil). *Brazilian Journal of Biology*, *66*, 421-430.

Magalhães, A., Nobre, D. S. B., Bessa, R. S. C., Pereira, L. C. C., & Costa, R. M. (2013). Diel variation in the biomass and productivity of *Acartia tonsa* (Copepoda: Calanoida) in a tropical estuary (Taperaçu, northern Brazil). *Journal of Coastal Research*, 65 (10065), 1164–1169.

Marcolin, C. R., Schultes, S., Jackson, G. A., & Lopes, R. M. (2013). Plankton and seston size spectra estimated by the LOPC and ZooScan in the Abrolhos Bank ecosystem (SE Atlantic). *Continental Shelf Research*, *70*, 74-87. https://doi.org/10.1016/j.csr.2013.09.022

Marcolin, C. R., Gaeta, S., & Lopes, R. M. (2015). Seasonal and interannual variability of zooplankton vertical distribution and biomass size spectra off Ubatuba, Brazil. *Journal of Plankton Research*, 37(4), 808-819. https://doi.org/10.1093/plankt/fbv035

Melo Júnior, M. D., Paranaguá, M. N., Schwamborn, R., Leitão, S. N., & Ekau, W. (2007). Fluxes of zooplankton biomass between a tidal estuary and the sea in Northeastern Brazil. *Brazilian Journal of Oceanography*, *55*, 239-249.

Moriarty, R., Buitenhuis, E. T., Le Quéré, C., & Gosselin, M. P. (2013). Distribution of known macrozooplankton abundance and biomass in the global ocean. *Earth System Science Data*, 5(2), 241-257. https://doi.org/10.5194/essd-5-241-2013

Neumann Leitão, S., Melo Junior, M. D., Porto Neto, F. D. F., Silva, A. P., Diaz, X. F. G., Silva, T. D. A. E., … Schwamborn, R. (2019). Connectivity between coastal and oceanic zooplankton from Rio Grande do Norte in the Tropical Western Atlantic. *Frontiers in Marine Science*, *6*, 287.

Omori, M. & T. Ikeda. (1984). Methods in Marine Zooplankton Ecology. *John Wiley & Sons*, New York, 332 pp.

Platt, T., & Denman, K. (1977). Organisation in the pelagic ecosystem. *Helgoländer Wissenschaftliche Meeresuntersuchungen*, *30*, 575-581.

Platt, T. & Denman, K. (1978). The structure of pelagic marine ecosystems. *Rapp. P-v. Reun. Cons. Int. Explor. Mer* 173, 60-65.

Platt, T. (1985). Structure of the marine ecosystem: its allometric basis. In Ecosystem theory for biological oceanography. Edited by R.E. Ulanowicz and T. Platt.*Canadian Bulletin of Fisheries and Aquatic Sciences* 213, 55–64.

Parsons TR (1969). The use of particle size spectra in determining the structure of a plankton community, Journal of the Oceanographical Society of Japan, 25(4):172-181.

Perez, M. F., & Sulkin, S. D. (2005). Palatability of autotrophic dinoflagellates to newly hatched larval crabs. *Marine Biology*, *146*(4), 771-780.

Quah, W. C., Chew, L. L., Chong, V. C., Chu, C., Teoh, C. Y., & Ooi, A. L. (2022). Does structural change in the zooplankton community affect larval fish feeding in anthropogenically disturbed tropical waters?. *Environmental Biology of Fishes*, *105*, 55-76. https://doi.org/10.1007/s10641-021-01189-2

Quiroga, E., Gerdes, D., Montiel, A., Knust, R., & Jacob, U. (2014). Normalized biomass size spectra in high Antarctic macrobenthic communities: linking trophic position and body size. *Marine Ecology Progress Series*, 506, 99-113.

R Core Team. (2022). R: A Language and Environment for Statistical Computing. *R Foundation for Statistical Computing*, Vienna, Austria, 2022, Version 4.1.3

RStudio Team, (2022). *RStudio: Integrated Development for R*, Version 2022.02.0. https://www.rstudio.com.

Ray, S., Berec, L., Straškraba, M., & Jørgensen, S. E. (2001). Optimization of exergy and implications of body sizes of phytoplankton and zooplankton in an aquatic ecosystem model. *Ecological Modelling*, 140(3), 219-234.

Rykaczewski, R. R., & Checkley Jr, D. M. (2008). Influence of ocean winds on the pelagic ecosystem in upwelling regions. *Proceedings of the National Academy of Sciences*, 105(6), 1965-1970.

Rodríguez, J. (1994). Some comments on the size-based structural analysis of the pelagic ecosystem. *Scientia Marina*, 58(1-2), 1-10.

Rossberg, A. G., Gaedke, U., & Kratina, P. (2019). Dome patterns in pelagic size spectra reveal strong trophic cascades. *Nature communications*, *10*(1), 4396. https://doi.org/10.1038/s41467-019-12289-0

San Martin, E., Harris, R. P., & Irigoien, X. (2006). Latitudinal variation in plankton size spectra in the Atlantic Ocean. *Deep Sea Research Part II: Topical Studies in Oceanography*, *53*(14-16), 1560-1572. https://doi.org/10.1016/j.dsr2.2006.05.006

Sartori, L. P., & Lopes, R. M. (2000). Seasonal variability of pelagic copepod assemblages on the inner shelf off Paraná, Brazil. *Nauplius*, 79-88.

Schwamborn, R. (2018). How reliable are the Powell–Wetherall plot method and the maximum-length approach? Implications for length-based studies of growth and mortality. *Reviews in Fish Biology and Fisheries*, *28*(3), 587-605.

Schwamborn, R., & Saint-Paul, U. (1996). Mangroves-forgotten forests?.Centre for Tropical Marine Ecology. *Natural Resources and Development*, *43*(44), 13-36.

Schwamborn, R. & Silva, T. A. (1996). Comparação da restistência de duas comunidades zooplanctônicas (Canal de Santa Cruz e Praia do Pilar, Itamaracá, Pernambuco, Brasil) ao choque hipoosmótico. Um estudo eco-fisiológico preliminar. *Trabalhos Oceanográficos*, UFPE, Recife, 24, 135-143.

Schwamborn, R., Ekau, W., Pinto, A. S., Silva, T. A., Saint-Paul, U. (1999). The contribution of estuarine decapod larvae to marine macrozooplankton communities in northeast Brazil. *Archive of Fishery and Marine Research*, 47 (2/3), 167–182.

Schwamborn, R., Neumann-Leitão, S., Silva, T. A., Silva, A. P., Ekau, W., & Saint-Paul, U. (2001). Distribution and dispersal of decapod crustacean larvae and other zooplankton in the Itamaracá estuarine system, Brazil. *Tropical Oceanography*, *29* (1), 1-18.

Schwamborn, R., Ekau, W., Silva, A. P. Schwamborn, S. H. L., Silva, T. A. Neumann-Leitão, S., & Saint- Paul, U. (2006). Ingestion of large centric diatoms, mangrove detritus, and zooplankton by zoeae of *Aratus pisonii* (Crustacea: Brachyura: Grapsidae). *Hydrobiologia*, 560(1), 1-13.

Schwamborn, D. F. M. C, Marcolin, C. R., Lins-Silva, N., Almeida, A. O., & Schwamborn, R. (2024). Asynchronous contributions of decapod life history stages to the zooplankton of tropical estuarine, coastal and shelf ecosystems - new insights from semi-automatic image analysis. *Journal of Marine Systems*, 242, 103943, ISSN 0924-7963. https://doi.org/10.1016/j.jmarsys.2023.103943

Shaber, K., & Sulkin, S. (2007). Feeding on dinoflagellates by intermediate and late stage crab zoeae raised in the laboratory and collected from the field. *Journal of experimental marine biology and ecology*, *340*(2), 149-159.

Sheldon, R. W., Prakash, A. & Sutcliffe Jr, W. H. (1972). The size distribution of particles in the ocean. *Limnology and oceanography*, *17*(3), 327-340. https://doi.org/10.4319/lo.1972.17.3.0327

Sheldon, R. W., Sutcliffe Jr, W. H., & Paranjape, M. A. (1977). Structure of pelagic food chain and relationship between plankton and fish production. *Journal of the Fisheries Board of Canada*, *34*(12), 2344-2353. https://doi.org/10.1139/f77-314

Silva, T., Neumann-Leitão, S., Schwamborn, R., Gusmão, L. M., & Nascimento-Vieira, D. A. (2003). Diel and seasonal changes in the macrozooplankton community of a tropical estuary in Northeastern Brazil. *Revista Brasileira de Zoologia*, Curitiba, 20, 439-446. Silva, A. P., Neumann-Leitão, S., Schwamborn, R., Gusmão, L. M., & Silva, T. A. (2004). Mesozooplankton of an impacted bay in North Eastern Brazil. *Brazilian Archives of Biology and Technology*, Curitiba, 47(3), 485-493.

Silva, A. J., Castro Melo, P. A. M., Neumann-Leitão, S., & de Melo Júnior, M. (2020). Non-predatory mortality of planktonic copepods in a reef area influenced by estuarine plume. *Marine Environmental Research*, *159*, 105024. https://doi.org/10.1016/j.marenvres.2020.105024

Souza, C. S., da Conceição, L. R., Freitas, T. S., Aboim, I. L., Schwamborn, R., Neumann-Leitão, S., & Mafalda, P. O. (2020). Size spectra modeling of Mesozooplankton over a tropical continental shelf. *Journal of Coastal Research*, 36(4), 795-804. https://doi.org/10.2112/JCOASTRES-D-19-00102.1

Sprules, W. G., & Barth, L. E. (2016). Surfing the biomass size spectrum: some remarks on history, theory, and application. *Canadian Journal of Fisheries and Aquatic Sciences*, 73(4), 477-495.

Sprules, W. G., & Munawar, M. (1986). Plankton size spectra in relation to ecosystem productivity, size, and perturbation. *Canadian Journal of Fisheries and Aquatic Sciences*, 43(9), 1789-1794. https://doi.org/10.1139/f86-222

Sterza, J. M., & Fernandes, L. L. (2006). Zooplankton community of the Vitória Bay estuarine system (Southeastern Brazil): Characterization during a three- year study. *Brazilian Journal of Oceanography*, São Paulo, 54(2-3), 95-105.

Sun, X., Sun, S., Li, C., & Wang, M. (2012). Seasonal change in body length of important small copepods and relationship with environmental factors in Jiaozhou Bay, China. *Chinese Journal of Oceanology and Limnology*, *30*(3), 404-409. http://dx.doi.org/10.1007/s00343-012-1140-9

Taniguchi, D. A. A., Franks, P. J. S., & Poulin, F. J. (2014). Planktonic biomass size spectra: An emergent property of size-dependent physiological rates, food web dynamics, and nutrient regimes. *Marine Ecology Progress Series*, *514*, 13-33. https://doi.org/10.3354/meps10968

Turner, J. T. (2004). The importance of small planktonic copepods and their roles in pelagic marine food webs. *Zoological Studies*, *43*(2), 255-266.

Vandromme, P., Nogueira, E., Huret, M., Lopez-Urrutia, A., González-Nuevo González, G., Sourisseau, M., & Petitgas, P. (2014). Springtime zooplankton size structure over the continental shelf of the Bay of Biscay. *Ocean Science*, *10*(5), 821-835.

van Duren, L. A., & Videler, J. J. (2003). Escape from viscosity: the kinematics and hydrodynamics of copepod foraging and escape swimming. *Journal of Experimental Biology*, *206*(2), 269-279.

Van Eynde, B., Vuylsteke, D., Christiaens, O., Cooreman, K., Smagghe, G., & Delbare, D. (2019). Improvements in larviculture of *Crangon crangon* as a step towards its commercial aquaculture. Aquaculture research, 50(6), 1658-1667.

Vidjak, O., Bojanić, N., Gladan, Ž. N., Skejić, S., SKEJIĆ, B., & GRBEC, B. (2016). First record of small tropical calanoid copepod Parvocalanus crassirostris (Copepoda, Calanoida,

Paracalanidae) in the Adriatic Sea. *Mediterranean Marine Science*, *17*(3), 627-633. http://dx.doi.org/10.12681/mms.1743

Vidondo, B., Prairie, Y. T., Blanco, J. M., & Duarte, C. M. (1997). Some aspects of the analysis of size spectra in aquatic ecology. *Limnology and oceanography*, *42*(1), 184-192.

Wang J, Zamar R, Marazzi A, Yohai V, Salibian-Barrera M, Maronna R, Zivot E, Rocke D, Martin D, Maechler M, & Konis K. (2019). Robust: Port of the S+ "Robust Library". R package version 0.4-18.2

Wang, L., Chen, J., Su, H., Ma, X., Wu, Z., Shen, H., ... & Xie, P. (2022). Is zooplankton body size an indicator of water quality in (sub) tropical reservoirs in China?. *Ecosystems*, 25(2), 308-319.

Wheeler, R. & Torchiano, M. (2016). Package lmPerm - Permutation Tests for Linear Models. https://cran.r-project.org/web/packages/lmPerm/lmPerm.pdf

Wiebe, P. H. (1970). Small-scale spatial distribution in oceanic zooplankton. *Limnology and Oceanography*, *15*(2), 205-217.

Woodward, G., Ebenman, B., Emmerson, M., Montoya, J. M., Olesen, J. M., Valido, A., & Warren, P. H. (2005). Body size in ecological networks. *Trends in ecology & evolution*, 20(7), 402-409.

Yahia, M. N. D., Souissi, S., & Yahia-Kéfi, O. D. (2004). Spatial and temporal structure of planktonic copepods in the Bay of Tunis (southwestern Mediterranean Sea). *Zoological studies*, *43*(2), 366-375.

Yurista, P., Kelly, J. R., & Miller, S. (2005). Evaluation of optically acquired zooplankton size-spectrum data as a potential tool for assessment of condition in the Great Lakes. *Environmental Management*, 35(1), 34-44. https://doi.org/10.1007/s00267-003-0298-5

Zhang, Z., Chen, H., Li, Y., Ge, R., Liu, G., Ali, S., & Zhuang, Y. (2023). Trait-based approach revealed the seasonal variation of mesozooplankton functional groups in the South Yellow Sea. *Marine Life Science & Technology*, 5(1), 126-140. https://doi.org/10.1007/s42995-022-00156-9

Zhou, M., & Huntley, M. E. (1997). Population dynamics theory of plankton based on biomass spectra. *Marine Ecology Progress Series*, 159, 61-73.

Zhou, M. (2006). What determines the slope of a plankton biomass spectrum?. *Journal of plankton research*, *28*(5), 437-448. https://doi.org/10.1093/plankt/fbi119

5 ARTIGO 3 – DECLINES IN COASTAL MACROZOOPLANKTON COMMUNITIES WITHIN A RECENT CLIMATE AND OCEAN TIPPING POINT IN THE TROPICAL SOUTH ATLANTIC

1 INTRODUCTION

Pelagic ecosystems are extremely dynamic, unstable, and often hardly predictable, due to continued nonlinear variations and interplays among innumerable abiotic and biotic variables. Change in such ecosystems may be discontinuous and drastic, leading to conspicuous regime shifts (Chavez *et al.*, 2003). A substantial body of evidence on marine ecosystem regime shifts comes from studies on ancient decadal-scale oscillations between small pelagic fish species of economic interest, such as sardines and anchovies (Chavez *et al.*, 2003; Díaz-Ochoa *et al.*, 2009; Alheit and Bakun, 2010).

More recently, several studies have shown that during the anthropocene, additionally to ancient decadal oscillations, unprecedented tipping points in climate, ocean and ecosystems occur due to global warming (Heinze *et al.*, 2021), with unexpected domino effects and nonlinear interactions between drivers and processes (Wunderling *et al.*, 2021). Such unidirectional regime shifts related to anthropogenic warming and complex climate change (e.g., increasing rainfall) have already been reported from several (mostly polar and temperate) regions, based on highly informative and sensible zooplankton time series (Jiao, 2009; Mackas and Beaugrand; 2010; Wells *et al.*, 2022). Zooplankton communities are extremely sensitive and responsive systems, dynamically and quickly responding to even the subtlest alterations, thus being potent "canary in the mine" signal amplifiers for early stages of deleterious climate and ocean change (Richardson, 2008) . Increasingly frequent extreme rainfall events have been recently reported from several parts of the world, including catastrophic flooding and landslides in coastal regions of Pernambuco State, northeastern Brazil, with calamitous socio-economic consequences and loss of human life (Marengo *et al.*, 2023). However, up to now, no ecosystem effects of such extreme events have been published in the scientific literature, for tropical pelagic ecosystems and fisheries.

One of the most important fundamental questions in climate research regards the interactions between ENSO (El Niño Southern Oscillation), anthropogenic warming, and

ecosystem responses (Cai *et al.*, 2015). Numerous studies have shown the effects of ENSO on coastal ecosystems in the Eastern Pacific (Fiedler, 2002; Ayón *et al.*, 2008; Aronés *et al.*, 2009; Lehodey *et al.*, 2020), where the most drastic and conspicuous variations occur. Also, strong El Niño (EN) events have been detected as key triggers for relevant ecosystem regime shifts in the Eastern Pacific, based on zooplankton time series (Ayón *et al.*, 2008).

Several recent studies have increased our understanding of ENSO effects on ecosystems in the Amazon region, where there is unusually severe drought during strong EN events (Li *et al.*, 2011; Tyaquiçã *et al.*, 2017; Brum *et al.*, 2018; Foltz *et al.*, 2019). Conversely, in the temperate climate regions of South Brazil, exceptionally high rainfall commonly occurs during EN events (Herrmann, 2014; Lima *et al.*, 2010; Tedeschi *et al.*, 2015). During the years 2015 and 2016, unprecedented SST anomalies were observed in the Pacific Ocean. This record-strength El Niño event, that received the nickname "Godzilla" (Schiermeier, 2015; Coria-Monter *et al.*, 2019), caused exceptional changes in sea surface temperature and chlorophyll a concentration, and had drastic consequences for mortality, biomass, growth, recruitment, and distribution of fishes, invertebrates and plankton, affecting marine ecosystems in many parts of the world (Jiao, 2009; Park *et al.* 2011; Coria-Monter *et al.*, 2019).

In recent years, there have been increasingly strong and frequent extreme rainfall events at the eastern coast of northeastern Brazil (coastal regions of the states of Paraíba, Pernambuco, and Alagoas, Fig. 1b) which have been associated with the ENSO cycle and SST fluctuations in the Tropical Atlantic (Hounsou-Gbo *et al.*, 2019; Marengo *et al.*, 2023). Little is known about the effects of ENSO and other global-scale phenomena on coastal zooplankton communities in the Southwestern Tropical Atlantic. This may also be due to the absence of zooplankton time series in this region.

Our objective was to test the hypothesis that interannual variations of tropical planktonic decapods (including species of socio-economic relevance) and other macrozooplankton can be explained by variations in global-scale climate indices (e.g., ONI and TSA), based on a 6-year time series (2013-2019) in a northeast Brazilian coastal marine protected area. Moreover, we intended to examine the potential effects of specific, well-defined climate phenomena, such as the strong 2015/16 EN and recurring extreme rainfall events, on these pelagic communities of substantial ecological and socio-economic relevance.

2 MATERIALS AND METHODS

2.1 Study Area

Tamandaré Bay (Pernambuco State, northeastern Brazil) extends over approximately 3 km² (Fig. 1). It is a semi-open bay protected by sandstone and coral reefs. It is connected to a lagoon-like shallow reef labyrinth to the north and mangrove estuaries to the south (Duarte, 1993; Maida and Ferreira, 1997). This semi-enclosed, reef-lined bay is under the seasonally varying influence of the large-scale plume of the Una River (Schwamborn *et al.*, 2024), which is the region's main watershed with a stretch of 290 km, and from the adjacent small Mamucabas and Ilhetas creeks, which empty directly into the southern part of the Bay. The adjacent continental shelf off Tamandaré has a series of sandstone and coral reef lines running parallel to the coast, as well as calcareous mudflats and rhodolite beds (Manso *et al.*, 2003; Camargo *et al.*, 2007; Schwamborn *et al.*, 2024).

The region of Tamandaré is characterized by socio-economically important tourism, sugar cane cultivation, small-scale artisanal penaeid shrimp fisheries (mostly *Xiphopenaeus kroyeri* and *Penaeus spp.*), as well as several other artisanal fisheries on fish and invertebrates in the adjacent mangroves and reef ecosystems (Coelho & Santos, 1993; Ferreira *et al.*, 2003; Silva & Santos, 2007; Mello & Souza, 2013; Alves *et al.*, 2023). The study area belongs to the “Costa dos Corais” Marine Protection Area, which extends over 120 km of coastline, including extensive estuarine mangroves, coral reefs, sandy beaches, and continental shelf (ICMBio - MMA).

The average annual precipitation (average from 1990 to 2020) in this area is 1,631 mm (Silva *et al.*, 2022), with strong fluctuations between dry (September to February, 367 mm, 22.5% of total precipitation) and rainy seasons (March to August, 1,264 mm, 77.5% of accumulated precipitation (Ferreira *et al.*, 2003; Grego *et al.*, 2009; Venekey *et al.*, 2011; Silva *et al.*, 2022). In coastal areas of Pernambuco State, the South Atlantic high-pressure system controls the trade wind regime (Domingues *et al.*, 2017). The wind regime exhibits significant seasonality (Rollnic and Medeiros, 2006), with strong southeasterly winds in the second half of the year. Low wind speeds occur in the first semester, with minimum wind speeds in March, April, and May (early rainy season) and weaker E-NE winds especially in December and January, coinciding with the main dry season. The peak windy season, with strong east-

southeast coastal winds, lasts from June to October and extends from the peak of the wet season to the early dry season (Schwamborn *et al.*, 2024).

2.2 Sampling

Sampling was carried out at three stations (B1 to B3), that were conceived for a long-term study of the pelagic ecosystems of Tamandaré Bay, Pernambuco State, northeastern Brazil (Fig. 1). Bi-monthly sampling campaigns were conducted over six years, from June 2013 to August 2019. Sampling always took place during the day, during new moon spring tides, at three fixed stations (Fig. 1) yielding a total of 107 samples. The sampling strategy in Tamandaré Bay was designed to minimize the influence of estuarine plumes and sample coastal marine zooplankton, with maximum marine influence (sampling during high tide, between 1:00 p.m. and 3:00 p.m.). Station 1 was located closer to adjacent reef ecosystems, while station 2, was approximately in the center of the Bay, being more influenced by offshore waters, and station 3 was closer to the Mamucabas and Ilhetas mangrove creeks (Fig. 1) Because the tidal regime was standardized to be the new moon, the exact hours and tidal situations (i.e., high tide) were constant and perfectly standardized across the entire time series.

During each field campaign, subsurface horizontal tows (0 to 60 cm depth layer) were carried out using a conical plankton net (mesh size: 300 μm, diameter: 60 cm, length: 2.5 m) equipped with a calibrated flowmeter (Hydro-Bios, Kiel) to estimate the filtered volume. The towing process took 5 minutes at a speed of 2 knots, at each station. *In situ* abiotic data (temperature, salinity, and Secchi depth) were obtained at each station using a CTD probe (YSI/SonTek CastAway) and a Secchi disk. All zooplankton samples were immediately placed in flasks with seawater and preserved with 4% formaldehyde (buffered with 0.5 g/L sodium tetraborate).

2.4. Climate indices, chlorophyll a, wind speed, rainfall, and Una river discharge

In addition to *in situ* abiotic data (temperature, salinity, and Secchi depth), several other datasets, obtained from external sources, were also considered as potentially relevant explanatory variables, such as satellite-derived chlorophyll a, global-scale climate indices (ONI, NAO, TSA, etc.), rainfall, wind speed and the discharge of the nearby Una River.

Local rainfall data were obtained from the Pernambuco State Agency of Waters and Climate (APAC: http://old.apac.pe.gov.br/meteorologia/monitoramento-pluvio.php). For each sampling day, we used the sum of local rainfall along five days (i.e., on the day of sampling and the four preceding days), at the meteorological station of Tamandaré. The optimal period of five days was chosen after correlation analysis between rainfall days and local water transparency and salinity data. Wind speed data were obtained from the ASCAT dataset (BENTAMY & FILLON, 2012). Satellite-derived chlorophyll a data were obtained from the NASA MODIS (https://modis.gsfc.nasa.gov/data/dataprod/chlor_a.php) sensor on the Aqua satellite (NASA Ocean Biology Processing Group, 2014; Savtchenko *et al.*, 2004). Monthly discharge of the nearby Una River (Fig. 1) at the Barreiros station (station nº 39590000) was obtained from the Brazilian National Water Agency (ANA), pre-processed and stored in the MARDAO dataset (Varona *et al.*, 2022).

The Oceanic Niño Index (ONI) index is used for the operational definition of El Niño (EN) and La Niña (LN) periods by the National Oceanic and Atmospheric Administration (NOAA). ONI data are regularly calculated as a three-month running mean of SST anomalies in the Niño 3.4 region (5º N - 5º S, 120º - 170º W), based on centered 30-year base periods, that are updated every 5 years. The North Atlantic Oscillation (NAO) index is based on the surface sea-level pressure difference between the Subtropical (Azores) high and the Subpolar Low. NAO data were obtained from the NOAA National Weather Center, Climate Prediction Center (https://www.cpc.ncep.noaa.gov/data/teledoc/telecontents.shtml).

The TSA (Tropical Southern Atlantic) index is an indicator of sea surface temperatures (SST) in the Gulf of Guinea and the Eastern Tropical South Atlantic Ocean (30°W to 10°E, 20°S to 0°). It does not include the Western Tropical South Atlantic Ocean (which would be where the study area is located). The study area (Tamandaré Bay) is located thousands of kilometers from the core of the TSA area, and the westernmost border of the TSA area lies

approximately 700 km from Tamandaré (Figure 2). TSA is a global-scale scale climate index that may potentially affect the study area through several processes, such as remote forcing, winds, ocean currents, and easterly disturbance waves (Marengo *et al.*, 2023). The TSA index is based on SST anomalies in the TSA area, which are calculated relative to a monthly climatological seasonal cycle of SST in the years 1982-2005 (Enfield *et al.*, 1999). TSA index data were obtained from the APEC Climate Center (https://www.apcc21.org/ser/indic.do?lang=en).

2.5. ZooScan analyses

In the laboratory, samples were divided into two size fractions by sieving with a mesh size of 1000 μm. This separation was important to avoid underestimating large organisms that are usually less abundant than small ones (Gorsky *et al.*, 2010). Each size fraction was split using a Motoda splitter (Omori and Ikeda, 1984) to create quantitative aliquots (subsamples) of approximately 1,000 to 2,000 objects per subsample.

The ZooScan device (Hydroptic model ZSCAN03), a modified scanner (resolution: 2400 dpi), was used to digitize the zooplankton samples. ZooProcess (http://www.obs-vlfr.fr/LOV/ZooPart/ZooScan) and Plankton Identifier (PkID) software were used to semi-automatically analyze and classify each subsample to produce digital images (i.e. “vignettes”) of all organisms. For each vignette, a vector of descriptive parameters was calculated. These parameters were used for semi-automated identification using the ECOTAXA (ecotaxa.obs-vlfr.fr) software and online database. The Random Forest algorithm (Breiman, 2001) was used to classify all vignettes, which were later visually checked (validated) by a specialist and separated into categories. This means that all classification errors were corrected manually. This procedure allowed the identification of planktonic decapods at the level of taxonomic groups and life stages (zoea, megalopa, protozoea, mysis, postlarva, juveniles, and adults).

2.6 Statistical analyses

To test for significant temporal (sampling months, sampling years, “rainy *vs* dry season” “pre-EN *vs* post-EN periods”, or “pre-EN, peak EN, post-EN periods”) and spatial (sampling stations) variations in key univariate parameters, including abiotic data, climate indices, and the zooplankton and decapod communities (total zooplankton abundance, total decapods abundance, abundance of key taxa), we used a simple univariate permutation test (univariate PERMANOVA) with 50,000 permutations (function “aovperm”, R package “permuco”, Frossard and Renaud, 2021). When there were three or more levels of the independent factor (e.g. “pre-EN, peak EN, post-EN periods”), and significant ($P < 0.05$) univariate PERMANOVA results, we conducted post-hoc pairwise testing, based on the the non-parametric Nemenyi rank comparison test (Nemenyi, 1963), using the function “kwAllPairsNemenyiTest” within the R package “PMCMRplus” (Pohlert, 2023).

Figure 1. Map of the study area and sampling stations (B1 to B3), in Tamandaré Bay, Pernambuco State, Brazil.

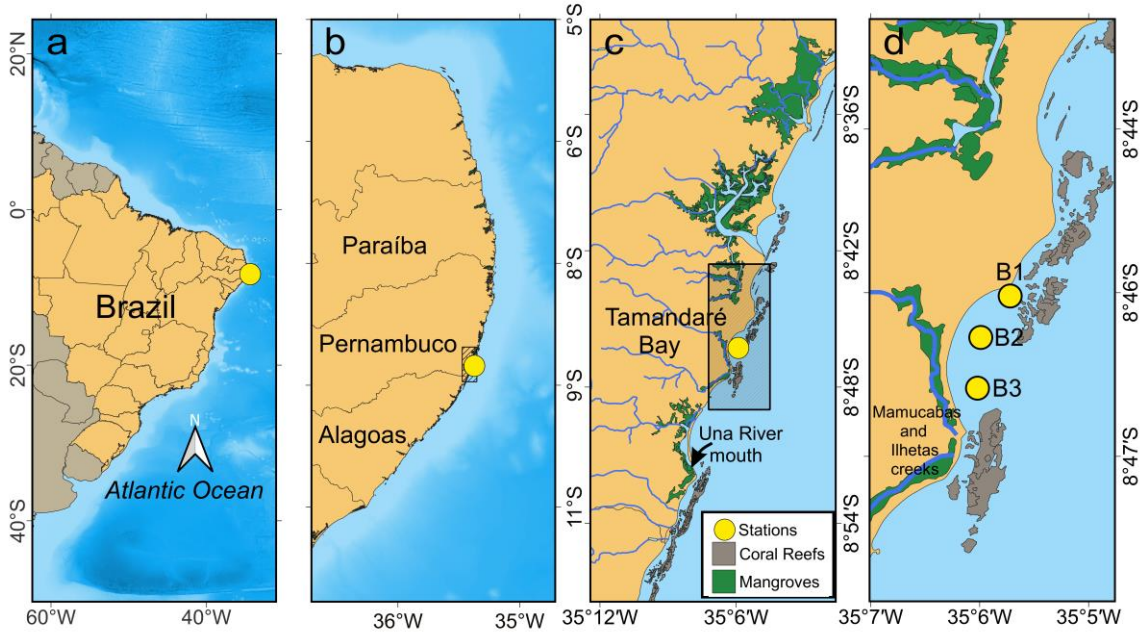

Fonte: A autora (2024).

Figure 2. Schematic representation of the Tropical South Atlantic (TSA) showing the extension of the TSA index region (large rectangle) and climate and ocean processes that spread from the TSA region westwards towards the study area (Tamandaré Bay, Pernambuco State, Brazil, brown circle in the map). Dashed purple arrows: schematic representation of the predominant trade winds in the peak dry (January) and peak rainy (July) seasons. Dashed brown arrows: atmospheric easterly disturbances (after Marengo *et al.*, 2023). Black arrows: ocean currents. TA: Tamandaré. BC: Brazil Current. NBUC: North Brazil Undercurrent. sSEC: southern branch of the South Equatorial Current.

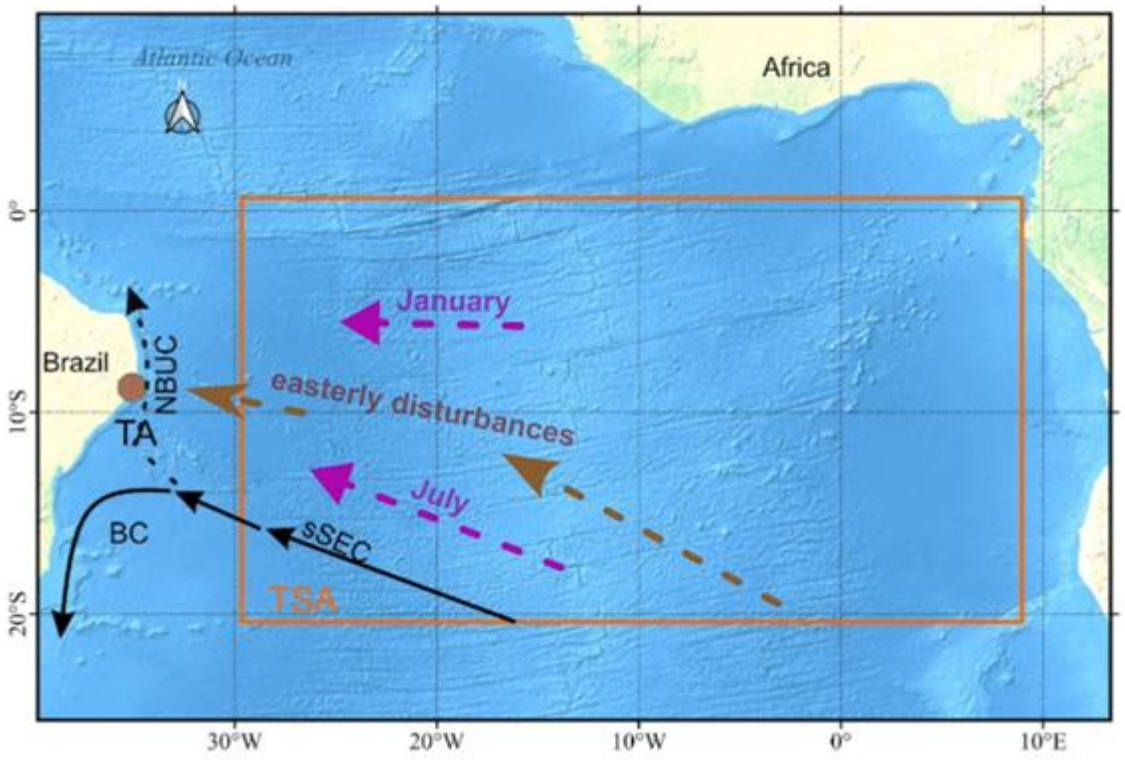

Fonte: A autora (2024).

Seasonal anomalies (difference between raw values and monthly means, for each month) were calculated for all biotic and abiotic parameters (except for ONI and TSA, which are already seasonal anomalies). Analyses based on raw data include elements of seasonal and interannual variability, while analyses based on monthly anomalies show interannual variability only.

Significant points of change in the time series were detected with batch sequential tests (i.e., batch change detection), based on sequential nonparametric Mann-Whitney tests (Ayón *et al.*, 2008). Also, we tested for significant abrupt changes in variability in the time series using a sequential Bartlett test for change in variance. Both sequential tests were applied using the "cpm" package in R (Ross, 2015). For each variable, such batch detection algorithms were applied to the raw time series data and to the seasonal (monthly) anomalies, except for climate indices that are already based on seasonal anomalies (such as ONI and TSA), where only the raw index data were used.

Univariate (one taxon *vs* one abiotic variable) and multiple linear models were constructed to explain the temporal variability of the most common key taxa (frequency of occurrence above 5%). Linear models were constructed and tested using raw abundance data, log10 (x+1)-transformed abundances, seasonal anomalies, and log10 (x+1)-transformed seasonal anomalies. For multiple linear models, the "best" combination of independent variables was chosen using a stepwise backwards approach, starting from the full model, and then stepwise excluding variables until the "best" multivariate linear model (best AIC value) was obtained, by applying the "step" function in the "MASS" R package (Venables and Ripley, 2002).

Relative contributions of each abiotic variable to the variability explained by multiple linear models were assessed by applying the "Relative importance" approach, using the "lmg" index (R^2 partitioned by averaging over orders, Lindeman *et al.*, 1980) within the "relaimpo" R package (Grömping, 2007). Statistical significance ($p_{crit} = 0.05$) of all linear models was tested with permutation tests, using 50.000 permutations, by applying the function "aovperm" within the "permuco" R package (Frossard and Renaud, 2021).

Redundancy Analysis (RDA) was conducted to identify whether the variability in zooplankton community structure (matrix of response variables) could be explained by environmental and climatology descriptors (matrix of explanatory variables). We included twelve taxa (the most common key taxa (frequency of occurrence above 5%) as a response matrix and a matrix of environmental and climatology descriptors (e.g., temperature, salinity, water transparency, wind speed, TSA index, Chlorophyll a) as independent matrices. We applied the Hellinger transformation to process the biological data (zooplankton abundance) before RDA (Legendre and Gallagher, 2001). Monte Carlo permutations (999 permutations) were used for testing the significance ($p < 0.05$) of environmental variables, and only significant

variables are shown in the RDA plots. One-way Multivariate Permutational Analysis of Variance (multivariate PERMANOVA, Anderson, 2017) was applied, with 20,000 permutations, to evaluate the significance of the RDA axis, to test the hypothesis that environmental and climatology descriptors are responsible for structuring the zooplankton abundance, and to test whether there are significant differences in community structure between pre- and post-EN periods. These analyses were carried out using the "vegan" package (Oksanen *et al.*, 2019) within the "R" software, language and environment (version 3.6.1, R Development Core Team, 2019).

3 RESULTS

3.1 Time series of climate indices and local abiotic variables

Climate indices, abiotic variables and macrozooplankton abundance displayed remarkable variation patterns throughout the study period (Figs. 3 to 7). The time series of the global-scale oceanic El Niño index (ONI) perfectly illustrates the peak of the record strength 2015/16 El Niño event (Fig. 3). Most strikingly, the 2015-2016 El Niño was characterized by unusually low rainfall in the study area (i.e., 2016 was a year almost without any rainy season). The TSA time series displayed a considerable increase in SST anomalies during the study period, with a conspicuous TSA warming event that occurred in the second semester of 2015, coinciding exactly with the peak of the 2015/16 EN event (Fig. 3).

Local rainfall at Tamandaré presented several prominent seasonal peaks (Fig. 3). Also, rainfall showed a considerable increase during the study period, with three extreme rainfall events (above 50 mm per month) in 2017, 2018, and 2019. Regular seasonality (rainy vs dry season) and extreme peaks in the rainy seasons of 2017, 2018, and 2019, were also conspicuously well reflected in the time series of the Una river discharge and in the salinity in Tamandaré Bay. Similar patterns were also observed in most other abiotic parameters, such as chlorophyll a, wind speed, salinity, temperature, and Secchi depth.

3.2 Zooplankton time series

A total of 169197 individual zooplankton vignettes (digital images) were individually analyzed, identified, and validated in this study. These vignettes were categorized into 49 taxonomic groups and life history stages, including several holo-, meroplankton, and decapod larvae groups. The twelve most frequent (key) taxa were copepods, chaetognaths, appendicularians, cnidarian medusae, gastropod veliger larvae, bryozoan cyphonautes larvae, teleost fish eggs, holoplanktonic luciferid shrimp adults, sergestid protozoea larvae, luciferid protozoea larvae, brachyuran crab zoeae, and penaeid shrimp (mostly *Penaeus* spp.) postlarvae.

Time series of total zooplankton, total decapods, and taxonomic groups (Figures 5 to 7) showed considerable seasonal and interannual variations, including peaks, troughs, trends, and conspicuous differences between pre-EN, peak EN and post-EN periods. Total zooplankton abundance and several common taxonomic groups (e.g., copepods, chaetognaths, appendicularians, and penaeid shrimp postlarvae) exhibited conspicuous decreasing trends in abundance. Total zooplankton, copepods and appendicularians displayed evident peaks in abundance during minimum-rainfall, maximum-transparency (Secchi depth of 8m) conditions in November 2015, at the very peak of the strong 2015/2016 EN event.

3.3 Trends, seasonality, points of change, regime shifts, and climate tipping points

Among all climate and ocean variables tested, permutation-based trend analysis ("variable x" vs Date, "permuco" R package, function "aovperm") revealed significant long-term trends for rainfall (increase, $p = 0.00015$), Una river discharge (increase, $p = 0.02$), salinity (decrease, $p = 0.02$), and TSA (increase in SST, $p = 0.0002$). Significant points of change ("cpm" R rackage) were detected for one abiotic variable (salinity) and one climate index (TSA) only (Figs. 2 and 3).

The monthly seasonality pattern of rainfall showed maxima from February to August (rainy season) and minimum mean rainfall from September to January (dry season). No significant points of change were detected in the time series, whether for rainfall raw data or monthly rainfall anomalies. The three extreme rainfall events observed in 2017, 2018, and 2019 were evident as outliers when analyzing the raw data, and also for anomalies. Thus, these three extreme rainfall events could not be explained by regular seasonality.

The seasonality of the Una river discharge showed a similar pattern, but with the period of minimum mean discharge (dry season) starting two months later, from November to January. Quite similarly to the rainfall data, the three extreme events of 2017, 2018, and 2019 were also well detectable in the Una River discharge raw data and seasonal anomalies. No significant points of change were detected for raw data or monthly Una river discharge anomalies

Wind speed displayed a pattern of strong stochastic variability within the seasonal cycle, except for an evident minimum in April and a strong maximum in July. Sea surface temperature (SST) measured *in situ* (at 1 m depth) followed a perfectly regular seasonal oscillation (seasonal

amplitude: 2.5 °C, with a maximum mean of 29.67 °C in March and minimum mean of 27.14 °C in August) without any interannual variations, regime shifts, or significant trends in the study period.

Similarly, water transparency (i.e., Secchi depth, m) also followed a perfectly regular seasonal oscillation (maximum mean of 7.9 m in November (early dry season) and minimum mean of 0.7 m in July (peak rainy and peak windy season)) without conspicuous regime shifts, points of change, nor any significant trends in the study period.

Satellite-derived Chlorophyll a followed a regular seasonal pattern, with minimum values from September to March (dry season), maximum values from April to August (rainy season, similar to Rainfall, Una river, Wind speed, and Secchi depth), with a clear and prominent maximum in June. Sea surface salinity (SSS) measured *in situ* (at 1 m depth) also showed a clear seasonality. Maximum salinities were measured in the dry season (in November, December, and January, max. mean SSS = 37.15). Minimum mean SSS was measured at the end of the rainy season, in August (min. mean SSS = 26.99). We did not detect any significant spatial effects (i.e., no differences among stations B1, B2, and B3) for SSS nor for any other abiotic variable ($p > 0.05$, function “aovperm”).

Among the abiotic variables tested, SSS (raw data and monthly anomalies) were the only ones to show significant interannual changes in median values (sequential batch Mann-Whitney tests) and in variability (sequential batch Bartlett tests). SSS raw data displayed three statistically significant points of change in median value (Fig. 4). Also, SSS raw data displays five points of change in variance, after Sept 2026 (Fig. 4). All significant changes in raw salinities occurred after September 2016. Before the strong EN event in 2015/16, there was a regular, low-variability period in salinity, with regular, low-amplitude seasonal oscillations (SSS oscillating seasonally between 35 and 37). After this event, there were alternating periods of low and high median SSS values and low and high spatial and temporal variability.

Among the climate indices tested, only one time series revealed a statistically significant point of change. A striking and highly significant ($p < 0.001$, sequential batch Mann-Whitney test) regime shift was detected within the TSA time series (Fig. 3). A clear and highly significant tipping point was detected in September 2015 (Fig. 3). Sea surface temperatures (SST) in the Tropical South Atlantic increased significantly and consistently after the strong 2015-2016 El Niño event. The mean TSA index before September 2015 was -0.013 (std. dev.: 0.145). After

September 2015, the Tropical South Atlantic was significantly warmer than before, with a TSA mean of 0.276 (std. dev.: 0.186). Thus, mean SST in the TSA region increased abruptly, by 0.288 degrees Celsius, when comparing the periods before and after September 2015. This change point coincides with the onset of the extremely strong EN (ONI with values above 1.5). Accordingly, univariate PERMANOVA yielded an extremely high significance of the effect of the factor "preEN, EN, postEN" for TSA, ($p < 0.0001$, aovperm).

Figure 3. Time series of local rainfall in Tamandaré (Brazil) and potentially relevant climate indexes. Rainfall (mm) in Tamandaré Bay (day of samplings and four days before), ONI (Oceanic Niño Index) in the Pacific Ocean, NAO (North Atlantic Oscillation) index and TSA (Tropical South Atlantic) SST index. Shaded areas represent the rainy season. Red arrow: significant ($p < 0.05$) point of change (tipping point) for median SSTs in the TSA area. Dashed horizontal lines: mean TSA values before and after the tipping point. Orange bar: peak of the strong 2015/16 El Niño event in the ONI region.

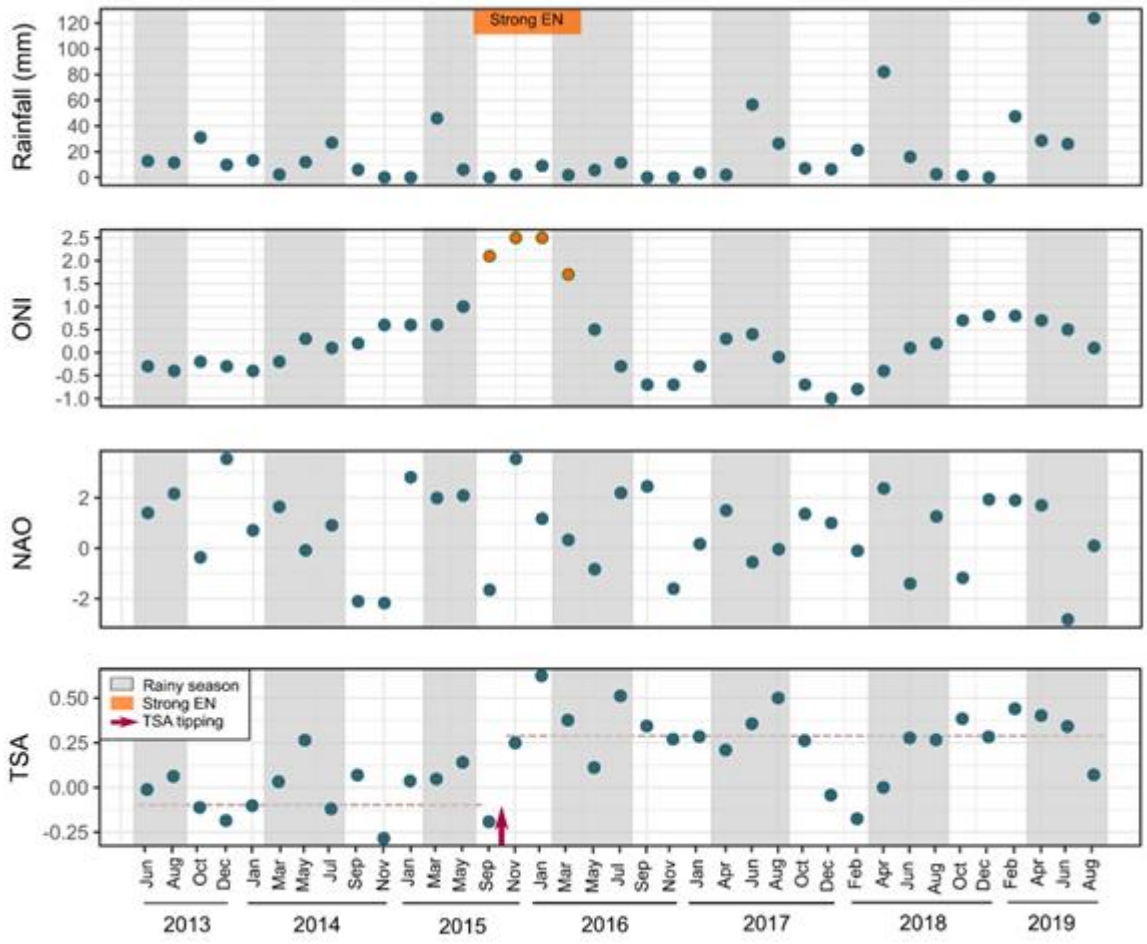

Fonte: A autora (2024).

Figure 4. Time series of abiotic data obtained over six years (2013-2019) in Tamandaré Bay, Brazil: temperature (ºC), salinity, Secchi depth (m), URD (Una River Discharge (m³/s)), Chla: (Chlorophyll *a* (mg/m³)) and wind speed (m/s) at three stations (B1, B2, and B3). Shaded areas represent the rainy season. Arrows represent significant ($p < 0.05$) points of change for medians (red) or variance (green). Orange bar: peak of the strong 2015/16 El Niño event.

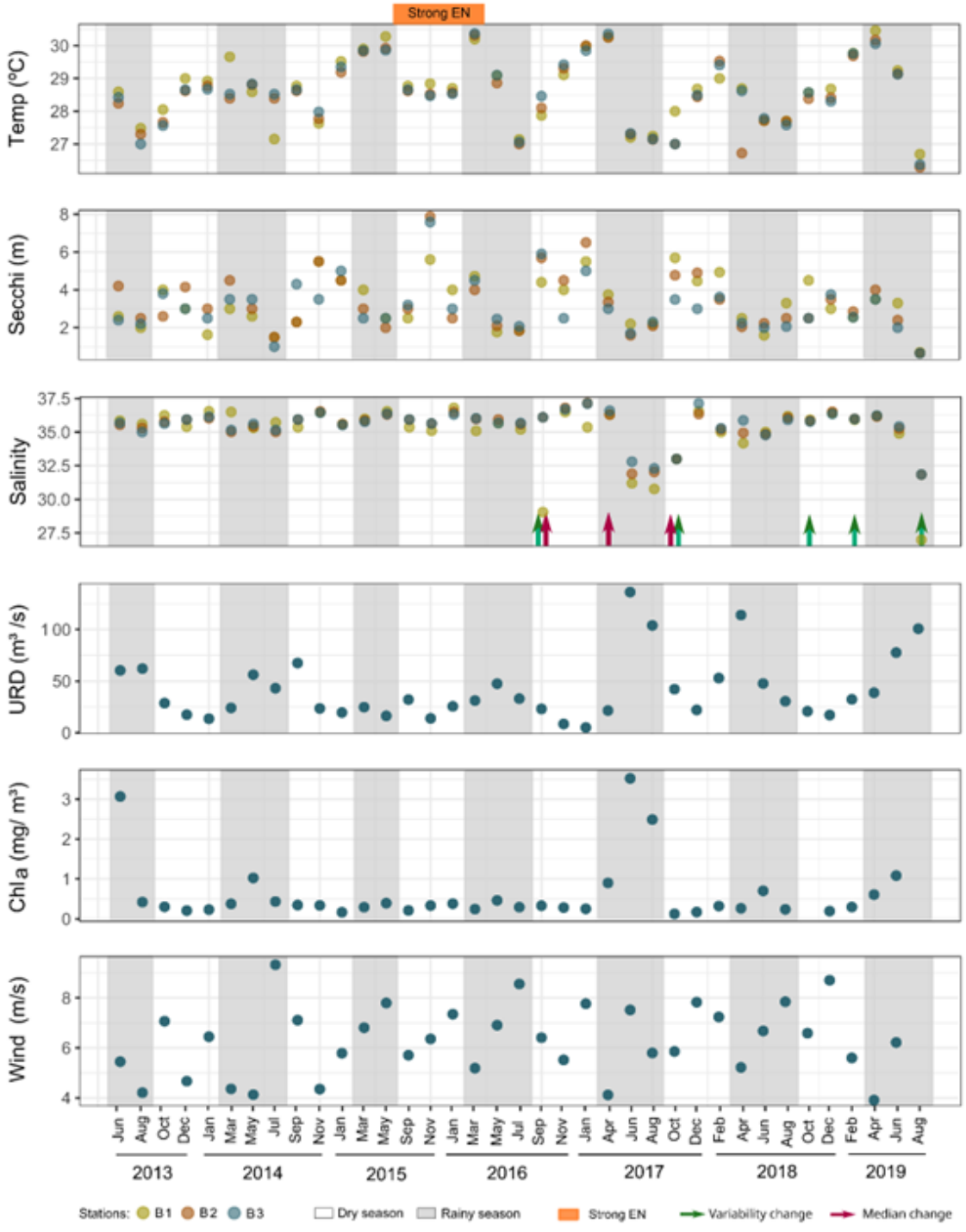

Fonte: A autora (2024).

Figure 5. Time series of the abundance (ind. m^{-3}) of total zooplankton, copepods, chaetognaths, appendicularians, fish eggs, and fish larvae. Samples (n = 107) were obtained bimonthly from June 2013 to August 2019 at three stations (B1, B2, B3), during 36 sampling campaigns in Tamandaré Bay, Brazil. Gray bars: rainy season. Orange bar: peak of the strong 2015/16 El Niño event. Note the logarithmic scale.

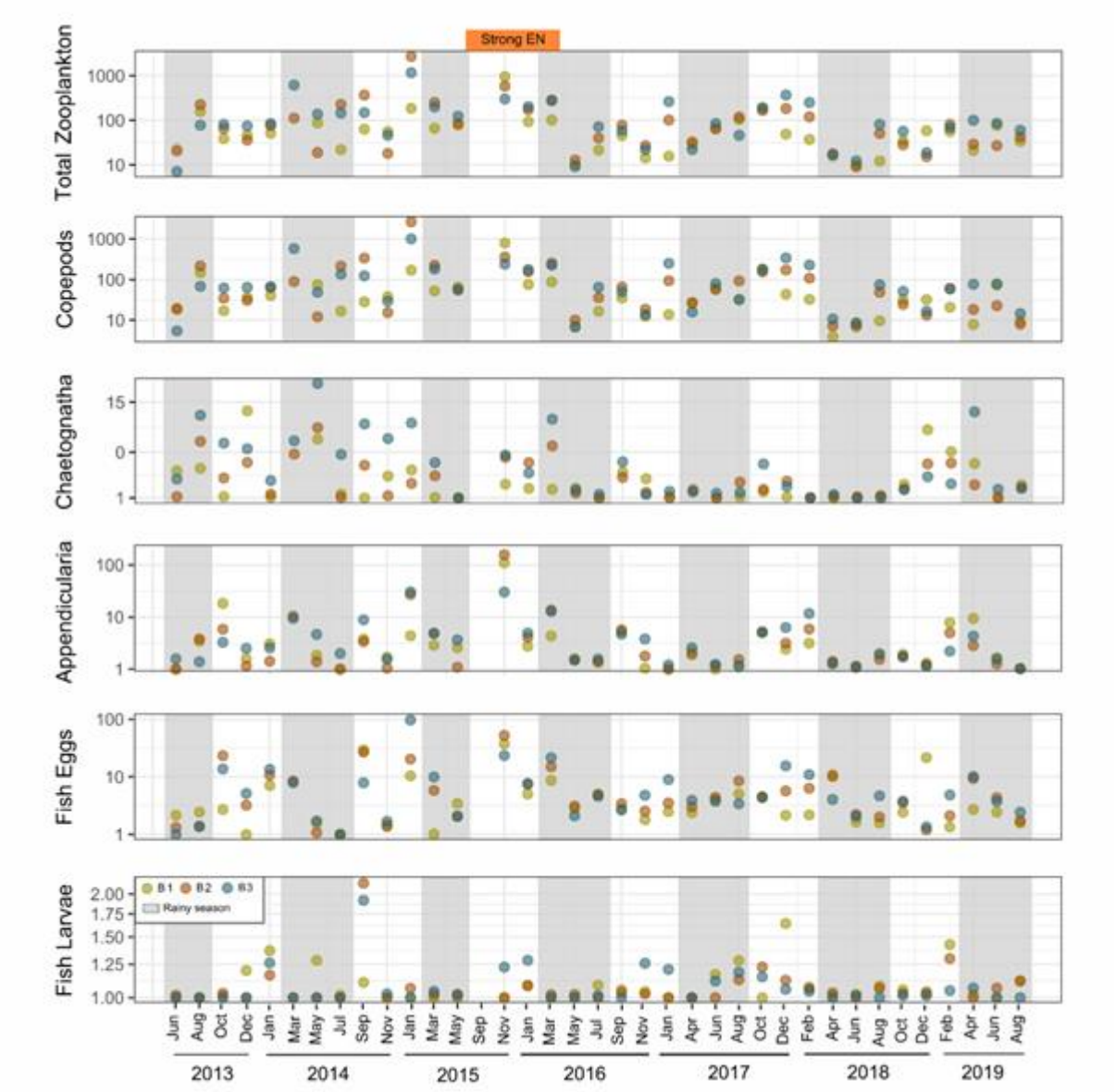

Fonte: A autora (2024).

Figure 6. Time series of the abundance (ind. m^{-3}) of total decapods and selected decapod taxa (brachyuran crab zoeae and megalopae, luciferid shrimp, adults and juveniles, anomuran (other than Porcellanidae) hermit crab zoeae, alpheid pistol shrimp zoeae). Samples (n = 107) were obtained bimonthly from June 2013 to August 2019 at three stations (B1, B2, B3), during 36 sampling campaigns in Tamandaré Bay, Brazil. Gray bars: rainy season. Orange bar: peak of the strong 2015/16 El Niño event. Note the logarithmic scale.

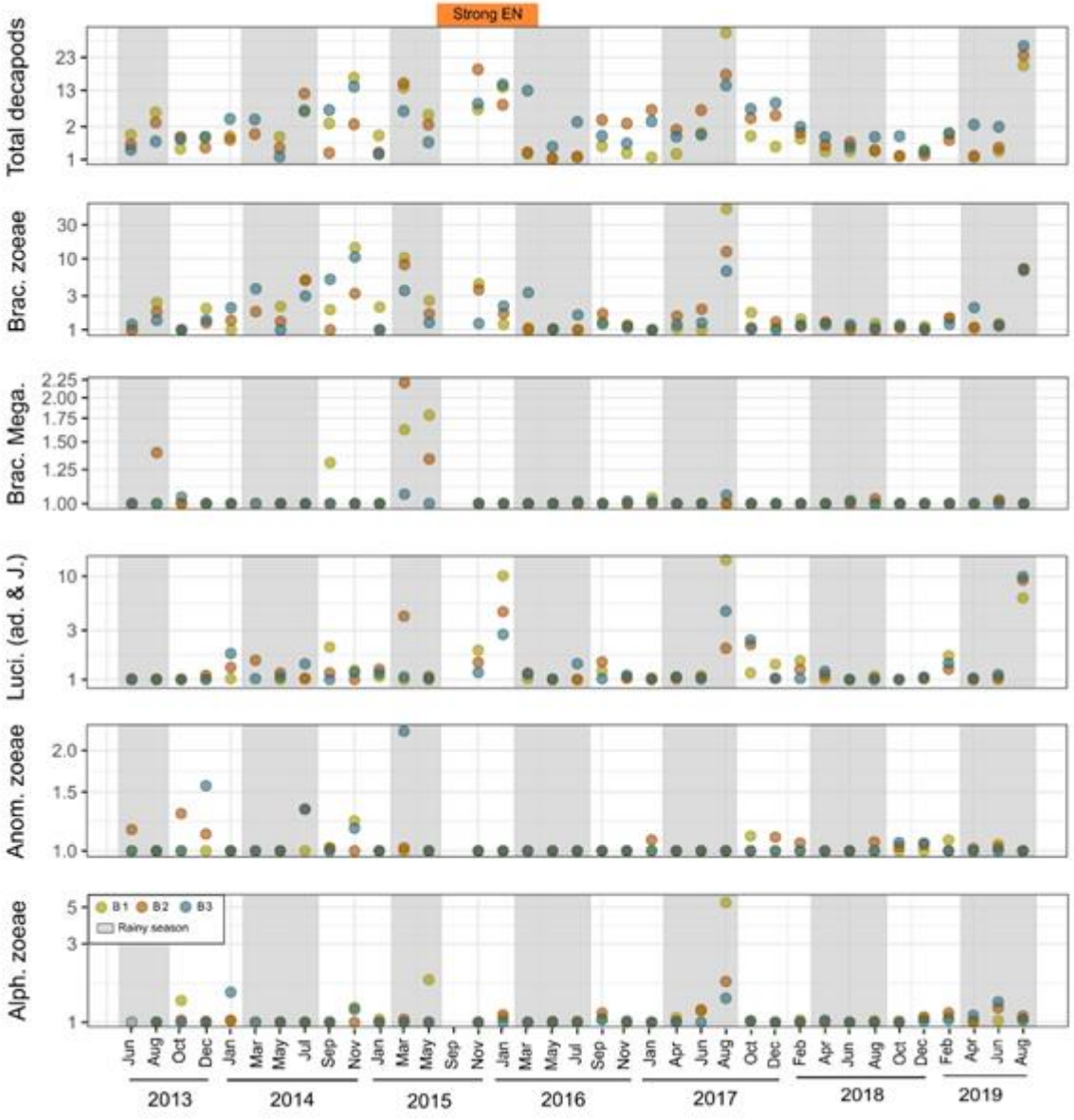

Fonte: A autora (2024).

Figure 7. Time series of abundance (ind. m^{-3}) of penaeid shrimp postlarvae, other caridean shrimp zoeae (other than Alpheidae), and cnidarian medusae. Samples (n = 107) were obtained bimonthly from June 2013 to August 2019 at three stations (B1, B2, B3), during 36 sampling campaigns in Tamandaré Bay, Brazil. Grey bars: rainy season. Orange bar: peak of the strong 2015/16 El Niño event. Note the logarithmic scale.

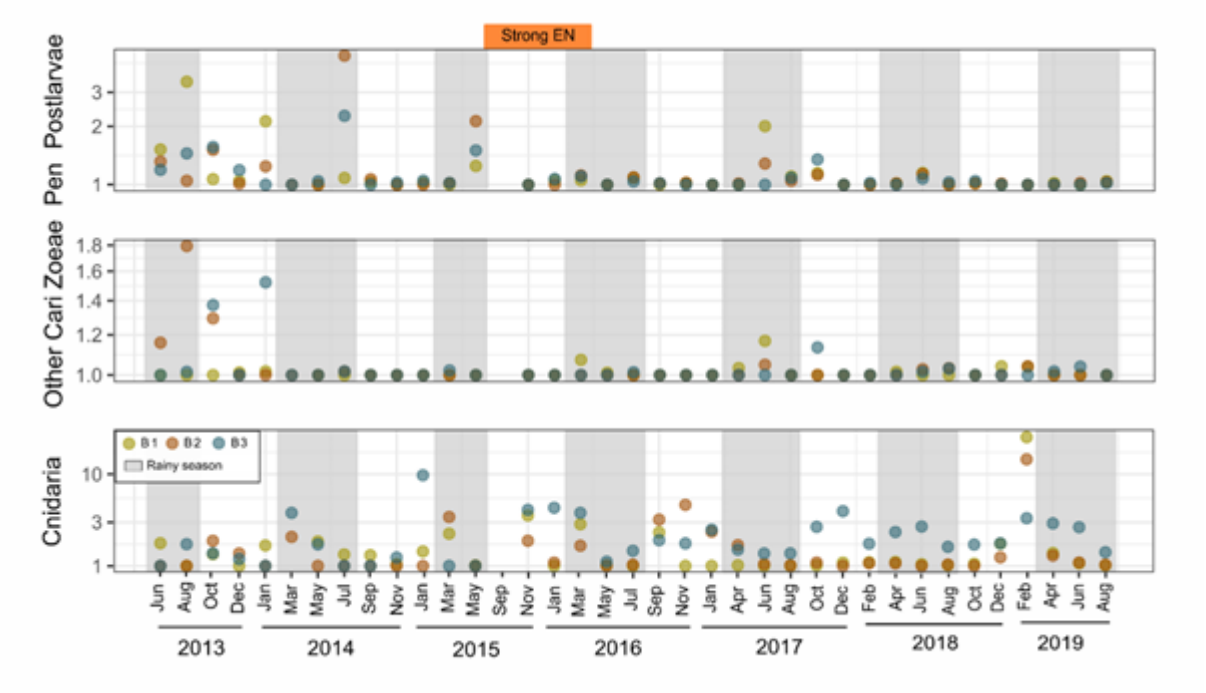

Fonte: A autora (2024).

3.4 Spearman correlation matrix

Non-parametric Spearman correlation analysis (Fig. 8) detected numerous correlations among abiotic parameters. For example, surface (1m) salinities in Tamandaré Bay were significantly correlated with local rainfall (sum of 5 days) and the Una River discharge. These correlations were highly significant, whether using raw data, or seasonal anomalies.

Figure 8. Correlation plots (non-parametric Spearman correlations) of monthly seasonal anomalies (below) and raw data (above), for abiotic variables, climate indices, and abundances of the 12 most frequent taxa. Non-significant correlations ($p > 0.05$) are shown as blank (white) spaces. Una: river discharge of the nearby Una River. Rainfall: 5-day sum of rainfall in Tamandaré. TSA: Tropical South Atlantic SST index, NAO: North Atlantic Oscillation index, ONI: Oceanic El Niño index. Samples (n = 107) were obtained bimonthly from June 2013 to August 2019 at three stations in Tamandaré Bay, Brazil.

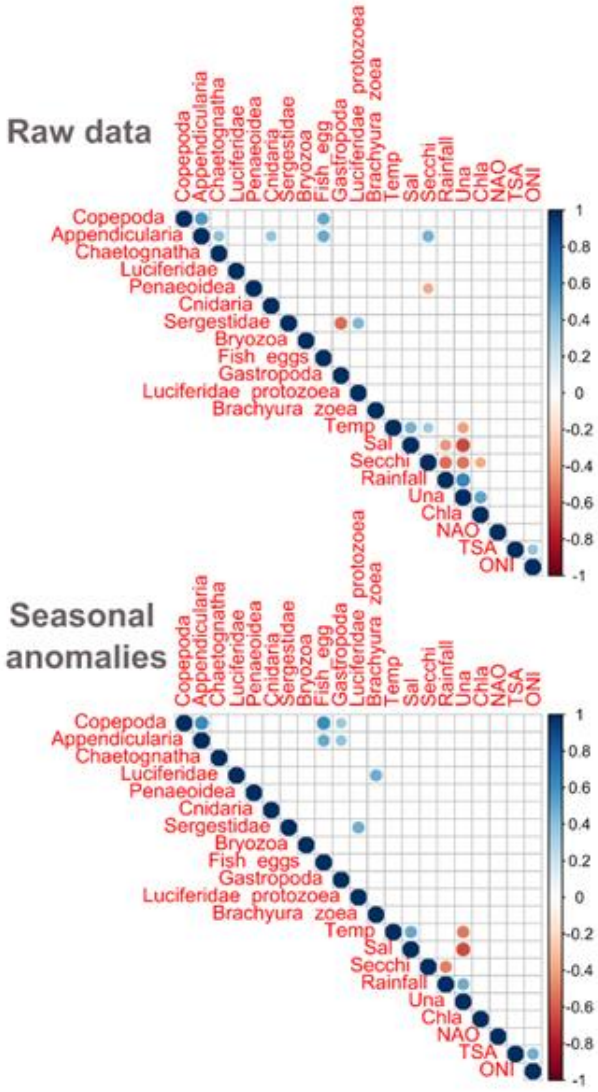

Fonte: A autora (2024).

Secchi Depth in Tamandaré Bay was significantly correlated with satellite-derived chlorophyll a, rainfall, and the Una river discharge. Also, Secchi depth was correlated with surface (1m) water temperature. Secchi depth seasonal anomalies were not correlated with temperature seasonal anomalies, showing that the temperature-Secchi relationship for raw data was exclusively due to seasonal covariance (i.e., a warm-water dry season with more transparent "blue waters", as opposed to a colder rainy season with "green waters" in the rainy sean). Yet, seasonal anomalies of Secchi depth and rainfall were correlated, showing a significant interannual covariance between these two variables. TSA and ONI were positively correlated, proving the strong influence of ENSO on SSTs in the TSA area (Fig. 8). No significant correlations with NAO were detected in this study.

3.5 Linear models, trends, seasonality, points of change, and PERMANOVA for total zooplankton, copepods, chaetognaths, appendicularians, penaeid postlarvae

Numerous significant linear models and univariate PERMANOVA results were obtained between spatio-temporal factors, biotic and abiotic variables, for total zooplankton abundance and for several key taxa.

3.5.a. Total zooplankton

Total zooplankton abundance displayed remarkable and highly significant temporal variations (Fig. 9). At the beginning, during the pre-EN period, there were relatively high abundances (median: 141.52 ind. m^{-3}), followed by a prominent peak (median: 326.25 ind. m^{-3}) during the strong EN, and finally, there was an extremely low abundance (median: 75.51 ind. m^{-3}) in the post-EN period. Univariate PERMANOVA revealed that the difference in total zooplankton abundance between time periods (pre-EN / peak EN / post-EN, Fig. 9) was highly significant ($p = 0.00002$, aovperm). Furthermore, post-hoc Nemenyi tests showed that all pairwise comparisons between these three time periods were statistically significant (Pre-EN *vs* peak EN: $p = 0.02$, Pre-EN *vs* postEN: $p = 0.008$, peak EN *vs* Post-EN, $p = 0.00002$).

Also, total zooplankton abundance exhibited a clear seasonality, with higher abundances in the dry season (Fig. 9). The difference between dry and rainy season, for total zooplankton abundance, was highly significant ($p = 0.005$, univariate one-way PERMANOVA, function “aovperm”).

Figure 9. Boxplots showing the total zooplankton (log_{10}-transformed) abundance *vs* season (dry and rainy) and *vs* time periods (pre-EN, peak EN and post-EN). Samples (n = 107) were obtained bimonthly from June 2013 to August 2019 at three stations in Tamandaré Bay, Brazil. All differences displayed in the plots were significant (univariate PERMANOVA and post-hoc Nemenyi test, $p < 0.05$).

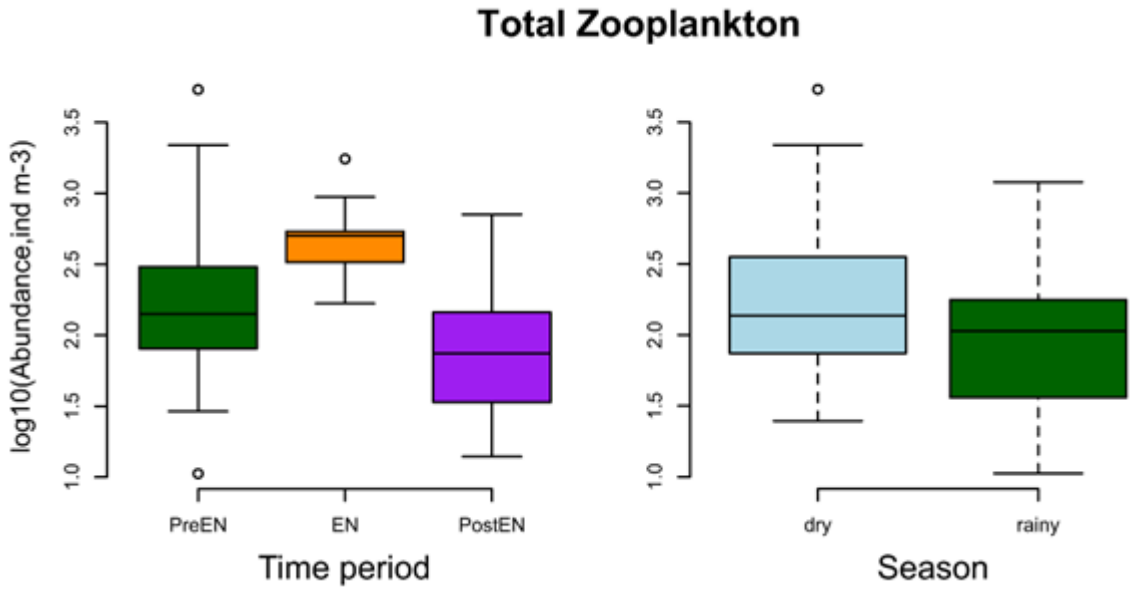

Fonte: A autora (2024).

3.5.b. Key holoplankton taxa (copepods, chaetognaths, and appendicularians)

Copepod abundance displayed a highly significant ($p = 0.004$, function "aovperm", log(x+1)transformed abundance vs Date) decreasing trend from 2013 to 2019. Also, copepod abundance (log(x+1)transformed abundance) showed a highly significant seasonal pattern ($p = 0.0002$, function "aovperm") and a highly significant ($p = 0.0006$, function "aovperm") positive correlation with Secchi depth (i.e., higher abundance in more transparent waters, Fig. 9). The relationship with Secchi depth is evidently due to the seasonal pattern of copepod abundance, with minimum abundance in the peak rainy season (minimum water transparency), from April to July (Fig. 10).

Similarly, the chaetognath abundance time series showcased another highly significant decline over the study period ($p = 0.0001$, function "aovperm", log(x+1)transformed abundance vs Date, Fig. 10). In contrast to the copepods, chaetognatha abundance did not display any significant linear relationships with Secchi depth, sampling month, or any other variables, possibly due to the higher overall variability in the chaetognatha data and much lower numbers. The spatial factor (stations B1, B2, and B3) was not significantly related to any taxonomic group, except for the two fragile gelatinous predators Chaetognatha ($p = 0.018$, aovperm), and Cnidaria ($p = 0.026$, aovperm), both with higher abundances at the southernmost station 3, which suffers less surf impact and turbulence from the wave-washed reefs that are located close to station 1.

Appendicularians did not present any significant linear trends or relationships with other variables. Yet, their abundance was highly significantly ($p = 0.0002$, aovperm) different between EN periods (pre-EN / EN / post-EN), with a prominent peak in the 2015/16 EN period ("blue water" conditions). Also, appendicularian abundance was highly significantly ($p = 0.0004$, aovperm) different between dry and rainy seasons, with much higher abundance in the dry season.

3.5.c. Penaeid shrimp postlarvae

The variability in abundance of penaeid shrimp postlarvae (mostly *Penaeus* spp.) was well explained by water transparency (Secchi depth), where "blue waters" with 4m or more Secchi depth were characterized by zero or extremely low abundances of penaeid postlarvae (Fig. 10).

The simple linear model of log10(x+1)transformed abundance of penaeid shrimp post-larvae vs Secchi depth was highly significant (p: 0.002, R^2 = 0.09, aovperm). Also, the Spearman rank correlation between abundance and Secchi depth was characterized by extremely high significance (p: 0.0001, Fig. 8).

The best multivariate linear model (best AIC) for penaeid shrimp postlarvae (raw data) was highly significant (p = 0.0004, R^2 = 0.164) and included three explanatory variables: Secchi depth, wind speed, and TSA (Tropical South Atlantic SST anomalies). Relative importance metrics ("lmg" index) showed that within this model, Secchi depth, wind speed, and TSA could explain 8.4, 2.9, and 5.1 % of the total variability in postlarval abundance, respectively.

The linear relationship between penaeid shrimp postlarvae (raw data) and Secchi depth is clearly due to the seasonal co-variance of these two variables. Penaeid postlarvae had their seasonal mean peak abundance in July, and mean Secchi depth also indicated the seasonal mean minimum in water transparency in July (Fig. 10). Accordingly, when analyzing seasonal anomalies instead of raw data, we observed no significant relationship between penaeid abundance anomalies and Secchi anomalies, whether testing with permutational linear models or with Spearman correlation tests (Fig. 8). This proves that the observed relationship between these two raw variables was based only on seasonal co-variance.

Yet, penaeid shrimp data were significantly related to another variable: time. Penaeid postlarvae abundances displayed a highly significant (p: 0.0004, R^2: 0.096, aovperm) and continuous linear decrease throughout the study period (Fig. 10). This linearly declining trend was highly significant for all transformations, whether using seasonal anomalies of penaeid postlarvae abundances, log10(x+min.+1)-transformed seasonal anomalies, raw abundances, or log10(x+1)-transformed raw abundance data. This shows a strong and consistent decline throughout the time series.

Also, seasonal anomalies of penaeid shrimp postlarvae abundances were significantly (p: 0.01, R^2: 0.058, aovperm) related to the TSA index. This linear relationship was significant ($p < 0.05$) for all transformations, whether using seasonal anomalies of penaeid postlarvae abundances, log10(x+min.+1)-transformed seasonal anomalies, raw abundances, or log10(x+1)transformed raw abundance data. This indicates the existence of a significant relationship between SSTs in the Eastern and Central Tropical South Atlantic (TSA index area) and shrimp recruitment in a coastal area of the Western Tropical South Atlantic (Tamandaré Bay).

Figure 10. Relationship between the log10 (x + 1) - transformed abundance of three selected key taxa (Copepods, Chaetognaths, and *Penaeus* spp. postlarvae) and explanatory variables Date, Secchi depth, TSA (Tropical South Atlantic SST anomalies) and sampling month. Samples (n = 107) were obtained bimonthly from June 2013 to August 2019 at three stations in Tamandaré Bay, Brazil.

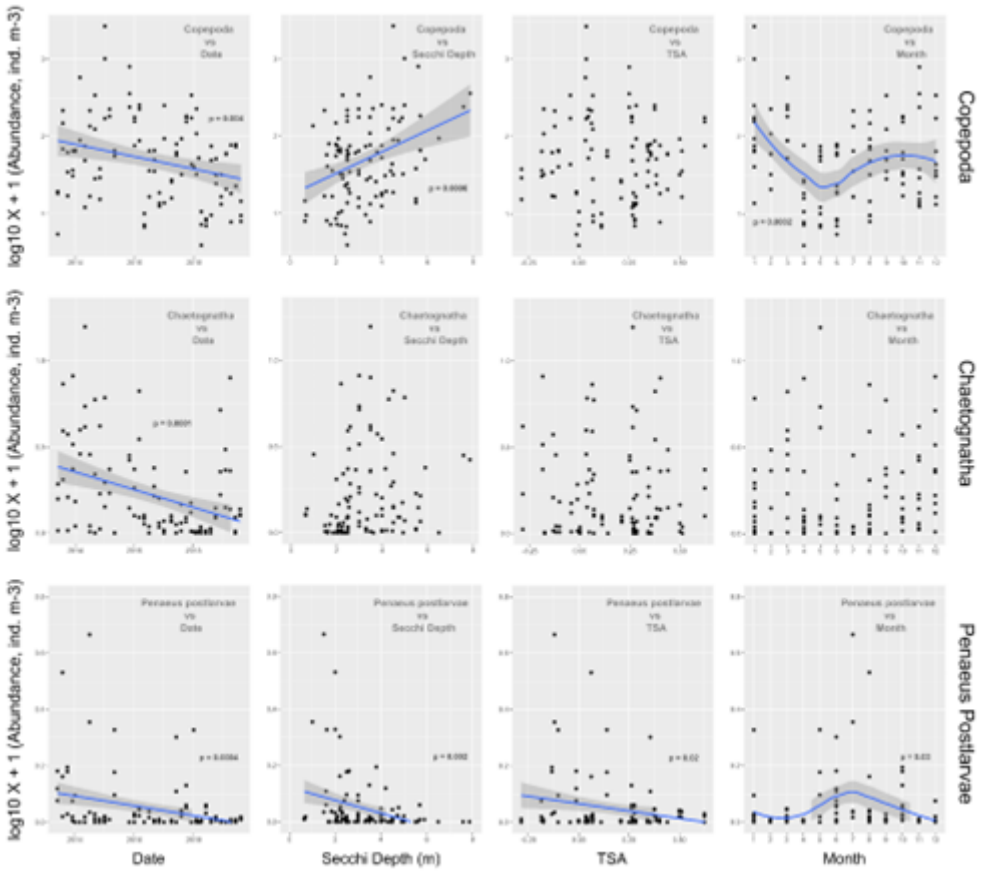

Fonte: A autora (2024).

3.6 Changes in macrozooplankton community structure (RDA and multivariate PERMANOVA)

Redundancy analysis (RDA, Fig. 11) showed that abiotic drivers can be used to explain 57% of the total variability in zooplankton community structure within the first two axes, where 37% and 20% of variance were explained by axes 1 and 2, respectively (Fig. 11). Most strikingly, the RDA ordination plot, based exclusively on the abundance of 12 key taxa, separated samples taken in pre-EN, peak strong EN, and post-EN periods very clearly (green, yellow, and purple symbols in the RDA plot, respectively, Fig. 11).

The RDA plot evidenced a clear interannual separation, illustrating the existence of three macrozooplankton communities: pre-EN, peak strong EN, and post-EN. The differentiation of pre- and post-EN communities (purple and green symbols in the RDA plots) showed considerable overlap, but spread the samples clearly along the first axis (post-EN samples being mostly on the left side of the plot, and pre-EN samples mostly to the right). The difference in community structure between pre-EN and post-EN periods was highly significant (multivariate PERMANOVA, pre-EN *vs* post-EN, $p < 0.0001$).

The strong 2015/16 EN event was evident only in the second axis (yellow symbols being in the upper portion of the plot). The difference in community structure between peak EN and the other periods was also highly significant (multivariate PERMANOVA, peak EN *vs* pre&post-EN, $p < 0.0001$).

Seasonality spread the samples considerably within years, and was statistically significant ($p = 0.02$, multivariate PERMANOVA, dry vs rainy season). Yet, seasonality did not lead to a consistent separation and ordination pattern throughout the first two RDA axes, showing the strong interannual variability, and the absence of a consistent seasonality pattern in this dataset, with highly variable seasonal patterns among taxonomic groups and years, especially in the period after the strong EN. Also, the use of Hellinger-transformed abundance (i.e., square-root-transformed relative abundance) and Bray-Curtis similarity will not consider the quantitative (total abundance) changes in absolute numbers, but only changes in relative composition, that were clearly dominated by interannual (not seasonal) variability. All samples taken in 2019 (and all 2018 rainy season samples) are located in the far left of the RDA diagram (post-EN). Conversely, most samples from 2013, 2014 and 2015 (post-EN) are located at the far right or at the center of the diagram. TSA and Rainfall both point towards the left (where

mostly post-EN samples are located), highlighting the excellent congruence of the RDA analysis, the increase in TSA and rainfall after the 2015/16 EN event and the existence of a relevant change in macrozooplankton community structure, driven by changes in TSA and rainfall. Copepods, gastropods, chaetognaths, luciferid shrimp, and *Penaeus* spp. postlarvae were distributed towards the right portion of the RDA plots (Fig. 10), due to their high abundances in the pre-EN period and decline after the strong EN. Appendicularians and copepods are placed upwards along the second axis, according to their peak abundance during the strong EN event (yellow symbols in the RDA plot).

Figure 11. Redundancy analysis (RDA) based on the abundance (ind.m^{-3}) of zooplankton communities (abundance of the most common key taxa with frequency of occurrence above 5%; response variables) versus environmental and climatology descriptors (explanatory variables). Cop: Copepoda; App: Appendicularia; Chae: Chaetognatha; Luc: Luciferidae (adults and juveniles); Pen: Penaeid postlarvae; Cni: Cnidarian medusae; Serg: Sergestid protozoeae; Bry: Bryozoan cyphonautes larvae; Fegg: Teleost fish eggs; Gast: Gastropod veliger larvae; Luc_p: Luciferid protozoea larvae, and Bra_z: Brachyuran crab zoeae. Samples (n = 107) were obtained bimonthly from June 2013 to August 2019 at three stations in Tamandaré Bay, Brazil.

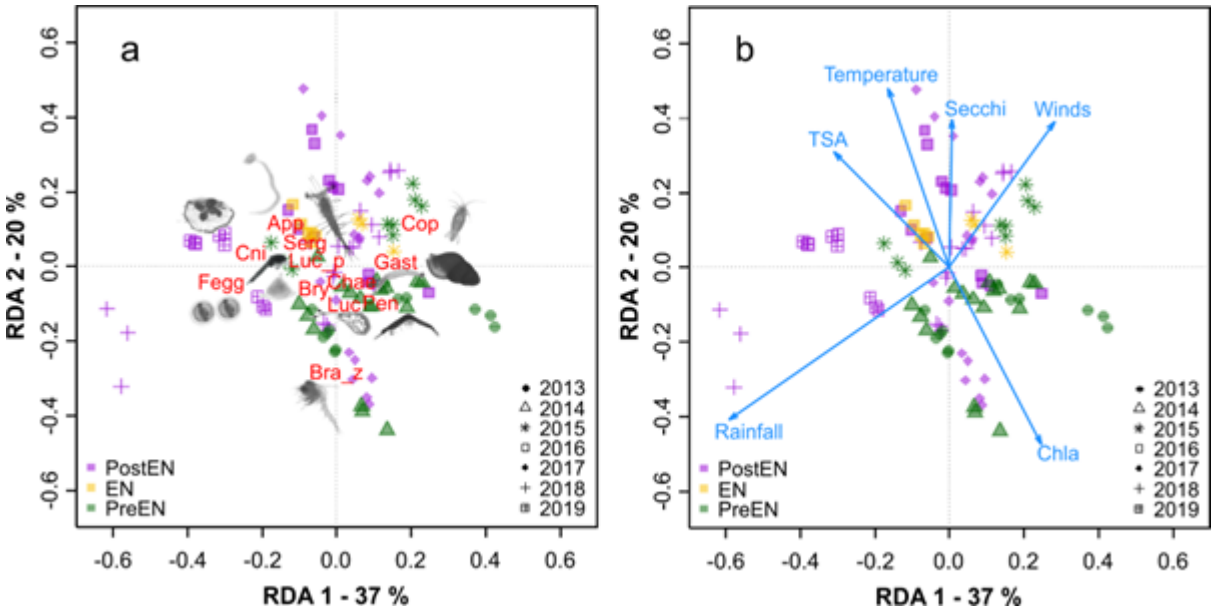

Fonte: A autora (2024).

Cnidarians and teleost eggs were placed on the left side of the RDA (Fig. 11), which is in accordance with their increased relative abundance during the post-EN period. These two groups did actually not show a significant increase in absolute numbers after the strong EN. However, since they were among the few groups not to show a decline in absolute numbers, their relative abundance increased considerably within a zooplankton community in general decline. Since the RDA is based on relative abundances (not absolute numbers), cnidarian medusae and fish eggs are highlighted on the right side of the plot, as the few “winners” of the recent ecosystem regime shift in Tamandaré Bay.

4 DISCUSSION

This is the first study to investigate a time series of seasonal and interannual variations of planktonic decapods and other macrozooplankton in the Southwestern Tropical Atlantic and to relate these variations to global-scale climate indices, such as ONI and TSA.

4.1 Seasonal vs interannual variability of abiotic conditions in the study region

Many abiotic and biological variables displayed a considerable seasonality, mainly driven by variations in rainfall in this coastal region with two well-defined seasons (rainy and dry). Salinities in Tamandaré Bay were significantly correlated with local rainfall (sum of 5 preceding days), and the Una river discharge, highlighting the excellent consistency within our data set. These correlations were highly significant for raw data and for seasonal anomalies, proving that there are significant seasonal and interannual components in this covariance, and significant interannual change in salinity (as proved by points–of-change testing and permutation-based trend analysis).

Conversely, Secchi depth was dominated by strong seasonal variations only and did not show any significant interannual changes. Secchi depth in Tamandaré Bay was significantly correlated with satellite-derived chlorophyll a, rainfall, and to the Una river discharge, as expected for a “green-water” / “blue-water” seasonal cycle driven by seasonally varying freshwater and nutrient inputs and wind-driven resuspension of nutrients from sediments (Schwamborn *et al.*, 2024). Also, Secchi depth was correlated with surface (1m) water temperature, showing the importance of the seasonal cycle, with less transparent waters in the cooler rainy season. Accordingly, Secchi depth seasonal anomalies were not correlated with temperature seasonal anomalies, or any other anomalies, proving that all significant relationships with Secchi depth were exclusively due to the strong seasonal variably in Secchi depth, the absence of any significant interannual long-term trends in Secchi depth, and strong seasonal covariance between Secchi depth and many other abiotic and biological variables**.**

Seasonal variations in community structure were weakly significant ($p = 0.02$, multivariate PERMANOVA), and this weak seasonality did not lead to a consistent separation

and ordination pattern of dry vs rainy season samples throughout the first two RDA plot, most likely due to strong interannual variability (extremely oligotrophic conditions in November 2015, and peak rainfall events at the end of the time series), and the absence of a consistent seasonality pattern in the biological dataset, with highly variable seasonal patterns among taxonomic groups and years, especially in the period after the strong EN. This may indicate a loss of regular seasonality in salinity, Secchi depth, and in community phenology, due to the combined impact of the strong 2015/16 EN and climate change. The initial regular pattern (pre-EN period) was disrupted during the strong EN, by unusually oligotrophic conditions (November 2015) and a completely failed rainy season (February to August 2016), followed by unusually strong rainfall and three extreme rainfall events (post-EN), all of which led to a loss of regularity in seasonal cycles. Similarly, Wells *et al.* (2022) reported a "complete breakdown of the seasonal cycle" at the end of their zooplankton time series in west Schotland, due to extremely increased rainfall.

4.2 Climate and ocean trends and regime shifts at the tipping point in 2015 / 2016

One important result of this study was that rainfall in the study area increased significantly ($p = 0.0004$) over the period from 2013 to 2019. We did not detect any significant change in water temperature in the study area, from 2013 to 2019, despite relevant global warming during this period. This apparent contradiction may be due to our relatively short time series and high overall variability in a relatively small and dynamic tropical bay. Another likely explanation for the lack of local warming in the surface waters of Tamandaré Bay may have been the combination of increased rainfall, cloud cover, and variability in winds, which may have masked the effects of global warming in the study region in the period from 2013 to 2019. Conversely, there was a significant warming of oceanic surface waters in the Eastern and Central Tropical South Atlantic (TSA, this study) in the study period. Thus, in contrast to small-scale temperature measurements at a local scale, large-scale analyses, that integrate and average over extensive ocean regions, can indeed show that global warming affected water temperatures in the Eastern and Central Tropical South Atlantic (TSA, this study) and elsewhere (Wiltshire *et al.*, 2009), even for a limited time series. Additionally, our study proved the occurrence of a unidirectional point of change (tipping point) in TSA temperatures during the 2015/16 record strength ("Godzilla") EN event.

Among all abiotic variables tested, salinity displayed the most striking and significant interannual changes (in median values and in variability). Significant changes in salinity occurred after the strong 2015/16 EN event. This illustrates that there was a "regular", low-variability pattern in salinity before the strong "Godzilla" EN event in 2015/16, and that after this EN event, there was a regime shift towards a highly dynamic "roller-coaster" mosaic of patterns ("up-and-down", "narrow-and-wide"), with alternating periods of low and high median SSS values and low and high variability.

This change in the seasonal SSS pattern is probably mediated by the increase in extreme rainfall events in the study area after September 2016. These variations in local salinity anomalies, after 2016, may also be due to variable combination effects of ever more common extreme rainfall events at the upper ranges of the Una River and other nearby river systems, rainfall events in other parts of the study area becoming more common, and varying incursions and mixtures of high-salinity waters from the adjacent shallow coral reef labyrinth, and low-salinity filaments from estuarine plumes derived from nearby mangrove creeks and river systems within a highly dynamic coastal system.

The relationship between increasing SSTs in the TSA area and more common and more extreme rainfall events in the study area has been well described and explained in several recent studies (Marengo *et al.*, 2023). Increasing heat content in the upper layers of the TSA leads to increased frequency and severity of easterly wave atmospheric disturbances that transport moisture from the TSA area towards the Northeast Brazilian Coast (Marengo *et al.*, 2023).

4.3 Time series in Tamandaré and elsewhere showcase zooplankton declines and regime shifts in pelagic ecosystems

Similarly to our results, Wells *et al.* (2022) also found global-warming-related increasing rainfall to be the key driver to explain the decline in zooplankton abundance in temperate coastal zooplankton on the west coast of Scotland. In spite of a completely different climatic and biogeographic setting, their extensive time series analysis yielded many similar results to our study. In spite of impressive global warming in the time period of their study, and increased SSTs in the adjacent North Atlantic, they did not find any increase in local water temperature (actually, a slight decrease), probably due to the dramatically increased rainfall in this coastal region. The overall climate change scenario described for the west coast of Scotland

is strikingly similar to the one observed in our study, with warming in the TSA index area and increased rainfall in the Tamandaré coastal region, located far leewards of the TSA index area.

Copepods and many other zooplankton were in decline in Loch Ewe, west Scotland (Wells *et al.* 2022). According to the authors, the drastic decline in numbers of most zooplankton taxa in Loch Ewe finally led to a "complete breakdown of the seasonal cycle" (Wells *et al.*, 2022). Similarly, in our study, we observed significant and drastic declines in numbers of total zooplankton and several taxa, such as copepods, chaetognaths, appendicularians, and penaeid shrimp postlarvae. Just like our investigation, Ayón *et al.* (2008) also detected relevant regime shifts in Peruvian zooplankton time series that were evidently triggered by strong EN events.

4.4 Shrimp postlarvae time series in Tamandaré and elsewhere

Several previous studies have investigated the variability in penaeid recruitment through the abundance of shrimp postlarvae, with strongly varying key results, as a function of the various shrimp species, life histories and ecosystems analyzed (Aragón-Noriega & Calderón-Aguilera 2000; Criales *et al.*, 2003; Heckler *et al.*, 2014).

Conversely to our study, Aragón-Noriega & Calderón-Aguilera (2000) observed that in the Upper Gulf of California (UGC), postlarvae of *Penaeus stylirostris* had greater abundance in years with lower salinity (1993 and 1997). In this particular system, the complete damming of the Colorado River had drastic negative consequences (including high salinities and zero freshwater flow) for the coastal nursery areas, and for the life cycle of *P. stylirostris.*

In the study by Criales *et al.* (2003), the abundance of postlarvae of the pink shrimp *Penaeus duorarum* in South Florida was investigated in the context of wind-driven postlarval transport form offshore waters into Florida Bay through inter-island channels, from October 1997 to June 1999. Postlarval transport displayed different patterns of magnitude and seasonality between Whale Harbor (WH) and Long Key (LK) inter-island channels. These channels connect the Atlantic Ocean with Florida Bay. In WH, there was an increase in the entry flow of post-larvae between spring-summer and winter, different from LK, with the most significant entry of post-larvae at the end of spring-summer, favored by winds and currents. Interestingly, there were also seasonal differences in body size. During the winter months,

postlarvae were significantly larger compared to the individuals collected in the summer months.

Our data clearly showed a significant decline in penaeid postlarvae throughout the study period (2013 to 2019). Conversely, Heckler *et al.* (2014) found no difference in the total abundance of juvenile seabob shrimp (*Xiphopenaeus kroyeri*, Heller, 1862) over 13 years, in four different areas of Ubatuba Bay, São Paulo State, southeastern Brazil. Clearly, the species, stage (postlarvae vs juveniles), life cycle, ecosystem structure, water masses, and climatology in this study are completely different from our study, with strong seasonal upwelling and intrusions of cold, nutrient-rich water masses in Ubatuba, and tropical waters in Tamandaré, located thousands of KMs to the north of Ubatuba. This exemplifies the importance of considering the specific peculiarities of each penaeid shrimp species, stage, and ecosystem in such time series analyses, and the inadequacy of any gross generalizations for penaeid shrimps.

4.5 Zooplankton communities in Tamandaré and elsewhere

Calanoid copepods are usually the dominant taxonomic group within the marine meso- and macrozooplankton, in units abundance, biovolume and biomass, in virtually all regions of the world oceans (Palomares-García *et al.*, 2013; Melo Júnior *et al.*, 2016). Among the calanoids, the species *Acartia (odontacartia) lilljeborgii* is very common and often numerically dominant in Tamandaré Bay and many other coastal areas of the Tropical Atlantic (Escamilla *et al.*, 2011; Silva *et al.*, 2004). This species showed a clear seasonal variability, with higher relative abundance in the dry season in a tropical coastal lagoon in the southern Gulf of Mexico (Escamilla *et al.*, 2011). This is similar to our results, where copepods had higher abundance in the dry season (maximum water transparency). With global warming and consequently increasing rainfall, as seen in our study, this dominant coastal marine species, *A. lilljeborgii* may possibly see its abundance reduced, while other, more estuarine copepods may dominate (Brito-Lolaia *et al.*, 2020; 2022; Brito-Lolaia *et al.*, in prep.).

Among appendicularians, the genus *Oikopleura* spp. is the most abundant in coastal waters of the Tropical Atlantic (Brito-Lolaia *et al.*, 2020; 2022). *Oikopleura* spp. are well adapted for life in oligotrophic waters due to their gelatinous “house”, a complex and ephemeral external structure used to capture small-sized food particles, which may concentrate particles

as small as 0.1 µm (Flood and Deibel, 1998). This ability gives them a considerable advantage in oligotrophic (microbial-loop-dominated) conditions, where there are less large-sized diatoms and small-sized unicellular organisms dominate the phytoplankton. Similarly to our study, a previous study in Tamandaré Bay showed that *Oikopleura* spp. had higher relative biomass in the dry season when the environment is more oligotrophic (Brito-Lolaia *et al.*, 2022) and explains its low abundance in the post-EN period, when the system was more eutrophic, with peaks in rainfall and Una River Discharge.

Chaetognaths constitute a group of marine carnivores that are widely distributed in coastal and oceanic waters of the world (Casanova, 1999). Similarly to our study, Schwamborn *et al.* (2024) observed little or no chaetognaths in estuarine waters in the Tamandaré region, proving that this is as an exclusively marine (not estuarine) taxon. *Sagitta* spp. is the most abundant and widely distributed chaetognath genus (Neumann-Leitão *et al.*, 1999; Melo *et al.*, 2020). Chaetognaths are avid predators of zooplankton and feed on a wide variety of taxa, but their main prey are usually copepods (Pearre Jr, 1980; Feigenbaum and Maris, 1984; Bone *et al.*, 1991; Stuart and Verheye, 1991). In our study, chaetognaths and copepods showed a congruent decline in their populations from 2013 to 2019, which may be due to a similar response to environmental drivers (e.g., salinity, pollutants, etc.), but also possibly also related to their prey-predator relationship, via a bottom-up food-web-mediated reduction of chaetognath numbers due to declining prey numbers. These two mechanisms (simultaneous response to changing environments, and bottom-up control), are not at all contradictory and may actually most likely be occurring simultaneously. Baier and Terazaki (2005) observed a predator-prey interaction in their study on arctic chaetognaths and copepods in the southeastern Bering Sea. In their study, chaetognath abundance and body size reflected variations in their prey, suggesting a possible bottom-up control (Baier and Terazaki, 2005). *Sagitta elegans* were larger and had low abundance when large copepods, *Calanus marshallae*, were most abundant in years of greatest ice extent, and were smaller and displayed high abundances when small copepods, such as *Pseudocalanus* spp. and *Acartia* spp. were dominant in relatively warm years, in the southeastern Bering Sea (Baier and Terazaki, 2005).

4.6 Trends and changes in ecosystem descriptors - explaining the decline

A significant decline in abundance was detected for total zooplankton and several key taxonomic groups such as copepods, chaetognaths, appendicularians, and *Penaeus* spp. postlarvae.

A continuous and significant linear decline in numbers was detected for copepods, chaetognaths, and *Penaeus* spp. postlarvae. For appendicularians, a decline was also observed, but it did not follow a consistent linear trend, but rather showed a stepwise pattern of change, with peak abundance at the strong EN event, and then significantly lower abundances in the post-EN (May 2016 to August 2019) period than in the preceding periods. The main difference between the appendicularian time series and the other key taxa (e.g., copepods, chaetognaths, and *Penaeus* spp. postlarvae) was the huge peak in appendicularian numbers during the exceptionally oligotrophic "blue water" conditions in the EN month of November 2015. While several other taxa (e.g., copepods), and total zooplankton, did actually also present an evident peak in abundance in November 2015, this peak was not as strikingly prominent as for appendicularians.

In principle, any temporal trends in biological variables should be explainable by a single abiotic variable or a discrete set of abiotic variables. However, for these taxonomic groups, no consistent seasonal and interannual preference for any given abiotic condition was observed. On the contrary, while shrimp postlarvae occurred seasonally in "green waters" during the months of May to October (rainy and windy season), copepods, appendicularians, and chaetognaths were more abundant during "blue water" conditions with high transparency. This apparent contradiction highlights the importance of distinguishing and carefully analyzing seasonal and long-term variability, processes, and drivers, for each taxonomic group. In the case of shrimp postlarvae, the seasonal patterns are mediated by seasonal changes in wind-driven cross-shelf transport. *Penaeus spp.* larvae are originated from hatching cohorts in the outer shelf and shelf break, that are transported by surface currents and winds towards the coast in the windy (and rainy) season. Wind-driven surface transport of shrimp postlarvae (and crab megalopae) has been widely documented. *Penaeus spp.* postlarvae are pre-settlement stages that are migrating from the continental shelf towards the nearby mangrove estuaries, and are well adapted to varying salinities.

Conversely, appendicularians (*Oikopleura* ssp., mainly and *O. dioica*) and chaetognaths are typically marine groups. In a recent analysis of spatial patterns, comparing estuarine and marine ecosystems in the study region, Schwamborn *et al.* (2024) showed that chaetognaths occur almost exclusively in marine, high-salinity waters. Thus, it should not be surprising that appendicularians and chaetognaths declined in the post-EN period with strong rainfall events and thrived in the low rain, "failed rainy season" during the 2015/16 EN.

Appendicularians and many other taxa showed significant variability between pre-EN end post-EN periods, with high abundance during the pre-EN phase, a conspicuous and significant peak in abundance in the EN event, followed by a plateau of significant let lower decline after EN, indicating a relevant ecosystem regime shift after the strong EN event. For total zooplankton and some taxonomic groups (e.g., copepods and appendicularians), the observed significant decrease within our time series may have been influenced by statistical effects of the peak during the record strength EN event. Penaeid shrimp postlarvae and chaetognaths, however, did not show any detectable peak during the EN event, and thus their significant decrease is most likely related to other effects, such as the increasingly extreme rainfall in the study area.

The observed decline in shrimp postlarvae is probably due to a complex variety of interacting factors and processes, such as bottom-up food-web effects (postlarvae being impacted by a decline their preys, such as copepods), due to a possible change in wind and current patterns that may affect their shoreward migration, increase in predators, such as cnidarian medusae, overfishing of parental shrimp stocks on the shelf, and increasing concentrations of pollutants (e.g., pesticides and microplastics), that are washed from the continent during extreme rainfall events. Undoubtedly, the Tamandaré Bay region has become less favorable for penaeid shrimp recruitment in the period from 2013 to 2019.

4.7 ENSO and the 2015/16 climate regime shift in the Tropical South Atlantic

Originally, this study was designed with the expectation to be able to investigate the effects of the El Niño Southern Oscillation (ENSO) on coastal ecosystems in northeastern Brazil. Surprisingly, the strong El Niño 2015/2016 did not show the expected effects (e.g., in water temperature) in this particular ecosystem. One main reason may be that this El Niño had strong effects in the Pacific, but the effect in the tropical Western Atlantic was felt most strongly in the southern regions (e.g. Argentina, Uruguay, and Southern Brazil) through coastal trapped

waves that had devastating effects in these regions, but did not reach far north as to affect coastal ecosystems in Pernambuco State, Brazil. This may explain why the ONI index and other El Niño related indices had no significant effects on the pelagic ecosystem in Tamandaré Bay. Conversely, the TSA index, composed of seasonal anomalies of the sea surface temperature in the Tropical South Atlantic, has proven to be an important and significant index for the abundance of penaeid shrimp postlarvae and many other organisms in the study region.

Considering wind, weather, and current patterns in the study area all have east-westwards transport patterns, it should be no surprise that the TSA index has an effect in Northeastern Brazil. Strong southeasterly winds in the second half of the year bring weather from the TSA region to Tamandaré. Atmospheric easterly wave disturbances that create extreme rainfall over Northeastern Brazil are formed in the TSA region. Also, the oligotrophic Tropical Surface Water masses found in Tamandaré originate from the TSA region (Fig. 2). More precisely, the extremely oligotrophic, warm, and saline southern branch of the South Equatorial Current (sSEC) flows in a northwesterly direction through the TSA region towards the Brazilian coast, where it bifurcates into the Brazil Current (BC) and the North Brazil Undercurrent (NBUC). The NBUC flows along the Pernambuco shelf break off Tamandaré (Fig. 2).

The TSA time series indicates a regime shift in 2015/16, with consistently warmer SST in the TSA region since the 2015/16 strong EN event, with a clear breakpoint (tipping point) in the second semester of 2015. Thus, ENSO seems to have a strong, but indirect effect in the study region. The strong EN event acted as a trigger for the observed regime shift in the TSA region, which then directly affected north-east Brazilian coastal ecosystems. Similarly, numerous studies (Ayón *et al.*, 2008; Aronés *et al.*, 2009) showed that regime shifts in the Pacific are also triggered by strong EN events. This is the first study to reveal a relevant climate and ecosystem tipping point (most likely triggered by the strong 2015/16 EN event) and to show the consequences of this climate regime shift for pelagic communities in a tropical coastal ecosystem.

4.8 Outlook

More recently, in May 2022, exceptionally heavy rainfall at the coast of northeastern Brazil (including Pernambuco state) led to catastrophic landslides and flash floods, with irreparable losses in urban and coastal areas (Marengo *et al.*, 2023). Such rainfall events have been explained by atmospheric easterly wave disturbances, that are related to the mounting heat content in the upper layers of the Tropical South Atlantic (Marengo *et al.*, 2023).

Our results indicate that the increase in vulnerability and risks for the recruitment of penaeid shrimp stocks due to increasingly intense and frequent extreme events must be urgently considered in the monitoring and management of ecosystems in Brazil and other tropical regions, for a truly precautionary approach to fisheries.

The currently ongoing record strength 2023/24 EN event has already (in December 2023) led to even higher temperatures in several parts of the world, including in the TSA index region. Our study showed that such strong EN events can trigger tipping point phenomena that lead to climate and ecosystem regime shifts in the Tropical Atlantic, with potentially detrimental consequences for coastal ecosystems and fisheries in the near future.

REFERENCES

Abualreesh, M. H. (2021). Biodiversity and contribution of natural foods in tiger shrimp (*Penaeus monodon*) aquaculture pond system: a review. AACL Bioflux, 14(3), 1715-1726.

Alheit, J., & Bakun, A. (2010). Population synchronies within and between ocean basins: apparent teleconnections and implications as to physical–biological linkage mechanisms. Journal of Marine Systems, 79(3-4), 267-285.

Alves, R. R. N., Pinto, M. F., Borges, A. K. M., & Oliveira, T. P. R. (2023). Fisheries and Uses of Coastal Aquatic Fauna in the Northernmost Brazilian Atlantic Forest. In Animal Biodiversity and Conservation in Brazil's Northern Atlantic Forest (pp. 229-255). Cham: Springer International Publishing.

Anderson, M.J., (2017). Permutational Multivariate Analysis of Variance (PERMANOVA). In: Balakrishnan, N., Colton, T., Everitt, B., Piegorsch, W., Ruggeri, F., Teugels, J.L.(Eds.), Wiley StatsRef: Statistics Reference Online. https://doi.org/10.1002/9781118445112.stat07841.

Aragón-Noriega, E. A., & Calderón-Aguilera, L. E. (2000). Does damming of the Colorado River affect the nursery area of blue shrimp Litopenaeus stylirostris (Decapoda: Penaeidae) in the Upper Gulf of California?. Revista de Biología Tropical, 48(4), 867-871.

Aronés, K., Ayón, P., Hirche, H. J., & Schamber, R. (2009). Hydrographic structure and zooplankton abundance and diversity off Paita, northern Peru (1994 to 2004)—ENSO effects, trends and changes. Journal of Marine Systems, 78(4), 582-598.

Aronés, K., Grados, D., Ayón, P., & Bertrand, A. (2019). Spatio-temporal trends in zooplankton biomass in the northern Humboldt current system off Peru from 1961-2012. Deep Sea Research Part II: Topical Studies in Oceanography, 169, 104656.

Ayón, P., Criales-Hernandez, M. I., Schwamborn, R., & Hirche, H. J. (2008). Zooplankton research off Peru: a review. Progress in Oceanography, 79(2-4), 238-255.

Baier, C. T., & Terazaki, M. (2005). Interannual variability in a predator–prey interaction: climate, chaetognaths and copepods in the southeastern Bering Sea. Journal of Plankton Research, 27(11), 1113-1125.

Bentamy, A.; Fillon, D. C. (2012). Gridded surface wind fields from Metop/ASCAT measurements. International journal of remote sensing, v. 33, n. 6, p. 1729–1754, .

Bondad-Reantaso, M. G., Subasinghe, R. P., Josupeit, H., Cai, J., & Zhou, X. (2012). The role of crustacean fisheries and aquaculture in global food security: past, present and future. Journal of invertebrate pathology, 110(2), 158-165. http://dx.doi.org/10.1016/j.jip.2012.03.010

Bone Q, Kapp H, Pierrot-Bults AC. (1991) The Biology of Chaetognaths. 1st ed. Oxford: Oxford University Press.

Botsford, L. W., Moloney, C. L., Hastings, A., Largier, J. L., Powell, T. M., Higgins, K., & Quinn, J. F. (1994). The influence of spatially and temporally varying oceanographic conditions on meroplanktonic metapopulations. Deep Sea Research Part II: Topical Studies in Oceanography, 41(1), 107-145. https://doi.org/10.1016/0967-0645(94)90064-7

Breiman, L., (2001). Random forests. Machine Learning, 45, 5–32. https://doi: 10.1023/A:1010933404324

Brito-Lolaia, M. *et al.* (2022) Can the stable isotope variability in a zooplankton time series be explained by its key species? Marine Environmental Research, v. 181, p. 105737.

Brito-Lolaia, M. *et al.* (2020) Micro- and mesozooplankton at the edges of coastal tropical reefs(Tamandaré, Brazil). Helgoland Marine Research, v. 74, 1.

Brum, M., Gutiérrez López, J., Asbjornsen, H., Licata, J., Pypker, T., Sanchez, G., & Oiveira, R. S. (2018). ENSO effects on the transpiration of eastern Amazon trees. Philosophical Transactions of the Royal Society B: Biological Sciences, 373(1760), 20180085. https://doi.org/10.1098/rstb.2018.0085

Cai, W., Santoso, A., Wang, G., Yeh, S. W., An, S. I., Cobb, K. M., ... & Wu, L. (2015). ENSO and greenhouse warming. Nature Climate Change, 5(9), 849-859.

Casanova J.P. (1999) Chaetognatha. In: Boltovskoy D, editor. South Atlantic Zooplankton. Leiden: Backhuys Publishers. pp. 1353–1374.

Chavez, F. P., Ryan, J., Lluch-Cota, S. E., & Ñiquen C, M. (2003). From anchovies to sardines and back: multidecadal change in the Pacific Ocean. science, 299(5604), 217-221.

Coelho, P. A., & Santos, M. C. F. (1993). Época da reprodução do camarão branco, Penaeus schmitti Burkenroad (Crustacea, Decapoda, Penaeidae) na região de Tamandaré. PE. Bol. Tecn. Cient. Cepene, 1, 157-169.

Coria-Monter, E., Salas de León, D. A., Monreal-Gómez, M. A., & Durán-Campos, E. (2019). Satellite observations of the effect of the “Godzilla El Niño” on the Tehuantepec upwelling system in the Mexican Pacific. Helgoland Marine Research, 73, 1-11.

Coria-Monter, Erik; Monreal-Gómez, María Adela; León, David Alberto Salas de; Durán-Campos, Elizabeth (2018). Impact of the “Godzilla El Niño” Event of 2015–2016 on Sea-Surface Temperature and Chlorophyll- a in the Southern Gulf of California, Mexico, as Evidenced by Satellite and In Situ Data. Pacific Science, 72(4), 411–422. doi:10.2984/72.4.2

Costlow, J. D., & Bookout, C. G. (1969). Temperature and meroplankton. Chesapeake Science, 253-255.

Coyle, K. O., & Paul, A. J. (1990). Abundance and biomass of meroplankton during the spring bloom in an Alaskan Bay. Ophelia, 32(3), 199-210. https://doi.org/10.1080/00785236.1990.10422031

Criales, M. M., Yeung, C., Jones, D. L., Jackson, T. L., & Richards, W. J. (2003). Variation of oceanographic processes affecting the size of pink shrimp (Farfantepenaeus duorarum) postlarvae and their supply to Florida Bay. Estuarine, Coastal and Shelf Science, 57(3), 457-468.

Mackas, D. L., Beaugrand, G. (2010). Comparisons of zooplankton time series, Journal of Marine Systems. Volume 79, Issues 3–4. Pages 286-304. ISSN 0924-7963. https://doi.org/10.1016/j.jmarsys.2008.11.030.

Díaz-Ochoa, J. A., Lange, C. B., Pantoja, S., De Lange, G. J., Gutiérrez, D., Muñoz, P., & Salamanca, M. (2009). Fish scales in sediments from off Callao, central Peru. Deep Sea Research Part II: Topical Studies in Oceanography, 56(16), 1124-1135.

Domingues, E.D.C., Schettini, C.A.F., Truccolo, E.C., Oliveira, J.C.D. (2017). Hydrography and currents on the Pernambuco continental shelf. Rbrh 22. https://doi.org/10.1590/2318-0331.0217170027.

Emerenciano, M. G., Rombenso, A. N., Vieira, F. D. N., Martins, M. A., Coman, G. J., Truong, H. H., ... & Simon, C. J. (2022). Intensification of penaeid shrimp culture: an applied review of advances in production systems, nutrition and breeding. Animals, 12(3), 236. https://doi.org/10.3390/ani12030236

Enfield, D. B., & Alfaro, E. J. (1999). The dependence of Caribbean rainfall on the interaction of the tropical Atlantic and Pacific Oceans. Journal of climate, 12(7), 2093-2103.

Escamilla, B.J.; Ordóñez-López, U.; Suárez-Morales, E. (2011). Spatial and seasonal variability of Acartia (Copepoda) in a tropical coastal lagoon of the southern Gulf of Mexico. Revista de Biología Marina y Oceanografía, 46 (3), pp. 379-390.

Feigenbaum, D. L.and Maris, R. C. (1984) Feeding in the chaetognatha.Oceanogr. Mar. Biol., Annu. Rev., 22, 343–392.

Ferreira, B.P., Maida, M., Cava, F., Messias, L.,(2003). Interações entre a pesca artesanal e o turismo em Tamandaré. In: APA Costa dos Corais. II Congresso sobre Planejamento e Gestão das Zonas Costeiras dos Países de Expressão Portuguesa. IX Congresso da Associação Brasileira de Estudos do Quaternário. II Congresso do Quaternário dos Países de Língua Ibérica.

Fiedler, P. C. (2002). Environmental change in the eastern tropical Pacific Ocean: review of ENSO and decadal variability. Marine Ecology Progress Series, 244, 265-283. doi:10.3354/meps244265

Flood, P., Deibel, D., (1998). The appendicularian house. In: The Biology of Pelagic Tunicates. Oxford University Press, New York, pp. 105–124.

Foltz, G. R., Brandt, P., Richter, I., Rodríguez-Fonseca, B., Hernandez, F., Dengler, M., ... & Reul, N. (2019). The tropical Atlantic observing system. Frontiers in Marine Science, 6, 206. https://doi.org/10.3389/fmars.2019.00206

Frossard, J., Renaud, O. (2021). Permutation tests for regression, ANOVA, and comparison of signals: the permuco package. J. Stat. Softw. 99, 1–32. https://doi. org/10.18637/jss.v099.i15.

Gorsky, G., Ohman, M. D., Picheral, M., Gasparini, S., Stemmann, L., Romagnan, J. B., Cawood, A., Pesant, S., Garcia-Comas, C., Prejger, F. (2010). Digital zooplankton image analysis using the ZooScan integrated system. Journal of Plankton Research, 32, 285–303. https://doi.org/10.1093/plankt/fbp124

Grego, C.K.S., Feitosa, F.A.N., Silva, M.H., Cunha, M.G.G.S., Nascimento Filho, G.A.N., (2009). Fitoplâncton do ecossistema estuarino do Rio Ariquindá (Tamandaré, Pernambuco, Brasil): variáveis ambientais, biomassa e produtividade primária. Atlântica, Rio Grande 31 (2), 183–198. https://doi.org/10.5088/atl.2009.31.2.183.

Grömping, U. (2007). Relative importance for linear regression in R: the package relaimpo. Journal of statistical software, 17, 1-27. https://doi.org/10.18637/jss.v017.i01

Gutiérrez, J. C., Ponce-Palafox, J. T., Pineda-Jaimes, N. B., Arenas-Fuentes, V., Arredondo-Figueroa, J. L., & Cifuentes-Lemus, J. L. (2016). The feeding ecology of penaeid shrimp in tropical lagoon-estuarine systems/Ecología alimentaria de camarones peneidos en los sistemas lagunar-estuarinos tropicales. Gayana, 80(1), 16.

Hao, M.C.; Dayal, U.; Keim, D.A.; Schreck, T. (2005). [IEEE IEEE Symposium on Information Visualization, 2005. INFOVIS 2005. - Minneapolis, MN, USA (Oct. 23-25, 2005)] IEEE Symposium on Information Visualization, 2005. INFOVIS 2005. - Importance-driven visualization layouts for large time series data. 203–210. doi:10.1109/infvis.2005.1532148

Heckler, G. S., da Costa, R. C., Fransozo, A., Rosso, S., & Munehisa Shimizu, R. (2014). Long-term patterns of spatial and temporal distribution in the seabob shrimp Xiphopenaeus kroyeri (Decapoda: Penaeidae) population in southeastern Brazil. Journal of Crustacean Biology, 34(3), 326-333. DOI: 10.1163/1937240X-00002231

Heinze, C., Blenckner, T., Martins, H., Rusiecka, D., Döscher, R., Gehlen, M., Gruber, N., Holland, E., Hov, Ø., Joos, F., Matthews J.B.R., Rødven, R., Wilson, S. (2021). The quiet crossing of ocean tipping points. Proceedings of the National Academy of Sciences Mar 2021, 118 (9) e2008478118; DOI: 10.1073/pnas.2008478118

Herrmann MLP, Alves DB. 2014. Síntese dos desastres naturais de 1980 a 2010. In Átlas de desastres naturais do Estado de Santa Catarina: período de 1980 a 2010, Herrmann MLP (ed). IHGSC/Cadernos Geográficos – GCN/UFSC: Florianópolis, 207–212.

Hounsou-Gbo, Gbèkpo Aubains, Jacques Servain, Moacyr Araujo, Guy Caniaux, Bernard Bourlès, Diogenes Fontenele, and Eduardo Sávio P. R. Martins. 2019. "SST Indexes in the Tropical South Atlantic for Forecasting Rainy Seasons in Northeast Brazil" Atmosphere 10, no. 6: 335.

Jiao, Y. (2009). Regime shift in marine ecosystems and implications for fisheries management, a review. Reviews in Fish Biology and Fisheries, 19, 177-191.

Legendre, P., & Gallagher, E. D. (2001). Ecologically meaningful transformations for ordination of species data. Oecologia, 129, 271-280.https://doi.org/10.1007/s004420100716

Lehodey, P., Bertrand, A., Hobday, A. J., Kiyofuji, H., McClatchie, S., Menkès, C. E., ... & Tommasi, D. (2020). ENSO impact on marine fisheries and ecosystems. El Niño Southern Oscillation in a changing climate, 429-451. https://doi.org/10.1002/9781119548164.ch19

Li, W., Zhang, P., Ye, J., Li, L., & Baker, P. A. (2011). Impact of two different types of El Niño events on the Amazon climate and ecosystem productivity. Journal of Plant Ecology, 4(1-2), 91-99. doi: 10.1093/jpe/rtq039

Lima, K. C., Satyamurty, P., & Fernández, J. P. R. (2010). Large-scale atmospheric conditions associated with heavy rainfall episodes in Southeast Brazil. Theoretical and Applied Climatology, 101, 121-135. DOI 10.1007/s00704-009-0207-9

Lindeman, R. H.; Merenda, P. F.; Gold, R. Z. Introduction to Bivariate and Multivariate Analysis. [s.l.] Scott, Foresman, 1980.

Mackas, D. L., & Beaugrand, G. (2010). Comparisons of zooplankton time series. Journal of Marine Systems, 79(3-4), 286-304. https://doi.org/10.1016/j.jmarsys.2008.11.030

Manso, V. D. A. V., Correa, I. C. S., & GUERRA, N. (2003). Morfologia e sedimentologia da plataforma continental interna entre as Praias Porto de Galinhas e Campos-Litoral Sul de Pernambuco, Brasil. Pesquisas em geociências, 30(2), 17-25.

Marengo, J. A., Alcantara, E., Cunha, A. P., Seluchi, M., Nobre, C. A., Dolif, G., ... & Moraes, O. L. (2023). Flash floods and landslides in the city of Recife, Northeast Brazil after heavy rain on May 25–28, 2022: Causes, impacts, and disaster preparedness. Weather and Climate Extremes, 39, 100545. https://doi.org/10.1016/j.wace.2022.100545

Mello, M. R. F., & Souza, R. V. C. C. (2013). 13936-Sistemas agroflorestais como uma alternativa de sustentabilidade no assentamento Jundiá de Cima, Tamandaré-PE. Cadernos de Agroecologia [Volumes 1 (2006) a 12 (2017)], 8(2).

Melo Júnior, M., Marcolin, C.R., Miyashita, L.K., Lopes, R.M., 2016. Temporal changes in pelagic copepod assemblages off Ubatuba, Brazil. Mar. Ecol. 37, 877–890. http://dx. doi.org/10.1111/maec.12366.

Monteiro, M., Cruz, J., Azeiteiro, U., Marques, S. C., Baptista, V., & Teodósio, M. A. (2023). Dynamics of Decapoda larvae communities in a southwest Iberian estuary: Understanding the impact of different thermal regimes. Estuarine, Coastal and Shelf Science, 294, 108547. https://doi.org/10.1016/j.ecss.2023.108547

NASA Goddard Space Flight Center, Ocean Ecology Laboratory, Ocean Biology Processing Group; (2014): MODIS-Aqua Ocean Color Data; NASA Goddard Space Flight Center, Ocean Ecology Laboratory, Ocean Biology Processing Group. https://oceancolor.gsfc.nasa.gov/ Accessed on 16/10/2023.

Nemenyi, P. 1963. Distribution-free Multiple Comparisons. Ph.D. thesis, Princeton University.

Neumann-Leitão S, Gusmão LM, Silva TDA, Nascimento-Vieira DA, Silva AP. Mesozooplankton biomass and diversity in coastal and oceanic waters off North-Eastern Brazil. Arch Fish Res. 1999; 47(2/3):153–165

Ockhuis, S., Huggett, J., & Sparks, C. (2017). The 'suitcase hypothesis': Can entrainment of meroplankton by eddies provide a pathway for gene flow between Madagascar and KwaZulu-Natal, South Africa?. African journal of marine science. https://doi.org/10.2989/1814232X.2017.1399292

Oksanen, J. *et al.* vegan: Community Ecology Package. 2019. R package version 2.5-6. Avilable online at https://CRAN. R-project. org/package= vegan .

Omori, M. & T. Ikeda. (1984). Methods in Marine Zooplankton Ecology. John Wiley & Sons, New York, 332 pp.

Palomares-García, R.J., Gómez-Gutiérrez, J., Robinson, C.J., 2013. Winter and summer vertical distribution of epipelagic copepods in the Gulf of California. J. Plankton Res. 35, 1009–1026. https://doi.org/10.1093/plankt/fbt052

Park, J. Y., J. S. Kug, J. Park, S. W. Yeh, and C. J. Jang. (2011). Variability of chlorophyll associated with El Niño–Southern Oscillation and its possible biological feedback in the equatorial Pacific. J. Geophys. Res. 116: C10001 (doi:10.1029/2011JC007056)

Pearre Jr S. (1980). Feeding by Chaetognatha: the relation of prey size to predator size in several species. Mar Ecol Prog Ser.; 3(2):125–134.

Pohlert, T. (2022). PMCMRplus: Calculate Pairwise Multiple Comparisons of Mean Rank Sums Extended. R package version 1.9.4. https://cran.r-project.org/web/packages/PMCMRplus/index.html

R Core Team. (2019) R: A Language and Environment for Statistical Computing. Vienna, Austria. URL: R Foundation for Statistical Computing. https://www.R-project.org/.

Richardson A.J. (2008) In hot water: zooplankton and climate change, ICES Journal of Marine Science, Volume 65, Issue 3, April, Pages 279–295, https://doi.org/10.1093/icesjms/fsn028

Ross, J.G. (2015). Parametric and Nonparametric Sequential Change Detection in R: The cpm Package. Journal of Statistical Software, 66, 1-20.

Sato, R.; Tanaka, Y.; Ishimaru, T. (2001). House production by *Oikopleura dioica* (Tunicata, Appendicularia) under laboratory conditions. J. Plankton Res., v. 23, p. 415– 423.

Savtchenko, A. *et al.* (2004). Terra and Aqua MODIS products available from NASA GES DAAC. Advances in Space Research, v. 34, n. 4, p. 710–714.

Schiermeier, Q. (2015). Hunting the Godzilla El Niño. Nature, 526(7574), 490.

Schwamborn, D. F. D. M. C., Marcolin, C. R., Lins-Silva, N., de Almeida, A. O., & Schwamborn, R. (2024). Asynchronous contributions of decapod life history stages to the zooplankton of tropical estuarine, coastal and shelf ecosystems-new insights from semi-automatic image analysis. Journal of Marine Systems, 242, 103943. https://doi.org/10.1016/j.jmarsys.2023.103943

Schwamborn, R., Ekau, W., Silva, A. P., Silva, T. A., & Saint-Paul, U. (1999). The contribution of estuarine decapod larvae to marine zooplankton communities in North-East Brazil. Archive of Fishery and Marine Research, 47(2/3), 167-182.

Silva, A. P.; Neumann-Leitão, S.; Schwamborn, R.; Gusmão, L. M.; Silva, T. A. (2004). Mesozooplankton of an impacted bay in North Eastern Brazil. Brazilian Archives of Biology and Technology, Curitiba, 47(3): 485-493.

Silva, U. M., & Santos, M. D. C. F. (2007). Biologia pesqueira do camarão sete-barbas, Xiphopenaeus kroyeri,(Heller, 1862)(DECAPODA, PENAEIDAE), na APA Costa dos Corais, Tamandaré (Pernambuco-Brasil). Bol. Tec. Cient. CEPENE, 15(2), 57-68.

Stuart, V. and Verheye, H. M. (1991) Diel migration and feeding patterns of the chaetognath, Sagitta friderici, off the west coast of South Africa. J. Mar. Res., 49, 493–515.

Tedeschi, R. G., Grimm, A. M., & Cavalcanti, I. F. (2015). Influence of Central and East ENSO on extreme events of precipitation in South America during austral spring and summer. International Journal of Climatology, 35(8), 2045-2064. DOI: 10.1002/joc.4106

Tyaquiçã, P., Veleda, D., Lefèvre, N., Araujo, M., Noriega, C., Caniaux, G., ... & Silva, T. (2017). Amazon plume salinity response to ocean teleconnections. Frontiers in Marine Science, 4, 250. https://doi.org/10.3389/fmars.2017.00250

Varona, H. L. *et al.* (2022) Monthly anomaly database of atmospheric and oceanic parameters in the tropical Atlantic Ocean. Data in Brief, v. 41, p. 107969.

Venables, W. N. *et al.* (2002). Exploratory multivariate analysis. Modern applied statistics with S, p. 301–330.

Venekey, V., Fonsêca-Genevois, V.G., Santos, P.J.P. (2011). Influence of the tidal and rainfall cycles on the population structure and density of Mesacanthion Hirsutum Gerlach (Nematoda, Thoracostomopsidae) on a tropical sandy beach (Tamandaré Bay, Pernambuco, Brazil). Braz. J. Oceanogr. 59 (3), 253–258, 2011.

Wells, S. R., Bresnan, E., Cook, K., Eerkes-Medrano, D., Machairopoulou, M., Mayor, D. J., Rabe, B., andWright, P. J. (2022) Environmental drivers of a decline in a coastal zooplankton community. ICES Journal of Marine Science, 79(3), 844–854. https://doi.org/10.1093/icesjms/fsab177

Williams, R. & Collins, N.R. (1986). Seasonal composition of meroplankton and holoplankton in the Bristol Channel. Mar. Biol. 92: 93-101.

Wiltshire, K. H., Kraberg, A., Bartsch, I., Boersma, M., Franke, H. D., Freund, J., ... & Wichels, A. (2010). Helgoland roads, North Sea: 45 years of change. Estuaries and Coasts, 33, 295-310. DOI 10.1007/s12237-009-9228-y

Wunderling, N., Donges, F.J., Kurths, J., Winkelmann, R. (2021). Interacting tipping elements increase risk of climate domino effects under global warming. Earth Syst. Dyn. 12, 601–619. https://doi.org/10.5194/esd-12-601-2021

6 CONSIDERAÇÕES FINAIS

Esta tese reúne evidências inéditas que conseguiram revelar e quantificar, pela primeira vez, os impactos dos decápodes planctônicos na estrutura dos ecossistemas costeiros tropicais, especialmente durante os seus picos sazonais em abundância e biovolume, no zooplâncton estuarino e marinho em três áreas de estudo na região de Tamandaré (Pernambuco, Brasil). Nossos resultados mostram que os espectros de tamanho, distribuídos de acordo com a distribuição de Pareto (ou "lei de potência"), são provavelmente moldados por interações estruturadas por tamanho, estratégias de nicho de tamanho específico dos táxons e processos de regulação "top-down" da cadeia alimentar. A ocorrência desses processos de regulação "top-down" depende da densidade dos predadores (zoeas de Brachyura). Também investigamos, pela primeira vez numa série temporal, as variações sazonais e interanuais de decápodes planctônicos e outros organismos do macrozooplâncton no Atlântico Tropical Sudoeste e relacionamos essas variações com índices climáticos em escala global, como ONI ("Oceanic El Niño Index") e TSA ("Tropical South Atlantic index") . Um ponto de inflexão ("tipping point") significativo (ponto de mudança, $p < 0{,}001$), com um aumento abrupto na TSM (temperatura superficial do mar), foi detectado no índice TSA (baseado na TSM no Oceano Atlântico Tropical Oriental e Central). Pós-larvas de camarões peneídeos (predominantemente *Penaeus* spp.) e outros grupos comuns do zooplâncton (por exemplo, copépodes, apendiculárias e quetognatos) apresentaram abundâncias significativamente mais baixas no período após o forte evento EN. O excepcionalmente forte evento EN (o "El Niño Godzilla ") de 2015-2016, em conjunto com o aquecimento antropogênico global, atuou como um gatilho ("trigger"), desencadeando uma mudança de regime de temperaturas na região da TSA, que afetou diretamente os ecossistemas costeiros estudados nesta tese. Este trabalho mostrou que séries temporais de zooplâncton tropical são capazes de captar as flutuações sazonais do zooplâncton ano após ano, podendo revelar possíveis anomalias nos ecossistemas.

Esta tese mostrou claramente que as larvas de Decapoda são importantes componentes do plâncton costeiro tropical, que respondem de forma significativa às variações climáticas, a exemplo das pós-larvas de camarões peneídeos. O declínio observado nas pós-larvas dos camarões deve-se provavelmente a uma variedade complexa de fatores e processos, tais como os efeitos "bottom-up" da cadeia alimentar (as pós-larvas são afetadas pelo declínio das suas presas, como os copépodes), devido a uma possível mudança nos padrões de vento e correntes

que podem afetar a sua migração para a costa, aumento de predadores, como medusas de cnidários, possível sobrepesca excessiva de estoques parentais de camarões na plataforma continental, e concentrações crescentes de poluentes (por exemplo, pesticidas e microplásticos), que são lavados do continente durante os eventos extremas (“enxurradas”) cada vez mais frequentes e intensos. Sem dúvida, a região da Baía de Tamandaré tornou-se menos favorável às pós-larvas dos camarões peneídeos e vários outros organismos do zooplâncton, no período de 2013 a 2019. O aumento da vulnerabilidade e dos riscos para o recrutamento dos estoques de camarões peneídeos no contexto dos eventos extremos cada vez mais intensos e frequentes deve ser considerado com urgência no monitoramento e manejo dos estoques pesqueiro e ecossistemas no Brasil e em outras regiões tropicais, para uma abordagem preventiva e sustentável ao manejo pesqueiro (“precautionary approach to fisheries”).

Esta tese mostrou que a combinação do uso do aparelho ZooScan com o banco de dados ECOTAXA, aplicado a uma série temporal de zooplâncton costeiro tropical, constitui uma abordagem com ferramentas poderosas para detectar e analisar as respostas ecossistêmicas à variabilidade climática.

REFERÊNCIAS

ALMEIDA, A. O. D. et al. Crustáceos decápodos estuarinos de Ilhéus, Bahia, Brasil. **Biota Neotropica**, v. 6, n. 2, 2006. DOI 10.1590/S1676-06032006000200024.

AlMEIDA, A. O. et al. Shallow-water anomuran and brachyuran crabs (Crustacea: Decapoda) from southern Bahia, Brazil. **Latin American Journal of Aquatic Research**, v. 38, p. 329-376. 2010. DOI. 10.3856/vol38-issue3-fulltext-2.

ALMEIDA, A. O. D. et al. Shallow-water caridean shrimps from southern Bahia, Brazil, including the first record of Sinalpheus ul (Rios and Duffy, 2007) in the southwestern Atlantic Ocean. **Zootaxa**, v. 3347, p. 1–35, 2012.

ANGER, K. The biology of decapod crustacean larvae. Lisse: **AA Balkema Publishers**. v. 14, p. 1-420, 2001.

ARONÉS, K. et al. Hydrographic structure and zooplankton abundance and diversity off Paita, northern Peru (1994 to 2004)—ENSO effects, trends and changes. **Journal of Marine Systems**, v. 78, n. 4, p. 582-598, 2009.

ATKINSON, A. et al. Increasing nutrient stress reduces the efficiency of energy transfer through planktonic size spectra. **Limnology and Oceanography**, v. 66, n 2, p. 422-437, 2021. DOI 10.1002/lno.11613.

AYÓN, P. et al. Zooplankton research off Peru: a review. **Progress in Oceanography**, v. 79, n. 2-4, p. 238-255, 2008.

AYÓN, P. et al. Long-term changes in zooplankton size distribution in the Peruvian Humboldt Current System: conditions favouring sardine or anchovy. **Marine Ecology Progress Series**, v. 422, p. 211-222, 2011. DOI 10.3354/meps08918.

BASHEVKIN, S. M.; MORGAN, S. G. Predation and competition. **The natural history of the Crustacea**, v.7, p. 360-382, 2020.

BERLINE, L. et al. Intercomparison of six Mediterranean zooplankton time series. **Progress in Oceanography**, v. 97, p. 76-91, 2012. DOI 10.1016/j.pocean.2011.11.011.

BLANCHARD, J. L. et al. From bacteria to whales: Using functional size spectra to model marine ecosystems. **Trends in Ecology and Evolution**, v. 32, p. 174–186, 2017. DOI 10. 1016/j.tree.2016.12.003.

BOUDREAU, S. A.; WORM, B. Ecological role of large benthic decapods in marine ecosystems: a review. **Marine Ecology Progress Series**, v. 469, p. 195-213, 2012. DOI 10.3354/meps09862.

BRACKEN, H. et al. The decapod tree of life: compiling the data and moving toward a consensus of decapod evolution. **Arthropod Systematics & Phylogeny.** v. 67, p. 99-116, 2009.

BRANDÃO, M. C.; GARCIA, C. A. E.; FREIRE, A. S. Large-scale spatial variability of decapod and stomatopod larvae along the South Brazil shelf. **Continental Shelf Research**, v. 107, p. 11-2, 2015. DOI org/10.1016/j.csr.2015.07.012.

CLARK, R. A.; FRID, C. L. J.; BATTEN, S. A critical comparison of two long-term zooplankton time series from the central-west North Sea. **Journal of Plankton Research**, v. *23*, n. 1, p. 27-39, 2001.

COURET, M. et al. Mesozooplankton size structure in the Canary Current System. *Marine* **Environmental Research**, v. 188, p. 105976, 2023. DOI 10.1016/j.marenvres.2023.105976.

D'INCAO, F. Espécies do gênero Lucifer Thompson, 1829 no litoral brasileiro (Decapoda: Luciferidae). **Nauplius**, v. 5, p. 139-145, 1997.

DICKIE, L. M.; KERR, S. R.; BOUDREAU, P. R. Size-dependent processes underlying regularities in ecosystem structure. **Ecological monographs**, v. 57, n. 3, p. 233-250, 1987. DOI 10.1111/gcb.12231.

EPIFANIO, C. E.; GARVINE, R. W. Larval transport on the Atlantic continental shelf of North America: a review. **Estuarine, coastal and shelf Science**, v. 52, n. 1, p. 51-77, 2001. DOI org/10.1006/ecss.2000.0727.

FIGUEIREDO, G. G. A. A. et al. Body size and stable isotope composition of zooplankton in the western tropical Atlantic. **Journal of Marine Systems**, v. 212, p. 103449, 2020. 10.1016/j.jmarsys.2020.103449.

FRECKMAN, D. W. et al. Linking biodiversity and ecosystem functioning of soils and sediments. **Ambio**, v. 26, n. 8, p. 556-562. 1997.

GAEDKE, U.; STRAILE, D. Daphnids-Keystone species for the pelagic food web structure and energy flow: a body size-related analysis linking seasonal changes at the population and ecosystem levels. **Advances in Limnology**, v. 53, p. 587-610, 1998.

GREVE, W. et al. Helgoland Roads meso-and macrozooplankton time-series 1974 to 2004: lessons from 30 years of single spot, high frequency sampling at the only off-shore island of the North Sea. **Helgoland Marine Research**, v. 58, p. 274-288, 2004. DOI 10.1007/s10152-004-0191-5.

HANSEN, H. J. Crustaces Decapodes (Sergestides) provenant des campagnes des yachts "Hirondelle" et "Princesse Alice" (1885-1915). **Résultats des Campagnes Scientifiques accomplies par le Prince Albert I de Monaco.** V. 64, p, 1-232, 1922.

HARVEY, A. C.; SHEPHARD, N. Structural time series models. in: G. S. Maddala, C. R. Rao and H. D. Vinod, eds., **Handbook of Statistics**, v. 11, Elsevier: Amsterdam, 1993.

HOBBIE, J. E. et al. A study of the distribution and activity of microorganisms in ocean water. **Limnology and oceanography**, v. 17, n. 4, p. 544-555, 1972. DOI. 10.4319/lo.1972.17.4.0544.

HOVEL, K. A.; MORGAN, S. G. Planktivory as a selective force for reproductive synchrony and larval migration. **Marine Ecology Progress Series**, v.157, p. 79-95, 1997.

JIAO, Y. Regime shift in marine ecosystems and implications for fisheries management, a review. **Reviews in Fish Biology and Fisheries**, v. 19, p. 177-191, 2009.

KE, Z. et al. Community structure and biovolume size spectra of mesozooplankton in the Pearl River estuary. **Aquatic Ecosystem Health & Management**, v. 21. n, 1, p. 30–40. 2018. DOI 10.1080/14634988.2018.1432948.

KERR, S. R. Theory of size distribution in ecological communities. **Journal of the Fisheries Board of Canada**, v. 31, n. 12, p. 1859-1862, 1974.

LIMA, F. A.; BUTTURI-GOMES, D.; MARTINELLI-LEMOS, J. M. Megalopa bloom of *Panopeus lacustris* (Decapoda: Panopeidae) on the Amazon Continental shelf. **Regional Studies in Marine Science**, v. 47, p. 101960, 2021. DOI 10.1016/j.rsma.2021.101960.

LINDLEY, J. A.; WILLIAMS, R.; CONWAY, D. V. P. Variability in dry weight and vertical distributions of decapod larvae in the Irish Sea and North Sea during the spring. **Marine Biology**, v. 120, p. 385–395, 1994. DOI 10.1007/BF00680212.

LOPES, R. M. et al. Zooplankton and ichthyoplankton distribution on the southern Brazilian shelf: an overview. **Scientia Marina**, v. 70, n. 2, p. 189-202, 2006. DOI org/10.3989/scimar.2006.70n2189.

MARCOLIN, C. R.; GAETA, S.; LOPES, R. M. Seasonal and interannual variability of zooplankton vertical distribution and biomass size spectra off Ubatuba, Brazil. **Journal of Plankton Research**, v. 37, n. 4, p. 808-819, 2015. DOI 10.1093/plankt/fbv035.

MCENNULTY, F. R. et al. A database of zooplankton biomass in Australian marine waters. **Scientific Data**, v. 7, n. 1, p. 297, 2020. DOI org/10.1038/s41597-020-00625-9.

MACKAS, D. L.; BEAUGRAND, G. Comparisons of zooplankton time series. **Journal of Marine Systems**, v. 79, n. 3-4, p. 286-304, 2010. DOI 10.1016/j.jmarsys.2008.11.030.

MACKAS, D. L. et al. Changing zooplankton seasonality in a changing ocean: Comparing time series of zooplankton phenology. **Progress in Oceanography**, v. 97, p. 31-62, 2012. DOI 10.1016/j.pocean.2011.11.005.

MARENGO, J. A. et al. Flash floods and landslides in the city of Recife, Northeast Brazil after heavy rain on May 25–28, 2022: Causes, impacts, and disaster preparedness. **Weather and Climate Extremes**, v. 39, p. 100545, 2023. DOI 10.1016/j.wace.2022.100545.

MAZZOCCHI, M. G. et al. Zooplankton associations in a Mediterranean long-term time-series. **Journal of Plankton Research**, v. 33, n. 8, p. 163-1181, 2011. DOI 10.1093/plankt/fbr017.

MELO JÚNIOR, M. et al. Fluxes of zooplankton biomass between a tidal estuary and the sea in northeastern Brazil. **Brazilian Journal of Oceanographic**, v. 55, n. 4, p. 239-249, 2007.

MELO JÚNIOR, M. et al. Composition of decapod larvae in a northeastern Brazilian estuarine inlet over a full tidal cycle. **Latin American Journal of Aquatic Research**, v. 44, p. 401–410. 2016. DOI 10.3856/vol44-issue2-fulltext-21.

MORIARTY, R. et al. 2013. Distribution of known macrozooplankton abundance and biomass in the global ocean. **Earth System Science Data**, v. 5, n. 2, p. 241-257, 2013. DOI 10.5194/essd-5-241-2013.

NG P. K. L.; GUINOT D.; DAVIE P. J. F. Systema brachyurorum: part I. An annotated checklist of extant brachyuran crabs of the world. **The Raffles Bulletin of Zoology**, v. 1, p. 1–286, 2008.

PLATT, T. Structure of the marine ecosystem: its allometric basis. In Ecosystem theory for biological oceanography. Edited by R.E. Ulanowicz and T. **Platt.Canadian Bulletin of Fisheries and Aquatic Sciences**, v. 213, p. 55–64, 1985.

PLATT, T.; DENMAN, K. Organisation in the pelagic ecosystem. **Helgoländer Wissenschaftliche Meeresuntersuchungen**, v. 30, p. 575-581, 1977.

PLATT, T.; DENMAN, K. The structure of pelagic marine ecosystems. Rapp. P-v. Reun. **Conseil International pour l'Éxploration de la Mer**, v. 173, p. 60-65, 1978.

RAY, S. et al. Optimization of exergy and implications of body sizes of phytoplankton and zooplankton in an aquatic ecosystem model. **Ecological Modelling**, v. 140, n. 3, p. 219-234, 2001.

RICHARDSON, A. J. In hot water: zooplankton and climate change. **ICES Journal of Marine Science**, v. 65. n. 3, p. 279-295, 2008. 10.1093/icesjms/fsn028.

ROCHA, G. R. et al. Seasonal budgets of organic matter in the Ubatuba shelf system, SE Brazil. I. Planktonic and benthic components. **Oceanologica Acta**, v. 26, n. 5-6, p. 487-495, 2003. DOI 10.1016/S0399-1784(03)00043-4.

RODRIGUES-INOUE, A. C. M., DOS SANTOS, A., MARTINELLI-LEMOS, J. M. Distribution patterns of Anomura, Axiidea and Gebiidea (Crustacea, Decapoda) larvae at the Amazon shelf. **Regional Studies in Marine Science**, v. 47, p. 101946, 2021. DOI org/10.1016/j.rsma.2021.101946.

RODRÍGUEZ, J. Some comments on the size-based structural analysis of the pelagic ecosystem. **Scientia Marina**, v. 58, n. 1-2, p. 1-10, 1994.

SAN MARTIN, E.; HARRIS, R. P.; IRIGOIEN, X. Latitudinal variation in plankton size spectra in the Atlantic Ocean. *Deep Sea Research Part II:* **Topical Studies in Oceanography**, v. 53, n. 14-16, p. 1560-1572, 2006. DOI 10.1016/j.dsr2.2006.05.006.

SANTANA, C. S. et al. Spatio-temporal variation of planktonic decapods along the leeward coast of the fernando de noronha archipelago. Brazil. **Brazilian Journal of Oceanography**. v. 66, p. 1–14, 2018. DOI 10.1590/s1679-87592018147206601.

SANTOS, P. S.; SOLEDADE, G. O.; ALMEIDA, A. O. Decapod crustaceans on dead coral from reef areas on the coast of Bahia, Brazil. **Nauplius**, v. 20, p. 145–169, 2012.

SANTOS, G. S. et al. Are tropical coastal reefs sinks or sources of mesozooplankton? A case study in a Brazilian marine protected area. **Coral Reefs**, v. 38, p. 1107–1120. 2019. DOI 10.1007/s00338-019-01860-2.

SARAIVA, A. Á. F.; PINHEIRO, A. P.; SANTANA, W. A. remarkable new genus and species of the planktonic shrimp family Luciferidae (Crustacea, Decapoda) from the Cretaceous (Aptian/Albian) of the Araripe Sedimentary Basin, Brazil. **Journal of Paleontology**, v. 92, n. 3, p. 459-465, 2018. DOI 10.1017/jpa.2018.5.

SCHWAMBORN, R.; BONECKER, A. C. T. Seasonal changes in the transport and distribution of meroplankton into a Brazilian estuary with emphasis on the importance of floating mangrove leaves. **Brazilian Archives of Biology and Technology**, v. 39, p. 451-462, 1996.

SCHWAMBORN, R. et al. The contribution of estuarine decapod larvae to marine macrozooplankton communities in northeast Brazil. **Archive of Fishery and Marine Research**, v. 47, n 2/3, p. 167–182, 1999.

SCHWAMBORN, R. et al. Distribution and dispersal of decapod crustacean larvae and other zooplankton in the Itamaracá estuarine system, Brazil. **Tropical Oceanography**, v. 29, n. 1, p. 1-18, 2001.

SCHWAMBORN, R. et al. How important are mangroves as a carbon source for decapod crustacean larvae in a tropical estuary?. **Marine Ecology Progress Series**, v. *229*, p. 195-205, 2002.

SHELDON, R. W.; PRAKASH, A.; SUTCLIFFE Jr, W. H. The size distribution of particles in the ocean. **Limnology and oceanography**, v. 17, n. 3, p. 327-340, 1972. DOI 10.4319/LO.1972.17.3.0327.

SHELDON, R. W.; SUTCLIFFE JR, W. H.; PARANJAPE, M. A. Structure of pelagic food chain and relationship between plankton and fish production. **Journal of the Fisheries Board of Canada**, v. 34, n.12, p. 2344-2353, 1977. DOI 10.1139/f77-314.

SPRULES, W. G.; BARTH, L. E. Surfing the biomass size spectrum: some remarks on history, theory, and application. **Canadian Journal of Fisheries and Aquatic Sciences**, v. 73, n 4, p. 477-495, 2016.

SPRULES, W. G.; MUNAWAR, M. Plankton size spectra in relation to ecosystem productivity, size, and perturbation. **Canadian Journal of Fisheries and Aquatic Sciences**, v, 43, n. 9, p. 1789-1794, 1986. DOI 10.1139/f86-222.

STEINBERG, D. K.; LANDRY, M. R. Zooplankton and the ocean carbon cycle. **Annual review of marine science**, v. 9, p. 413-444, 2017.

STENECK, R. S. et al. Creation of a gilded trap by the high economic value of the Maine lobster fishery. **Conservation Biology**, v. 25, p. 904−912, 2011.

SEKIGUCHI, H. Distribution of larvae of P*innixa rathbuni* Sakai (Decapoda: Pinnotheridae) in Ise bay and its neighboring coastal waters, central Japan part 3. Aggregation of the benthic adult population with reference to the spatial distribution of the planktonic larvae. **Journal of the Oceanographical Society of Japan**, v. 39, p. 119-128, 1983.

SOUZA, C. S. et al. Size spectra modeling of Mesozooplankton over a tropical continental shelf. **Journal of Coastal Research**, v. 36, n. 4, p. 795-804, 2020. DOI 10.2112/JCOASTRES-D-19-00102.1.

TOON, A. et al. Decapod phylogenetics and molecular evolution. In **Decapod crustacean phylogenetics.** p. 27-42, 2016. CRC Press.

VANDROMME, P. et al. Springtime zooplankton size structure over the continental shelf of the Bay of Biscay. **Ocean Science**, v. 10, n. 5, p. 821-835, 2014.

VALDÉS, L. et al. A decade of sampling in the Bay of Biscay: What are the zooplankton time series telling us?. **Progress in Oceanography**, v. 74, n. 2-3, p. 98-114, 2007. DOI 10.1016/j.pocean.2007.04.016.

VALENTIN, J. L.; MONTEIRO-RIBAS, W. M. Zooplankton community structure on the east-southeast Brazilian continental shelf (18–23 S latitude). **Continental Shelf Research**, v. 13 n. 4, p. 407-424, 1993. DOI 10.1016/0278-4343(93)90058-6.

WELLS, S. R. et al. Environmental drivers of a decline in a coastal zooplankton community. **ICES Journal of Marine Science**, v. 79, n. 3, 844–854, 2022. DOI 10.1093/icesjms/fsab177.

ZHOU, M.; HUNTLEY, M. E. Population dynamics theory of plankton based on biomass spectra. **Marine Ecology Progress Series**, v. 159, p. 61-7, 1997.

APÊNDICE A – ARTIGO PUBLICADO (JOURNAL OF MARINE SYSTEMS)

Journal of Marine Systems 242 (2024) 103943

Contents lists available at ScienceDirect

Journal of Marine Systems

journal homepage: www.elsevier.com/locate/jmarsys

Asynchronous contributions of decapod life history stages to the zooplankton of tropical estuarine, coastal and shelf ecosystems - new insights from semi-automatic image analysis

Denise Fabiana de Moraes Costa Schwamborn [a,b], Catarina R. Marcolin [c], Nathália Lins-Silva [b], Alexandre Oliveira de Almeida [a], Ralf Schwamborn [a,b,*]

[a] Programa de Pós-Graduação em Biologia Animal, Federal University of Pernambuco, Recife, PE, Brazil
[b] Zooplankton Laboratory, Department of Oceanography, Federal University of Pernambuco, Recife, PE, Brazil
[c] Environmental Science Training Center, Federal University of Southern Bahia, Porto Seguro, BA, Brazil

ARTICLE INFO

Keywords:
Decapoda
Brachyuran crabs
Penaeid shrimps
Dispersal
Recruitment
ZooScan
Brazil
Tropical Atlantic

ABSTRACT

Decapod crustaceans include many species of socioeconomic importance and are key components of pelagic ecosystems, both as adults and as larval forms. Knowledge on seasonal and spatial synchronicity of planktonic larvae in coastal tropical ecosystems is fundamental to understand the dynamics of these complex ecosystems. The objective of the present study was to quantify the contributions of decapods to the zooplankton in adjacent tropical estuarine, coastal and shelf ecosystems, while considering their seasonal life cycles and probable dispersal strategies. We evaluated the contributions of decapod biomass and biovolume in three distinct ecosystems: Rio Formoso estuary, Tamandaré bay, and Pernambuco continental shelf off Tamandaré, northeastern Brazil. Zooplankton samples were taken bimonthly from June 2013 to May 2015, with a 300 µm mesh net, and analyzed using a ZooScan equipment. Decapods were the second most important organisms (after copepods), in abundance, biomass and biovolume, in all sampling areas. Total decapods contributed on average with 33.6%, 4.4% and 7.1% relative abundance and 30.9%, 30.9%, and 15.2% relative biovolume in estuary, bay, and shelf areas, respectively. Overall, the most relevant decapod taxa and stages found in the three sampling areas were brachyuran crab zoeae and megalopae, penaeid shrimp postlarvae (mostly *Penaeus* spp.), holoplanktonic luciferids (adults, protozoeae and mysis), anomuran zoeae (mostly Paguridae and Diogenidae hermit crabs), pistol shrimp zoeae (Alpheidae), and porcelain crab zoeae (Porcellanidae). Brachyuran zoeae contributed with up to 81.3% abundance and up to 69% biovolume, in the estuary. Penaeid postlarvae comprised up to 28.1% of total abundance and up to 94.7% of total biovolume, on the shelf. These postlarvae were transported shorewards from the offshore shelf. Decapod contributions were especially relevant during massive larval release events of crab zoeae and during shoreward migration of pre-settlement stages. Seasonal peaks were clearly asynchronous between taxa and areas. Possible functional relationships between copepods and key decapod groups are discussed, as well as the processes triggering and regulating the input of larvae. Our results show the importance of quantitative, semi-automatic approaches and the relevance of decapod larvae for pelagic food webs in tropical coastal areas.

1. Introduction

Decapod crustaceans include many species of interest to fisheries and aquaculture (e.g., shrimps, crabs and lobsters). They are key components of estuarine and marine zooplankton communities, as holoplanktonic adults and as meroplanktonic larvae (Schwamborn et al., 2001). Many studies on planktonic decapods have been based on visual counting (i.e., abundance), and the abundance composition of planktonic decapod assemblages has thus been intensively studied in numerous tropical areas (Schwamborn et al., 2001; Melo Júnior et al., 2016; Costa and Schwamborn, 2016; Santana et al., 2018; Santos et al., 2019). Yet, there are considerable knowledge gaps regarding the biomass and biovolume composition of tropical estuarine and coastal zooplankton, especially regarding the contributions of meroplankton,

APÊNDICE B – TABELA SUPLEMENTAR

Table B1: TAXONOMIC SUMMARY OF ALL ZOOPLANKTON GROUPS IDENTIFIED DURING THIS STUDY.

Phylum **Porifera** Grant, 1836	Order **Harpacticoida** Sars, 1903
Phylum Sarcodina Schmard, 1871	Order Siphonostomatoida Thorell, 1859 (**Parasite Copepods**)
Order **Foraminifera** d'Orbigny, 1826	Order **Monstrilloida** Sars, 1903
Phylum **Cnidaria** Verril, 1865	**Copepoda (nauplii)**
Class **Anthozoa** Ehrenberg, 1834	Subclass **Cirripedia** Burmeister, 1834 (**nauplii and cypris**)
Phylum **Mollusca** Cuvier, 1795 (**various**)	Class Malacostraca Latreille, 1802
Class **Gastropoda** Cuvier, 1797 (**veliger**)	Order **Stomatopoda** Latreille, 1817 (**pseudozoea**)
Class **Bivalvia** Cuvier, 1797 (**veliger**)	Order **Decapoda** Latreille, 1803 (**various**)
Phylum Annelida Lamarck, 1809	Suborder Dendrobranchiata Bate, 1888
Class **Polychaeta** Grube, 1850 (**larvae and adults**)	Superfamily Penaeoidea Rafinesque, 1815
Phylum Arthropoda von Siebold, 1848	**Penaeus spp.** Fabricius, 1798
Class Pycnogonida Latreille, 1810	Family **Luciferidae** Dana, 1852 (**mysis, protozoea and adults**)
Order **Pantopoda** Gerstäcker, 1863	Family **Sergestidae**Dana, 1852 (**mysis, protozoea and adults**)
Phylum Crustacea Pennant, 1977	Suborder Pleocyemata Burkenroad, 1963
Class Hexapoda	Infraorder **Caridea** Dana, 1852
Subclass **Insecta**	Family **Alpheidae** Rafinesque, 1815 (**various**)
Class Maxillopoda Dahl, 1956	Family **Palaemonidae** Rafinesque, 1815
Subclass **Ostracoda** Latreille, 1806	Family **Processidae** Ortmann, 1986
Subclass Copepoda Milne-Edwards, 1840	Family **Hippolytidae**Spence Bate, 1888
Order Calanoida Sars, 1903	Infraorder **Anomura** MacLeay, 1838 (**zoea and megalopa**)
Family Calanidae Dana, 1849	Family **Paguridae** Latreille, 1803 (l**arvae**)
***Neocalanus* spp.**Sars G.O., 1925	Family **Diogenidae** Ortmann, 1892
Family Paracalanidae Giesbrecht, 1892	Family **Porcellanidae** Haworth, 1825 (**zoea**)
***Calocalanu* sspp.** Giesbrecht, 1888	Infraorder **Axiidea**de Saint Laurent, 1979
Parvocalanus crassirostris(Dahl F., 1894)	Infraorder **Gebiidea** Saint Laurent, 1979
***Paracalanus* spp.**Boeck, 1865	Infraorder Stenopodidea Spence Bate, 1888
Family Eucalanidae Giesbrecht, 1892	Family **Stenopodidae** Claus, 1872
***Paraeucalanus* spp.**Geletin, 1976	Infraorder **Brachyura** Latreille, 1803 (**zoea and megalopa**)
Family Euchaetidae Giesbrecht, 1893	Order **Mysida** Boas, 1883 (**Various**)
***Euchaeta* spp.** Philippi, 1843	Order **Cumacea**Kröyer, 1846 (**Various**)
Family Centropagidae Giesbrecht, 1892	Order **Amphipoda** Latreille, 1816 (**various**)
***Centropages* spp.**	Order **Isopoda** Latreille, 1817 (**adults**)
Family Pseudodiaptomidae Sars, 1902	Phylum **Bryozoa** Ehrenberg, 1831 (l**arvae**)
***Pseudodiaptomus* spp.** Herrick, 1884	Phylum Chordata Batenson, 1885
Family Temoridae Giesbrecht, 1892	Subphylum Tunicata Lamarck, 1816
***Temora* spp.** Baird, 1850	Class Ascidiacea Grzimek, 1974
Family Pontellidae Dana, 1853	Order PhlebobranchiaLahille, 1887
***Calanopia* spp.** Dana, 1852-1853	Family **Ascidiidae** Herdman, 1880 (**larvae**)
***Labidocera* spp.**Lubbock, 1853	Class **Appendicularia** Lohmann, 1913
Family Acartiidae Sars, 1903	Class ThaliaceaVan der Haeven, 1850
***Acartia* spp.** Dana, 1846	Order **Doliolida** Delage &Hérouard, 1898
Calanoida others	Order Salpida Forbes, 1853
Order Cyclopoida Burmeister, 1834	Family SalpidaeLahille, 1888
Family Corycaeidae Dana, 1852-1853	**Salpa sp.** Forskål, 1775
***Corycaeus* spp.** Dana, 1845	Phylum **Chaetognatha** (Leuckart, 1894)
***Farranula* spp.** Wilson CB., 1932	Subphylum Vertebrata Brusca & Brusca, 1990
Family OncaeidaeGiesbrecht, 1893	Superclass Pisces (Linnaeus, 1758)
***Oncaea* spp.** Philippi, 1843	Class Actiopterygii Carroll, 1988
Family Oithonidae Dana, 1853	**Fish (eggs and larvae)**
***Oithona* spp.** Baird, 1843	

APÊNDICE C – EXEMPLOS DE VINHETAS OBTIDAS ATRAVÉS DO *ZOOSCAN*, REFERENTES ÀS COLETAS FEITAS ENTRE 2013 E 2019 NA BAÍA DE TAMANDARÉ, ESTUÁRIO DO RIO FORMOSO E PLATAFORMA CONTINENTAL AO LARGO DE TAMANDARÉ (PE-BRASIL).

Apêndice C.1 - Vinhetas obtidas através do *ZooScan* nas coletas feitas na **Baía de Tamandaré**: 2013 - 2019 (PE-Brasil).

CNIDARIA

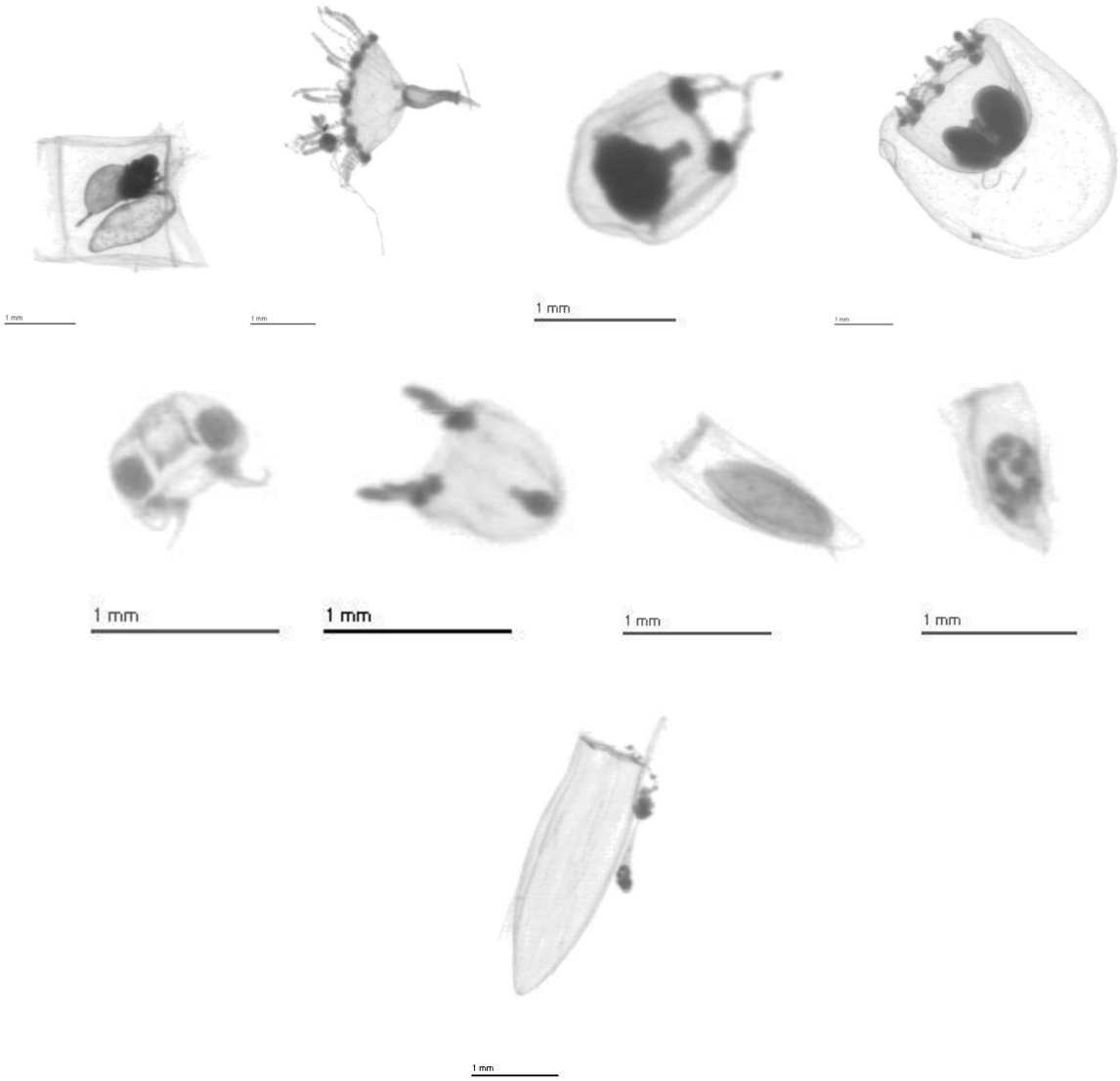

CHAETOGNATHA

BIVALVIA

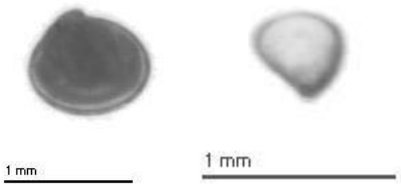

GASTROPODA

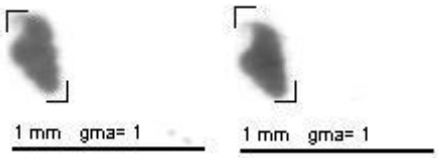

POLYCHAETA

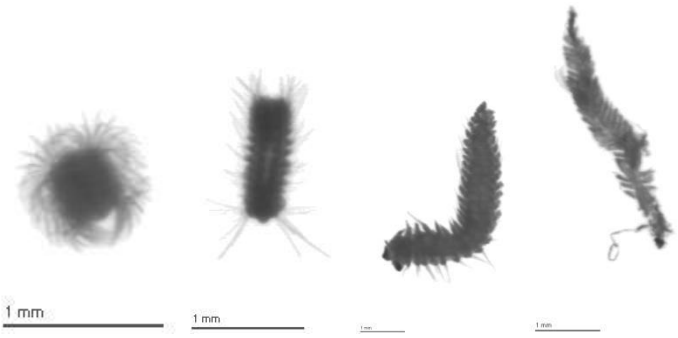

COPEPODA CALANOIDA

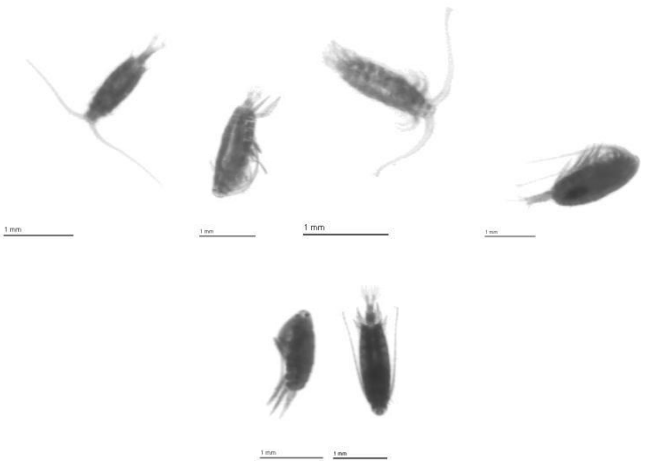

COPEPODA CYCLOPOIDA

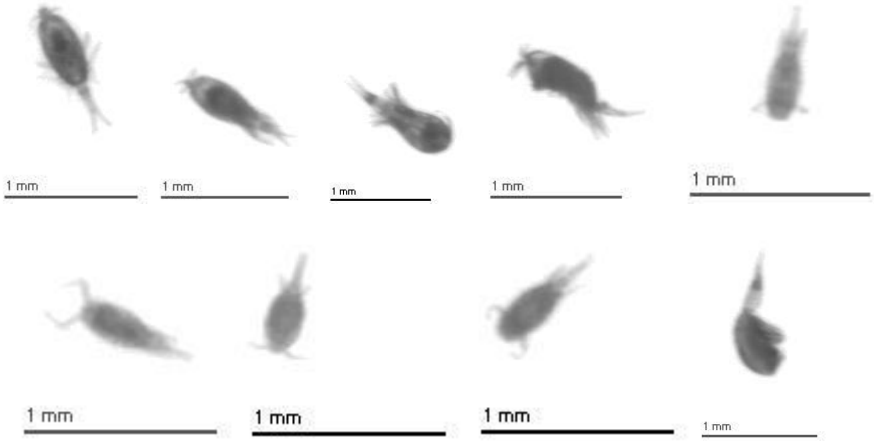

COPEPODA HARPACTICOIDA

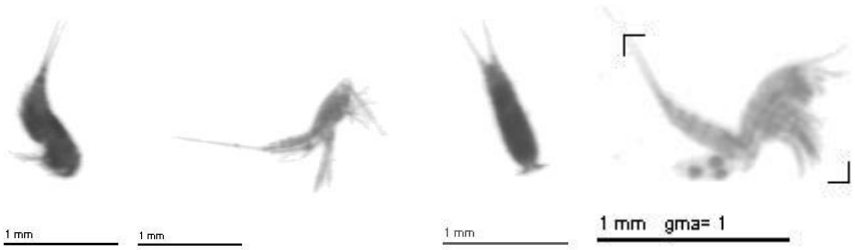

COPEPODA (Parasitas)

COPEPODA Monstrilloida

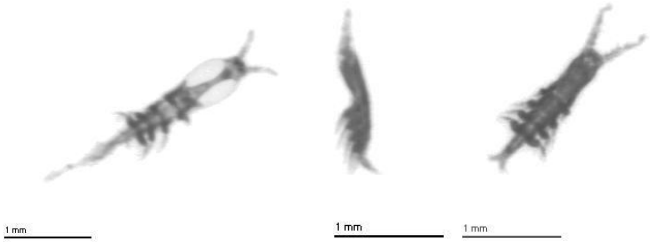

CUMACEA

STOMATOPODA

AMPHIPODA

MYSIDA

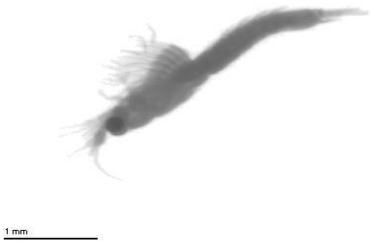

DECAPODA

LUCIFERIDAE (Adultos e juvenis)

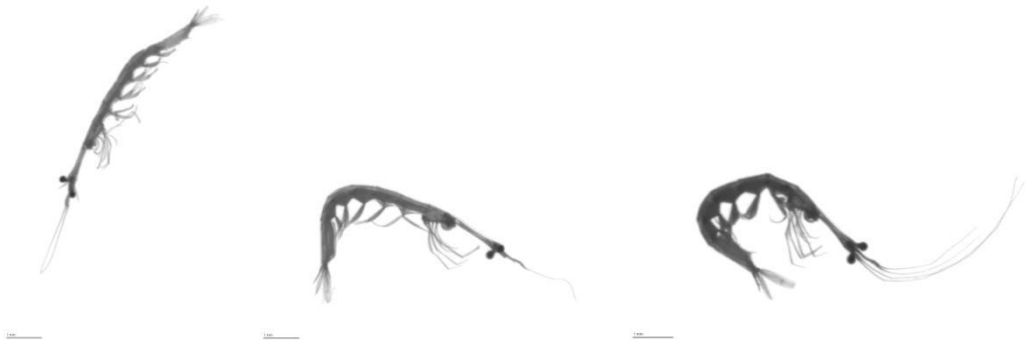

LUCIFERIDAE (Mísis)

LUCIFERIDAE (Protozoeas)

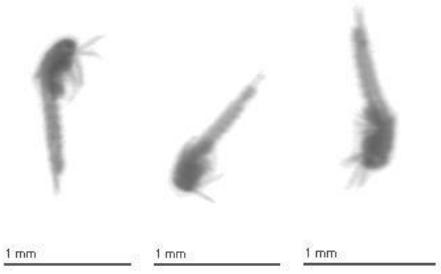

PENAEUS (Pós -larvas)

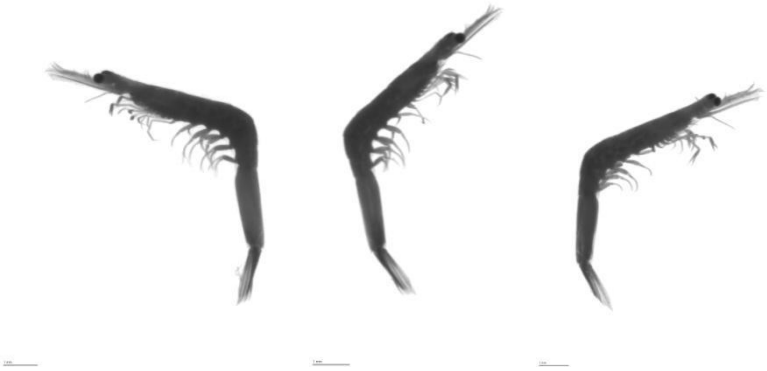

SERGESTIDAE (larvas)

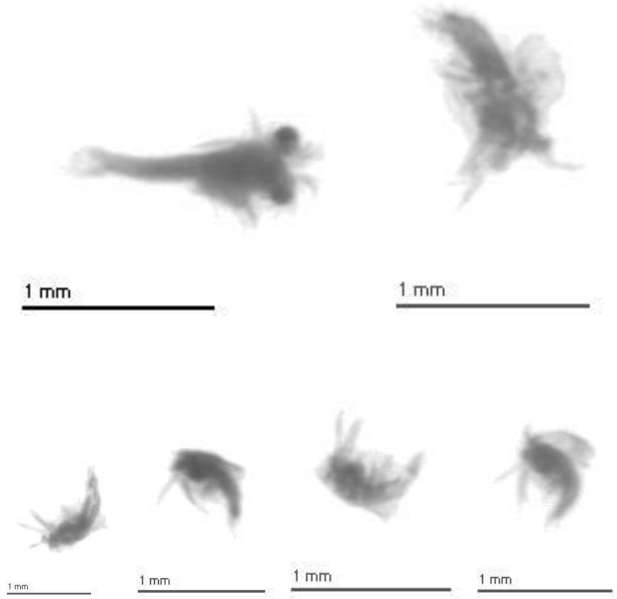

ACETES sp. (Sergestidae), juvenis e adultos

ANOMURA, fam. PORCELLANIDAE (Zoeas)

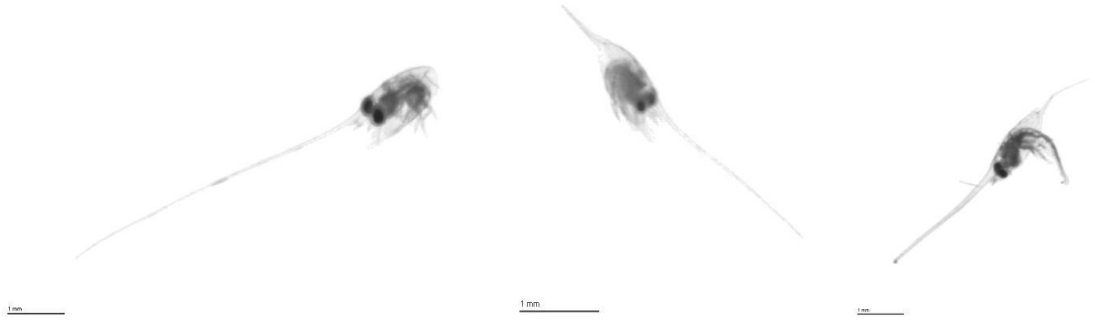

Morfotipo ANOMURA (Anomuros exceto fam. Porcellanidae, unclui Paguroidea, inclui Upogebiidae e outros Gebiidea e similares, zoeas)

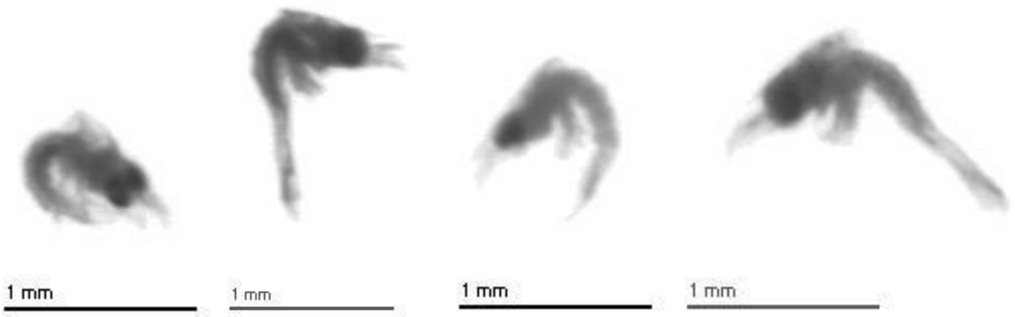

AXIIDEA (Zoeas)

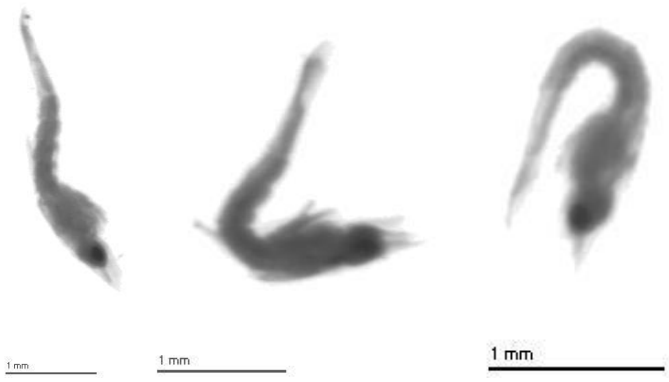

CARIDEA, fam. ALPHEIDAE (Zoeas)

CARIDEA, fam. PALAEMONIDAE (Zoeas)

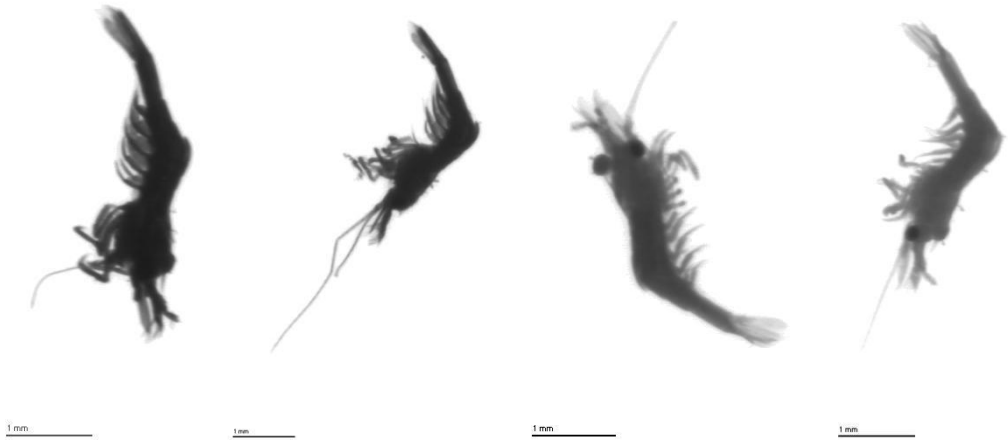

CARIDEA, fam. PROCESSIDAE (Zoeas)

BRACHYURA, fam. PORTUNIDAE (Juvenil)

BRACHYURA (Megalopas)

BRACHYURA (juvenil)

BRACHYURA (Zoeas)

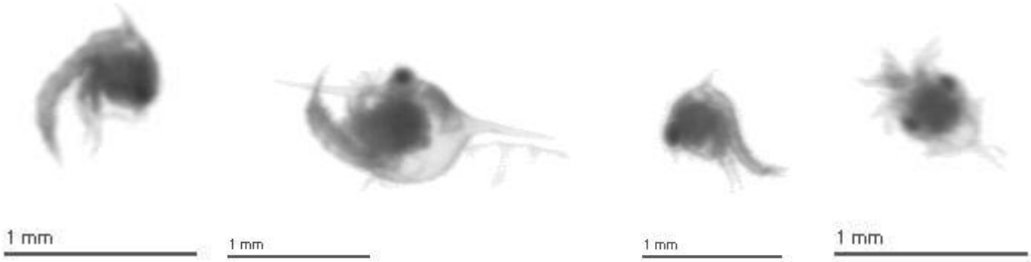

PAGUROIDEA (Megalopa)

ISOPODA

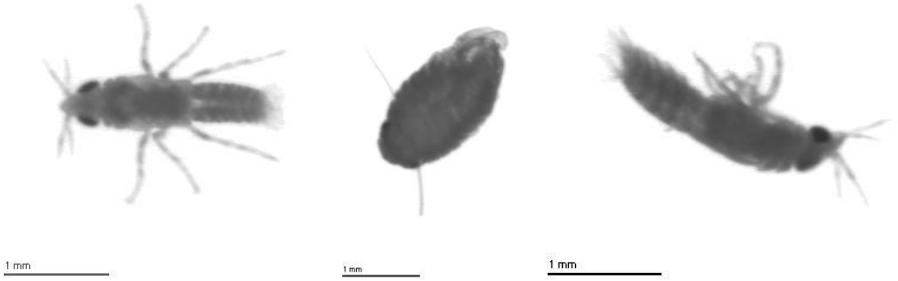

APPENDICULARIA

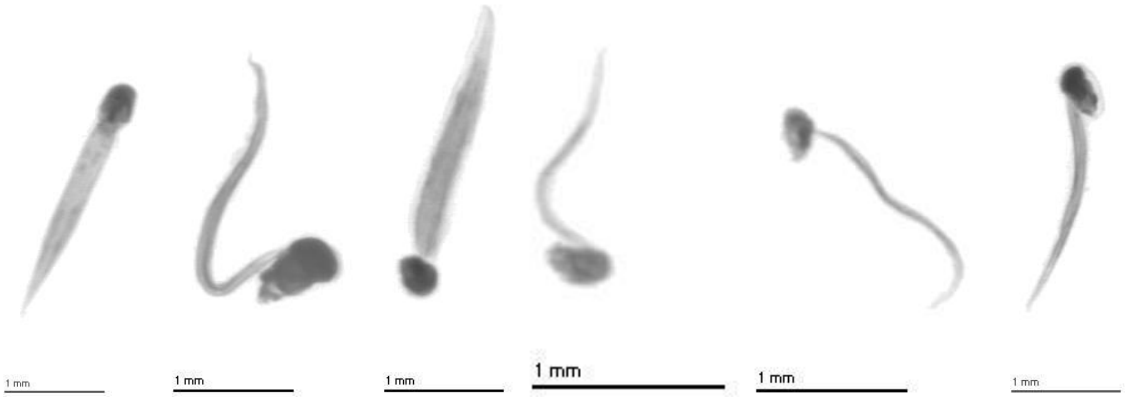

DOLIOLIDA

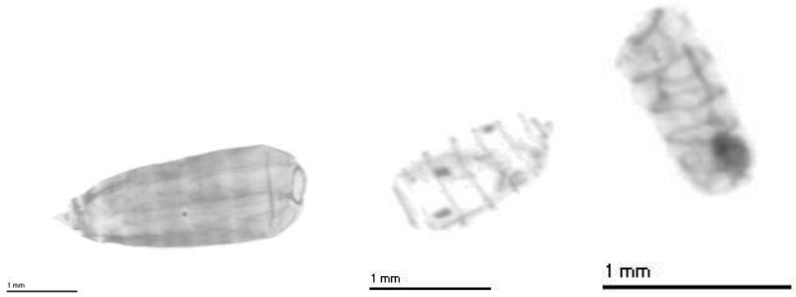

TELEOSTEI (Larvas)

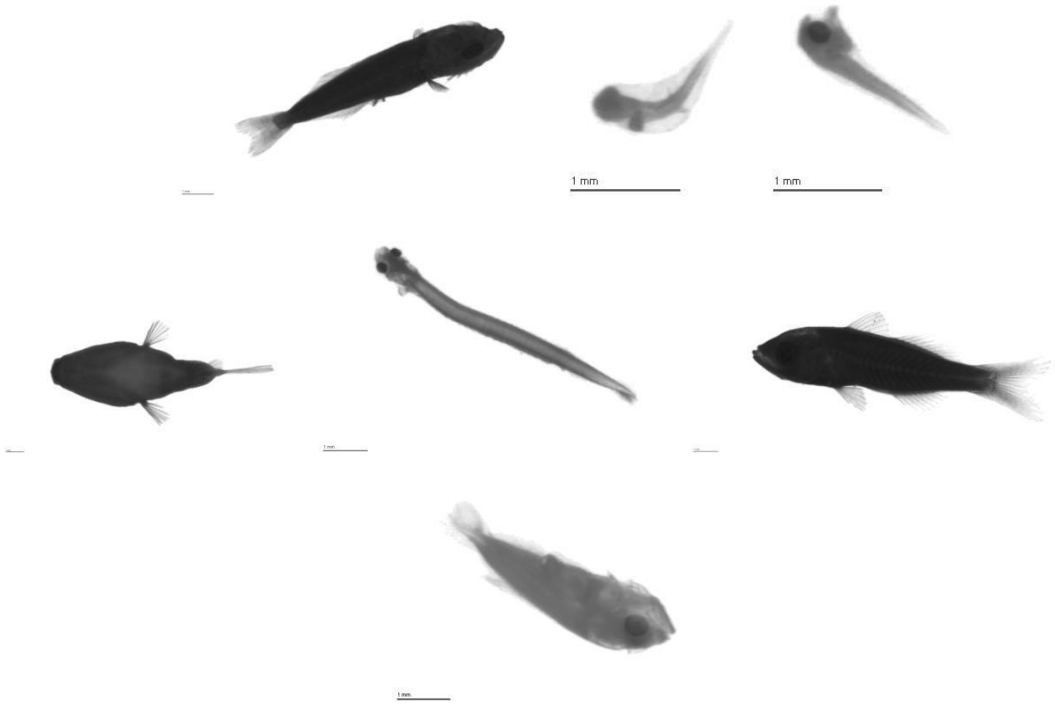

TELEOSTEI (Ovos)

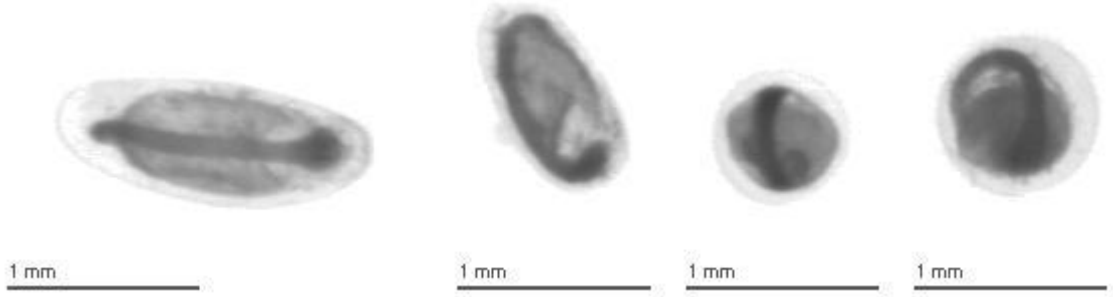

Apêndice C.2 - Vinhetas obtidas através do *ZooScan* nas coletas feitas no **Estuário do Rio Formoso**, Tamandaré: 2013 - 2015 (PE-Brasil).

CNIDARIA

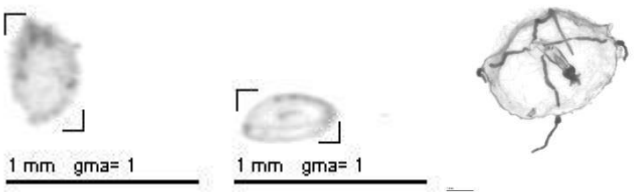

CHAETOGNATHA

GASTROPODA

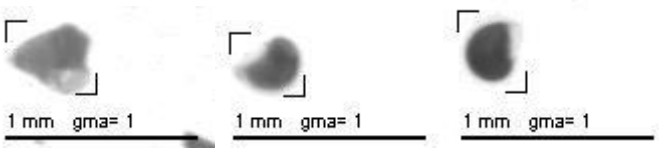

MOLLUSCA

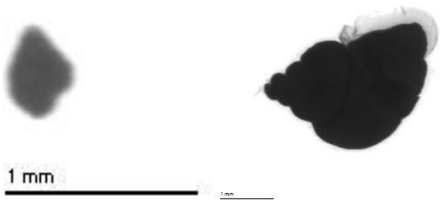

POLYCHAETA

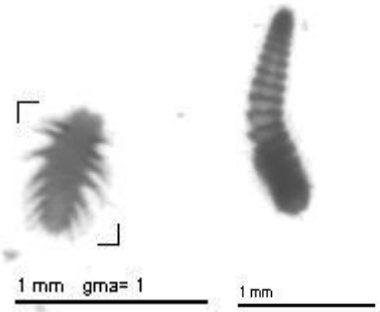

COPEPODA CALANOIDA

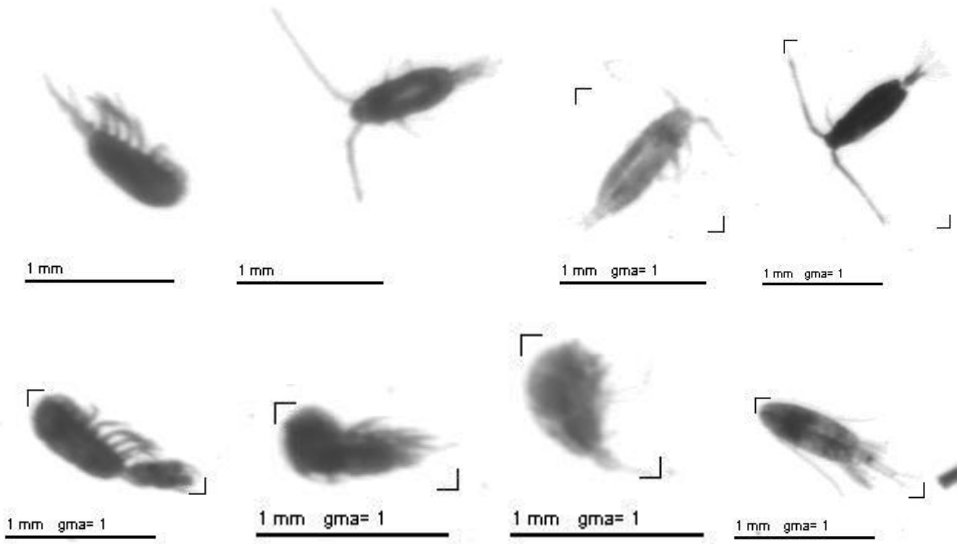

COPEPODA CYCLOPOIDA

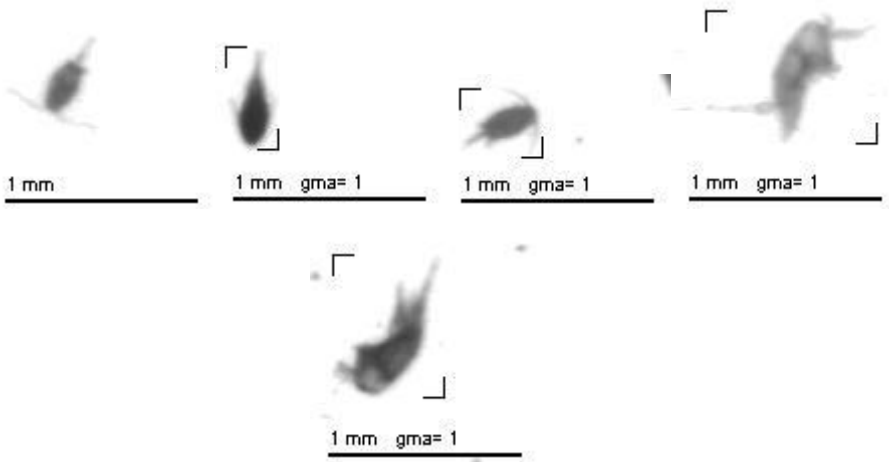

COPEPODA HARPACTICOIDA

ISOPODA

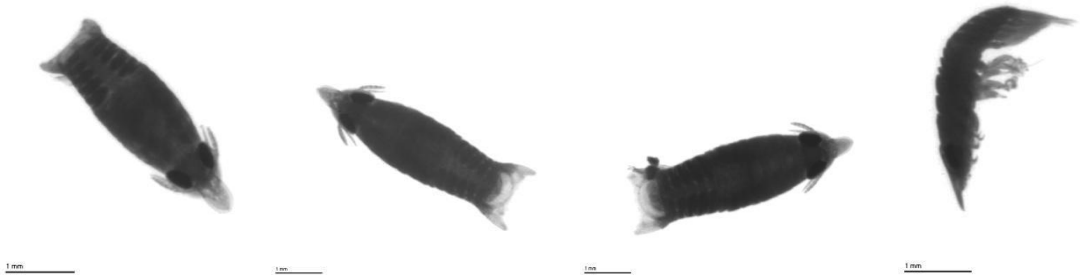

AMPHIPODA

CUMACEA

STOMATOPODA

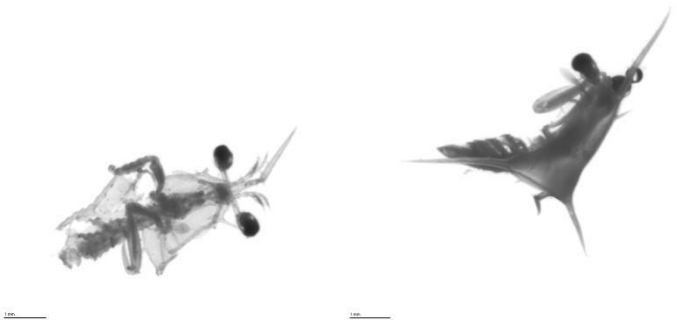

DECAPODA

LUCIFERIDAE (Adultos e juvenils)

LUCIFERIDAE (Protozoeas)

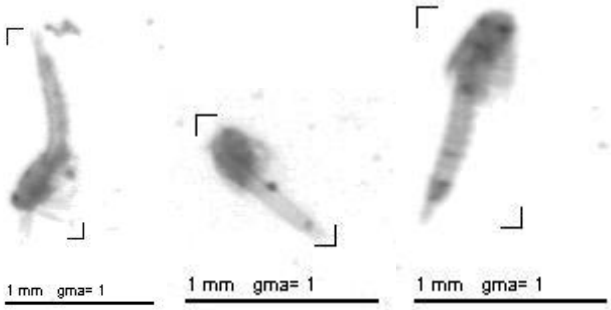

LUCIFERIDAE (Mísis)

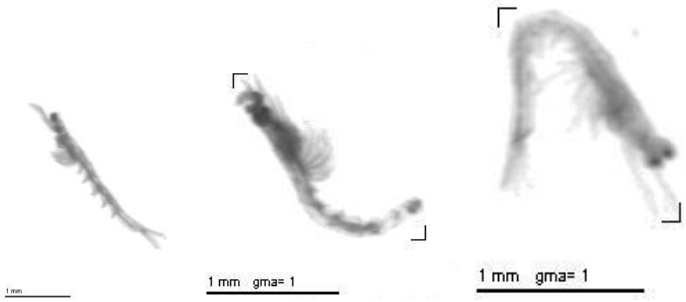

STENOPODIDEA (Zoeas)

PENAEUS (Pós - larvas)

ANOMURA, fam. PORCELLANIDAE (Zoeas)

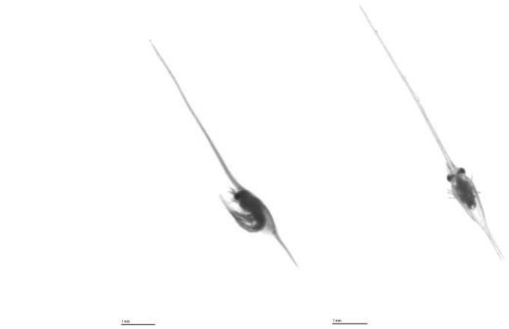

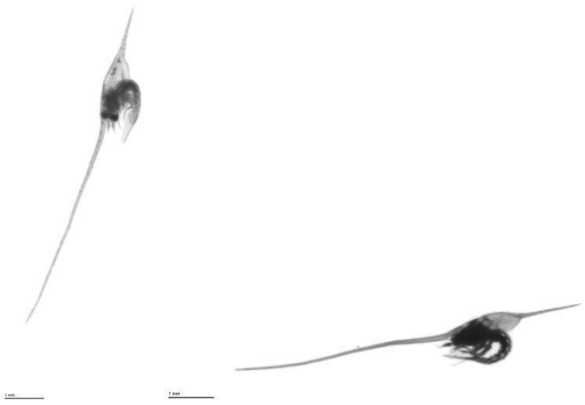

Morfotipo ANOMURA (Anomuros exceto fam. Porcellanidae, unclui Paguroidea, inclui Upogebiidae e outros Gebiidea e similares, zoeas)

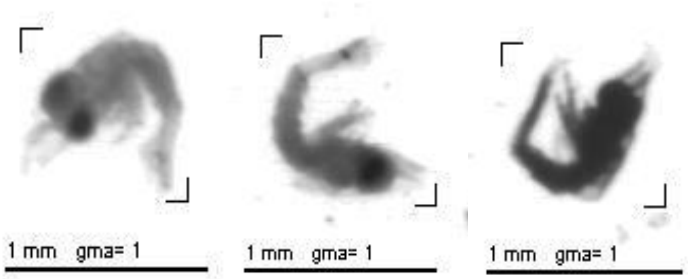

CARIDEA, fam. ALPHEIDAE (Zoeas)

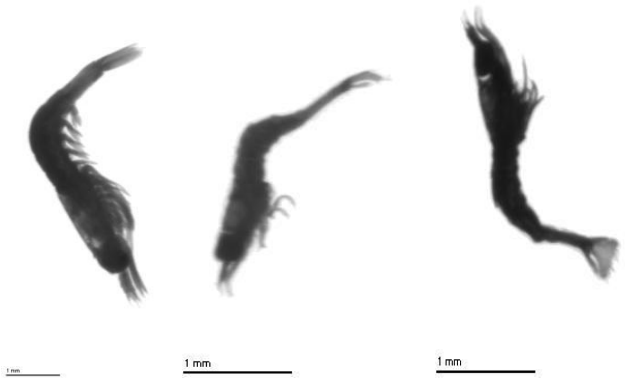

BRACHYURA (Zoeas)

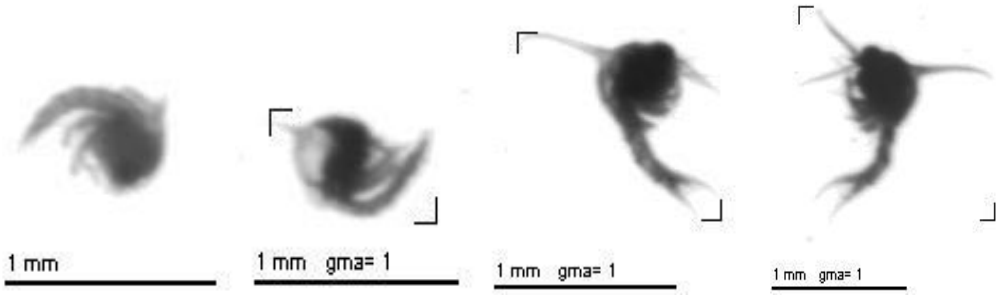

APPENDICULARIA

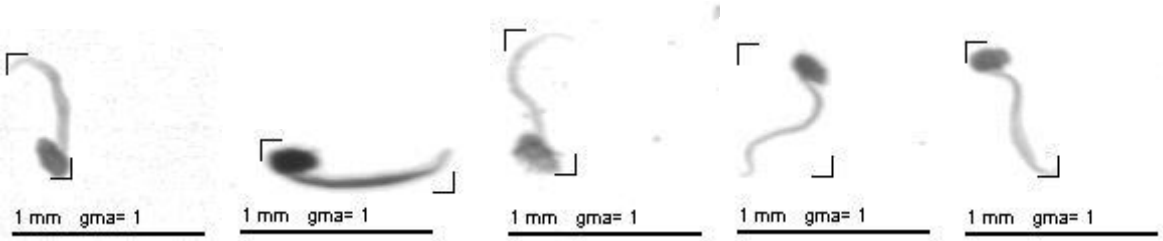

TELEOSTEI (Larvas)

TELEOSTEI (Ovos)

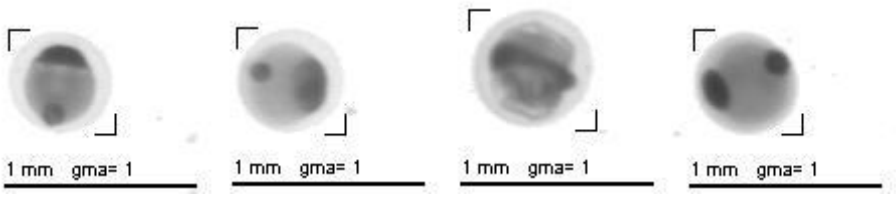

Apêndice C.3 - Vinhetas obtidas através do *ZooScan* nas coletas feitas na **Plataforma Continental** ao largo de Tamandaré: 2013 - 2015 (PE-Brasil).

CNIDARIA

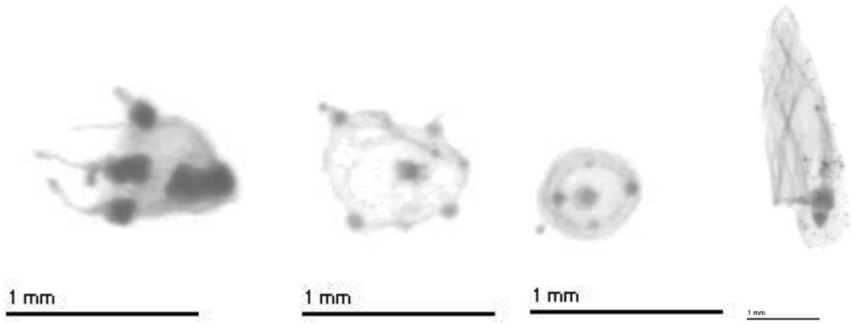

CHAETOGNATHA

AMPHIPODA

POLYCHAETA

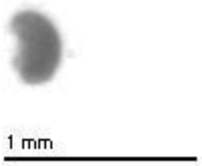

GASTROPODA

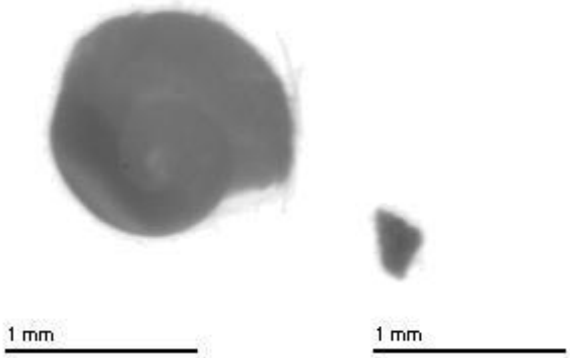

COPEPODA CALANOIDA

COPEPODA CYCLOPOIDA

COPEPODA HARPACTICOIDA

COPEPODA, Parasita

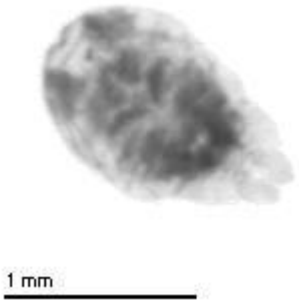

DECAPODA

LUCIFERIDAE (Adulto e juvenil)

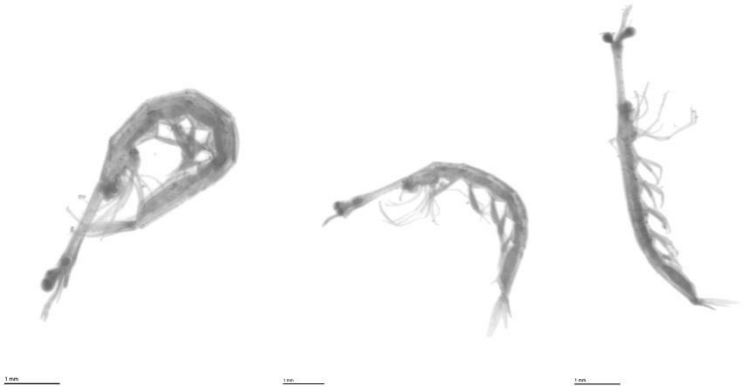

LUCIFERIDAE (Mysis)

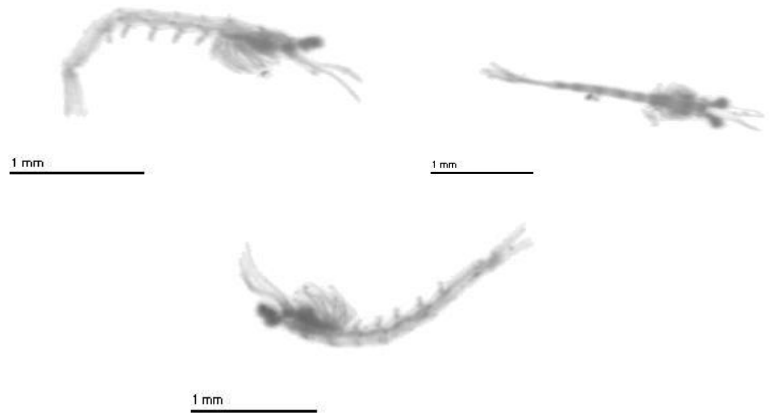

PENAEUS (Pós-larvas)

Morfotipo ANOMURA (Anomuros exceto fam. Porcellanidae, unclui Paguroidea, inclui Upogebiidae e outros Gebiidea e similares, zoeas)

CARIDEA, fam. ALPHEIDAE (Zoeas)

BRACHYURA (Zoeas)

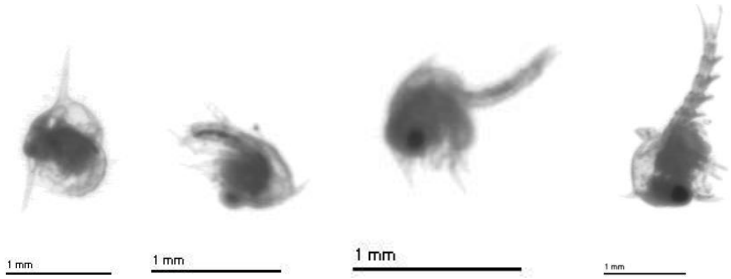

BRACHYURA (Megalopas)

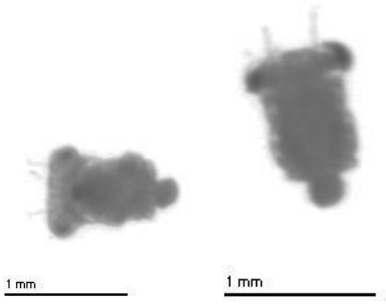

APPENDICULARIA

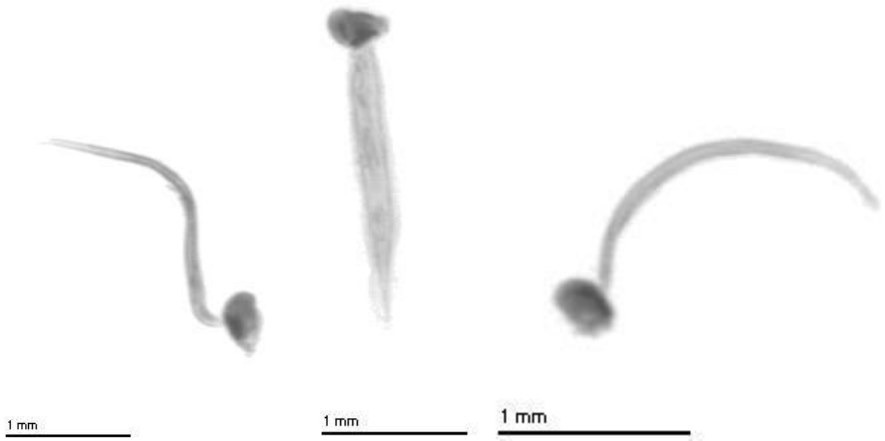

TELEOSTEI (Larvas)

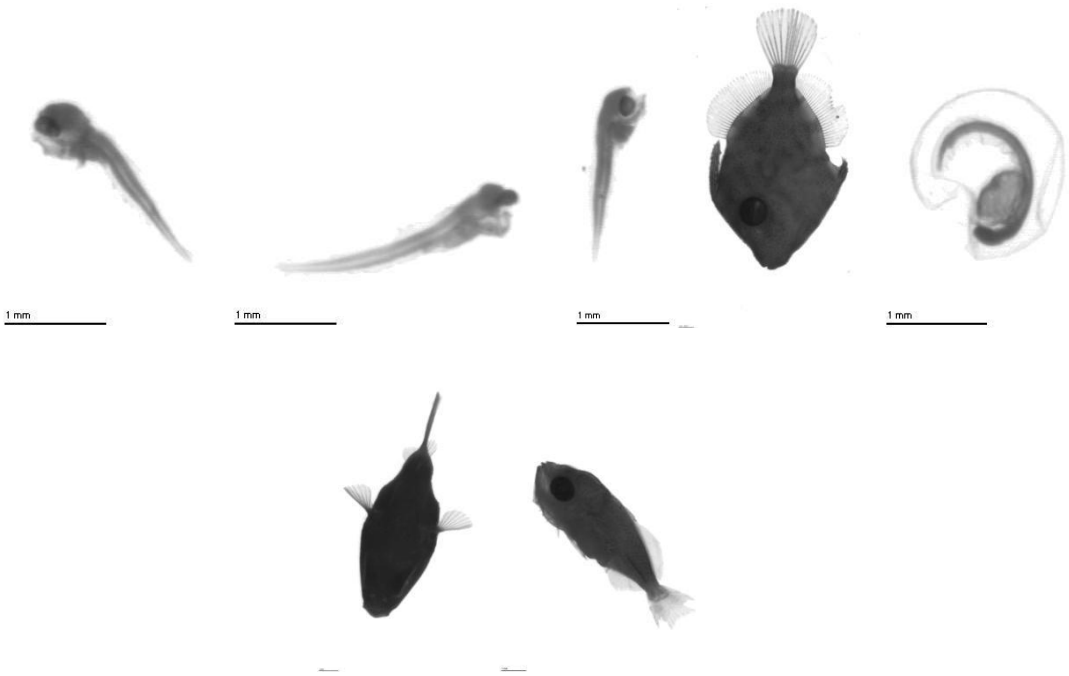

TELEOSTEI (Ovos)